Profiling the DNA damage response dynamics at sub-lethal and lethal temozolomide doses

Hartwig Visser

Faculty of Health and Applied Sciences, University of the West of England, Bristol

April 2023

A thesis submitted in partial fulfilment of the requirements of the University of the West of England, Bristol for the degree of Doctor of Philosophy

Abstract

Context: Confronted with DNA damage, cells can undergo cell cycle arrest and DNA repair, or cell death. However, communal DNA damage response (DDR) proteins involved in each of these cell fates, has confounded attempts to unravel the molecular nuances that drive cell fate determinations.

Aim: This study sought to identify whether distinct molecular signatures in the form of DDR protein and miRNA expression exist to underpin cell fate decisions.

Methods: Human lymphoblastoid (TK6) cells were exposed to a temozolomide (TMZ) dose range to identify sub-lethal and lethal doses. These doses (30 μM and 900 μM, respectively) were used for all subsequent experiments. TMZ-induced effects were determined based on DDR protein levels (immunoblotting), DNA damage accumulation (immunofluorescence), cell fate (flow cytometry), and miRNA expression (RNA sequencing and qRT-PCR). Mimics of identified miRNAs were over-expressed in TK6 cells and functional analysis performed with flow cytometry and immunoblotting.

Results: TK6 cells exposed to 30 μM TMZ (30TMZ) preferentially underwent G_2 arrest whereas 900 μM (900TMZ) caused apoptosis, identifying these as sub-lethal and lethal doses respectively. ATR-γH2Ax-Chk1-p53 pathway was significantly upregulated among 900TMZ-treated cells when compared to 30TMZ. Collectively, 31 miRNAs were differentially expressed when comparing 30TMZ-, and 900TMZ-treated cells to control-treated cells. Among these, miR-29b-3p, miR-363-5p, and miR-485-3p were determined to be significantly downregulated in response to 900TMZ-treated cells when compared to 30TMZ-treated cells. Moreover, p53 and miRNAs (miR-29b-3p, miR-363-5p, and miR-485-3p) were regulated in opposing directions following TMZ exposure, alluding to a possible miRNA-regulatory role for p53 in this context. Over-expression of miR-29b-3p or miR-363-5p individually or in combination did not affect cell fate.

Conclusion: TK6 cells exposed to a lethal dose of TMZ expresses a unique molecular profile in the form of significantly upregulated ATR-γH2Ax-Chk1-p53 signalling, along with significant downregulation of miR-29b-3p, miR-363-5p, and miR-485-3p when compared to sub-lethally-treated TK6 cells. This suggests these miRNAs to be DDR-responsive and thus, provides a link between DDR proteins and miRNA regulation. This is the first time these miRNAs have been reported in TK6 cells in the context of the DDR and these, along with the other differentially expressed miRNAs identified here, may prove useful as diagnostic biomarkers, druggable targets in future therapies, or become therapies in itself.

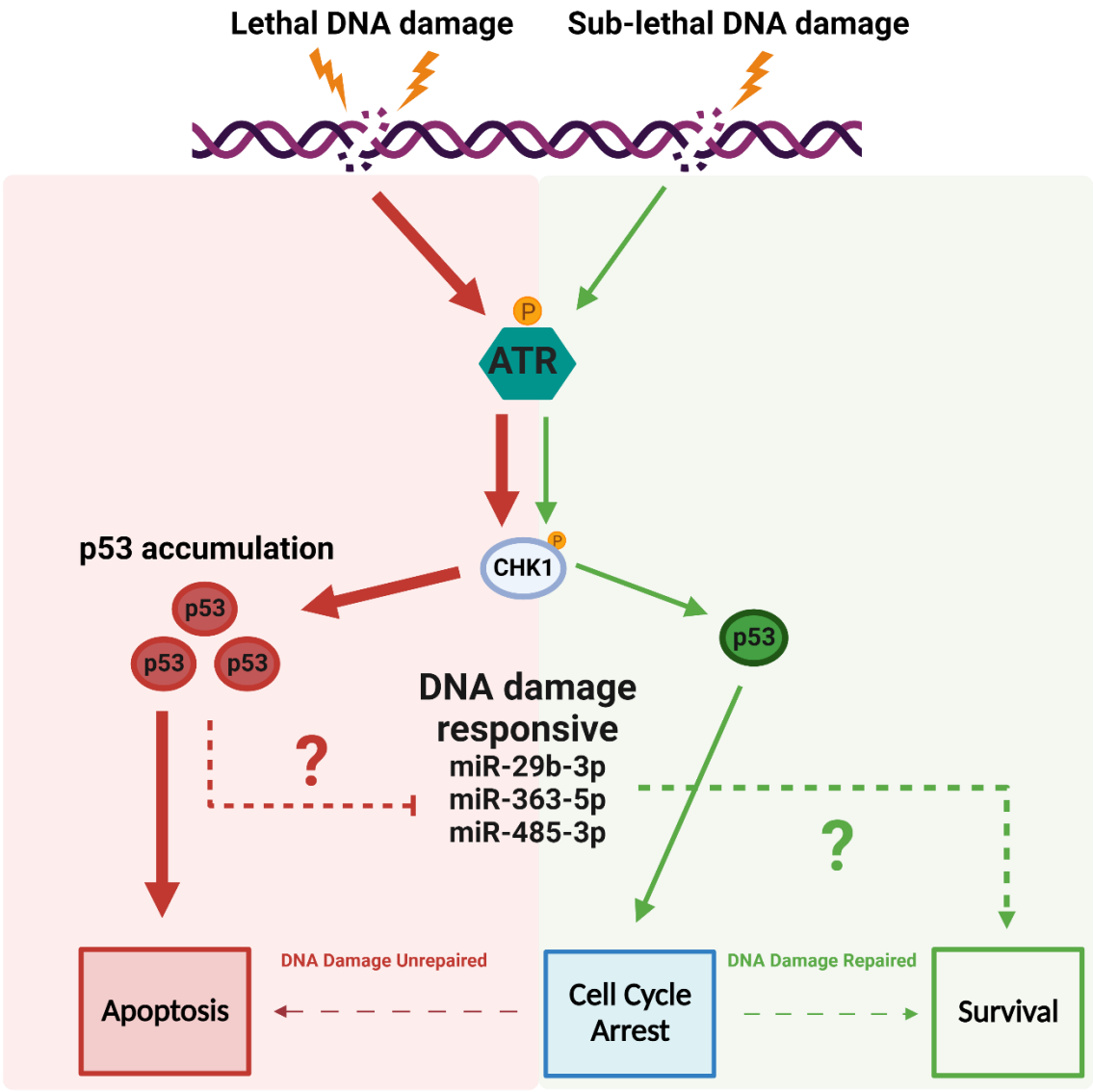

Acknowledgements

I would like to thank my supervisor, Dr Adam D Thomas, for his continued support throughout this PhD. Your enthusiasm for research and trust in my abilities allowed me to develop as an independent researcher. Your motivational catchphrase, "*It's a marathon, not a sprint*" will forever resonate with me.

To all my fellow PhD students, both those who have completed and those still in the grind, thank you for the lively environment that made PhD life slightly more tolerable.

To the technical team, especially Dr Katy Hayward, Alison Halliday, and Dave Corry, thank you for all your assistance and putting up with my overwhelming demeanour, concerns, and hour-long chats. The labs would not have been the same without you!

To Miriam Atom and Favour Oweisana, thank you for your contribution to the immunofluorescence microscopy component of this project.

To my lovely wife Toni Vonk, thanking you is pointless because it doesn't begin to describe how thankful I am for your continued love and support throughout all the sleepless nights, overnight experiments, and panic attacks. Without you I would have dropped out in year 1.

To UKEMS and UWE (specifically CRIB), thank you for the financial support that made this project possible.

Research Outputs

Kaina, B., Thomas, A.D., Visser, H., Hengstler, J.G., Frötschl, R. (2021). Do Carcinogens Have a Threshold Dose? The Pros and Cons. In: Reichl, FX., Schwenk, M. (eds) *Regulatory Toxicology*. https://doi.org/10.1007/978-3-030-57499-4_55

Visser, H., & Thomas, A. D. (2021). MicroRNAs and the DNA damage response: How is cell fate determined? *DNA Repair*, *108*, 103245. https://doi.org/10.1016/j.dnarep.2021.103245

Visser, H., & Thomas, A. D. (2021). MicroRNAs, damage levels, and DNA damage response control. *Trends in Genetics*, *37*(11), 963-965. https://doi.org/10.1016/j.tig.2021.06.018

Contents

List of figures

List of tables

Abbreviations

30TMZ – 30 μM temozolomide
900TMZ – 900 μM temozolomide
AATK – apoptosis associated tyrosine kinase
AGO – argonaute
ANOVA – analysis of variance
APAF1 - apoptotic protease activating factor 1
ATM - ataxia-telangiectasia
ATR - ataxia telangiectasia and Rad3-related
ATRIP – ATR interacting protein
Bcl-2 - B-cell lymphoma 2
Bcl-xL - B-cell lymphoma-extra large
BER – base excision repair
BNIP2 – Bcl-2 Interacting Protein 2
BOK - Bcl-2 related ovarian killer
BRCA1 – breast cancer 1
BTG1 - B-cell translocation gene 1
CAD - caspase-activated deoxyribonuclease
CASC2 - cancer Susceptibility 2
CDC25 - cell division cycle 25
Cdk – cyclin dependent kinase
cFLIP - cellular FLICE-like inhibitory protein
Chk1 – checkpoint kinase 1
Chk2 – checkpoint kinase 2
circHIPK3 – circular homeodomain-interacting protein kinase 3
CKI – cyclin dependent kinase inhibitor
CML - chronic myelogenous leukaemia
COL1A1 - collagen Type I Alpha 1 Chain
CPD - cyclopyrimidine dimers
CPM – counts per million
CRMP1 - collapsin response mediator protein
CytoC – cytochrome C

DAPI - 4′,6-diamidino-2-phenylindole
DDB2 - damage Specific DNA Binding Protein 2
DDR – DNA damage response
DDX5 - DEAD box helicase 5
DE – differentially expressed
DED – death effector domain
DISC – death induce signalling complex
DMSO – dimethyl sulfoxide
DNA – deoxyribonucleic acid
DNA pol - deoxyribonucleic acid polymerase
DNA-PK - DNA-dependent protein kinase
DNMT3A - DNA methyl-transferase
Dox - doxorubicin
DP5 – death protein 5
DROSHA - double-Stranded RNA-Specific Endoribonuclease
DSB – double strand breaks
E2F – E2 factor
EGFR – epidermal growth factor receptor
ERAD - ER-associated degradation
ERCC1 - excision repair cross-complementation protein
EtOH - ethanol
EXE - extra-embryonic ectoderm
FADD – Fas-associated death domain
FAS - Fas Cell Surface Death Receptor
FASL – Fas ligand
FBS – foetal bovine serum
FITC - fluorescein isothiocyanate
FOXO - forkhead box protein O
FOXP1 - forkhead box protein P1
FSC-A – forward scatter area
FSC-H – forward scatter height
G_1 – gap 1
G_2 – gap 2
GABRE - gamma-aminobutyric acid receptor subunit epsilon
GADD45a - growth arrest and DNA-damage-inducible protein
GO:BP – gene ontology: biological process
GP78 – glycoprotein 78
hESC - human embryonic stem cells
HIF1 – hypoxia-inducible factor 1
HIPK2 – homeodomain-interacting protein kinase 2
HMEC - human mammary epithelial cells
HMT - histone methyltransferase
HRR – homologous recombination repair
HUS1 - HUS1 Checkpoint Clamp Component
HUS1 - HUS1 Checkpoint Clamp Component
IAP – inhibitor of apoptosis protein
ICAD – inhibitor of caspase-activated deoxyribonuclease
IFN-γ – interferon gamma
IGF1 – insulin-like growth factor 1
IGF1R - insulin-like growth factor receptor
IL-1β – interleukin 1β
IR – ionizing radiation
JNK - c-Jun N-terminal kinase

KSRP - KH-type splicing regulatory protein
LNA – locked nucleic acid
LPEseq – local pooled error test for RNA sequence data
LPS – lipopolysaccharide
LRP1 - low-density lipoprotein receptor-related protein
LXRα - liver X-receptor α
MADD - mitogen-activated kinase activating death domain containing protein
Mcl-1 - induced myeloid leukaemia cell differentiation protein
MDC1 - mediator of DNA damage checkpoint 1
MDM2 – mouse double minute 2 homologue
MeOH - methanol
mESC - murine embryonic stem cells
MGMT – methylguanine methyltransferase
miRNA - microRNA
MMR- mismatch repair
MNNG - N-methyl-N-nitro-N-nitrosoguanidine
MOMP – mitochondrial outer membrane permeabilisation
MRE11 – meiotic recombination 11
*N*3-meA – *N*3-methyladenine
*N*7-meG – *N*7-methylguanine
NAIP - neuronal apoptosis inhibitory protein
NBS1 - Nijmegen breakage syndrome 1 protein

NER – nucleotide excision repair
NF-κβ – nuclear factor- κβ
NHEJ – non-homologous end joining
NK-cell – natural killer cell
NSCLC – non-small cell lung carcinoma
O^6-meG – O^6-methylguanine
P53AIP1 – p53-regulated apoptosis-inducing protein 1

P53BP1 – p53 binding protein 1
PAGE – polyacrylamide gel electrophoresis
PARP1 - poly (ADP-ribose) polymerase
pATR – phospho-ATR
PBS – phosphate buffered saline
pChk1 – phospho-Chk1
pChk2 - phospho-Chk2
PDCD4 – programmed cell death protein 4
PI – propidium iodide
PLK2 – polo-like kinase 2
PLK4 - polo-like kinase 2
pRb – protein retinoblastoma
Pre-miRNA – precursor miRNA
Pri-miRNA – primary miRNA
PRKDC - protein kinase, DNA activated, catalytic subunit
PRKG1 - protein kinase CGMP-dependent 1
PTEN - phosphatase and tensin homolog deleted on chromosome 10
PTM – post-translational modification
PUMA – p53 upregulated modulator of apoptosis
PVT1 - plasmacytoma variant translocation 1
qRT-PCR – quantitative real-time polymerase chain reaction
RIPA – radioimmunoprecipitation assay
RISC – RNA-induced silencing complex
RNA – ribonucleic acid
RPA – replication protein A
RPM – revolutions per minute
RPMI – Roswell park memorial institute
RT – room temperature
S - synthesis
SCLC – small cell lung carcinoma
SD – standard deviation
SDS – sodium dodecyl-sulfate
Ser - serine
SET8 - lysine Methyltransferase 5A
SIAH – seven in absentia homologue
siRNA – small interfering RNA
SIRT1 – sirtuin 1
SMAC - second mitochondria-derived activator of caspase
SMAD4 - mothers against decapentaplegic homolog 4
SMYD2 - SET and MYND domain containing 2
SOX2 - SRY-box transcription factor 2
SRSF10 - serine and arginine rich splicing factor
SSB – single strand break
SSC-A – side scatter - area
SSC-H – side scatter - height
STAR – spliced transcripts alignment to a reference
STAT3 - signal transducer and activator of transcription
TBS – tris-buffered saline
TBS-T – tris-buffered saline-tween 20
Thr - threonine
TLS – translesion synthesis
TMM - trimmed mean of M-values
TMZ - temozolomide
TNF-α – tumour necrosis factor-α
TopBP1 - DNA topoisomerase 2-binding protein 1
TRAF - TNF receptor-associated factor
TRAIL - TNF-related apoptosis-inducing ligand
TREX - three-prime exonuclease
UTR – untranslated region
UV – ultraviolet
VE - visceral endoderm
WEE1 - Wee1-like protein kinase
WIP1 - p53-induced protein phosphatase
XIAP – X-linked inhibitor of apoptosis protein
XPC - Xeroderma Pigmentosum, complementation group C
XPO5 – exportin 5
XRCC - X-ray repair cross-complementing protein
YY1 – yin yang 1
γH2Ax - H2A histone family member X

Preface

Human cells are in a constant state of genotoxicity. Endogenously, many biological processes required for physiological homeostasis leads to the generation of molecules capable of DNA damage (Tubbs and Nussenzweig, 2017). For example, cellular respiration generates reactive oxygen species that can cause DNA adducts (Auten and Davies, 2009). Exogenous sources of genotoxicity can be incidental (e.g., UV exposure), or as part of a treatment regime (e.g., chemotherapy) to combat cancer. DNA damage perceived by cells need to be dealt with to prevent the propagation of genomic instability and maintain DNA replicative fidelity (Tubbs and Nussenzweig, 2017). Following DNA damage, a complex signalling network, collectively termed, the DNA damage response (DDR), ensues. The DDR can initiate pro-survival strategies such as cell cycle arrest and repair the damage, or initiate programmed cell death (e.g., apoptosis) if the damage is substantial and exceeds cellular DNA repair capabilities (Surova and Zhivotovsky, 2013). While several forms of cell death exists, this thesis will focus on apoptosis. These cell fates (cell cycle arrest/DNA repair and apoptosis) are dependent on the amount of DNA damage experienced by the cell. Consequently, in response to ‘sub-lethal’ DNA damage, cells are likely to arrest, repair and survive, whereas ‘lethal’ damage results in apoptosis. How cells determine the appropriate cell fate remains a topic of debate, but it stands to reason that each of these cell fates are underpinned by a specific molecular mechanism(s) to ensure an appropriate and proportional physiological response. For example, considering the aforementioned example of cellular respiration, if this always resulted in cell death, humans would cease to exist. By the same token, if the DDR inappropriately initiates a survival strategy when cell death is required, this could facilitate cancer development or chemoresistance.

It is possible that in response to sub-lethal or lethal DNA damage, a characteristic DDR protein profile is brought about, serving as a molecular cue in favour of a particular cell fate. Additionally, miRNAs are involved in guiding both pro-, and anti-apoptotic cell fates. Thus, it is likely that the final cell fate outcome is determined by a specific miRNA expression pattern. Unravelling the molecular components involved in cell fate determination can have important implications for cancer prognosis and chemotherapeutic efficacy. Specifically, a clear understanding of the molecular mechanisms that drive cell fate can be utilised to assess chemotherapeutic efficacy, and lead to the discovery of novel druggable targets to improve chemotherapy. Moreover, identifying molecular signatures associated with either a 'pro-death' or 'pro-survival' cell fate could eventually be harnessed to mimic specific cell fate signatures as a form of cancer therapy, thus foregoing the use of toxic chemotherapy.

Hypothesis:

1. There is a change in a certain DDR protein profile at 'sub-lethal' and 'lethal' TMZ doses that drives cell fate.
2. DDR protein changes likely regulates, or is regulated by specific miRNAs.

Aims:

1. Identify the dynamics of key DDR proteins at sub-lethal and lethal TMZ doses at specific time-points.
2. Identify differentially expressed miRNAs between sub-lethal and lethal TMZ doses at specific time-points (based on Aim 1).
3. Manipulate miRNA levels and observe its effects on cell fate (based on Aim 2).

Chapter 1

Assessing TK6 cell fate changes in response to sub-lethal and lethal temozolomide doses

1.1. Introduction

1.1.1. DNA damage response and cell fate at a glance

The DNA damage response (DDR) fundamentally serves to maintain DNA replicative fidelity by preventing the propagation of damaged DNA that may manifest as mutations and subsequent diseases (Jan and Hoeijmakers, 2001; Matt and Hofmann, 2016). DNA damage is the detrimental structural alteration of DNA molecules that impedes its normal function and may result in cellular injury (Kaufmann and Paules, 1996). As DNA replication occurs during the cell cycle, tightly regulated mechanisms exist throughout cell division to monitor and ensure high fidelity DNA synthesis. These mechanisms not only detect DNA replication errors, but is fundamental to the DDR as DNA damage is also detected. Although the DDR will be discussed at length throughout this thesis, a brief overview is as follows: Cell cycle regulatory mechanisms comprise restriction points (checkpoints) at G_1/S, S, G_2/M and M-phase of the cell cycle, capable of arresting progression in response to detrimental cues, such as DNA damage (Visconti, Monica, and Grieco, 2016), that can result from endogenous (e.g., reactive oxygen species), or exogenous (e.g., xenobiotics or ultraviolet radiation, UV) sources (Hakem, 2008). In turn, cell cycle arrest provides an opportunity for DNA repair, or preparation for programmed cell death (e.g., apoptosis) if the damage is too severe and irreparable.

1.1.2. Cell cycle regulation and DNA damage repair

Principle components of cell cycle regulation include cyclins and cyclin-dependent kinases (Cdks). A full review of cell cycle regulation is beyond the scope of this thesis. Briefly, cyclin-Cdk dimerisation activates its kinase activity, which in turn phosphorylates specific target proteins in order to traverse each cell cycle checkpoint. In response to DNA damage, cell cycle progression is arrested, typically by inhibitory intervention of

the aforementioned process. For example, active cyclin-Cdk dimers in G_1-phase phosphorylates protein retinoblastoma (pRb), thereby liberating E2F transcription factors that upregulate G_1/S promoting proteins. Contrarily, DNA damage disrupts cyclin-Cdk dimerisation, thereby preventing pRb phosphorylation and subsequent cell cycle progression (Vermeulen, van Bockstaele, and Berneman, 2003).

Following cell cycle arrest, DNA repair attempts will commence. DNA repair mechanisms function in a damage-specific manner (**Fig. 1**), though repair pathways are not mutually exclusive (Kumar *et al*., 2020; Kumar, Raja, and van Houten, 2020). Broadly, DNA repair constitute five main pathways: base excision repair (BER), nucleotide excision repair (NER), mismatch repair (MMR), homologous recombination repair (HRR), and non-homologous end joining (NHEJ). An extensive review of DNA repair pathways is provided by Chatterjee and Walker (2017). Briefly, DNA repair mechanisms can be partitioned as functioning at the nucleotide level (e.g., BER, NER, MMR) or strand level (e.g., HRR, NHEJ). While BER mainly responds to non-helix distorting damage (e.g., deamination or oxidation) (Krokan and Bjørås, 2013), NER repairs bulky lesions capable of distorting the DNA helix (e.g., UV-induced cyclopyrimidine dimers, CPDs) (Schärer, 2013). MMR is tasked with removing mispaired bases, albeit from DNA replication errors, or DNA damage induction (Li, 2008; Pećina-Šlaus *et al*., 2020). On the other hand, HRR (Li and Heyer, 2008) and NHEJ (Trenner and Sartori, 2019) are fundamental DNA double strand break (DSB) repair pathways, and are arguably the most important in terms of cell fate, as DSBs are considered the most lethal DNA lesions (Trenner and Sartori, 2019). Of note, while these five pathways constitute the main DNA repair pathways, other contributors to DNA repair exist. For example, methylguanine methyltransferase (MGMT) is a repair enzyme that removes alkyl adducts as part of the direct DNA repair response (Gutierrez,

Thompson, and O'Connor, 2018). Direct repair, as the name suggests, is a means of direct reversal/removal of DNA adducts, and as such, are not pathways *per se*.

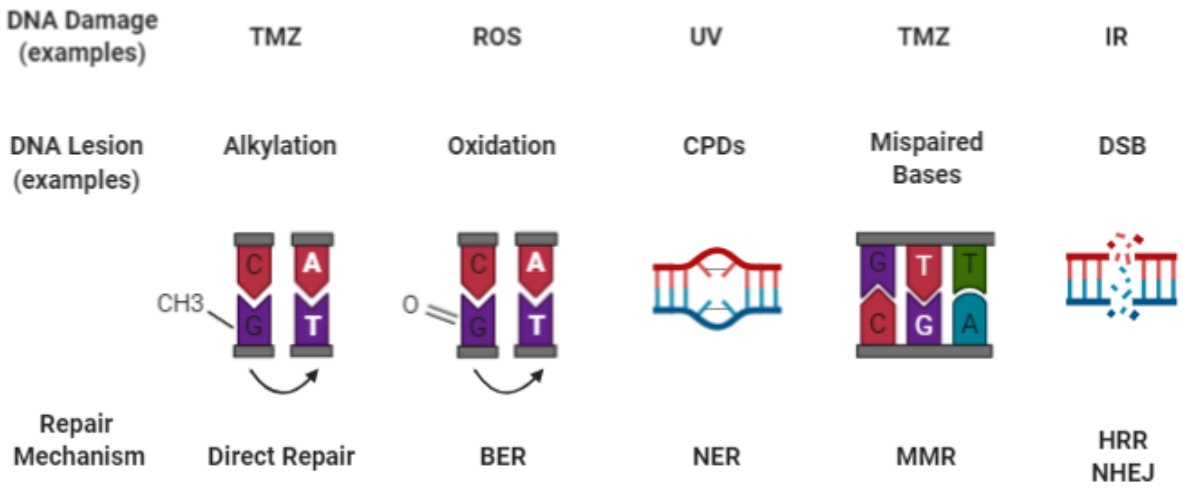

Figure 1. Overview of key DNA repair mechanisms.

This figure illustrates the utility of different DNA repair mechanism in response to specific DNA lesions, along with example sources of specific DNA damage lesions. Direct repair directly reverses/removes DNA adducts (e.g., methyl adducts). BER, NER, and MMR functions at the nucleotide level with BER repairing non-helix distorting damage (e.g., oxidation or deamination), whereas NER repairs 'bulky' adducts capable of helix distortion (e.g., cyclopyrimidine dimers). MMR serves to recognise and repair mispaired bases that could result from DNA damage or replication errors. HRR and NHEJ functions at DNA strand level and repairs strand breaks such as DSB caused by IR. Created on license from BioRender.com.

1.1.3. DDR cascade

1.1.3.1. DNA damage sensing and signal transduction

To accommodate an efficient DDR, DNA damage is detected by specialised sensor proteins including; MRE11-RAD50-NSB1 (MRN complex) (Syed and Tainer, 2018), RPA-ATRIP, XRCC6/5, and their respective phosphatidylinositol 3-kinase related kinases (PIKK): ataxia telangiectasia mutated (ATM), ataxia telangiectasia and Rad3-related (ATR), and DNA-dependent protein kinases (DNA-PK) (Roos, Thomas, and Kaina, 2016; Menolfi and Zha, 2020). Detection, in turn, brings forth a rapid DDR. DNA damage sensors are activated based on the type of DNA damage perceived. For example, while RPA-ATRIP detects DNA single strand breaks (SSBs) (Zou, Stephen, and Elledge, 2003), the MRN complex actively detects DSBs (Espinosa-Diez *et al*., 2018). This makes sense as their respective binding partners, ATR and ATM are generally distinguished as being able to sense SSBs and DNA replication fork stalling (ATR), or DSBs (ATM) (Cimprich and Cortez, 2008; Maréchal and Zou, 2013; Zeman and Cimprich, 2014). Subsequently, ATM and ATR phosphorylates downstream transducer proteins, including checkpoint kinases 1 and 2 (Chk1/2) (Bartek and Lukas, 2003) to propagate ‘damage signals’. ATM is widely considered to phosphorylate Chk2, whereas Chk1 is phosphorylated by ATR. However, this is a dated notion as functional interplay has been described between these pathways. For example, ATM is capable of phosphorylating Chk1 (Gatei *et al*., 2003), and reciprocally, ATR can phosphorylate Chk2 (Wang *et al*., 2006). It is worth noting that while Chk1/2 are perhaps the best known downstream targets of ATR/ATM phosphorylation, other targets are equally important to the DDR. For example, ATM phosphorylates the histone H2A, forming γH2Ax foci at DSB sites, and is thus an indicator of DSBs. In turn, γH2Ax facilitates DNA

repair protein recruitment at damaged sites (Stiff *et al*., 2004; Podhorecka, Skladanowski, Bozko, 2010).

Phosphorylated Chk1/2 (pChk1/2) is active and capable of signal transduction. Given its predominant association with ATR, Chk1 becomes phosphorylated in response to a broad range of stresses, including replication stress and SSBs. Concordantly, Chk1 has a broad range of functions (Dai and Grant, 2010; Zhang and Hunter, 2014). However, its functions in cell cycle arrest are frequently cited. For example, pChk1 is known to induce cell cycle arrest through inhibition of CDC25A-C (Zhang and Hunter, 2014). CDC25 is a family of dual-specificity phosphatases that promote cell cycle progression by removing inhibitory phosphoryl groups from Cdks (positive regulators of cell cycle progression) (Shen and Huang, 2012). CDC25 isoforms feature during specific cell cycle phases i.e., CDC25A (G_1/S phase), and CDC25B/C (G_2/M phase) (Zannini, Delia and Buscemi, 2014; Zhang and Hunter, 2014). Additionally, pChk1 activates the cell cycle inhibitory kinase, Wee1-like protein kinase (WEE1) (Lee, Kumagai, and Dunphy, 2001). Another well-known function of pChk1 is that of phosphorylating tumour suppressor protein, p53. pChk1 can phosphorylate p53 at serine 20 (ser20) thereby promoting its stability (Shieh *et al*., 2000; Zhang and Hunter, 2014; Hernandez-Valencia *et al*., 2018). Both pChk1 and pChk2 have also been suggested to promote cell cycle arrest through phosphorylation of pRb (negative regulator of cell cycle) at ser612, thereby promoting its repressive interaction with E2F-1 (transcriptional promoter of cell cycle) (Inoue, Kitagawa, and Taya, 2007). Similar to pChk1, pChk2 inhibits cell cycle progression through inhibition of CDC25A/C, thus regulating G_1/S and G_2/M phase progression respectively (Zannini, Delia and Buscemi, 2014). Moreover, pChk2 is also capable of phosphorylating p53 at ser20 (Hirao *et al*., 2000; Shieh *et al*., 2000).

1.1.4. The role of p53 in the DDR

When the DDR is inactive (unstressed conditions), p53 is maintained at low levels. This is achieved by proteasomal degradation facilitated by ubiquitin ligases that ubiquitinates p53, thereby recruiting 26S proteasomes. A prominent ubiquitin ligase is mouse double minute 2 homologue (MDM2), and it is widely accepted that p53 phosphorylation at ser20 inhibits p53-MDM2 interaction and subsequent degradation (Moll and Petrenko, 2003). P53 activation is a point of convergence for the majority of cascades within the DDR. Functioning as a transcription factor for several genes regulating cell cycle arrest, DNA repair (processes directed at survival), and apoptosis (Helton and Chen, 2007; Williams and Schumacher, 2016), the importance of p53 in the DDR and cell fate determination is evident (**Table 1**). The function of p53 is tied to its post-translational modification (PTM) status (discussed hereafter). This facilitates its functional selectivity, given that cell cycle arrest and DNA repair functions cannot be reconciled with apoptogenic functions, as these are seemingly opposing cell fates. While apoptosis is programmed cell death, arrest and repair functions are supportive of a cell survival outcome. Arguably, these outcomes are contingent on the severity of DNA damage (e.g., sub-lethal or lethal).

Table 1. Transcriptional and direct targets of p53

Biological System	Target	p53 Regulation	Reference
Cell cycle arrest	GADD45a	Upregulated	Han *et al*. (2019)
	p21 (CDKN1A)	Upregulated	El-Deiry *et al*. (1993)
	BTG2	Upregulated	Tsui *et al*. (2018)
DNA repair	XPC	Upregulated	Adimoolam and Ford (2002)
	RAD51	Repressed	Arias-Lopez *et al*. (2006)
	XPB	Direct recruitment to lesion	Chang *et al*. (2008)
	XPA, DDB2 (XPE), DNA Pol H	Upregulated	Kannappan *et al*. (2018)
	RAD51, RAD54	Repressed	Linke *et al*. (2003)
	Pol H	Upregulated	Liu and Chen (2006)
	Pol B	Upregulated	Seo *et al*. (2002)
Apoptosis	TRAIL-R3	Upregulated	De Almodóvar *et al*. (2004)
	Bcl-2	Repressed	Deng *et al*. (2006)
	BBC3 (PUMA)	Upregulated	Han *et al*. (2001) Nakano and Vousden (2001)
	TRAIL	Upregulated	Kuribayashi *et al*. (2008)
	DR4	Upregulated	Liu *et al*. (2004)
	CD95 (FASR)	Upregulated	Müller *et al*. (1998) Schilling *et al*. (2009)
	P53AIP1	Upregulated	Oda *et al*. (2000)
	BAX	Upregulated	Thornborrow *et al*. (2002)
	ACER2	Upregulated	Xu *et al*. (2017)
	APAF1	Upregulated	Yun *et al*. (2016)
Other	MDM2	Upregulated (low damage)	Mayo *et al*. (2005)
	PTEN	Upregulated (high damage)	
	USP49	Upregulated	Tu *et al*. (2018)

1.1.5. The role of PTMs in the DDR

PTMs dictate DDR dynamics. Some of the most extensively researched PTMs include phosphorylation, acetylation, and ubiquitination. Of these, phosphorylation is perhaps best understood. Phosphorylation is a staple topic among DDR research, as many DDR proteins (e.g., ATM, ATR, Chk1, and Chk2) are kinases. From DNA damage induction to cell cycle arrest and response execution, the DDR predominantly constitutes a relay of phosphorylations between regulatory kinases that drive the DDR. Consequently, DDR activity may be regarded as contingent on a balance between phosphorylation and dephosphorylation (Freeman and Monteiro, 2010). Simplistically, phosphorylation often serves to activate, whereas dephosphorylation deactivates (Freeman and Monteiro, 2010). For example, ATM/ATR phosphorylates (activates) Chk1/2, which phosphorylates p53. Concordantly, p53-induced protein phosphatase (WIP1) has been demonstrated to 'switch off' the DDR by dephosphorylating ATM and p53 (Macurek *et al*., 2013). However, it is worth noting that phosphorylation can also be deactivating. For example, ATM phosphorylates MDM2, thereby inducing a conformational change that disrupts polyubiquitination, and subsequent degradation of p53 (Cheng *et al*., 2009). Likewise, dephosphorylation is not synonymous with deactivation as it is well-known that pRb exerts its E2F repressive effects in a hypo-phosphorylated state.

These seemingly opposing functions of phosphorylation may be attributable to its position. Positioning of phosphoryl groups are known to elicit differential effects. For example, Chk1 phosphorylation on ser317 and ser345 is closely linked to its biological functionality in response to DNA damage (Niida *et al*., 2007; Wilsker *et al*., 2008). However, loss of ser317 phosphorylation impedes G_2/M checkpoint activation, whereas loss of ser345 is incompatible with cell viability in colorectal cancer cells (Wilsker *et al*., 2008). Furthermore, embryonic stem cells with mutated ser317 does not support

checkpoint activation, while mutated ser345 results in mitotic catastrophe (Niida *et al*., 2007). Chk2 functionality is also tied to differential phosphorylation. For example, phosphorylation on threonine 68 (thr68) is an initiating event, induced by DNA damage, that catalyses the structural modification of Chk2 to allow subsequent autophosphorylation, and full activation (Zannini, Delia, and Buscemi, 2014). Whereas phosphorylation at ser456 functions to stabilise Chk2 by preventing polyubiquitination and subsequent proteasomal degradation (Kass *et al*., 2007).

How PTMs regulate differential p53 functions remain a topic of debate. However, a recurring hypothesis is that specific PTMs correlate with the severity of DNA damage, and the position of subsequent PTMs determine p53 function. For example, p53 serves as an 'arrestor' when phosphorylated on ser15 and ser20 (Jabbur, Huang and Zhang, 2000; Loughery *et al*., 2014), while further phosphorylation at ser46 switches p53 functioning to 'killer', in favour of an apoptotic phenotype (Mayo *et al*., 2005; Smeenk *et al*., 2011). While pChk1/2 phosphorylates p53 at ser20, both ATM and ATR are capable of phosphorylating p53 at ser15, which promotes p53 stability and function primarily by disrupting p53-MDM2 interaction (Canman *et al*., 1998; Nakagawa *et al*., 1999; Tibbetts *et al*., 1999; Saito *et al*., 2002). Furthermore, while several kinases, including homeodomain-interacting protein kinase (HIPK2) (He *et al*., 2019), DYRK2 (Taira *et al*., 2007), ATM (Kodama *et al*., 2010), and p38 have been suggested to phosphorylate p53 at ser46 (Perfettini *et al*., 2005; Liebl and Hofmann, 2019), He *et al*. (2019) provides compelling evidence that HIPK2 is the principal kinase that phosphorylates ser46 upon DNA damage, as its inhibition diminished p53 (ser46) levels ≈ 4-fold in glioblastoma cells following TMZ treatment. Moreover, the authors demonstrated HIPK2 stabilisation to be contingent on ATM/ATR-mediated inhibition of seven in absentia homolog (SIAH1). SIAH1 is an E3 ubiquitin ligase that facilitates HIPK2 proteolysis, and has been

shown to be phosphorylated by both ATM and ATR at ser19, thereby disrupting SIAH1-HIPK2 interaction (Winter *et al*., 2008).

The function of p53 (ser46) has gained much attention in recent years, specifically regarding its role in apoptosis. Although still debated, a recurring hypothesis is that p53 (ser46) specifically promotes apoptosis by becoming more selective to pro-apoptotic gene promoters. For example, differential p53 target gene selectivity is reported by Smeenk *et al*. (2011) that observed increased p53 (ser46) among apoptotic cells. Particularly, genes involved in p53 signalling were significantly enriched. Importantly, the authors demonstrated the dependence of target gene selection on p53 (ser46), but not ser15, as phosphorylation at ser15 did not yield a similar target gene selection. Another example includes the observations by Oda *et al*. (2000) that demonstrated upregulation of apoptosis mediator, p53-regulated apoptosis-inducing protein (p53AIP1), to be dependent on p53 (ser46). Furthermore, mutation of ser46 reduced apoptosis. The authors hypothesised that initial p53 PTMs, including phosphorylation at ser15 and ser20 drives cell cycle arrest and repair functions, whereas later phosphorylation at ser46 drives apoptosis. This was supported by the observation that loss or mutation of p53 (ser46) does not affect p21 or p53R2 (DNA repair protein) (Wang *et al*., 2009) expression, whereas their expression correlated with ser15 phosphorylation. Additionally, observations by Mayo *et al*. (2005) demonstrated p53 (ser46) in response to ‘high dose’ chemotherapy, whereas this was not observed with the ‘low dose’. P53 (ser46) brought about increased selectivity for p53AIP1 and phosphatase and tensin homologue deleted on chromosome 10 (PTEN). PTEN is a tumour suppressor that augments apoptosis by inhibiting the pro-survival phosphoinositide-3 kinase (PI3K)-AKT signalling pathway (Carracedo and Pandolfi, 2008). Consistent with the notion of p53(ser46)-dependent pro-apoptotic promotor

selectivity, Feng, Hollstein, and Xu (2006) demonstrated downregulation of several pro-apoptotic genes in p53 (ser46)-alanine mutants, including Bcl-2 associated X protein (BAX) and p53 upregulated modulator of apoptosis (PUMA), following DNA damage induction.

It is important to recognise that, while phosphorylation constitutes principle PTMs driving p53 function, these are not 'stand-alone' and are often complemented by other PTMs, such as acetylation (Tang *et al*., 2008) and methylation (Shi *et al*., 2007). P53 acetylation is fundamental to diminish MDM2-induced proteolysis, and interference at p53-responsive promoters (Tang *et al*., 2008; Loewer *et al*., 2010). For example, p53 lysine residue (e.g., lys120, lys370, and lys382) acetylation has been demonstrated to diminish p53-MDM2 interaction. This acetylation also interferes with MDM2 recruitment to the p21 promoter. Moreover, loss of p53 acetylation can diminish PUMA, BAX, and p21 expression levels (Tang *et al*., 2008). Akin to p53 (ser46)-mediated pro-apoptotic gene selectivity, acetylation at lys120 increases apoptotic protease activating factor (APAF1) expression, thus promoting apoptosis (Yun *et al*., 2016). Therefore, the regulation of deacetylases are of importance. Sirtuin 1 (SIRT1) is a histone deacetylase that is known to deacetylate p53 (Yang *et al*., 2015; Ren *et al*., 2019), particularly at lys382 (Reed and Quelle, 2015). Moreover, SIRT1 can also inhibit p300, a histone acetyltransferase that acetylates p53 (Bouras *et al*., 2005). Incidentally, HIPK2 can inhibit SIRT1 (Conrad *et al*., 2016). Regarding methylation, this PTM also affects p53 activity, as p53 (lys382) methylation by histone methyltransferase (HMT), SET8, impairs p21 and PUMA transactivation (Shi *et al*., 2007). Similarly, Zhu *et al*. (2016) observed another HMT, SMYD2, along with SET8 to methylate p53 at lys382 and lys370 respectively. Methylation was tied to p53 transcriptional inhibition as knock-down of either HMT resulted in increased transcription of PUMA and p21.

1.1.6. Apoptosis at a glance

It is clear that strategic p53 PTMs can signify a commitment to cell death, and although the relationship between these PTMs and apoptosis execution requires clarification, it likely facilitates the upregulation of several pro-apoptotic proteins (**Table 1**). Since its discovery in 1979 (Soussi, 2010), p53 has become nearly synonymous with apoptosis, and is often cited as the 'guardian of the genome'. A full review of apoptosis is covered in **3.1.1** (**Chapter 3**). Briefly, apoptosis comprises two main pathways, intrinsic and extrinsic. The intrinsic pathway relies on pro-apoptotic proteins to compromise the mitochondrial membrane, which in turn leaks cytochrome C (cytoC) into the cytoplasm. CytoC serves as a molecular signal to continue with apoptosis, forming the apoptosome. The apoptosome, which is a construct of cytoC, APAF1, and caspase-9 (cysteine protease), ultimately activates executioner caspases (e.g., caspase-3/7) that digest cellular components. Similarly, the extrinsic pathway relies on caspase activation, though, its molecular cues are derived from death receptors (e.g., FAS ligand receptor, FASR). Moreover, in contrast to intrinsic apoptosis, extrinsic apoptosis relies on caspase-8/10 to activate executioner caspases-3/7 (Elmore, 2007; Galluzzi *et al*., 2018).

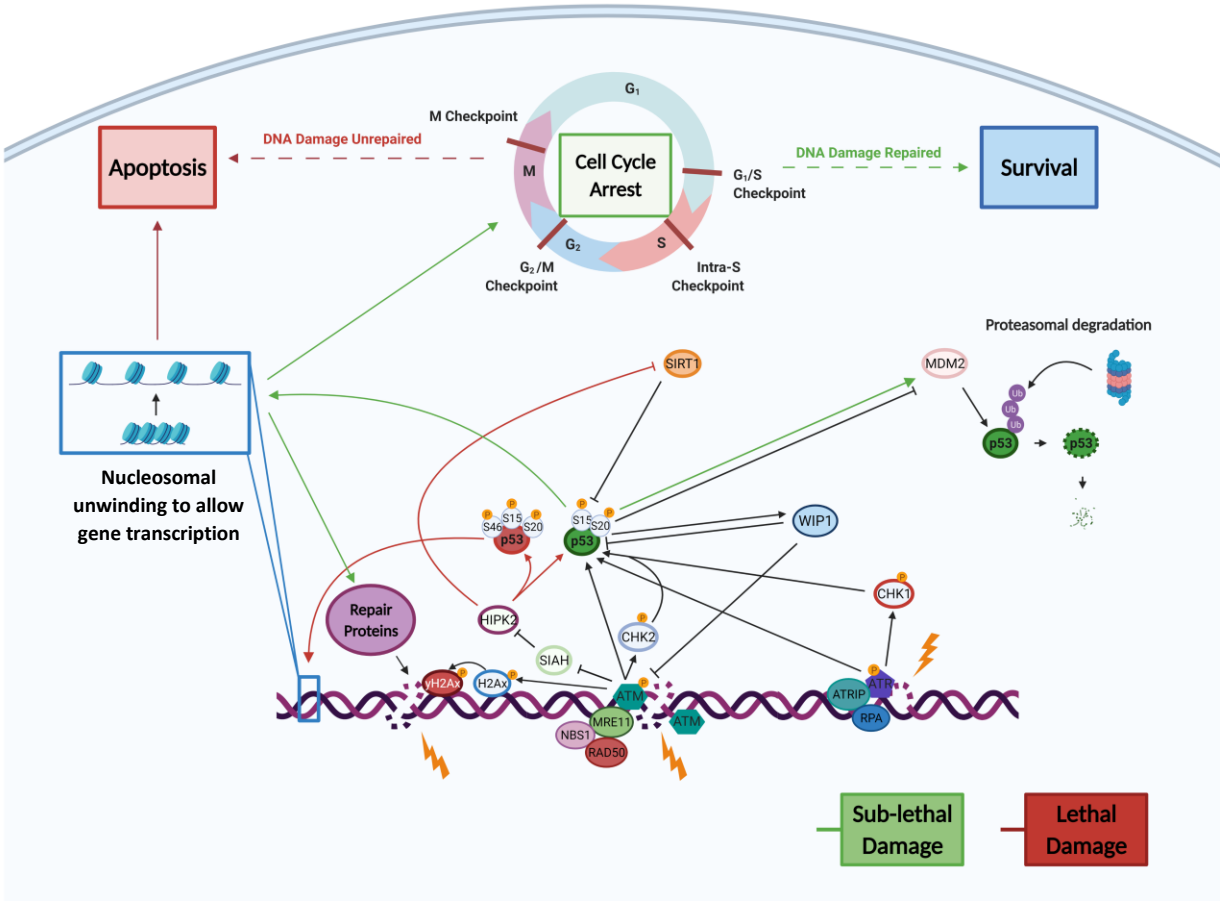

Figure 2. Typical DDR pathway in the context of sub-lethal and lethal DNA damage.

DNA damage is detected by ATM, or ATR that propagate 'damage signals' to Chk1/2 by means of phosphorylation. In turn, pChk1/2 further propagate the signal, resulting in p53 activation. Depending on the severity of the DNA damage, signalling may follow the 'sub-lethal damage' route, if the damage is tolerable/repairable, resulting in cell cycle arrest, DNA repair, and ultimately survival. However, if DNA damage is too severe, signalling may follow the 'lethal damage' route resulting in transcriptional activation of pro-apoptotic proteins, eventuating in apoptosis. Arrows represent activation whereas blunted ends indicate inhibition. Note: Image taken from Visser and Thomas (2021) and used with permission. Created on license from BioRender.com.

1.1.7. Rationale

This chapter brings into focus the concept that a single DDR pathway can manifest different cell fates (**Fig. 2**). Focussing on apoptosis (pro-death) and cell cycle arrest/DNA repair (pro-survival) as exemplar cell fates, what remains enigmatic is the molecular cues that promote either cell fate to prevail. Several theories have been suggested to govern cell fate following DNA damage, of which many are centred on a delicate balance between pro-survival and pro-death signalling (Adams and Cory, 2007; Nowsheen and Yang, 2012; Roos, Thomas, and Kaina, 2016). Thus, a reasonable assumption is that cell fate is determined by the intensity of the signalling in favour of either outcome. For example, Li *et al*. (2011a) observed that when cells are exposed to different levels of DNA damage, those exposed to greater levels of DNA damage are more likely to undergo cell death, whereas lower-exposed cells may survive. The authors also observed a positive correlation between the level of DNA damage and nuclear accumulation of DDR proteins. Relatedly, Speidel, Helmbold, and Deppert (2006) demonstrated high dose irradiation (known to cause DNA damage) to induce apoptosis, while low doses resulted in cell cycle arrest. Thus, a reasonable assertion is that greater levels of DNA damage, by intensifying DDR signalling, tips the balance of DDR signalling in favour of cell death. Moreover, a review by Roos, Thomas, and Kaina (2016) provides compelling arguments that ‘low level’ DNA damage is tolerated by cells in terms of initiating repair, and ultimately survival mechanisms. Whereas ‘high level’ or sustained damage initiates cell death. Although the intensity of DDR signalling has been correlated with the level, and duration of exposure to DNA damage (Zhang, Liu, and Wang, 2011; Nair, Bagheri, and Saini, 2015), the exact molecular mechanism that drives the ‘decision’ to abandon cell survival attempts in favour of apoptosis remains unclear.

Another critical consideration relates to the period *after* DNA damage. Specifically, while dose, and by extension, DNA damage intensity, is the *de facto* driver of cell fate decision-making, time is arguably equally important. In context of assessing lethality or genotoxicity, it is not unreasonable to assume that measurements taken at different times post-exposure might result in different conclusions. In support of the latter, consider how, for example, DNA repair might influence cell fate. It is known that endogenous DNA repair mechanisms safeguard the genome against DNA mutant propagation by repairing damaged DNA (Li *et al*., 2021). By the same token, the effectiveness of DNA damaging agents is contingent on the ability of cellular DNA repair mechanisms to resolve the resulting DNA lesions. For example, temozolomide (TMZ) (the test article used here) is an alkylating agent known to induce DNA damage by predominantly causing *N*3-meA, *N*7-meG, and O^6-meG adducts. While *N*3-meA and *N*7-meG adducts are the most abundant, they are considered to be less toxic than O^6-meG adducts given the competence of BER to resolve the former lesions and the limited availability of MGMT that resolves O^6-meG lesions (Kaina *et al*., 2007; Fan *et al*., 2013; Ito *et al*., 2013; Strobel *et al*., 2019). Thus, for cells exposed to TMZ, any assessment of genotoxicity would have to consider endogenous MGMT levels. However, MGMT is a ‘suicide enzyme’, repairing lesions at the expense of itself. Specifically, MGMT transfers the alkyl adduct onto itself, resulting in its inactivation (Kaina *et al*., 2007; Gouws and Pretorius, 2011). Consequently, indications of genotoxicity will become more obvious as MGMT levels deplete and, reciprocally, DNA damage lesions accrue with *time*. This exemplifies an example of how DNA repair might undermine DNA damaging agents, however, consideration must also be given to genotoxicity that may result from DNA repair. For example, the genotoxicity of TMZ is, at least in part, suggested to result from DNA repair intermediates that accumulate during repair

attempts over several cell cycles (York and Modrich, 2006; Mojas, Lopes, and Jiricny, 2007; Quiros, Roos, and Kaina, 2010; De Zio, Cianfanelli, and Cecconi, 2013; Fuchs *et al*., 2021). Thus, it is not unreasonable to assume an initial 'restrained genotoxicity' might be observed, prior to breaching a stochastic threshold after which a specific cell fate ensues. The concept of inherent DNA damage thresholds is gaining traction and along with DNA repair, a host of other factors (e.g., cell and DNA damage type) may influence it (Kaina *et al*., 2021). It is likely that time post-exposure to DNA damaging agents is inextricably linked to DNA damage thresholds and thus, cell fate. Therefore, this chapter identifies how specific DDR proteins change over time in response to sub-lethal and lethal DNA damage, and speculates on how changes in the level of these DDR proteins may be contributing factors to differential cell fates.

Aim:

1. Identify the dynamics of key DDR proteins at sub-lethal and lethal TMZ doses at specific time-points.

1.2. Methods

1.2.1.Tissue culture

The human B-lymphoblastoid TK6 suspension cell line (American Type Culture Collection, CRL-8015, Virginia, USA) was used as they are p53 competent and able to elicit a complete DDR (Hashimoto *et al*., 2012). Cells were incubated under standard conditions (37°C and 5% CO_2) in complete Roswell Park Memorial Institute (RPMI) medium (GlutaMAX) (Thermo Fisher Scientific, Loughborough, UK) containing 10% foetal bovine serum (FBS) (complete medium) (Thermo Fisher Scientific, Loughborough, UK). Cells were maintained at densities of < 1 x 10^6 cells/mL in accordance with supplier recommendations. Unless otherwise stated, all experiments were performed at cell densities of ≈ 1.5 x 10^5 – 2 x 10^5 cells/mL at the time of treatment. To ensure optimal growth conditions, cells were maintained for at least 5 days prior to TMZ treatment, adding fresh complete medium as required. In all cases, unless otherwise stated, 'biological replicates' refer to independent experiments conducted on TK6 cell cultures raised from respective cryovials i.e., for each biological replicate a fresh TK6 cell stock cryovial was revived from liquid nitrogen or -80°C storage.

1.2.2. Dose responses and subsequent TMZ treatments

1.2.2.1. Establishing sub-lethal and lethal TMZ doses

TMZ was selected as test article given its half-life of ≈ 1 - 2 h *in vitro* (Wesolowski, Rajdev, and Mukherji, 2010; Chen *et al*., 2014; Liu *et al*., 2014), thus supporting our 1 h TMZ exposure protocol discussed hereafter. This contrasts with certain other alkylating agents such as *N*-methyl-*N*-nitrosourea (MNU) that has an *in vitro* half-life of only 8 min (Miyamoto *et al*., 1988). Moreover, our research group has previous experience with

using TMZ *in vitro*. TMZ powder (Merck, Dorset, UK) was dissolved in dimethyl sulfoxide (DMSO) (Merck, Dorset, UK) to 100 mM stock solutions and stored at - 80 °C until use. These were further diluted with DMSO to prepare the TMZ doses for subsequent experimentation. Cells were exposed to final concentrations of 0 (1% DMSO solvent control), 10, 30, 70, 100, 250, and 900 µM TMZ for 1 h, respectively. This concentration range was selected to encompass typical intratumoural and plasma TMZ concentrations following cancer treatment (Berte *et al*., 2016; Beltzig, Stratenwerth, and Kaina, 2021; Knizhnik *et al*., 2013), and also included an 'extreme' dose (900 µM), to ensure an apoptotic cell fate, as previously observed within our research group (Thomas, A.D., personal communication, 2019). Subsequently, treatment was terminated by TMZ removal and phosphate-buffered saline (PBS) (Thermo Fisher Scientific, Loughborough, UK) washing, after which cells were resuspended in fresh, complete RPMI to re-establish initial cell densities, and were re-incubated for a further 24 h under standard conditions. This time-point was selected to ensure sufficient DNA damage (in the form of DSBs) have occurred, prompting the formation of γH2Ax foci (indicator of DSBs) (De Zio, Cianfanelli, Cecconi, 2013), and the induction of apoptosis.

1.2.2.2. γH2Ax foci visualisation by immunofluorescence of TMZ dose response samples

Following the 24 h incubation, cells were counted, washed with tris-buffered saline (TBS), and fixed with ice-cold 100% methanol (MeOH) (Thermo Fisher Scientific, Loughborough, UK) (15 min). Fixed cells were washed with TBS and subsequently 5 x 10^4 cells were incubated with 0.1 % triton-X (Thermo Fisher Scientific, Loughborough, UK) for 10 min at room temperature (RT). Following another TBS wash, cells were incubated in 5% goat serum (Thermo Fisher Scientific, Loughborough, UK), made in TBS, for 30 min at RT. Subsequently, cells were incubated with an anti-γH2Ax (D7T2V)

antibody (Cell Signaling Technology, Leiden, Netherlands) for 2 h at RT, at a 1/150 final dilution. After incubation, cells were spun onto slides in cytofunnels using a Cytospin centrifuge (Thermo Fisher Scientific, Loughborough, UK) at 800 rpm for 8 min. Slides were air dried (10 min), TBS-washed for 5 min, and incubated with Alexa Fluor 568 goat anti-mouse secondary antibody (Life Technologies, Leicestershire, UK) (diluted 1/500 in 5% goat serum) for 1 h at RT. Slides were subsequently TBS-washed and incubated with 0.5 µg/ml DAPI (Merck, Dorset, UK) for 10 min before mounting coverslips with Mowiol mounting medium (Merck, Dorset, UK). Visualisation was performed on a Nikon Eclipse 80i fluorescent microscope and 140 – 1100 cells per sample were scored for γH2Ax foci. Scores were classified as groups: γH2Ax negative (< 7 foci/cell) or γH2Ax positive (≥ 7 foci/cell) based on typical scoring parameters classifying 5 - 10 foci as positive (Avondoglio *et al*., 2009; Toyooka, Ishihama, and Ibuki, 2011). Scoring γH2Ax foci provides confirmation of the level and type of damage being caused at specific TMZ doses.

1.2.2.3. Annexin V measurement of TMZ dose response samples

TK6 cells were treated exactly as for γH2Ax foci visualisation. Annexin V analysis was performed with an Annexin V-FITC kit (Miltenyi Biotec, Surrey, UK), according to manufacturer specifications, to detect apoptotic cells following TMZ exposure. Twenty-four hours post-exposure, 3 x 10^5 cells were sampled, centrifuged (160 X g, 6 min), and resuspended in 1 x binding buffer. Subsequently, this suspension was centrifuged (300 X g, 10 min) and resuspended in Annexin V-FITC antibody (diluted 1/10 v/v in 1 x binding buffer), followed by a 15 min incubation in the dark. After this, cells were washed in binding buffer and centrifuged (300 X g, 10 min), before being resuspended in ≈ 1 µg/mL propidium iodide (PI) (prepared 1/100 v/v in 1 x binding buffer). Analysis was performed on a BD Accuri C6 flow cytometer. A medium flow rate was used and TK6

cells were gated based on size and granularity indicated with an SSC-A vs. FSC-A scatter plot. Doublet exclusion was based on both FSC-A vs. FSC-H, and SSC-A vs. SSC-H scatter plots. PI positive cells and Annexin V positive cells (indicated by FITC) were detected in the FL2-A and FL1-A channels respectively. Following this, the TK6 population was gated to identify; PI and Annexin V double negative, PI positive, Annexin V positive, and PI and Annexin V double positive cells, to identify live, necrotic, and apoptotic cells respectively. At least 10000 single cells were recorded in the FL2-A vs. FL1-A channel for each sample.

1.2.3. DDR protein profiling in response to TMZ

1.2.3.1. TK6 treatment with 30TMZ and 900TMZ

TK6 cells were exposed to DMSO, 30 µM (30TMZ), and 900 µM (900TMZ). Treatment was the same as **1.2.2.1**, with the exception of using 4 h, 18 h, and 36 h post-exposure as sampling times. This experimental setup allows characterisation of DDR protein levels at both sub-lethal and lethal doses over a sufficient time span, allowing DNA damage to manifest. This is based on the doubling time of TK6 cells (≈ 12 - 18 h) (Hashimoto and Todo, 2013; Brüsehafer *et al*., 2016; Lorge *et al*., 2016), and considering that TMZ-induced DNA damage requires at least two replicative cycles (Quiros, Roos, and Kaina, 2010). DMSO treatments were used as time-matched controls. In anticipation of TK6 cell doubling, samples were supplemented with an equal volume fresh complete RPMI ≈ 18 - 24 h post-exposure, to maintain the original cell density.

1.2.3.2. Immunoblotting TMZ-treated samples and controls

Protein extraction

Following treatments, all samples and controls underwent protein extraction. Samples were centrifuged (433 X g) for 5 min at 4°C, and PBS washed to remove residual serum. Following two subsequent wash cycles, cell lysis was achieved by resuspending samples in radioimmunoprecipitation assay (RIPA) buffer (Merck, Dorset, UK), containing protease and phosphatase inhibitor (1/100 v/v) (Halt™, Thermo Fisher Scientific, Loughborough, UK), and incubating on ice for 15 min with intermittent vortexing. Proteins were extracted as a supernatant following centrifugation (8000 X g) for 10 min at 4°C. These were stored at - 80°C until further analysis.

Protein quantification and polyacrylamide gel electrophoresis

Protein concentration was determined spectrophometrically using the DC assay (BioRad, Hertfordshire, UK) according to manufacturer specifications. Depending on the protein probed for, 10 – 50 µg protein was used for immunoblotting. Extracted proteins were prepared in 1 x sodium dodecyl-sulfate (SDS)-PAGE sample loading buffer (from 6 x Laemmli buffer: SDS (10.57% w/w), bromophenol blue (0.05% w/w) (Merck, Dorset, UK; Thermo Fisher Scientific, Loughborough, UK), dithiothreitol (8.19% w/w), glycerol (52.14% w/w) (Thermo Fisher Scientific, Loughborough, UK), tris-HCl (0.5 M pH 6.8) (10.57% w/w, dH_2O (18.49% w/w)). Following this, samples were heated at 95°C for 3 min, cooled, and loaded onto 6 - 15% polyacrylamide gels (prepared according to BioRad specifications), depending on protein size. PageRuler™ Plus or HiMark™ (Thermo Fisher Scientific, Loughborough, UK) protein standards were used depending on the molecular weight of the proteins probed for. Electrophoresis was performed at 100 V in running buffer (SDS (0.1% v/v),10 x tris-glycine (10% v/v) (Merck, Dorset, UK; Thermo Fisher Scientific, Loughborough, UK), dH_2O (89.9% v/v)).

Immunoblotting

Proteins were transferred to nitrocellulose membranes overnight (4°C) at 100 mA or 30 V (depending on protein size), or for 2 h at 300 mA on ice, in transfer buffer (MeOH (10% v/v) (Thermo Fisher Scientific, Loughborough, UK), 10 x tris-glycine (10% v/v), dH_2O (80% v/v)). Key DDR proteins were targeted for analysis. For a complete list of proteins targeted and antibodies used see **Table 2**.

Table 2. Primary antibodies validated and used for immunoblotting

Protein	Species	Clonality	Dilution	Supplier	Clone
β-actin	Mouse	Monoclonal	1/2000-1/2500	Cell Signaling	8H10D10
Chk1	Mouse	Monoclonal	1/1000-1/1250	Cell Signaling	2G1D5
pChk1	Rabbit	Monoclonal	1/1000-1/1250	Cell Signaling	133D3
Chk2	Mouse	Monoclonal	1/1000-1/1250	Cell Signaling	1C12
pChk2	Rabbit	Monoclonal	1/1000-1/1250	Cell Signaling	C13C1
P53	Mouse	Monoclonal	1/1000-1/1250	Cell Signaling	DO-1
γH2Ax	Rabbit	Monoclonal	1/1000-1/1250	Cell Signaling	20E3
ATR	Mouse	Monoclonal	1/1000-1/1250	Santa Cruz	C-1
pATR	Rabbit	Polyclonal	1/1000-1/1250	Cell Signaling	-

* Proteins preceded by ‘p’ indicates phosphorylated form.

Following protein transfer, membranes were incubated in 5% bovine serum albumin (BSA) (Thermo Fisher Scientific, Loughborough, UK) prepared in TBS-T (TBS, 0.1% tween 20) for 1 h at RT. Primary antibody incubation was done overnight at 4°C or for 1 h at RT. Antibody dilutions used are indicated in **Table 2**. Following this, membranes were washed three times in TBS-T for 5 min. Subsequently, membranes were incubated with the appropriate secondary antibodies (IRDye goat anti-rabbit/goat anti-mouse) (Licor, Cambridge, UK), diluted 1/15000 (v/v in TBS-T), for 1 h at RT. To simultaneously detect total and phospho-proteins of the same target, primary antibodies for each were from different species, and secondary antibodies were tagged with different fluorescent labels. Excess antibodies were removed with three 10 min wash cycles in TBS-T. Subsequent visualisation was performed on a Licor Odyssey Fc imaging system (LI-COR Biosciences, Nebraska, USA). Protein normalisation was performed with lane normalisation factors calculated from β-actin (loading control), and phospho-proteins were further normalised against respective total proteins where relevant (**Appendix A**). Fold changes were calculated by comparing each sample to its respective, time-matched, DMSO control.

1.2.4. Cell cycle analysis

TK6 cells were exposed to DMSO, 30TMZ, and 900TMZ. Treatment and sampling times were the same as for **1.2.3.** All samples were counted, centrifuged (400 X g) for 5 min, and 1 x TBS/PBS washed (twice). Subsequently, cells were fixed in ice-cold MeOH (100%) for 10 - 15 min, at RT. Samples that were not immediately processed were stored after fixation, at - 20 °C for no longer than one week. Following this, 2 - 3 x 10^5 cells were sampled for analysis. Note, for each experiment the number of cells sampled were kept constant between individual samples. Adjustment of the number of cells sampled was only required when cell loss during processing impeded subsequent

analysis. Sampled cells were centrifuged (600 - 5000 X g) for 5 min and incubated at RT for 1 h in 1 x PBS-diluted RNAse A (30 µg/mL) (Thermo Fisher Scientific, Loughborough, UK). Following this, PI (Thermo Fisher Scientific, Loughborough, UK) was added to each sample to a final concentration of 40 µg/mL and analysed using a BD Accuri C6 flow cytometer. A medium flow rate was used and TK6 cells were gated based on size and granularity indicated with a SSC-A vs. FSC-A scatter plot. Doublet exclusion was based on both FSC-A vs. FSC-H, and SSC-A vs. SSC-H scatter plots. Following these exclusions, at least 5000 single cells were recorded in the FL2-A channel for each sample. PI positive cells were detected as a histogram in the FL2-A channel, after which cell cycle phases were gated for 4 h, 18 h, and 36 h samples respectively, using time-matched DMSO-treated samples to define G_1, S, and G_2 populations.

1.2.5. Annexin V analysis

TK6 cells were exposed to DMSO, 30TMZ, and 900TMZ. Treatment and sampling times was the same as **1.2.4**. Analysis was performed as described in **1.2.2.3**.

1.2.6. Statistical analysis

Statistical analyses were performed using IBM SPSS Statistics v.28. Normality was assessed using Shapiro-Wilk test. Parametric data was analysed with either independent sample t-test or one-way ANOVA with Tukey's test or Dunnett's test as a post-hoc test depending on the type and number of comparisons made. Non-parametric data was assessed with Mann-Whitney U test. Correlations between time and γH2Ax foci and apoptosis, respectively, were performed with Kendall's tau-b. Correlation between γH2Ax foci and apoptosis were performed with Spearman's rank correlation. To ensure balanced correlations, three simple random sampling iterations were used to

correct unpaired sample sizes when performing Spearman correlations. This resulted in multiple correlation combinations, and thus, resulting p-values were averaged. However, statistical significance was only considered if each combination had an association in the same direction and had a $p < 0.05$, otherwise it was assumed that no correlation exists. For all statistics, $p < 0.05$ was considered statistically significant.

1.3. Results

1.3.1. Assessing the genotoxicity of TMZ doses

To assess the genotoxicity of TMZ, TK6 cells were exposed to TMZ doses ranging 0 (DMSO) – 900 μM and sampled 24 h post-exposure. Subsequently, γH2Ax was used as an indicator of DSBs, and by extension, genotoxicity. Only 900TMZ yielded a significantly decreased γH2Ax negative population (**p = 0.008**), whereas the γH2Ax positive population significantly increased (**p = 0.008**) when compared with the DMSO control (**Fig. 3**)**.**

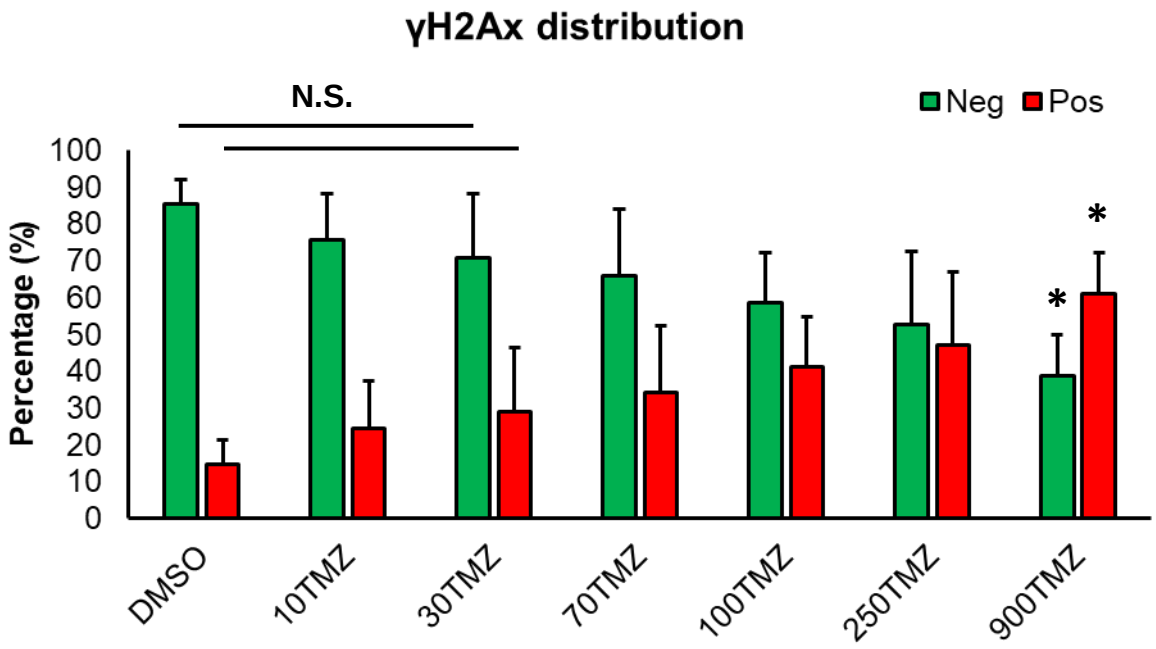

Figure 3. Distribution of γH2Ax positive and negative TK6 cells 24 h post-exposure to TMZ.

TK6 cells were treated with a dose range of TMZ for 1 h, after which treatment was terminated and cells were further incubated for 24 h in fresh complete RPMI. Cells with ≥ 7 γH2Ax foci were classified as 'γH2Ax positive' (red) while < 7 were classified as 'γH2Ax negative' (green). The percentage γH2Ax positive cells show a positive relationship with increasing TMZ dose, while the reverse is true for γH2Ax negative cells. Particularly, the only dose significantly influencing γH2Ax foci as compared to DMSO, was 900TMZ. Normality was assessed with Shapiro-Wilk test while mean differences between TMZ-treated and DMSO controls were assessed for statistical significance using a one-way ANOVA with Dunnett's test post-hoc. For 30TMZ only two biological replicates were available for analysis and therefore normality was not assumed. Thus, a Mann-Whitney U test was used to compare 30TMZ against the DMSO control. In all other cases the data is representative of three biological replicates (**n = 3**) ***** Indicates statistical significance ($p < 0.05$). Data represents mean + SD (error bars). N.S. (not significant).

Given that no other doses yielded a significant difference, 900TMZ was selected as the lethal dose. For the sub-lethal dose, 30TMZ was selected as this did not significantly affect γH2Ax levels (**p = 0.8**) and is within range of the intratumoural and typical plasma concentrations achieved following patient treatment with TMZ (Berte *et al*., 2016; Beltzig, Stratenwerth, and Kaina, 2021). The effect of DMSO, 30TMZ, and 900TMZ on γH2Ax foci formation can be seen in **Fig. 4**. Foci formation was more wide-spread (present in more cells) and had a greater accumulation per cell among 900TMZ-treated cells compared to the DMSO control, whereas 30TMZ demonstrated some γH2Ax foci accumulation but to a much lesser extent when compared to 900TMZ-treated cells. Moreover, unlike 30TMZ, 900TMZ-treated cells showed prominent morphological changes indicative of apoptosis, including nuclear condensation and fragmentation (Saraste and Pulkki, 2000).

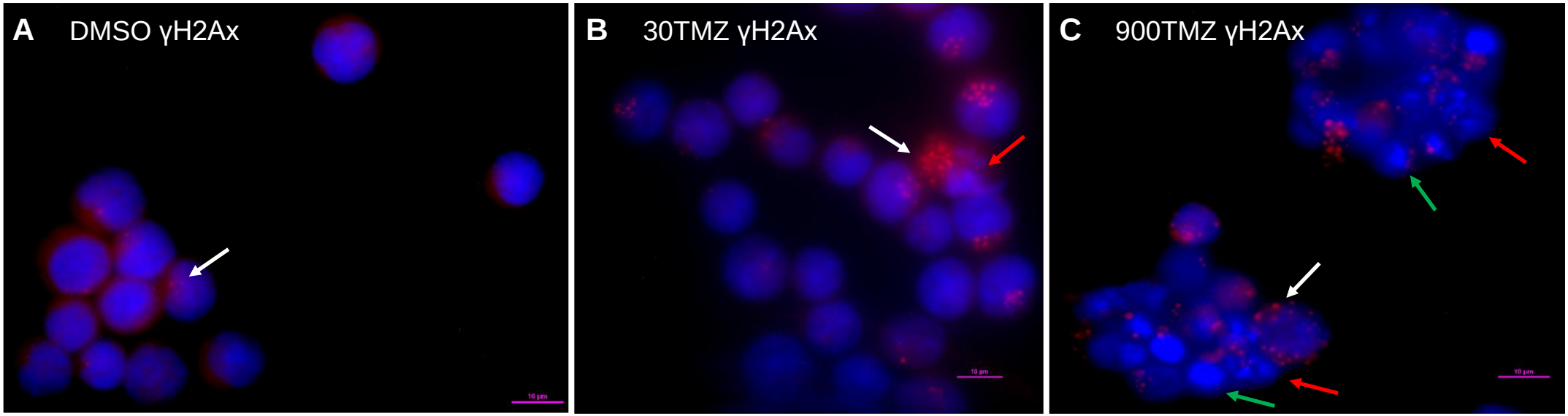

Figure 4. Immunofluorescence micrographs of γH2Ax foci in TK6 cells.

TK6 cells were treated with DMSO and a range of TMZ doses for 1 h. Samples were collected 24 h post-exposure and processed for immunocytochemistry. Cells were probed with a primary mouse antibody against γH2Ax, and the primary antibody was detected with Alexa Fluor 568 goat anti-mouse secondary antibody. White arrows indicate examples of γH2Ax foci, while red and green arrows indicate apparent nuclear fragmentation and nuclear condensation respectively, both likely resulting from apoptosis. Of particular note is the prominent increase in γH2Ax foci among TMZ-treated cells (**B** and **C**) as compared to those treated with DMSO (**A**). Furthermore, compared to either DMSO (**A**) or 30TMZ-treated cells (**B**), 900TMZ-treated cells (**C**) show clear morphological indications of apoptosis. Scale bars represents 10 μm.

To determine if an association exists between TMZ dose and γH2Ax foci formation, Kendall's tau-b correlation was performed (**Fig. 5**). Indeed, a significant (**$p < 0.001$**) positive association was observed between increasing γH2Ax-positive cells and increasing TMZ dose. Similarly, a significant (**$p < 0.001$**) negative association was observed between the percentage-γH2Ax negative cells and increasing TMZ dose.

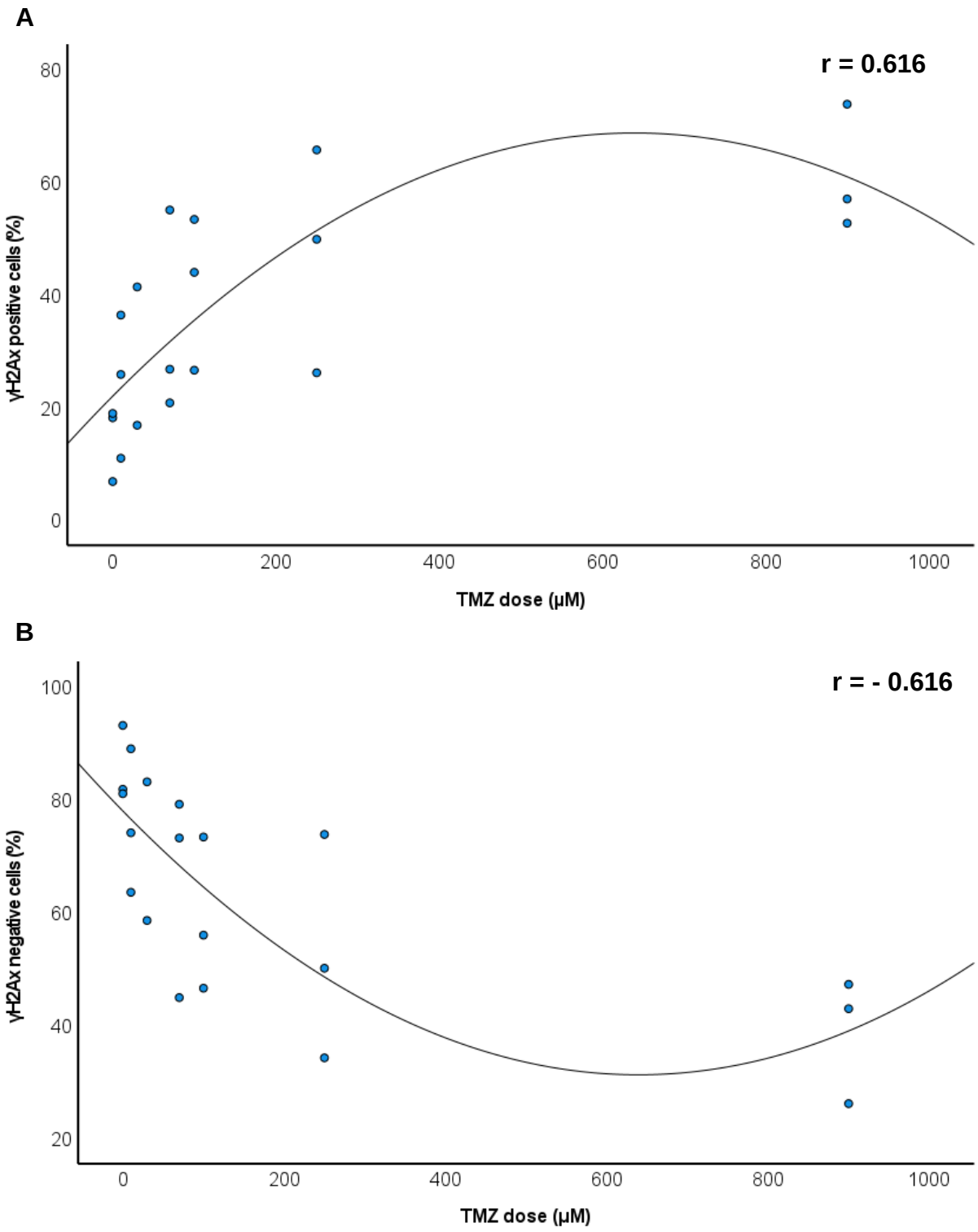

Figure 5. Correlation between γH2Ax foci formation and TMZ dose.
TK6 cells were treated with DMSO or a dose range of TMZ for 1 h, after which treatment was terminated and cells were further incubated for 24 h in fresh complete RPMI. Cells with ≥ 7 γH2Ax foci were classified as 'γH2Ax positive' while < 7 were classified as 'γH2Ax negative'. Kendall's tau-b correlation demonstrates a significant non-linear positive association between γH2Ax positive cells and TMZ dose (**A**), whereas the reverse is true for γH2Ax negative cells (**B**). Data represents individual samples of three (**n = 3**) biological repeats, except for 30TMZ where only two biological repeats were available.

1.3.2. Assessing lethality of TMZ doses

To determine whether the observed genotoxicity manifests as apoptosis, TK6 cells exposed to TMZ (0 – 900 µM) were assessed by flow cytometry for phosphatidylserine (**Fig. 6**), a membrane protein exposed during apoptosis that has a high affinity for annexin V (Lee *et al*., 2013). Exploiting the phosphatidylserine-annexin V interaction, the fraction of apoptotic TK6 cells was quantified. Compared to the DMSO control, only 250TMZ and 900TMZ significantly increased apoptosis (**p = 0.027** and **p < 0.001**) 24 h post-exposure, as indicated by the percentage annexin V positive cells. However, at 30TMZ, no increase in apoptosis (**p = 0.999**) was observed when compared to the DMSO control. These observations correspond with our γH2Ax foci accumulation data and thus confirms that TMZ-induced genotoxicity culminates in apoptosis.

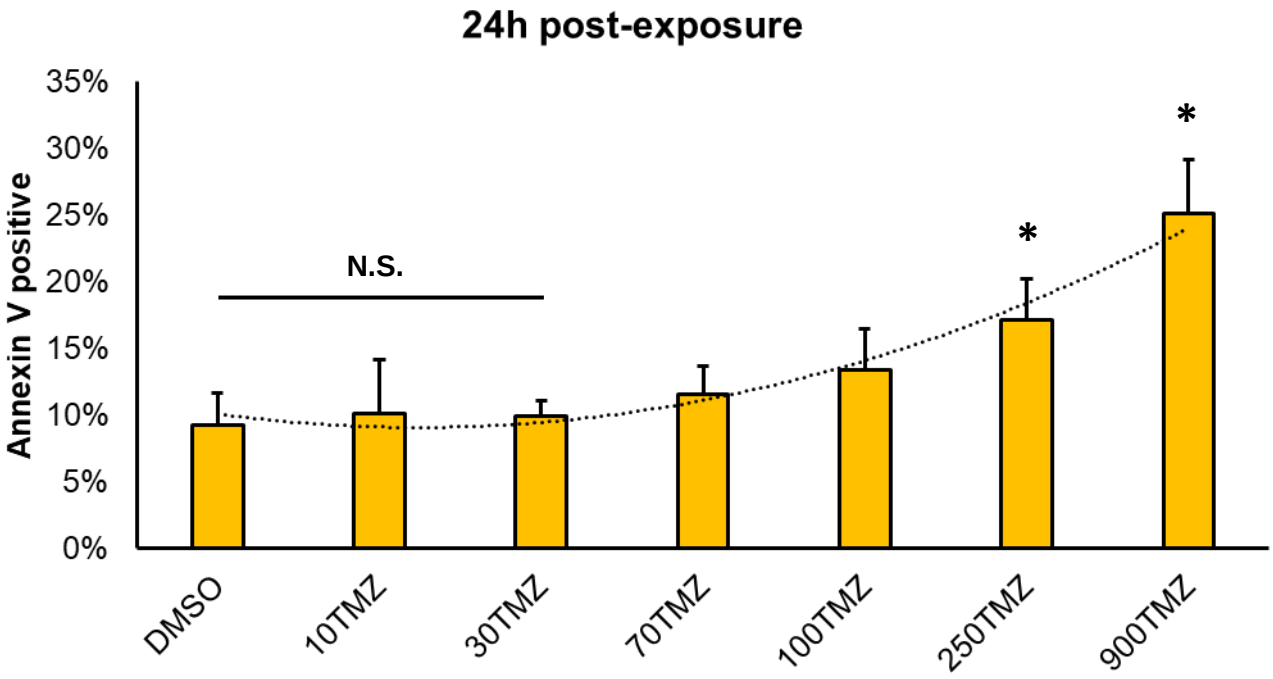

Figure 6. Apoptosis levels of TK6 cells exposed to a TMZ dose range.

TK6 cells were treated with DMSO and a range of TMZ doses for 1 h. Samples were collected 24 h post-exposure, probed with Annexin V-FITC and analysed with flow cytometry. Percentage annexin V positive cells increases with TMZ dose, reaching statistical significance at 250TMZ and 900TMZ as compared to the DMSO control. Of note is the non-significant relationship between 30TMZ and DMSO. Normality was assessed with Shapiro-Wilk test while mean differences between any TMZ dose and DMSO were assessed for statistical significance using a one-way ANOVA and Dunnett's test post-hoc. ***** Indicates statistical significance ($p < 0.05$). Data is representative of three biological repeats (**n = 3**). Data represents mean + SD (error bars). N.S. (not significant).

To determine if an association exists between the level of apoptosis and TMZ dose, Kendall's tau-b correlation was performed (**Fig. 7**). Indeed, a significant (**p < 0.001**) positive association was observed between annexin V positive cells and increasing TMZ dose. Given the positive correlation between increasing apoptosis, γH2Ax positive cells and increasing TMZ dose, respectively, we sought to determine if a relationship also exists between γH2Ax foci formation and apoptosis. Unfortunately, the nature of our data limits the statistical appropriateness of such a correlation. Nonetheless, statistical appropriateness aside, an approximation of the relationship between γH2Ax foci formation and apoptosis can be seen in **Appendix B**. Indeed, a statistically significant (**p = 0.019**) positive correlation was observed between annexin V positive and γH2Ax positive cells, whereas a significant (**p = 0.019**) negative correlation was observed between annexin V positive and γH2Ax negative cells. However, this relationship is not apparently linear.

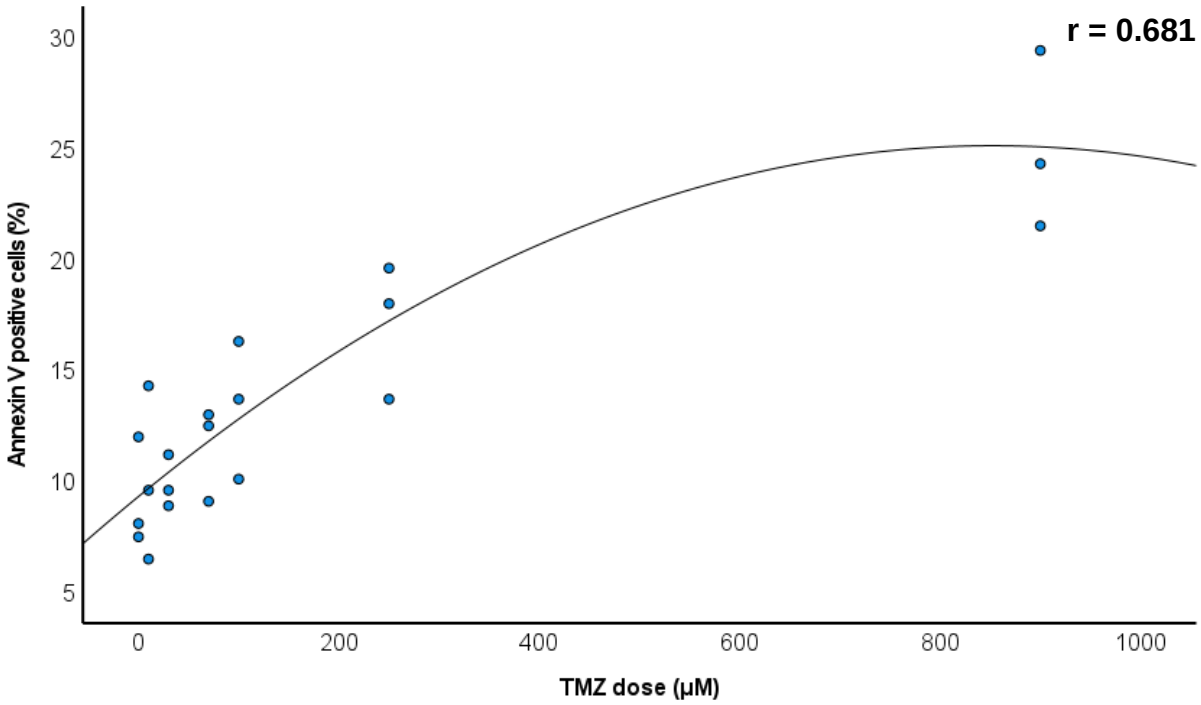

Figure 7. Correlation between Annexin V positive cells and TMZ dose.

TK6 cells were treated with DMSO and a range of TMZ doses for 1 h. Samples were collected 24 h post-exposure, probed with Annexin V-FITC and analysed with flow cytometry. Kendall's tau-b correlation demonstrates a significant non-linear positive association between Annexin V positive cells and TMZ dose. Data represents individual samples of three (**n = 3**) biological repeats.

1.3.3. Assessing the influence of time after TMZ treatment on cell cycle distribution and apoptosis

To determine the influence of TMZ treatment on TK6 cell fate at 4 h, 18 h, and 36 h post-exposure, cell cycle analysis (**Fig. 8**) and annexin V analysis (**Fig. 9**) was performed using flow cytometry. The overall cell cycle distribution at 4 h was comparable between 30TMZ and 900TMZ, only showing a slightly, but significantly, increased (**$p = 0.012$**) S-phase accumulation among 900TMZ-treated cells. At 18 h post-exposure, 900TMZ-treated cells exhibited a significant reduction (**$p < 0.001$**) in the G_1-phase when compared to that of 30TMZ-treated cells. In contrast, there were significantly more (**$p = 0.026$**) G_1-phase cells among 900TMZ-treated cells 36 h post-exposure when compared to that of 30TMZ-treated cells. However, at the same time-point, the G_2 fraction of 900TMZ-treated cells was significantly decreased (**$p = 0.035$**) when compared to that of time-matched 30TMZ-treated cells. Of note, these differential responses to 30TMZ and 900TMZ resulted in 30TMZ-treated cells having a cell cycle distribution that was inverse to that observed among DMSO-treated cells, in terms of G_1 and G_2 fractions, 36 h post-exposure.

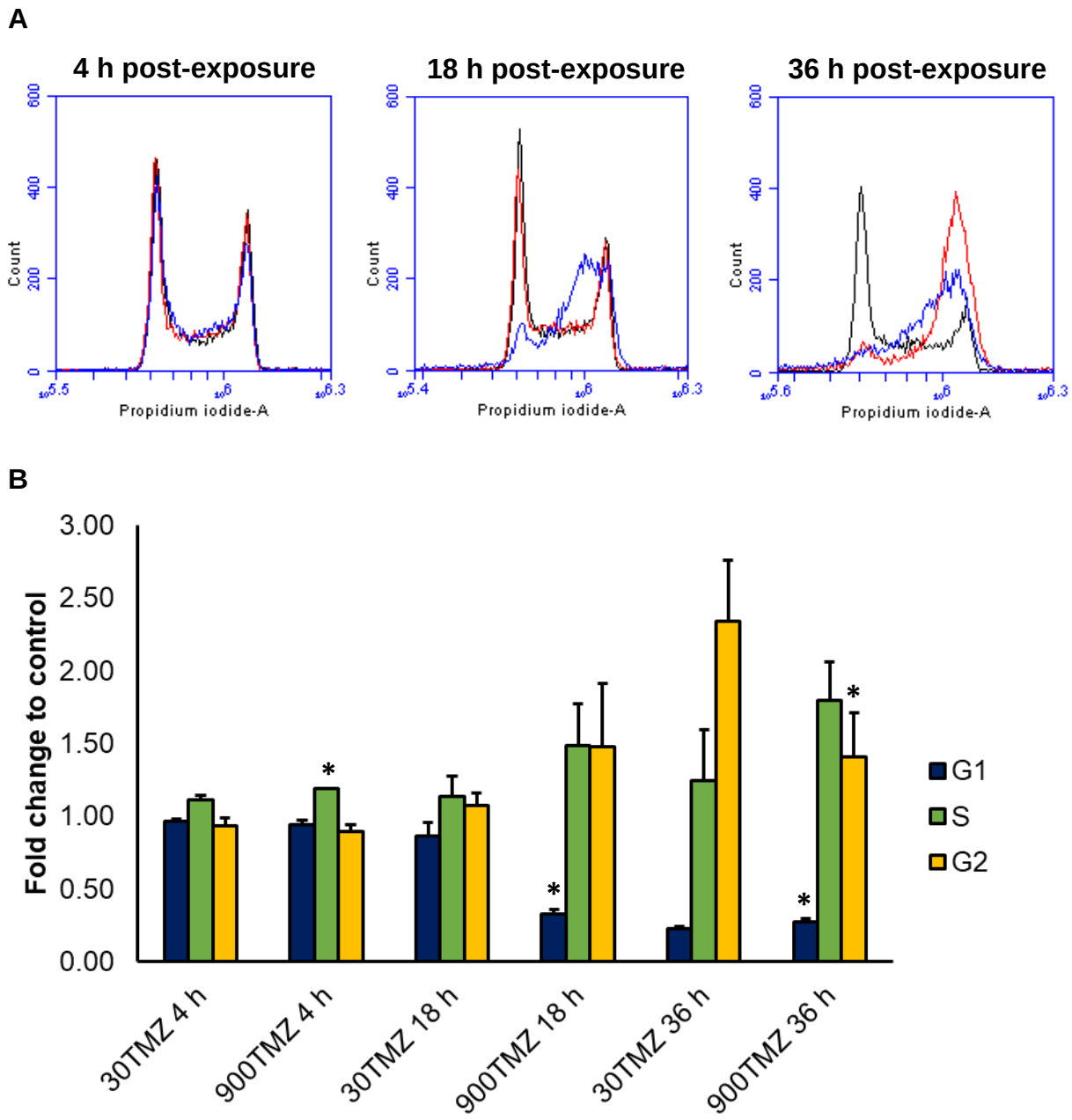

Figure 8. Cell cycle distribution of TK6 cells post-exposure to TMZ.

TK6 cells were sampled 4 h, 18 h, and 36 h post-exposure to TMZ, and 2 – 3 x 10^5 cells were used for flow cytometry. At least 5000 single cells were analysed for each sample. Histograms (**A**) illustrate the cell cycle distribution of DMSO (**black**), 30TMZ (**red**), and 900TMZ (**blue**) treated cells at respective time-points. There is a notable shift from G_1 fraction to G_2 among TMZ-treated cells over time, with 900TMZ-treated cells having faster kinetics to this effect (**A** and **B**). Moreover, the G_2 fraction of 900TMZ-treated cells 36 h post-exposure is significantly less compared to time-matched 30TMZ-treated cells. Normality was assessed with Shapiro-Wilk test while mean differences between cell cycle phases (G_1, S, and G_2) of 30TMZ and 900TMZ were assessed for statistical significance using an independent sample t-test. * Indicates statistical significance ($p < 0.05$) and is based on time-matched comparisons between 900TMZ and 30TMZ. Data is representative of three (**n = 3**) biological repeats. Data represents mean + SD (error bars).

As with cell cycle distribution, a similar level of apoptosis between 30TMZ and 900TMZ was observed 4 h post-exposure. However, a significant difference was observed 18 h (**p = 0.035**) and 36 h (**p = 0.021**) post-exposure, between 30TMZ-, and 900TMZ-treated cells. Notably, when comparing 30TMZ 4 h post-exposure to those 36 h, no significant difference (**p = 0.342**) was observed in the apoptotic fraction. However, the same comparison among 900TMZ-treated cells revealed a significant increase (**p = 0.014**) in apoptotic cells 36 h post-exposure.

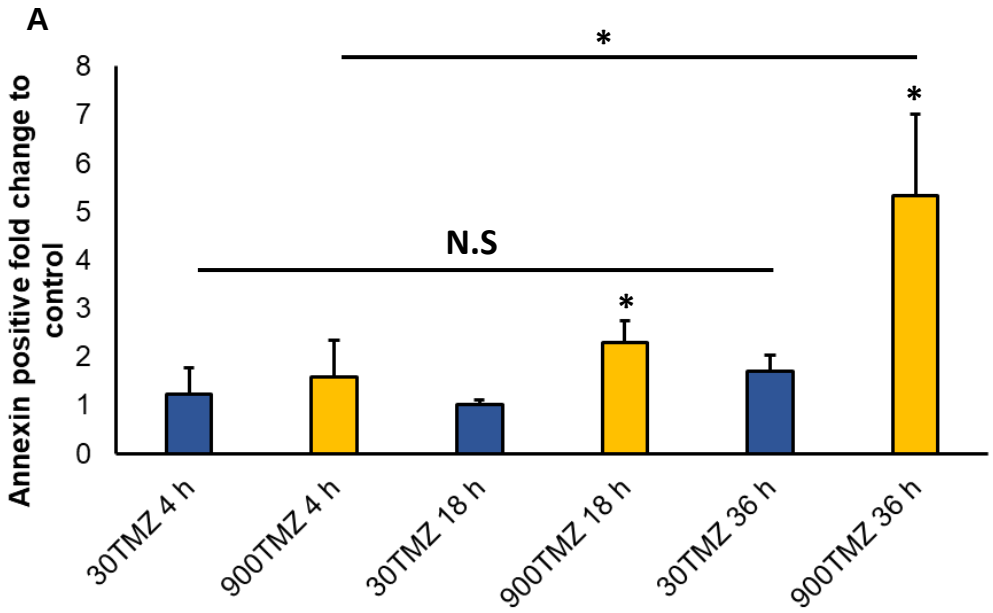

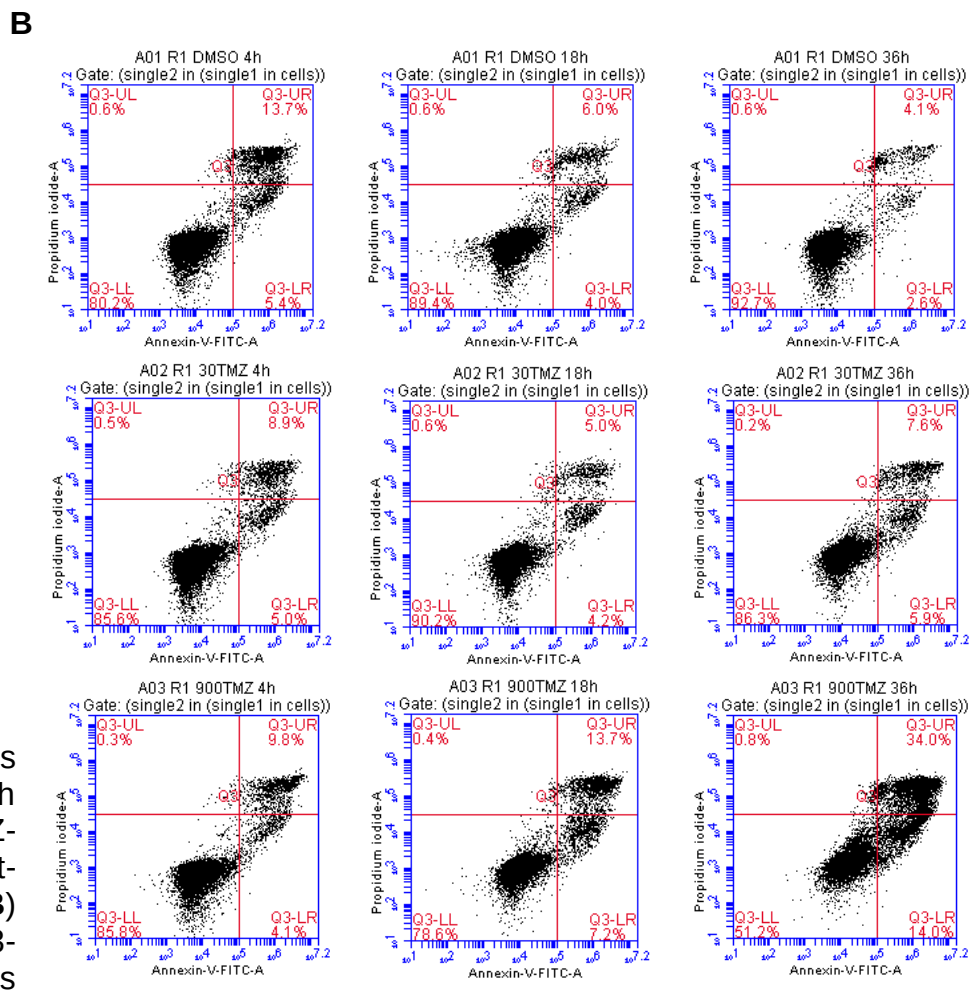

Figure 9. Apoptosis of TK6 cells at different times post-exposure to TMZ.

TK6 cells were sampled 4 h, 18 h, and 36 h post-exposure to TMZ, and 3 x 10^5 cells were used for flow cytometry. At least 10000 single cells were analysed for each sample. Overall, cell viability remains comparable between DMSO-, and 30TMZ-treated cells over time, while that of 900TMZ markedly declines after 18 h post-exposure with a reciprocal increase in the apoptotic fraction (**A** and **B**). Images (**B**) illustrate the gating strategy for determining annexin V positive cells (Q3-UR + Q3-LR) among DMSO or TMZ-treated cells at respective time-points. Q3-LL represents the surviving fraction while Q3-UL is indicative of debris or necrotic cell death. Normality was assessed with Shapiro-Wilk test while mean differences between the proportion of annexin V positive cells of time-matched 30TMZ and 900TMZ samples were assessed for statistical significance using an independent sample t-test. One-way ANOVA with Tukey's post-hoc test was used to test for any mean differences within 30TMZ-, and 900TMZ-treated groups respectively. * Indicates statistical significance ($p < 0.05$). * With connecting line shows specific statistically significant ($p < 0.05$) comparisons. Data is representative of three (**n = 3**) biological repeats. Data represents mean + SD (error bars). N.S. (not significant).

1.3.4. Assessment of DDR proteins 4 h, 18 h, and 36 h post-exposure to 30TMZ and 900TMZ doses.

To determine if 30TMZ and 900TMZ treatment results in differential DDR responses, key DDR proteins were quantified by immunoblotting (**Fig. 10**). Given the doubling time of TK6 cells (12 - 18 h) and the requirement of two replicative cycles for TMZ-induced damage to fully manifest, DDR proteins were assessed at 4 h, 18 h, 36 h post-exposure to TMZ. All DDR proteins assessed followed similar dynamics, that is, an increase in protein levels with increased time post-TMZ exposure. This was specifically apparent among 900TMZ-treated cells that showed significantly increased protein levels at most time-points when compared with 30TMZ-treated cells (**Table 3**). Specifically, 36 h post-exposure, 900TMZ-treated cells had significantly greater levels of all DDR proteins (pATR, γH2Ax, pChk1, pChk2, and p53) measured. Similarly, at 4 h and 18 h post-exposure, 900TMZ-treated cells had significantly greater DDR protein levels for all proteins, except γH2Ax (4 h) and pChk2 (18 h) as compared to time-matched 30TMZ-treated cells. Overall, γH2Ax and pChk1 appear to be the most responsive to TMZ, showing the largest fold increases over time. Specifically, γH2Ax levels among 900TMZ-treated cells were elevated 14.8-fold, 18 h post-exposure as compared to DMSO, whereas that of 30TMZ-treated cells was elevated 1.9-fold. Moreover, 36 h post-exposure, γH2Ax levels among 900TMZ-treated cells further increased to 32.3-fold, whereas that of 30TMZ-treated cells increased to 12.5-fold. Similarly, the levels of pChk1 was elevated 21.1-fold for 900TMZ-treated cells, whereas that of 30TMZ-treated cells was elevated 3.3-fold, as compared to DMSO controls 36 h post-exposure. Of note, 4 h post-exposure, pChk1 levels were elevated 6.1-fold among 900TMZ-treated cells whereas that of 30TMZ-treated cells was elevated 1.8-fold. Among all proteins tested, this is the highest, early (4 h post-exposure), observed increase in protein levels.

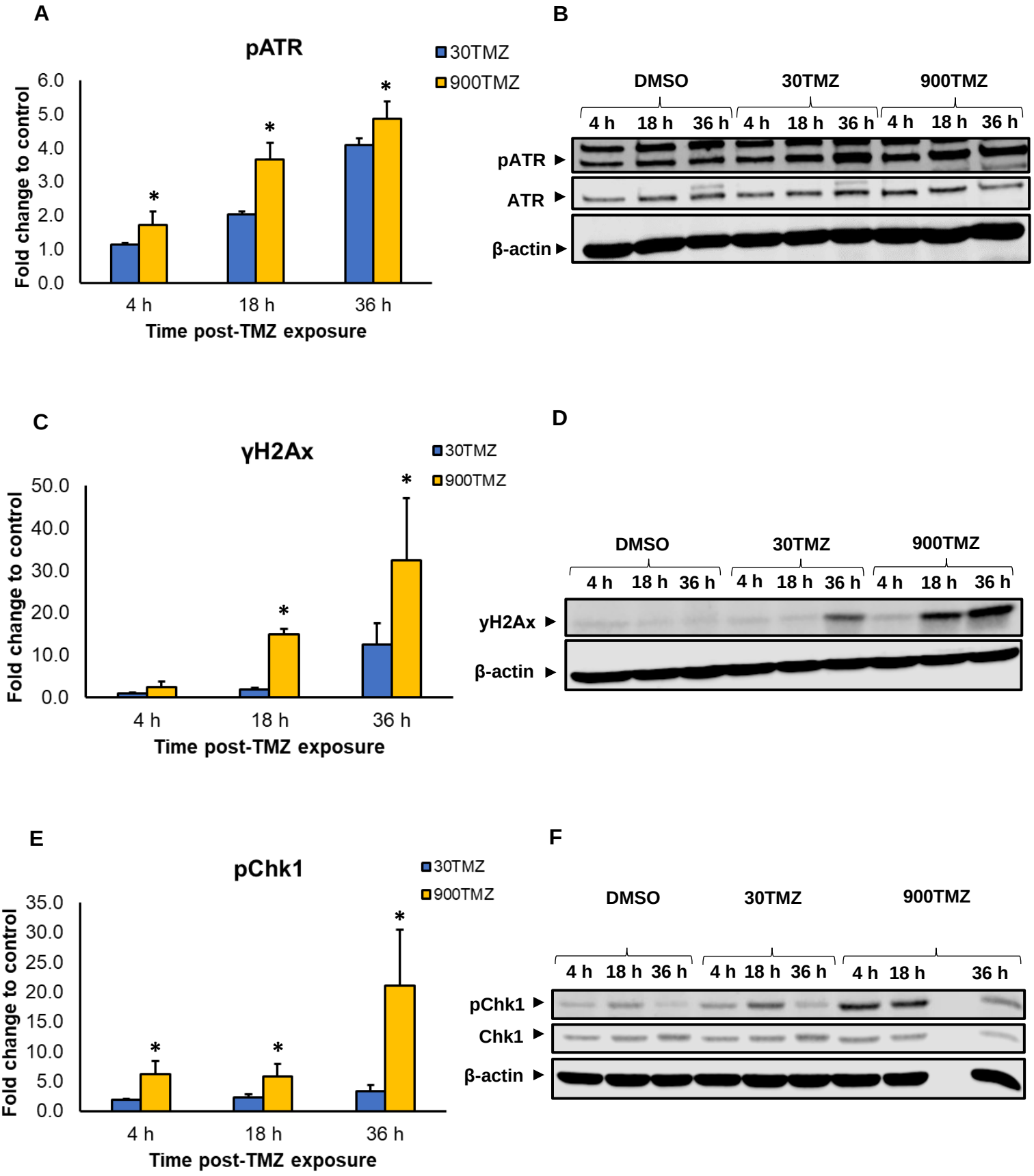
A
pATR
30TMZ
900TMZ
Fold change to control
6.0
5.0
4.0
3.0
2.0
1.0
0.0
4 h
18 h
36 h
Time post-TMZ exposure
B
DMSO
30TMZ
900TMZ
4 h 18 h 36 h 4 h 18 h 36 h 4 h 18 h 36 h
pATR
ATR
β-actin
C
γH2Ax
30TMZ
900TMZ
Fold change to control
50.0
40.0
30.0
20.0
10.0
0.0
4 h
18 h
36 h
Time post-TMZ exposure
D
DMSO
30TMZ
900TMZ
4 h 18 h 36 h 4 h 18 h 36 h 4 h 18 h 36 h
γH2Ax
β-actin
E
pChk1
30TMZ
900TMZ
Fold change to control
35.0
30.0
25.0
20.0
15.0
10.0
5.0
0.0
4 h
18 h
36 h
Time post-TMZ exposure
F
DMSO
30TMZ
900TMZ
4 h 18 h 36 h 4 h 18 h 36 h 4 h 18 h 36 h
pChk1
Chk1
β-actin

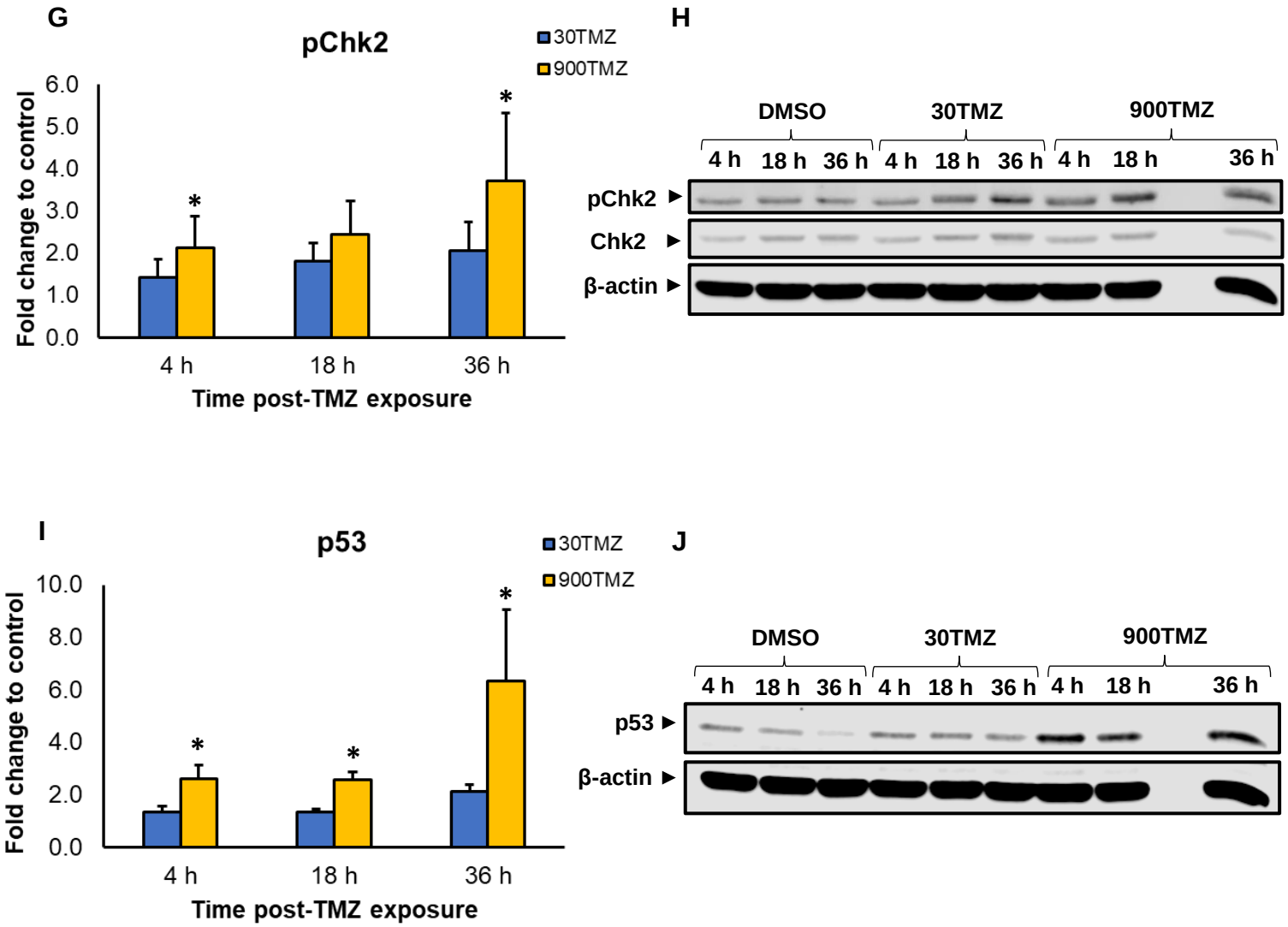

Figure 10. DDR protein profile following TMZ treatment.

Phosphorylated and total protein levels of key DDR proteins were analysed by immunoblotting. TK6 cells were sampled 4 h, 18 h, and 36 h post-exposure to TMZ, protein extracted, and 10 - 50 µg protein was used for immunoblotting. In response to TMZ, all protein levels increased over time, with the most significant increases observed 36 h post-exposure to 900TMZ (**A** – **J**). The most TMZ-responsive proteins appear to be γH2Ax (**C** and **D**) and pChk1 (**E** and **F**) based on the magnitude of protein elevation post-exposure. Normality was assessed with Shapiro-Wilk test while mean differences between time-matched 30TMZ and 900TMZ samples were assessed for statistical significance using an independent sample t-test. ***** Indicates statistical significance ($p < 0.05$). Data is representative of at least five (**n = 5**) biological repeats. Data represents mean + SD (error bars).

Table 3. P-values for comparison of time-matched control normalised protein levels between 30TMZ-, and 900TMZ-treated cells

	Time post-exposure to TMZ		
	4 h	**18 h**	**36 h**
pATR	0.008	<0.001	0.003
γH2Ax	0.052	<0.001	0.037
pChk1	<0.001	<0.001	0.001
pChk2	0.048	0.09	0.035
p53	<0.001	<0.001	0.013

1.4. Discussion

Human cells are in a constant state of genotoxicity from endogenous and exogenous sources (Auten and Davies, 2009; Jenkins *et al*., 2010; Tubbs and Nussenzweig, 2017). DNA damage events perceived by cells need to be dealt with to maintain genomic stability and DNA replicative fidelity (Tubbs and Nussenzweig, 2017). Depending on the type and amount DNA damage, a cell can either undergo cell cycle arrest and repair the damage, or initiate apoptosis if the damage is substantial and exceeds its repair capabilities (Surova and Zhivotovsky, 2013). The 'decision' to undergo either cell cycle arrest/DNA repair or commit to apoptosis implies the existence of specific molecular cues that remains enigmatic. This underpins the rationale for this thesis in which sub-lethal (30 μM) and lethal (900 μM) TMZ doses were determined empirically at specific time-points, at which the magnitude of the DDR between these doses differed significantly.

Recall that TMZ-induced DNA damage predominantly comprises *N*3-meA, *N*7-meG, and O^6-meG adduct formation, with O^6-meG being the most detrimental given the limited availability of the suicide enzyme, MGMT, that resolves O^6-meG lesions (Kaina *et al*., 2007; Gouws and Pretorius, 2011; Fan *et al*., 2013; Strobel *et al*., 2019). Thus, when O^6-meG lesions exceed the available MGMT, the lesions remain unrepaired and eventually form DSBs which is the most detrimental form of DNA damage (Trenner and Sartori, 2019). How, exactly, O^6-meG adducts result in DSBs remain a topic of debate, but a popular hypothesis is the MMR futile cycle. The MMR futile cycle is believed to occur when O^6-meG is mistakenly read as adenine by DNA polymerase, thus pairing it with thymine. This thymine then becomes recognised by MMR machinery as a mispaired base and is removed. However, since the actual O^6-meG lesion is not repaired, thymine is reinserted, thus facilitating the futile cycle. The continuous cycling

of MMR leads to the accumulation of SSBs, which eventually give rise to DSBs, though, the exact underlying mechanism that results in DSB formation is unclear (York and Modrich, 2006; Mojas, Lopes, and Jiricny, 2007; De Zio, Cianfanelli, and Cecconi, 2013; Fuchs *et al*., 2021).

The ability of TMZ to induce DSBs was exemplified in this study by the detection of a dose-dependent increase in γH2Ax foci in TK6 cells (**Figs. 3** and **4**). Interestingly, only 900TMZ resulted in a significant increase in foci when compared to the DMSO control, 24 h post-exposure. In line with the observed γH2Ax response, analysis of apoptotic levels revealed that only 250TMZ and 900TMZ were able to significantly induce apoptosis 24 h post-exposure, whereas lower doses did not, when compared to DMSO controls (**Fig. 6**). As well as supporting the use of 30TMZ as a sub-lethal dose, this observation also alludes to the existence of DNA damage thresholds within TK6 cells. Traditionally, a linear no-threshold (LNT) model has been assumed regarding genotoxic compounds and DNA damage induction. Specifically, the linear model theorises that there is no lower limit to increased genotoxicity above cellular background levels, but rather that the amount of DNA damage increases linearly with genotoxic dose (Jenkins *et al*., 2010). Consequently, a linear relationship between DNA damage and cell fate is also implied. While a significant positive association was observed between γH2Ax foci formation and TMZ dose, and likewise, apoptosis and TMZ dose (**Figs. 5** and **7**), these associations are not apparently linear. Moreover, when assessing the average apoptosis levels from our dose-response curve (**Fig. 6**), a seemingly plateaued response up to 30TMZ is observed which does not fit with the LNT model. Admittedly, it could be argued that the disparity between the highest TMZ doses (250TMZ and 900TMZ) caused an inherent skewness in the data distribution. However, this does not account for the aforementioned plateaued response. It is possible that an apoptotic cell

fate was yet to occur for doses of 30TMZ or lower. This has been observed in low dose irradiated leukaemia cells among which the apoptotic fraction did not differ significantly from untreated controls 24 h post-exposure, but did increase significantly 48 h post-exposure (Xin *et al*., 2014). While this poses a scenario in which cell fate deteriorates over-time, it is also important to consider DNA damage resolution over time. This is demonstrated by Speidel, Helmbold, and Deppert (2006) that observed murine fibroblasts to undergo temporary cell cycle perturbations within 11 h following 'low dose' UV or γ-irradiation, but homeostasis was restored within 68 h following treatment. Contrarily, 'high dose' UV exposure resulted in apoptosis 24 h - 30 h post-exposure, as indicated by increased cleaved caspase-3 protein and sub-G_1 levels, and 68 h post-exposure most cells were apoptotic. Considering these studies, the impact of both *time* and *dose* shifts into focus and could be determining factors in cell fate. Another consideration is that at 30TMZ (or lower), resulting DNA damage lesions do not saturate endogenous DNA repair mechanisms, and thus the damage is tolerated, or genotoxicity from specific TMZ-induced lesions is yet to manifest (discussed later). Nonetheless, the observed plateaued response until 30TMZ either indicates DNA repair in effect, damage resolution, or a delay in cell fate decision making, all of which leans in favour of the existence of thresholds and different mechanisms that allows a differential response depending on the extent of DNA damage (Kaina *et al*., 2021).

Notwithstanding our observations (**Figs. 5 - 7**), the LNT model is increasingly being challenged (Jenkins *et al*., 2010; Kaina *et al*., 2021). To consolidate our observations in context of a non-linear dose-response, we sought to determine if γH2Ax foci formation and apoptosis levels were correlated (**Appendix B**), based on the premise that if the LNT model held true in our experimental setup, it is reasonable to expect a linear relationship. Indeed, increased γH2Ax foci formation showed a significant positive

correlation to apoptosis levels, while decreased γH2Ax foci accumulation had a significant negative correlation to apoptosis levels. However, these correlations are not apparently linear. In fact, these correlations are more reminiscent of a polynomial distribution. Specifically, the initial percentage of annexin V positive cells and γH2Ax positive cells appears approximately stable, with a noticeable incline only apparent beyond 40% γH2Ax positive cells. Admittedly, the nature of this data does not lend itself to this type of correlation, and thus, conclusions are tentative. Nevertheless, the collective data may be indicative of the existence of a DNA damage threshold in TK6 cells.

Furthermore, the distribution of γH2Ax foci is telling. For example, despite having been part of the exact same cellular population and having been exposed to the same concentration of TMZ, individual cells did not respond unilaterally in γH2Ax foci accumulation (**Fig. 4**). Using 30TMZ-treated cells (**Fig. 4B**) as an example, it is particularly apparent in that frame of view where 40% - 50% of cells are considered γH2Ax negative, while others are clearly γH2Ax positive. Moreover, even among those that are γH2Ax positive, there are clear differences in the amount of γH2Ax accumulation. As cell cycles are not naturally synchronised it is plausible that the graded response to TMZ is contingent on cells being in different stages of the cell cycle, and thus, TMZ induced DNA damage may be detected sooner for some cells than others. Moreover, depending on the current phase a cell resides in, different DNA repair mechanisms may be in operation (Vindigni and Gonzalo, 2013; Chatterjee and Walker, 2017). For example, homologous recombination is known to function during S-, and G_2-phases, but not G_1, due to a requirement for sister chromatids as a repair template (Fugger and West, 2016). Moreover, certain BER enzymes have been reported to have higher activity in G_1, compared to G_2 of cervical cancer cells (Chaudhry, 2007).

Additionally, this activity was enhanced following γ-irradiation. Incidentally, the majority of TMZ-induced lesions are repaired by BER (Zhang, Stevens, and Bradshaw, 2012). Thus, it is clear how cell cycle dependent DNA repair can influence the response of TK6 cells to TMZ. It is also tempting to speculate that an internal 'dose-response' occurs that depends on the bio-, and physicochemical interactions between TMZ and the dynamic cellular culture environment. A simplistic representation of this would be physical exposure of TK6 cells to TMZ. TK6 cells are suspension cells and thus their localisation in culture is dynamic and may influence the degree of TMZ exposure. For example, if cells settle in one area more densely than others, it stands to reason that underlying cells may be less exposed to TMZ. This may also bring about concentration gradients, altering the rate that TMZ enters certain cells. This is especially possible for TMZ as it does not require specialised transport machinery to enter cells, but rather enters by passive diffusion (Zhou and Gallo, 2009).

To explore the possibility that time might be a critical factor in determining the cellular response to DNA damage, analyses were performed 4 h, 18 h, and 36 h post-exposure to TMZ. This provides a wide time-frame to observe any shift in cell fate or DDR protein dynamics, along with allowing at least two replicative cycles for TMZ-induced damage to manifest, as is suggested for TMZ (Quiros, Roos, and Kaina, 2010). DNA content analysis showed distinct changes in cell cycle distribution at 18 h and 36 h post-exposure when comparing 30TMZ and 900TMZ. Specifically, at 18 h post-exposure, 900TMZ-treated cells exhibited a significantly decreased G_1-phase fraction as compared with its 30TMZ-treated counterpart. Moreover, 36 h post-exposure, 900TMZ-treated cells had a significantly increased G_1-phase fraction along with a decreased G_2-phase fraction when compared to its respective 30TMZ counterparts (**Fig. 8**). Interestingly, given the overall similar distribution between 30TMZ and 900TMZ 4 h

post-exposure, and 30TMZ-treated cells, 18 h post-exposure, identifies 18 h as a point of departure for 900TMZ-treated cells given its noticeably altered cell cycle distribution as compared to time-matched, 30TMZ-treated cells. However, this does not exclude the possibility that this departure could have initiated between 4 h - 18 h post-exposure. Overall, the effect of TMZ treatment on cell cycle distribution can be summarised by fewer cells in the G_1-phase and an accumulation of cells in S-, and G_2-phases. The ability of TMZ to induce G_2/M arrest has been described (Hirose, Berger, and Pieper, 2001; Caporali *et al*., 2004). For example, Caporali *et al*. demonstrated G_2/M arrest in TK6 and U2OS (osteosarcoma) cells following 12.5 μM and 25 μM TMZ treatment respectively. Compared with our observations 36 h post-30TMZ exposure, the magnitude of their time-matched TK6 cell cycle perturbations after TMZ exposure appear less prominent. Nonetheless, a comparable pattern in cell cycle perturbations was observed pertaining to a decreased number of cells in G_1-phase and increased S-phase accumulation 36 h following TMZ exposure. However, there was little evidence of G_2 accumulation. These differences are likely due to the difference in TMZ dose used (12.5 μM vs. 30 μM). However, U2OS cells sampled 48 h after 25 μM TMZ treatment showed a level of G_2/M arrest comparable to our own, 36 h after 30TMZ treatment. Regarding the disparity in cell cycle distribution between 30TMZ-, and 900TMZ-treated cells, it is likely that both doses initially followed the same damage response as evidenced by similar cell cycle distributions 4 h post-exposure, after which the response kinetics for 900TMZ was more expeditious, causing the divergence in cell cycle distribution observed between 30TMZ and 900TMZ at 18 h post-exposure. This assertion is supported by the overall similarity in cell cycle distribution of 30TMZ-treated cells 36 h post-exposure when compared with 900TMZ-treated cells 18 h post-exposure. Finally, 36 h post-exposure to TMZ, 900TMZ-treated cells showed a

significantly decreased number of cells in G_2-phase when compared with 30TMZ-treated cells. Additionally, the number of G_1-phase cells among 900TMZ-treated cells were significantly greater when compared with 30TMZ-treated cells, however, this was likely a consequence of the significantly reduced cells in G_2-phase. This disparity is possibly the result of 30TMZ preferentially causing G_2/M arrest as opposed to apoptosis, whereas the reverse is true for 900TMZ. This is supported by the significantly greater proportion of apoptotic cells among 900TMZ-treated cells when compared to 30TMZ-treated cells, 36 h post-exposure, as will be described hereafter (**Fig. 9**).

Measuring the apoptotic response following TMZ exposure revealed a significantly greater proportion of apoptotic cells among 900TMZ-treated cells when compared to 30TMZ-treated cells at 18 h and 36 h post-exposure (**Fig. 9**). Importantly, when comparing changes in apoptotic fractions within 30TMZ and 900TMZ groups respectively, no significant changes were observed between 4 h and 36 h post-exposure among 30TMZ-treated cells, while 900TMZ-treated cells showed as statistically significant increase 36 h post-exposure when compared to those 4 h post-exposure. This confirms that 30TMZ remains preferentially sub-lethal throughout the experimental time-frame, while 900TMZ becomes lethal. Note that our classification of a 'sub-lethal' dose is one that preferentially results in G_2 arrest in response to TMZ, whereas a 'lethal' dose preferentially results in apoptosis.

The underlying cause of the differential responses to apoptosis and cell cycle distribution between 30TMZ-, and 900TMZ-treated cells may be the result of different TMZ-induced adducts. Recall that TMZ causes *N*3-meA, *N*7-meG, and O^6-meG adducts. *N*3-meA and *N*7-meG constitutes the bulk of TMZ-induced adducts but are rapidly repaired by BER (Zhang, Stevens, and Bradshaw, 2012), and thus, is not the likely cause of the observed G_2/M arrest following TMZ treatment, especially not 36 h

post-exposure. Nonetheless, these adducts may contribute to an apoptotic cell fate in DNA repair defective cells, or if sufficiently high levels of adducts are present that could disrupt the replisome, ultimately causing DSBs (Roos and Kaina, 2013). In fact, it has been reported that BER intermediates drive DSB formation by interfering with replication (Ensminger *et al*., 2014). Thus, it is possible that for 900TMZ-treated cells, BER-dependent DNA lesions is sufficiently abundant to disrupt the replisome and promote DSB formation, thus contributing to apoptosis. However, in most instances, O^6-meG is considered the most genotoxic lesion (Kaina *et al*., 2007; Quiros, Roos, and Kaina, 2010). This is especially true for cells, like TK6, that are deficient in MGMT (Chapman, Doak, and Jenkins, 2015; Lorge *et al*., 2016), the enzyme responsible for O^6-meG repair (Goldmacher, Cuzick Jr, and Thilly, 1986; Kaina *et al*., 2007). O^6-meG has been reported to require at least two replicative cycles for genotoxicity to manifest (Quiros, Roos, and Kaina, 2010). This has been attributed to the MMR-futile cycle that resolves the O^6-meG:T mispair, however, since the lesion itself is not repaired, the O^6-meG:T mispair reforms during the second replicative cycle post-exposure to the methylating agent. This futile attempt continuously produce SSBs as a DNA repair intermediate and causes replisome uncoupling, which can lead to replication fork collapse and subsequent DSB formation (De Zio, Cianfanelli, Cecconi, 2013; Li, Pearlman, and Hsieh, 2016). Moreover, based on observations in Chinese hamster ovarian cells (CHO-9), apoptosis following a toxic dose (10 μM) treatment with *N*-methyl-*N*-nitro-*N*-nitrosoguanidine (MNNG), that also produces O^6-meG, occurs out of the G_2/M-phase (Quiros, Roos, and Kaina, 2010). The same study also showed that MGMT-transfected CHO-9 cells did not result in G_2/M arrest following MNNG treatment, as was observed for untransfected CHO-9 cells. This suggests O^6-meG as the driving force for both G_2/M arrest and apoptosis. In relation to our own findings, this implies that the G_2/M arrest

and subsequent apoptosis observed following TMZ exposure is predominantly caused by O^6-meG. This could explain why the level of apoptosis was significantly greater while the G_2-phase fraction was significantly less in 900TMZ-treated cells when compared to 30TMZ-treated cells. Specifically, it is likely that at 30TMZ the accumulating O^6-meG lesions are much less than in 900TMZ-treated cells, in which the propensity for DSB formation would be higher given an excessive amount of SSBs, forming as a consequence of MMR futile cycling. Therefore, it is reasonable to assume that at 36 h post-exposure, 30TMZ-treated cells were arresting in G_2/M but did not yet accumulate sufficient DNA damage to induce a predominantly apoptotic cell fate, whereas in 900TMZ-treated cells, G_2/M arrest already began 18 h post-exposure and rapidly transitioned to an apoptotic cell fate, giving rise to an apparently stifled G_2/M arrest when compared to 30TMZ-treated cells. Interestingly, these observations suggest that TK6 cells are able to tolerate O^6-meG lesions associated with 30TMZ, despite being MGMT deficient, for at least 36 h post-exposure. Moreover, while our observations for 30TMZ-treated cells are in agreement with those of Quiros, Roos, and Kaina in terms of the time-frame associated with O^6-meG DNA damage manifestation, observations for 900TMZ-treated cells are disparate. Specifically, the authors suggest the second replicative cycle to be a key node in the response to O^6-meG. However, we observed a significant increase in apoptosis among 900TMZ-treated cells, 18 h post-exposure when compared with 30TMZ-treated cells. Given the replication time of TK6 cells (12-18 h), this would, at the latest, place these cells within the early to mid-second replicative cycle post-exposure to TMZ. Admittedly, the authors benefitted from using a synchronised cell system that would provide a more accurate timed response to genotoxic insult, whereas our cells were unsynchronised.

It is clear that TK6 cells exposed to different TMZ doses exhibit different responses. Thus, the question becomes, what mechanism drives this differential response to sub-lethal and lethal TMZ doses? To address this question, the level of key DDR proteins were analysed (**Fig. 10**). DDR proteins assessed were pATR (thr1989), γH2Ax (ser139), pChk1 (ser345), pChk2 (thr68), and p53. Our results showed that for most comparisons between 900TMZ-, and 30TMZ-treated cells, 900TMZ-treated cells resulted in a significantly greater elevation of DDR protein levels (**Table 3**). This was particularly true at 36 h post-exposure. A similar pattern was observed at 4 h and 18 h post-exposure, except for γH2Ax (4 h) and pChk2 (18 h) that were not significantly different when comparing 30TMZ-, and 900TMZ-treated cells. These observations are supported by that of Eich *et al*. (2013) that predominantly ascribes the effects of TMZ on cell fate to ATR-γH2Ax-Chk1 signalling in glioblastoma and melanoma cell lines. Our results extend these observations to TK6 cells and provides insight into earlier DDR kinetics (4 h, 18 h, 36 h) at both sub-lethal (30TMZ) and lethal (900TMZ) doses, as their observations were typically 48 h (and beyond) post-exposure to 100 μM TMZ. Moreover, the authors determined γH2Ax foci formation to be ATR-dependent based on observations made 48 h following 1 μM TMZ exposure in glioblastoma cells in which ATM or ATR was selectively knocked down. While this might have been appropriate for their experimental setting, our findings provide a direct time-, and dose-matched comparison of γH2Ax levels in the context of ATR signalling. Interestingly, while the processing of O^6-meG adducts into DSBs have been reported to require two replicative cycles, presumably to allow sufficient time for MMR futile cycling to precipitate O^6-meG:T mispairs to DSBs (Kaina, Margison, and Christmann, 2010; Quiros, Roos, and Kaina, 2010), we observed a significant increase in γH2Ax among 900TMZ-treated cells when compared to 30TMZ-treated cells, 18 h post-exposure, at which time, TK6 cells

are unlikely to have progressed beyond the mid-second replicative cycle. This calls into question the previously proposed two replication cycle requirement, and perhaps even the involvement of MMR in TMZ induced genotoxicity, at least at this early time-point. Admittedly, γH2Ax accumulation was more pronounced at the later time-point (36 h), though, the question remains, if not by MMR futile cycling, what causes early γH2Ax accumulation? One possible explanation is that the initial *N*7-meG and *N*3-meA lesions formed are sufficiently abundant in 900TMZ-treated cells, and this floods the DNA repair system causing considerable accumulation of SSBs as a by-product of BER. Consequently, this could progress to DSB formation (Caldecott, 2003; Ensminger *et al*., 2014). It is not unreasonable to expect that such an increase in DSBs would correspond with an increase in apoptosis. Indeed, the level of apoptosis among 900TMZ-treated cells were significantly increased when compared with 30TMZ-treated cells 18 h post-exposure.

While our observations support other studies that identify ATR signalling as a key DDR component of alkylating agent-induced DNA damage (Quiros, Roos, and Kaina, 2010; Noonan *et al*., 2012; Ito *et al*., 2013), it is curious that pChk2 appears to have a subordinate role compared to pChk1. This assertion is based not only on the fact that pChk1 was consistently significantly elevated among 900TMZ-treated cells, whereas for pChk2, this was only true at 4 h and 36 h post-exposure as compared to 30TMZ-treated cells; but also, on the difference in order of magnitude between pChk1 and pChk2 levels that clearly favours pChk1 as the dominant signal transducer. This was particularly apparent 36 h post-exposure among 900TMZ-treated cells (**Fig. 10**). On one hand, these results could imply that pChk2 is not a critical component in effecting different TMZ-induced cell fates, at least not to the same extent as pChk1. On the other hand, it is possible that pChk2 might be a more kinetically active signal transducer than pChk1

and does not require the same level as pChk1. Alternatively, pChk1 and pChk2 may function in a tissue-specific manner. It has recently been shown that Chk1 is more active in primary lung cells than breast cells, whereas the reverse was true for Chk2 (van Jaarsveld *et al*., 2020). Thus, it is possible that pChk1 may be more functionally active and have a greater involvement than pChk2 in effecting cell fates in TK6 cells. Analysis of apoptotic levels supports the latter assertion as 900TMZ-treated cells showed significantly increased levels of apoptosis compared to 30TMZ-treated cells at both 18 h and 36 h post-exposure. Consequently, if pChk2 contributed toward this cell fate, it is not unreasonable to expect a proportional elevation in its levels at both these time-points, as opposed to only 36 h, as was observed for all other proteins measured (**Fig. 10; Table 3**). Taken together, these observations partly contrast those of Noonan *et al*. (2012) that demonstrated Chk1 and Chk2 to have comparable kinetics in TK6 cells in response to 0.1 µg/mL MNNG (high dose) or 0.01 µg/mL MNNG (low dose). Specifically, the magnitude of increasing Chk2 kinase activity between 20 h - 36 h post-exposure was similar to that observed for pChk1 (ser317) when comparing high or low dose MNNG-treated cells, respectively. Collectively, this suggests a dose-, and time-dependent role for Chk2 that may be equipotent to Chk1 in response to MNNG, a role that cannot be reconciled with our observations, especially among 900TMZ-treated cells, using a similar acting alkylating agent, TMZ. Given the overall similarity in the adduct spectrum caused by TMZ and MNNG and considering that both rely on O^6-meG as the main genotoxic lesion, these are unlikely sources of the observed differences (Wyatt and Pittman, 2006; Klapacz *et al*., 2016; Strobel *et al*., 2019). Therefore, drug dose might underpin these differences. Specifically, it is tempting to speculate that unlike the observations by Noonan *et al*., the activity of pChk1 far exceeded that of pChk2 among 900TMZ-treated cells because this dose surpasses a stochastic

threshold that favours ATR over ATM signalling. Consequently, this might explain the predominant kinetics of pChk1 when compared to pChk2, as ATR preferentially activates Chk1 (Rundle *et al*., 2017). This is plausible given that MMR, which is known to function in response to O^6-meG, results in ATR-Chk1 activation (Yoshioka, Yoshioka, and Hsieh, 2006; Gupta *et al*., 2018). Furthermore, as Chk1 shares multiple downstream targets with Chk2, it is not unreasonable to assume functional redundance of Chk2 in this context, thus negating its activation (Bartek and Lukas, 2003). It is also worth considering that, although not to the same extent as pChk1, pChk2 levels were significantly increased 4 h and 36 h post-900TMZ exposure as compared with 30TMZ-treated cells. Thus, considering that pChk1 may be the dominant signal transducer in TK6 cells, and that pChk2 may be functionally redundant in this context, it is possible that this pChk2 elevation is a 'spill over' effect stemming from ATR activity, rather than directed functional activation, as ATR has been shown to phosphorylate Chk2 (Matsuoka *et al*., 2000; Wang *et al*., 2006). However, as the cumulative effect of different TMZ and MNNG doses used in our study and that of Noonan *et al*., respectively, cannot be compared directly, these suggestions remain speculative.

The importance of pChk1 activation is highlighted by Ito *et al*. (2013), suggesting pChk1 as an initial responder to TMZ-induced DNA damage. Specifically, the authors ascribe an early (3 h post-TMZ exposure) response by pChk1 to *N*3-meA and *N*7-meG lesions following glioblastoma cell exposure to 100 μM TMZ. Similarly, our observations show a 1.8-fold (30TMZ) and 6.1-fold (900TMZ) increase in pChk1 compared with DMSO controls, 4 h post-exposure. However, it should be noted that the authors relied on a 3 h treatment regime, whereas our TMZ exposures were only 1 h. The extended treatment time seems counterintuitive as TMZ only has a half-life of 1.8 h (Wesolowski, Rajdev, and Mukherji, 2010). Thus, the observations by Ito *et al*. would amount to 5 h post-

exposure, in context of our study. Therefore, combined with our usage of a sub-lethal dose (30TMZ), and observations as early as 4 h post-exposure, our findings emphasise the importance of pChk1 in response to TMZ and informs an earlier time-point, in TK6 cells. Nonetheless, the authors allude to *N*3-meA and *N*7-meG adducts being the pChk1 activating event, whereas O^6-meG sustains it. It is tempting to speculate that this adduct relay is what underpins the differential DDR observed between 30TMZ and 900TMZ. Specifically, the cumulative *N*3-meA and *N*7-meG burden among 900TMZ-treated cells likely exceeds that of 30TMZ-treated cells and would explain why lethally-treated TK6 cells showed elevated DDR kinetics at early time-points. Moreover, the overall O^6-meG burden among 900TMZ-treated cells also likely exceeds that of 30TMZ-treated cells, thus explaining the sustained and progressive DDR activation among 900TMZ-treated cells that exceeded that of 30TMZ-treated cells.

Given that p53 is stabilised by PTMs facilitated by upstream DDR kinases such as ATR, Chk1, and Chk2, it is not unexpected that the levels of p53 was significantly increased at every time-point among 900TMZ-treated cells, when compared to 30TMZ-treated cells. Notwithstanding the similar pattern of activation that can be followed from pATR-γH2Ax-pChk1-p53, the importance of p53 in response to TMZ has been described (Gupta, Sathishkumar, and Ahmed, 2010; Blough *et al*., 2011; He and Kaina, 2019). Specifically, both cell cycle arrest and apoptotic eventualities observed following TMZ exposure would, at least partly, be regulated by the transcriptional activities of p53 that effects these cell fates. For example, Gupta, Sathishkumar, and Ahmed (2010) demonstrated a stark reduction in apoptosis among p53 siRNA transfected pancreatic cancer cells 48 h post-exposure to 500 µM TMZ treatment.

Collectively, this chapter identifies 30TMZ and 900TMZ as sub-lethal and lethal doses, capable of preferentially inducing cell cycle arrest and apoptosis, respectively, within 36

h post-exposure. While these eventualities only became apparent 18 h post-exposure (depending on the dose), the DDR protein signalling that preceded it was evident from 4 h post-exposure. Specifically, intensity of pATR-γH2Ax-pChk1-p53 signalling appears to drive the differential response observed for 30TMZ and 900TMZ. However, it is not clear if/how this pathway facilitates cell fate to selectively diverge into cell cycle arrest or apoptosis, nor is it clear if the pathway itself is modulated by apical DNA damage responsive molecules to effect cell fate.

Chapter 2

Assessing miRNA expression at sub-lethal and lethal TMZ doses

2.1. Introduction

2.1.1. Overview

DDR protein interactions are physiologically complex and often convoluted by multifaceted cross-talk and/or ambivalent functions. The extensive cross-talk between DDR proteins emphasise the importance of understanding the dynamics of their regulation, as the regulation of specific proteins may influence other, seemingly functionally distinct proteins. In this regard, miRNAs may provide some insight. MiRNAs are small (≈ 20 nucleotides) non-coding RNA sequences that are known to function as regulators of gene expression (Ling, Fabbri, and Calin, 2013; Wang and Taniguchi, 2013). Specifically, miRNAs naturally exist to inhibit gene expression, and can be transcribed from its target mRNA as a natural antagonist (Gao *et al*. 2012; Wang and Taniguchi, 2013). For example, miR-338-3p has been demonstrated to inhibit its host gene, apoptosis-associated tyrosine kinase (AATK) in rat neuroblastoma cells (Kos *et al*., 2012). Thus, miRNAs are fitting candidates as potential molecular arbiters of a tightly regulated DDR, and cell fate.

2.1.2. MiRNA biogenesis

MiRNAs are embedded throughout the genome and can be intronic or intergenic. While intronic miRNAs are part of the intron portion of its host gene, and thus co-transcribed with it, intergenic miRNAs can be regarded ‘independent’ transcripts with its own promotor region (Hu and Gatti, 2011). MiRNAs are predominantly transcribed by RNA polymerase II (Lee *et al*., 2004), forming primary miRNA (pri-miRNA). The unique hairpin structure of pri-miRNA allows recognition by a microprocessor complex that cleaves pri-miRNA to form precursor miRNA (pre-miRNA). Main components of the microprocessor complex are the ribonuclease, DROSHA and its RNA-binding partner,

PASHA (Denli *et al*., 2004). Together, these can interact with, and cleave, pri-miRNA to pre-miRNA (Denli *et al*., 2004). Pre-miRNAs are transported from the nucleus to the cytoplasm by EXPORTIN-5 (XPO5). In the cytoplasm, pre-miRNA is further cleaved by another ribonuclease, DICER, to an ≈ 20 nucleotide duplex. This constitutes the mature miRNA that becomes integrated into the RNA-induced silencing complex (RISC). However, only one strand of the miRNA duplex becomes integrated (guide strand), while the other is digested (passenger strand). In its simplest form, RISC consists of mature miRNA and argonaute proteins (AGO) (Pratt and MacRae, 2009). Integrated miRNA is protected from digestion by AGO proteins and serves as a guide strand to seek out mRNA with complementarity to its 5' 'seed sequence' to facilitate translational inhibition or degradation (Feng *et al*. 2011; Hu and Gatti, 2011; Hermeking, 2012). The type of mRNA regulation is contingent on the degree of complementarity between the miRNA seed sequence and its target mRNA. While exact complementarity can result in AGO-mediated mRNA cleavage, partial complementarity is subject to translational inhibition (Höck and Meister, 2008) (**Fig. 11**). In this way, miRNAs can regulate gene expression either negatively, as previously mentioned, or positively, by inhibiting other inhibitors.

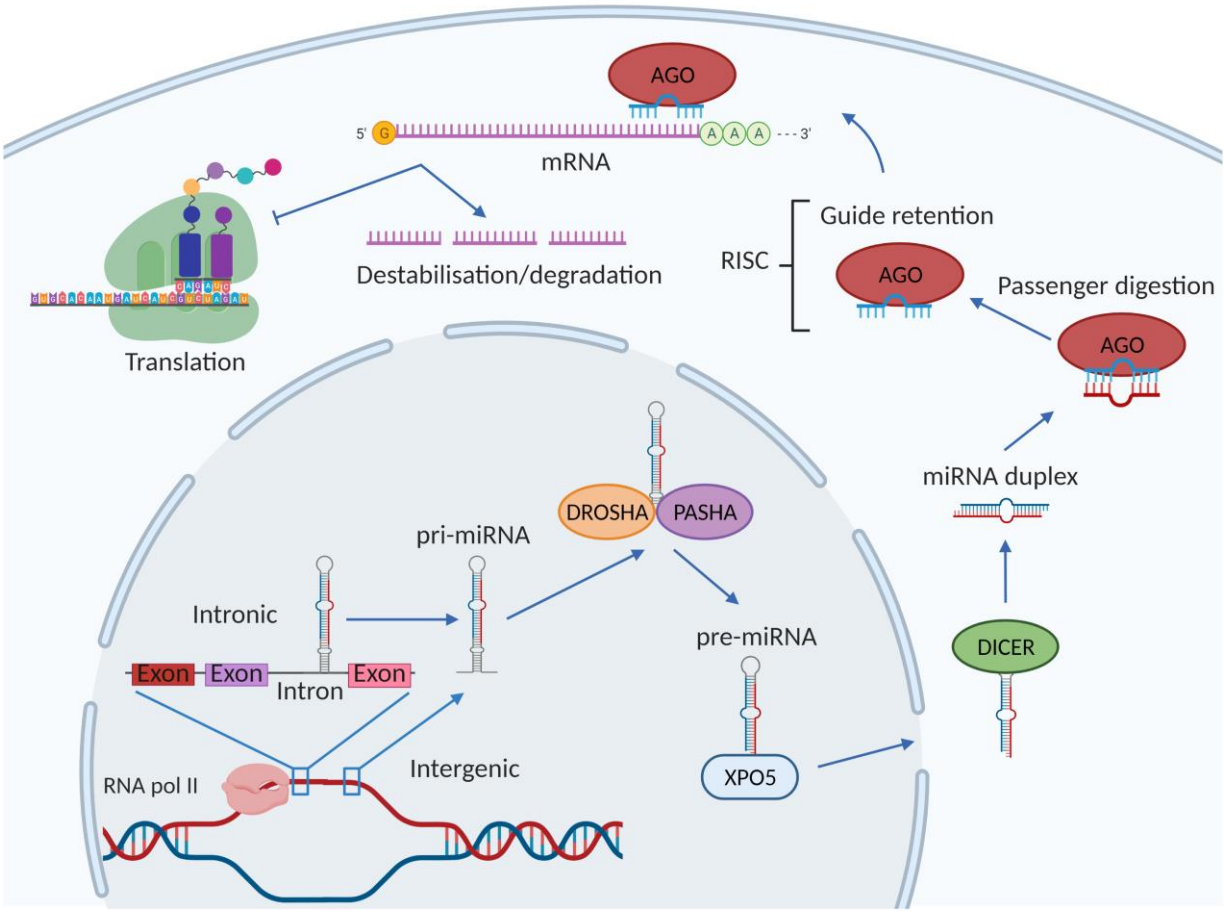

Figure 11. Overview of miRNA biogenesis.

MiRNAs can be intronic or intergenic and is predominantly transcribed by RNA polymerase II into pri-miRNA. DROSHA and PASHA recognises the hairpin structure of pri-miRNA and cleaves it into pre-miRNA which is transported into the cytoplasm by XPO5. In the cytoplasm, DICER cleaves pre-miRNA to produce mature miRNA that can integrate with AGO proteins, ultimately forming a RISC capable of translational inhibition or mRNA degradation, depending on the degree of miRNA sequence complementarity with its target mRNA. Note: Image taken from Visser and Thomas (2021) and used with permission. Created on license from BioRender.com.

Considering the gene regulatory role of miRNAs, the importance of any entity capable of miRNA regulation cannot be overstated. In this context, DDR proteins are known to influence miRNA biogenesis. For example, ATM can induce biogenesis of multiple miRNAs (e.g., miR-16) in a KH-type splicing regulatory protein (KSRP)-dependent manner (Zhang *et al*., 2011). KSRP is a splicing regulatory protein (Min *et al*., 1997) that regulates the biogenesis of a subset of KSRP-dependent miRNAs (Trabucchi *et al*., 2009; Zhang *et al*., 2011). As described by Trabucchi *et al*. (2009), KSRP forms part of both DROSHA and DICER microprocessor complexes and enhances miRNA biogenesis. Mechanistically, KSRP promotes mature miRNA synthesis through high affinity binding to a terminal loop in pre-miRNA sequences. However, whether this is also its pri-miRNA binding mechanism to promote pre-miRNA synthesis was less clear. Nonetheless, KSRP depletion did impair pre-miRNA synthesis thus implicating KSRP in pri-miRNA processing. Zhang *et al*. (2011) provides insight regarding KSRP-mediated pri-miRNA processing, suggesting it to be contingent on ATM-dependent phosphorylation. This PTM improves KSRP-pri-miRNA interaction, and subsequent maturation. Breast cancer 1 (BRCA1) has also been reported to promote miRNA biogenesis (Kawai and Amano, 2012). Specifically, BRCA1 can directly interact with DROSHA and RNA binding protein, DDX5, to facilitate pri-miRNA processing. Moreover, BRCA1 can also directly interact with the stem-loop structure of pri-miRNAs via its DNA binding domain. Ultimately, BRCA1 is capable of promoting the expression of several miRNAs including let-7a and miR-16 (Kawai and Amano, 2012). Interestingly, these were among the miRNAs that showed pronounced reduction (40% – 70%) upon KSRP knock-down in the study by Trabucchi *et al*. Therefore, considering that KSRP-mediated pri-miRNA processing is ATM-dependent, and that BRCA1 is a substrate for ATM (Gatei *et al*., 2000), the importance of ATM as a core regulator of, at least, a subset

of miRNAs is evident. While this is one example of miRNA biogenesis in the context of the DDR, it is reasonable to assume that other DDR proteins, especially those capable of transcriptional regulation, can influence miRNA biogenesis to facilitate specific cell fates.

2.1.3. MiRNAs and DNA damage sensing

To maintain DNA integrity, DNA damage is efficiently detected by DNA damage sensors; MRN complex (Syed and Tainer, 2018), RPA-ATRIP, XRCC6/5, and their respective partners: ATM, ATR, and DNA-PK (**Chapter 1**; Roos, Thomas, and Kaina, 2016; Menolfi and Zha, 2020). Detection, in turn, brings forth a rapid DDR. However, it is important to recognise that the DDR is not limited to linear cascade activation. Rather, several DDR proteins can elicit, necessarily, multiple reactions and is reliant on functional interplay. For example, ATM facilitates recruitment of the MRN complex to DSB sites, which in turn promotes further recruitment of ATM (Wang *et al*., 2014a; Syed and Tainer, 2018). Additionally, ATM phosphorylates the histone H2A, forming γH2Ax foci at DSB sites, which facilitates DNA repair protein recruitment (Stiff *et al*., 2004; Podhorecka, Skladanowski, Bozko, 2010).

The molecular highway that is the DDR is clearly complex, yet, often narrowly viewed in the context of protein dynamics. However, miRNAs can influence the DDR. For example, Espinosa-Diez *et al*. (2018) demonstrated miR-494 upregulation within 1 h following γ-irradiation. This led to MRN complex inhibition in human endothelial cells, promoting a senescent phenotype. In this instance, it is reasonable to assume that MRN inhibition can have knock-on effects given its role in ATM recruitment to DSBs. By extension, this can influence γH2Ax formation. Thus, if γH2Ax formation happened to be the focus of research, but failed to form at DSBs, it may be, mistakenly, assumed

that ATM is defective. However, in this case, miR-494-mediated inhibition of the MRN complex impeded γH2Ax formation.

Other damage sensing proteins are also subject to miRNA regulation. For example, X-ray repair cross-complementing protein (XRCC5), which is a component of the DNA-PK binding partner heterodimer, XRCC6/5 (Hanakahi and West, 2002), is a direct target of miR-526b, and its repression can promote cell cycle arrest and apoptosis in transfected lung cancer cells (Zhang *et al*., 2014a). Furthermore, Hu *et al*. (2010) demonstrated that miR-421 transfected cervical carcinoma cells exhibit a phenotype reminiscent of ataxia telangiectasia, indicated by ATM downregulation and diminished S-phase arrest and cell survival following irradiation. Moreover, miR-421 expression seems to be driven by the expression of N-Myc, an oncogenic transcription factor (Beltran, 2014). Mechanistically, the authors suggest N-Myc to upregulate miR-421, which in turn inhibits ATM at its 3' UTR. The authors tested their model in neuroblastoma cells with varying endogenous N-Myc levels, and indeed, an inverse relationship was observed between ATM and N-Myc expression, whereas a positive relationship was observed between N-Myc and miR-421. Similarly, Liao *et al*. (2015) demonstrated that miR-383 suppresses ATR expression by targeting its 3' UTR in epidermoid carcinoma cells. However, signal transducer and activator of transcription (STAT3) was demonstrated to rescue ATR expression by antagonising the miR-383 promotor. Another example is described by Wang *et al*. (2013) that demonstrated miR-185 to inhibit ATR in transfected renal carcinoma cells, promoting an apoptotic phenotype in response to irradiation.

It is clear that miRNAs feature in the negative regulation of upstream DDR activity. However, this regulation is not always suppressive, and can promote expression. For example, miR-15b can upregulate phosphorylated ATM (pATM) levels in lung epithelial cells 24 h after IR-induced DNA damage, by targeting WIP1 (Rahman *et al*., 2014).

Although the authors only reported increased pATM protein expression 24 h after IR, it is likely to have occurred much earlier as miR-15b levels peaked 2 h after IR. Moreover, γH2Ax and p53 (ser15) levels were also elevated in miR-15b expressing cells 2 h after IR, as compared to non-miR-15b expressing controls. Interestingly, the effect of miR-15b on pATM was dependent on IR, suggesting miR-15b to augment, or be augmented by other DNA damage responsive proteins.

2.1.4. MiRNAs and DNA damage response transducers

As discussed in **Chapter 1**, typical transducers of the DDR, and downstream targets of the ATM/ATR pathway, include Chk1/2 (Bartek and Lukas, 2003). Though these are by no means the only DDR transducers, they do represent those most extensively researched. Yet, literature linking miRNAs to Chk1, and particularly Chk2 is limited. Nevertheless, Xie *et al*. (2014) demonstrated miR-497 to negatively regulate Chk1 levels in hepatocellular carcinoma patient samples, owing to an 8-mer complementarity at the 3' UTR of Chk1 mRNA. Similarly, Liu *et al*. (2015) showed Chk1 repression by miR-195 in transfected non-small cell carcinomas (NSCLC), *in vitro*. Adding validity to this observation, the authors analysed clinical data from the *Cancer Genome Atlas* and found a significant negative correlation between miR-195 and Chk1 expression among NSCLC patients. Lezina *et al*. (2013) also demonstrated Chk1 repression in miR-16 and miR-26a transfected lung adenocarcinomas, *in vitro*. The authors suggested miR-16 and miR-26a to be post-transcriptionally and transcriptionally regulated, respectively, by p53 in response to sub-lethal doxorubicin (dox) treatment (0.5 μM) (Yang, Kemp, and Henikoff, 2015; Cheng *et al*., 2017). Therefore, these miRNAs may function specifically in a genotoxicological context, as p53 is stabilised during genotoxicity (**Chapter 1**). These miRNAs were further identified to target WEE1, promoting an apoptotic phenotype (Duan *et al*., 2018). However, while both are able to inhibit Chk1, miR-26a

seems to act predominantly in a synergistic capacity with miR-16 to inhibit WEE1. While miRNAs can directly inhibit their targets, indirect inhibition is also possible. For example, miR-126 can promote apoptosis, *in vitro*, by inhibiting polo-like kinase (PLK-4). Promotion of apoptosis results from disruption of the novel interaction between PLK-4 and ATR, thus impairing the ATR-Chk1 cascade (Bao *et al*., 2018). The authors allude to the promoted apoptosis being a consequence of impaired DNA repair, which is a logical conclusion, as inhibition of ATR (given its role in SSB repair) would promote SSB to DSB progression, which is among the most lethal forms of DNA damage (De Zio, Cianfanelli, Cecconi, 2013).

Chk2 is a target of miR-182-5p in transfected embryonic kidney and breast cancer cells, *in vitro* (Krishnan *et al*., 2013). The authors confirmed binding sites for miR-182-5p in Chk2 mRNA, implying direct inhibition. Inhibition of Chk2 propagated an impaired HRR phenotype, as Chk2 positively regulates BRCA1, which promotes HRR (Zhang *et al*., 2004; Hu *et al*., 2014). Moreover, while this was not addressed by the authors, inhibition may also be indirect. Among the network of putative miR-182-5p targets (e.g., RAD17 and p53 binding protein, p53BP1), some are capable of interfering with Chk1/2 activation. For example, RAD17 was significantly inhibited by miR-182-5p and is an important facilitator of the ATR-Chk1 cascade (Shiotani *et al*., 2013). Furthermore, p53BP1 is a known substrate of ATM and important for Chk2 activation (Irene *et al*., 2003; Perona *et al*., 2008; Lee *et al*., 2010). When checkpoint kinases are inhibited, an expected outcome is decreased cyclin-dependent kinase inhibitors (CKIs) and increased cyclins (regulatory proteins that promote cell cycle progression), as the cell cycle would now favour proliferation, rather than arrest. This is, in part, because checkpoint kinases are upstream activators of p53 that function, initially, to arrest the cell cycle through CKI (e.g., p21) upregulation (Sullivan *et al*., 2018). CKIs can be

classified as two families, INK (p15, 16, 18, and 19) and CIP/KIP (p21, 27, 57). While INK CKIs target CDK4/6 to disrupt interaction with its partnering cyclin D, CIP/KIP CKIs target the cyclin-Cdk dimers forming between cyclins D, E, and A and their respective Cdks. Ultimately, the net effect of either INK or CIP/KIP CKIs is a disabled kinase activity of cyclin-Cdk dimers, thus preventing cell cycle progression (Karimian, Ahmadi, and Yousefi, 2016; Abbastabar *et al*., 2018). Huang *et al*. (2015a) demonstrates this in miR-191 transfected osteosarcoma cells causing direct Chk2 inhibition, which caused a subsequent p21 and p27 downregulation, and concomitant upregulation of several cyclins, thereby promoting proliferation.

2.1.5. MiRNAs and DDR mediators

2.1.5.1. MiRNAs and p53

Perhaps the most widely researched DDR mediator, and tumour suppressor, is p53 (Helton and Chen, 2007; Zhang, Liu, and Wang, 2011; Williams and Schumacher, 2016). Through transactivation or repression, p53 regulates several genes regulating cell cycle arrest, DNA repair, and apoptosis (**Chapter 1**; Helton and Chen, 2007; Williams and Schumacher, 2016). As previously discussed, during basal conditions p53 is maintained at low levels by MDM2, but upon DNA damage, p53 phosphorylation disrupts the p53-MDM2 interaction (**Chapter 1**). However, less is known about the regulation of MDM2 itself. A comprehensive *in silico* study by Moore *et al*. (2015) suggests several feedback loops, orchestrated by p53 that hinders the p53-MDM2 interaction. P53 is suggested to induce transcription of miR-192, miR-34a, and miR-29a that either directly or indirectly inhibits MDM2. While miR-192 targets MDM2 directly, miR-34a inhibits transcription factor Yin Yang 1 (YY1) that upregulates MDM2. Incidentally, YY1 is also a direct target of miR-7-5p in glioblastoma multiforme cells (Jia

et al., 2019a). Similarly, miR-29a targets WIP1, a phosphatase that dephosphorylates MDM2 at ser395, thereby stabilising it and improving p53-MDM2 interaction (Lu *et al*., 2008). In the context of oncogenesis, excessive inhibition of WIP1 may elicit a bifurcated cell fate. WIP1 has been demonstrated to 'switch off' the DDR by dephosphorylating ATM and p53 (Macurek *et al*., 2013). Thus, WIP1 inhibition can result in an aberrantly sustained DDR, prohibiting cell cycle progression, and likely facilitate excessive apoptosis. By the same token, a sustained DDR may benefit oncogenesis by promoting DNA repair, which undermines the desired effect of many chemotherapeutic strategies.

Bearing in mind that p53 also induces MDM2 as a form of negative regulation (Moll and Petrenko, 2003), it can be said that p53 facilitates a network of negative and positive feedback loops that are believed to manifest as p53 pulsation. In response to DNA damage, the levels of p53 increase, generating pulses which is hypothesised to direct cell fate (Chen *et al*., 2013a). It has been suggested that mild to moderate DNA damage stimulates a series of p53 pulses in an attempt to repair, rather than kill the cell. This is suggested to be achieved by the pulsing of p53, causing gradual DDR protein accumulation (prompting cell cycle arrest and DNA repair), rather than one potent p53 pulse that would cause rapid DDR protein (and by extension pro-apoptotic proteins) accumulation when extensive and/or sustained DNA damage occurs (Chen *et al*., 2013a). While this notion has gained much attention, Moore *et al*. relied solely on the presence or absence of these p53 oscillations in breast cancer cells with drug-induced DSBs as biological validation of their proposed p53-miRNA-MDM2 network. Indeed, it does support their *in silico* model, however, it does leave the possible presence of additional intermediary proteins, or the involvement of other miRNAs that may result in, or contribute to, p53 pulsation, an open question. For example, miR-194, miR-215

(Pichiorri *et al*., 2010), and miR-605 (Xiao *et al*., 2011) have all been shown to disrupt p53-MDM2 interaction.

Rahman *et al*. (2014) observed decreased MDM2 and increased p53 (ser15) phosphorylation in miR-15b/16-2 transfected human bronchial epithelial cells (HBEC) following irradiation. These observations were attributed to possible WIP1 inhibition by miR-15b, along with augmentation of the ATM-Chk1-p53 cascade. Taken together, the study suggests a pro-survival role for miR-15b as the survival fraction was increased in miR-15b transfected HBEC cells following irradiation. This may be related to the IR dose used (4 Gy), which may be considered sub-lethal based on the findings of Ifeadi and Garnett-Benson (2012) that described doses < 10 Gy as sub-lethal in colorectal cancer cells. MiR-15b/16-2 transfected cells demonstrated, among others, increased levels of pATM, pChk1, and p53 (ser15) in response to IR, compared to non-transfected cells. This suggests an active DDR, and while seemingly counterintuitive to a survival outcome, it is possible that the DDR is predominantly geared towards arrest and repair rather than apoptosis. This is supported by four observations: 1) the percentage of RAD51 positive cells were significantly greater for miR-15b/16-2 transfected cells after 5 h of IR compared to non-transfected cells. RAD51 is a core HRR protein (Li and Heyer, 2008), 2) miR-15b/16-2 transfected cells exhibit greater G_2/M arrest fractions after IR, 3) the authors only reported upregulated p53 (ser15), which is proposed to promote arrest/repair functions rather than cell death, whereas p53 (ser46) would have been more suggestive of an apoptotic phenotype (discussed hereafter), 4) miR-15b/16-2 transfected cells exhibited an increased overall survival fraction following IR. Admittedly, increased levels of cleaved poly (ADP-ribose) polymerase (PARP1) and BID (indicators of apoptosis, discussed in **2.1.7** and **Chapter 3**) were also reported, though this is not unexpected as some cells are still expected to undergo apoptosis if DNA damage

exceeds the capabilities of DNA repair machinery. Interestingly, the authors did not report on Chk2, which is the primary downstream target of ATM, while Chk1 is typically a substrate for ATR. However, the authors did comment on RAD51 (functions in DSB repair) (Krejci *et al*., 2012) and γH2Ax (indicator of DSB) (De Zio, Cianfanelli, Cecconi, 2013) induction by miR-15b/16-2. Thus, it would be interesting to include pChk2 expression studies, as ATM-Chk2-p53 activation typically follows IR and subsequent DSBs (**Chapter 1**). Admittedly, this mutually exclusive allocation of ATM-Chk2 and ATR-Chk1 pathways is deprecated as functional interplay occurs between them, as previously mentioned (**Chapter 1**). Nonetheless, the inclusion of Chk2 is warranted as it is a fundamental component of the DDR.

2.1.5.2. MiRNAs and p53 PTM

As with several DDR proteins, PTMs such as phosphorylation and acetylation are critical for complete p53 functionality (Loughery *et al*., 2014; Roos, Thomas, and Kaina, 2016). Recall (**Chapter 1**), p53 executes different functions based on the number and position of phosphorylations (Jabbur, Huang, and Zhang, 2000; Mayo *et al*., 2005; Smeenk *et al*., 2011; Loughery *et al*., 2014; Roos, Thomas, and Kaina, 2016). Importantly, p53 (ser46) is clearly implicated in apoptosis, and while the exact kinase(s) responsible for this PTM remains uncertain, mounting evidence implicate ATM, DYRK2, p38, and HIPK2 (Perfettini *et al*., 2005; Taira *et al*., 2007; Kodama *et al*., 2010; He *et al*., 2019; Liebl and Hofmann, 2019). Consequently, the mechanism(s) involved in regulating these kinases are potentially key determinants of cell fate. Interestingly, each of these kinases are reported to be repressed by miRNAs. In addition to miR-421-mediated inhibition of ATM (previously discussed), DYRK2 is a direct target of miR-622 in transfected colorectal cancer cells (Wang *et al*., 2017). Similarly, miR-499 has been reported to directly target DYRK2 in rat cardiomyocytes (Wang *et al*., 2014b). Moreover,

miR-124 was shown to directly inhibit p38 in transfected murine microglial cells (Yao *et al*., 2019). Furthermore, miR-141 has been shown to directly target HIPK2 in transfected human kidney cells (Huang *et al*., 2015b). Finally, HIPK2 has also been shown to be a direct target of miR-222-3p in transfected gastric cancer cells. Perhaps not surprisingly, ectopic expression of miR-222-3p in these cells significantly diminished apoptosis, exemplifying the overall potential of miRNAs to determine cell fate (Tan *et al*., 2017).

While these observations implicate miRNAs as potential influencers of p53 phosphorylation, consideration must also be given to other PTMs that influence p53 activity. Recall, p53 acetylation is fundamental to its stability and function (Tang *et al*., 2008; Loewer *et al*., 2010; Yun *et al*., 2016). Therefore, the regulation of deacetylases (e.g., SIRT1) are important determinants of p53-dependent cell fates. SIRT1 is a target of miR-449 and miR-34a (Lizé, Pilarski, and Dobbelstein, 2009). MiR-449 is upregulated by E2F1, a family member of cell cycle promoting transcription factors. Interestingly, E2F1 is DNA damage responsive, resulting in its stabilisation and shifts to pro-apoptotic tendencies (Biswas and Johnson, 2012). In particular, E2F1 can directly upregulate p73 (p53 related protein) via its promotor to induce apoptosis, as demonstrated by Stiewe and Pützer (2001) that used modified osteosarcoma cells expressing a drug-inducible E2F1 transcript to induce p73 expression. MiR-449 induction may add to the pro-apoptotic capability of E2F1 as its substrate, SIRT1, hinders p53 activity (**Chapter 1**). Importantly, p53 acetylation is central to both its arrest/repair and apoptotic functions. Thus, the outcome of SIRT1 inhibition on cell fate would depend on the presence and severity of DNA damage. Similarly, miR-34a targets SIRT1 and is proposed to be directly induced by p53 (Moore *et al*., 2015). This makes sense, as literature prominently implicates miR-34a as pro-apoptotic (Chang *et al*., 2007; Rokhlin *et al*., 2008; Kato *et al*., 2009; Jia *et al*., 2019b). MiR-506-3p is also reported to directly target SIRT1 and

promote apoptosis in miR-506-3p transfected ovarian cancer cells (Xia *et al*., 2020). However, this was attributed to a SIRT1-AKT-forkhead box-protein (FOXO3a) axis where SIRT1 would activate AKT (pro-survival protein), which in turn inhibits FOXO3a (a tumour suppressor protein) (Santo *et al*., 2013; Xia *et al*., 2020). Among others, FOXO3a can promote apoptosis indirectly by facilitating the repression of anti-apoptotic protein, B-cell lymphoma extra-large (Bcl-xL) (Burgering and Medema, 2003), or directly by transactivating the pro-apoptotic protein, BIM (Sanphui and Biswas, 2013). Thus, miR-506-3p is capable of liberating the tumour suppressive activity of FOXO3a by targeting SIRT1. Taken together, miRNA mediated inhibition of SIRT1 may play a fundamental role in facilitating both cell survival and apoptosis.

Another PTM of p53 is methylation. Recall that, like phosphorylation and acetylation, methylation also influences p53 activity (Shi *et al*., 2007; Zhu *et al*., 2016). Therefore, the regulation of HMTs, such as SET8, demonstrated to target p53 (Shi *et al*., 2007; Zhu *et al*., 2016) has important implications for cell fate determination. Incidentally, Yu *et al*. (2013) demonstrated miR-7 to inhibit SET8 in transfected breast cancer cells. Moreover, ectopic expression of miR-7 caused apoptosis and increased breast cancer cell susceptibility to chemotherapeutic drugs, VP-16 and camptothecin. This suggests miRNAs can potentially be used to promote apoptosis by liberating the pro-apoptotic transcriptional activity of p53 from inhibitory methylation, by HMTs.

2.1.5.3. p53-mediated miRNA expression

Clearly, PTM of p53 is imperitive to its role in the DDR, and specifically its transcriptional activity. These p53 PTMs have largely been explored in context of p53 stabilisation and transactivation of DDR genes. However, it is likely that DDR-responsive miRNAs form part of the transcriptional and/or post-transcriptional repertoire of p53. In fact, p53 has

been reported to directly transactivate miR-34a by binding to its promotor (Tarasov *et al*., 2007). Moreover, miR-34a transfection resulted in G_1/S arrest and apoptosis in osteosarcoma and NSCLC cells respectively. Furthermore, Nakazawa, Dashzeveg, and Yoshida (2014) proposed miR-1915 to be DNA damage responsive by virtue of p53-mediated pri-miR-1915 to pre-miR-1915 processing, and ultimately facilitating apoptosis by targeting Bcl-2. Additionally, p53 transactivates miR-22 by directly interacting with its host gene *C17orf91* in response to DNA damage (Tsuchiya *et al*., 2011). MiR-22 was also shown to facilitate p21 repression, thereby sensitising transfected colorectal cancer cells to apoptosis in response to dox (Tsuchiya *et al*., 2011). These examples firmly point to a p53-mediated regulation of miRNA expression in response to DNA damage.

2.1.6. MiRNAs and DNA damage response effectors

The initial response to DNA damage is cell cycle arrest to provide an opportunity for DNA repair, or preparation for apoptosis if the damage is too severe and irreparable. As mentioned previously, cyclins and Cdks are principal components of the cell cycle that dimerise to facilitate cell cycle progression by phosphorylating specific target proteins. Thus, disruption of cyclin-Cdk dimers initiates cell cycle arrest. Like much of the DDR, the cell cycle is regulated by a series of phosphorylation/dephosphorylation events, regulation of which is critical for cell cycle arrest or progression. Recall, CDC25a is a phosphatase that promotes cell cycle progression by removing inhibitory phosphoryl groups from Cdks (Shen and Huang, 2012). Pothof *et al*. (2009) demonstrated miR-16 to be upregulated in cervical cancer cells following UV exposure, which resulted in direct CDC25a inhibition. MiR-16 transfection also resulted in G_1-phase accumulation, even in the absence of UV. Thus, as CDC25a is a critical regulator of the G_1/S-phase checkpoint (Blomberg and Hoffmann, 1999), the accumulation of cells in G_1 further suggests miR-16-mediated CDC25a inhibition. Relatedly, Yan *et al*. (2012) provided an

in silico model of E2F negative regulation by miR-449 that targets Cdk6, cyclin E, and CDC25a. Several other cyclins are targets of miRNAs, for example, miR-16 targets cyclin D1 (Mobarra *et al*., 2015), along with cyclin D3 and cyclin E1 (Liu *et al*., 2008).

While miRNAs can target cyclins and Cdks to promote cell cycle arrest, miRNAs can also target CKIs in favour of cell cycle progression. For example, CKI p27 is inhibited by miR-221 and miR-222 promoting a more aggressive glioblastoma phenotype, *in vitro* (Gillies and Lorimer, 2007). However, while the authors demonstrated that endogenous miR-221/222 could suppress p27 at a protein level, only miR-221 was shown to target the 3' UTR of p27 directly. Admittedly, bioinformatic analysis demonstrated two potential target sites for both miRNAs. Moreover, the authors suggested miR-221 and miR-222 to be co-regulated, thus, presumably, they extended their observations of miR-221 to miR-222. Therefore, it is possible that miR-222 relies on intermediary proteins to facilitate indirect inhibition of p27. Furthermore, the assertion that miR-221/222 promotes a more aggressive glioblastoma phenotype was based on reduced proliferation, and the accumulation of cells in G_1-phase, observed after DICER inhibition. While this supports the notion of p27 inhibition, it does not explicitly identify miR-221 and miR-222 as the inhibitors.

Another frequently referenced miRNA substrate is p21. For example, Dolezalova *et al.* (2012) demonstrated that endogenous miR-302 (cluster) is upregulated in human embryonic stem cells (hESCs) following UV irradiation. Moreover, the authors suggest p21 to be a direct target of the miR-302 cluster as inhibition of miRNA biogenesis proteins caused p21 upregulation, whereas additional miR-302 cluster co-transfection antagonised this upregulation. Interestingly, despite p53 and pro-apoptotic protein accumulation following UV radiation, hESCs had no detectable p21 expression. This could be explained by the observed apoptotic phenotype of UV irradiated cells, as p21

mainly functions to induce cell cycle arrest in an attempt at repair and survival, which precedes commitment to apoptosis (Abbas and Dutta, 2009). It is tempting to speculate that miR-302 cluster-mediated repression of p21 may be a mechanism to sensitise hESCs to apoptosis, as these are known to be highly susceptible to apoptosis, given its role as precursors to various cell types (Liu, Lerou, Lahav, 2014). Similarly, miR-106b can promote G_1/S-phase cell cycle progression by targeting p21 in miR-106b transfected human mammary epithelial cells (HMECs), *in vitro* (Ivanovska *et al*., 2008). Several lines of evidence suggested that miR-106b transfection promotes cell cycle progression, including an increased accumulation of S-phase cells, an expedited growth curve, and accumulation of cells in G_1-phase after miR-106b inhibition. The authors attributed these observations to negative regulation of p21 by miR-106b, as miR-106b was able to reduce p21 mRNA and protein levels in transfected HMECs. Furthermore, p21 knock-down recapitulated the phenotype of miR-106b transfected HMECs. Intriguingly, miR-106b was able to disengage a dox-induced G_1/S checkpoint, a phenotype mimicked by p21 inhibition. P21 is also directly inhibited by miR-33b-3p in NSCLC cells in response to cisplatin-induced DNA damage (Xu *et al*., 2016). The authors demonstrated downregulation of endogenous miR-33b-3p following apparently lethal doses of cisplatin (Freeburg, Goyeneche, and Telleria, 2009; Ahmed and Jamil, 2011; Barr *et al*., 2013). Additionally, miR-33b-3p transfection promoted cell viability as evidenced by increased proliferation and G_1/S progression following cisplatin treatment (Xu *et al*., 2016). Furthermore, the opposite effect was observed in cisplatin-resistant counterparts of the same cells when miR-33b-3p was inhibited and treated with cisplatin, suggesting miR-33b-3p as the possible cause of cisplatin resistance. Interestingly, miR-33b-3p was suggested to promote DNA repair as indicated by reduced γH2Ax levels following cisplatin treatment of miR-33b-3p transfected NSCLC

cells. This was supported by a significant upregulation of excision repair cross-complementation protein (ERCC1), a component of NER, coupled with significant downregulation of p21 in miR-33b-3p transfected NSCLC cells (Xu *et al*., 2016). This makes sense as cisplatin is an alkylating agent known to generate 'bulky' DNA adducts which are repaired by NER (Schärer, 2013; Rocha *et al*., 2018). Mechanistically, the authors confirmed involvement of these proteins as conduits for the observed pro-survival phenotype as ERCC1 silencing and transfecting cells with p21 constructs devoid of the miR-33b-3p binding site effectively reversed the effects of miR-33b-3p following cisplatin treatment. Although, it is not clear whether miR-33b-3p is capable of preventing the formation of γH2Ax foci, or merely assist its reduction by promoting DNA repair, as the initial timing after cisplatin treatment in miR-33b-3p transfected cells and subsequent γH2Ax measurement was not clearly stated. Moreover, when timed γH2Ax levels were measured, it was not obvious whether time-points represented post-exposure or continuous exposure. However, if the data demonstrating a reduction of γH2Ax in miR-33b-3p transfected cells following cisplatin treatment represents a measurement immediately after treatment, it could imply miR-33b-3p to be a rapid responder to DNA damage, perhaps even assuming a damage sensor role and preventing the accumulation of γH2Ax by promoting the NER pathway, as implied by the authors.

2.1.7. MiRNAs and DNA repair

As discussed in **Chapter 1**, BER, NER, MMR, HRR, and NHEJ encompass the main constituents of a tightly regulated, damage type-dependent, DNA repair response. Arguably, HRR and NHEJ are the most critical, considering their role in DSB repair. Given the toxicity of DSBs, miRNA-mediated regulation of DSB repair enzymes can alter cell fate in response to DSBs. For example, PARP1 is a proposed target of miR-7-5p

(Luo *et al*., 2018; Lai *et al*., 2019). Importantly, PARP1 functions in several DNA repair pathways including NER (Robu *et al*., 2013), BER (Reynolds *et al*., 2015), and modulates HRR (Hu *et al*., 2014; Lai *et al*., 2019). The inhibition of PARP1 by miR-7-5p manifests as impaired HRR, resulting from downregulated BRCA1 (Luo *et al*., 2018; Lai *et al*., 2019), a tumour suppressor protein that promotes HRR (Hu *et al*., 2014). Furthermore, miR-7-5p-mediated PARP1 inhibition also results in indirect RAD51 downregulation (Lai *et al*., 2019). Thus, miR-7-5p indirectly impairs HRR by directly inhibiting PARP1. Consequently, cell fate is altered by miR-7-5p in an HRR-dependent manner as miR-7-5p transfection was able to significantly reduce the dox IC_{50} in dox-resistant small-cell lung cancer cells (SCLCs) (Lai *et al*., 2019). Moreover, lymphoblastoid cell transfection with miR-7-5p prominently increased the proportion of apoptotic cells both with, and, interestingly, without hydroquinone treatment (Luo *et al*., 2018). This suggests that miR-7-5p is sufficient to prompt apoptosis, even at basal DNA damage levels, which, in addition to HRR inhibition, may be attributable to the inhibition of other DNA repair pathways that involve PARP1 (as previously mentioned). Of note, Luo *et al*. demonstrated that endogenous miR-7-5p levels decrease with increasing doses of hydroquinone, suggesting that miR-7-5p might exist to limit excessive DNA repair during homeostasis to maintain genome stability, but becomes downregulated in response to DNA damage to allow DNA repair.

Notwithstanding indirect inhibition of RAD51 by miR-7-5p (mentioned previously), direct inhibition is also possible. For example, miR-103 and miR-107 directly target both RAD51 and its paralogue RAD51D, resulting in impaired HRR (Huang *et al*., 2013). Transfection of osteosarcoma cells with either miR-103 or miR-107 reduced cellular viability in response PARP1 inhibitor (PARPi) or cisplatin treatment compared with untransfected cells. This suggests these miRNAs augment the inhibitory effect of

PARPi, possibly by compounding its inhibitory effects on HRR. Moreover, miR-103/107-mediated inhibition of HRR also explains the observed reduction in cell viability in response to cisplatin, as these cells would be less capable to repair resulting DSBs. Incidentally, miR-103 also directly targets three-prime exonuclease (TREX1), *in vitro* (Wilson *et al*., 2016), which has been demonstrated to augment PARP1 stability and function (Miyazaki *et al*., 2014), thus further linking miR-103 to HRR inhibition. RAD51 was also shown to be directly inhibited by miR-34a/b/c-5p (miR-34s), in a partially p53-dependent manner (Chen *et al*., 2019). Transfection of colon carcinoma cells with any of these miRNAs caused a significant increase in apoptotic rate in the absence of induced DNA damage. In line with impaired HRR resulting from RAD51 inhibition by miR-34s, transfected cells also demonstrated increased γH2Ax accumulation, suggestive of impaired DSB repair. While miR-34s can independently inhibit RAD51 (and by extension HRR), the authors noted RAD51 inhibition to be more pronounced in $p53^{wild\text{-}type}$, than $p53^{-/-}$ cells transfected with miR-34s. This suggests RAD51 inhibition to be partially p53-dependent, which might be explained by a possible p53-miR-34 positive feedback loop as suggested by Moore *et al*. (2015) (previously discussed). Moreover, a comprehensive screen by Piotto *et al*. (2018) revealed RAD51 as a direct target of miR-96-5p, along with BRCA2, XRCC5, and protein kinase, DNA activated, catalytic subunit (PRKDC) as direct targets of miR-19a-3p, miR-218-5p, and miR-874-3p respectively. While RAD51 and BRCA2 function in HRR, XRCC5 and PRKDC are part of the NHEJ pathway (Piotto *et al*., 2018). XRCC5 has also been demonstrated to be a target of miR-526b as a means of inducing apoptosis (Zhang *et al*., 2014a). Notwithstanding DSB repair, miRNAs also influence other repair pathways. For example, miR-192 hinders NER in liver carcinoma cells by directly targeting NER components, ERCC3/4 (Xie *et al*., 2011).

These examples demonstrate the potential role of miRNAs as regulators of DNA repair, and how it can sway cell fate in response to DNA damage, or even bring about a certain cell fate independent of exogenous DNA damage. Moreover, literature clearly implicates miRNAs as integral modulators of the DDR. This sheds new light on the well-accepted notion that if DNA damage is *too severe*, cell fate is directed towards cell death, as miRNAs can seemingly shift the tolerance to DNA damage by impeding DNA repair mechanisms. By the same token, the ubiquitous involvement of miRNAs in the DDR complicate genotoxicity studies as their influence can sway the DDR to a cell fate that cannot be reconciled with doses administered. Thus, three aspects will determine cell fate in response to DNA damage: 1) the level of damage, 2) the repair capability of the cell, and 3) the expression of DNA damage responsive miRNAs.

2.1.8. Rationale

This chapter brings into focus the ubiquitous involvement of miRNAs in DDR regulation and cell fate decision-making. However, despite the plethora of literature implicating individual miRNAs in a DDR context, few studies address miRNA profiles that may function as a collective to bring about specific responses. Moreover, the potential for distinct miRNA profiles to be indicative of specific cell fates remain to be fully realised. At this point, it is important to realise that while miRNAs were selected as the subject of investigation for this thesis, it does not undermine the involvement, or preclude future investigation of other gene regulatory mechanisms e.g., siRNAs or lncRNAs. Simply, as previously discussed, miRNAs has a wide-spread and well-documented involvement in the DDR pathway which can aid interpretation of our findings in context of literature.

As a logical first step, this chapter set forth to identify DNA damage responsive miRNAs in the context of sub-lethal and lethal DNA damage, and performed functional

enrichment analysis to assess the predictive value of the identified DNA damage-responsive miRNAs and its associated cell fate. Clinically, the identification of miRNA profiles indicative of specific cell fates could have important therapeutic, diagnostic, and prognostic implications. Furthermore, as one of the most commonly used cell lines for genotoxicity assessment, identification and eventual characterisation of miRNAs expressed within TK6 cells can inform future studies. To the best of our knowledge, this is the first study to assess side-by-side sub-lethal and lethal TMZ dose effects on miRNA expression in TK6 cells, and it identifies multiple miRNAs that have not yet been reported in a DNA damage context.

Aim:

1. Identify differentially expressed miRNAs between sub-lethal and lethal TMZ doses at specific time-points (based on Chapter 1 aim).

2.2. Methods

2.2.1. MiRNA sequencing

2.2.1.1. RNA extraction and purification

TK6 cells were exposed to DMSO, 30TMZ, and 900TMZ. Treatment was the same as described in **Chapter 1** (**1.2.3.1**). Following treatment, RNA was extracted using the Zymo Research Quick RNA mini-Prep kit (R1054) (Cambridge Biosciences, Cambridge, UK) according to manufacturer specification. Briefly, samples were centrifuged (500 X g) for 5 min and resuspended in lysis buffer. All subsequent centrifugations were at 10000 X g. Subsequently, lysates were vortexed (briefly), centrifuged for 1 min, and the supernatant was transferred to a filter column assembly for repeat centrifugation to remove genomic DNA. Following this, an equal volume of ethanol (100%) was added to the flow-through and mixed. This mixture was added to another column assembly and centrifuged for 30 s to allow RNA purification. RNA, retained in the column, was subsequently washed with wash buffer, and incubated with DNase for 15 min at RT to remove any residual DNA. Following incubation, the columns were centrifuged for 30 s before adding RNA prep buffer, after which columns were centrifuged again for 30 s. This was followed by two wash cycle centrifugations, 30 s and 2.5 min respectively. Subsequently, 50 µL nuclease-free water was added and centrifuged for 45 s to elute purified RNA.

2.2.1.2. RNA quantification and quality assessment

Purified RNA was quantified using NanoDrop ONE (Thermo Fisher Scientific, Loughborough, UK). RNA quality was externally assessed as part of a small RNA sequencing service (**Appendix C**).

2.2.1.3. MiRNA sequencing

Purified RNA samples were sequenced by Genewiz (New Jersey, USA). Small RNA library preparation was done using a TruSeq Small RNA library preparation kit (Illumina, California, USA) and paired-end sequencing was performed with an Illumina HiSeq sequencing system.

Sequence cleaning

Unless otherwise stated, all sequence analyses were performed within the Galaxy platform (https://usegalaxy.org) (Afgan *et al*., 2018). Quality control analysis was performed on raw small RNA sequences using FastQC (v.0.11.8) (https://www.bioinformatics.babraham.ac.uk/projects/fastqc/) to determine (among others), base sequence quality (Q-score), base quality loss originating from the flow cell, average sequence Q-score, sequence length distribution, and any adapter sequence contamination (added as part of the sequencing process). Subsequently, sequencing adapters were removed from raw sequences, and reads becoming shorter than 10 bases were discarded using Trim-Galore (v.0.6.3) (https://github.com/FelixKrueger/TrimGalore), as mature miRNAs are not expected to be < 10 bases. Following this, sequences were further trimmed using Trimmomatic (v.0.38) (Bolger, Lohse, and Usadel, 2014). Beginning at the 5' end of each read, sequences were trimmed once the average of four bases dropped below a Q-score of 25. Subsequently, extremely poor quality bases (Q-score < 3) were removed from either end of the reads. Reads were also filtered to include only those with an average Q-score > 30. Following this, all remaining reads were truncated to only include reads up to a maximum length of 25 bases, starting from the beginning (5') of the read, as miRNAs are not expected to be larger than 25 bases. Following this, reads were subjected to another FastQC analysis to ensure the data "clean-up" was successful.

Sequence alignment

Cleaned sequences were aligned to high confidence mature miRNA sequences provided by miRBase (ftp://mirbase.org/pub/mirbase/CURRENT/). Sequence alignment was performed using the RNA alignment tool, STAR (v.2.7.5b) (Dobin *et al*., 2013). STAR parameters were adjusted to ensure at least 18 bases are aligned to the reference miRNA sequences. Effectively, this nullifies all reads shorter than 18 bases, as mature miRNA sequences are not expected to be shorter than 18 bases. Mismatch allowance was set to 5% of the read length, thus for every 20 bases, 1 base can be mismatched. In cases where a read mapped to multiple reference sequences, parameters were set to retain only one of these reads selected in a quasi-random manner. This prevents over-estimation of multi-mapped reads, but also prevents under-representation of these reads as a common approach is to either include or exclude all multi-mapped reads.

2.2.2. Differential miRNA expression analysis

Read counts for all aligned miRNAs were retrieved using the Samtools IDXstats tool (v.2.0.3) (Li *et al*., 2009). These counts were then imported to RStudio (v.4.0.0) where the Bioconductor packages; *EdgeR* (v.3.30.3) (Robinson, McCarthy, and Smyth, 2010) and *Limma* (v.3.44.3) (Ritchie *et al*., 2015) were used to calculate counts per million (CPM) and subsequently filter read alignments to only include those miRNAs with a CPM greater/equal to a threshold corresponding with at least 10 reads. This is a method generally considered for filtering, in this case, lowly expressed miRNAs (Chen, Lun, and Smyth, 2016). Moreover, in order to be retained, this threshold must have been met at least once per miRNA across all samples. This ensures that ‘lowly expressed’ miRNAs

are not included in downstream analyses. Using CPM normalises read counts to account for library size variations.

To determine whether any miRNAs were differentially expressed (DE) between samples, miRNA read counts were analysed using the local pooled error (LPEseq) method in RStudio (Gim, Won, and Park, 2016). This method allows extrapolation of differentially expressed genes from RNA sequencing data without replicates. Subsequently, adjusted p-values (Benjamini-Hochberg corrected p-values) (q-values) were ordered (increasing order) and filtered to retain only miRNAs with $q < 0.05$. Further normalisation of any identified DE miRNAs were performed using the *calcNormFactors* function in *EdgeR*, utilising the trimmed mean of M-values (TMM) method to calculate normalisation factors for each library that would effectively 'correct' counts as a function of library size. As read counts inherently follow a non-normal distribution, the logarithm (log2) of the normalised counts were calculated. Subsequently, the z-score for each DE miRNA was calculated for each sample, based on the average log2(CPM) for all samples, and plotted as a heatmap using *Heatmap.2* (v.3.0.1). To identify any miRNA expression patterns among different samples, hierarchical clustering was performed based on Euclidean distance.

2.2.3. Functional enrichment analysis of DE miRNAs

To determine if specific biological processes are associated with DE miRNAs, functional enrichment analysis was performed with GeneCodis 4 (https://genecodis.genyo.es/) (García-Moreno *et al*., 2022). DE miRNAs at specific time-points after 30TMZ and 900TMZ exposure was arranged in decreasing order of significance and using the Wallenius test to correct for gene length bias, functional enrichment was determined within the gene ontology (GO): biological process (BP) database.

2.2.4. MiRNA validation with qRT-PCR

To validate DE miRNAs identified from RNA sequencing data, qRT-PCR was performed. First strand cDNA synthesis was performed using the miRCURY Locked Nucleic Acid (LNA) Reverse Transcription kit (Qiagen, Manchester, UK). Other than adjusting the total input RNA to 400 ng, cDNA synthesis was performed according to manufacturer specifications. To monitor the efficiency of cDNA synthesis and the PCR, the synthetic RNA, UniSp6 (12 fmol) was added to the cDNA synthesis reaction mixture (1/20 v/v) after being prepared according to manufacturer specifications. For full details on the reaction mixture composition and cDNA synthesis conditions, see **Table 4** and **5**.

Table 4. cDNA synthesis reaction mixture composition

Component	miRCURY LNA miRNA PCR Assay
5x miRCURY RT Reaction Buffer	4 µL
RNase-free water	3 µL
10x miRCURY RT Enzyme Mix	2 µL
UniSp6	1 µL
Template RNA (40 ng/µL)	10 µL
Total volume	**20 µL**

Note – template RNA is pre-diluted in nuclease free (NF) water to 40 ng/µL.

Table 5. cDNA synthesis conditions

Step	Time	Temperature
RT step	60 min	42°C
Reaction inactivation	5 min	95°C
Storage	Indefinitely	4°C

Following cDNA synthesis, qPCR was performed with the miRCURY LNA SYBR Green PCR kit (Qiagen, Manchester, UK) according to manufacturer specifications, using an Applied Biosystems StepOnePlus™ real-time PCR system (Thermo Fisher Scientific, Loughborough, UK). Details of the reaction mixture setup and amplification conditions can be found in **Table 6** and **7**. Primers used for miRNA targets were purchased from Qiagen (Manchester, UK), and included hsa-miR-29b-3p (cat. YP00204679), hsa-miR-363-5p (cat. YP00204173), and hsa-miR-485-3p (cat. YP00206055), while U6 (cat. YP00203907) was used for endogenous control amplification. UniSp6 (cat. YP00203954) was used to monitor cDNA synthesis and qPCR amplification efficiency.

Table 6. qPCR reaction mixture composition

Component	Volumes
2x miRCURY SYBR Green Master Mix	5 µL
ROX Reference Dye	0.5 µL
Primer	1 µL
cDNA template (diluted 1/60)	3.5 µL
RNase-free water	-
Total reaction volume	10 µL

Note – cDNA is pre-diluted (1/60) in NF water.

Table 7. qPCR amplification conditions

Step	Time	Temperature
PCR initial heat activation	2 min	95°C
Denaturation	10 s	95°C
Combined annealing/extension	60 s	56°C
Number of cycles	40	
Melting curve analysis		60 - 95°C

Analysis of amplification data was performed using the delta-delta Ct method of relative quantification of gene expression. Using this method, Ct values for the endogenous control, U6, was used to normalise miRNA expression among DMSO-, and TMZ-treated samples. Subsequently, TMZ-treated miRNA expression levels were controlled against respective time-matched DMSO-treated samples and expressed as fold changes.

2.2.5. Statistical analysis

Statistical analyses were performed using IBM SPSS Statistics (v.28). Normality was assessed using Shapiro-Wilk test. Parametric data was analysed with either independent sample t-test, one-way ANOVA with Tukey's test as a post-hoc test, or Welch's ANOVA with Dunnett's T3 test as a post-hoc test depending on the nature of the data, and the type and number of comparisons made. Non-parametric data was assessed with either Mann-Whitney U test or Kruskal-Wallis test with Bonferroni test as a post-hoc test depending on the number of comparisons made and nature of the data. Correlations between p53 or miRNA levels with time post-TMZ exposure were performed with Kendall's tau-b. Correlations between p53 and miRNAs were performed using Spearman's correlation. To ensure balanced correlations, three simple random sampling iterations, for each unpaired time-point, were used to correct unpaired sample sizes when performing Spearman correlations. As all time-points (4 h, 18 h, and 36 h) were collectively used for a correlation, all combinations resulting from different sampling iterations were respectively correlated. Resulting p-values were averaged, however, statistical significance was only considered if each combination had an association in the same direction and had a $p < 0.05$, otherwise it was assumed that no correlation exists. For all statistics, $p < 0.05$ was considered statistically significant.

2.3. Results

2.3.1. Differentially expressed miRNAs in sub-lethal-, and lethal-treated TK6 cells

To determine whether 30TMZ and 900TMZ produces differentially expressed miRNA patterns, TK6 cells were exposed to these doses, sampled 4 h, 18 h, and 36 h post-exposure, and were sequenced for small RNA. Using LPEseq, differentially expressed miRNAs were identified. Collectively, 31 DE miRNAs were identified of which 21 was unique to 900TMZ-treated cells, whereas 30TMZ-treated cells displayed 8 when compared with DMSO-treated cells. Additionally, two miRNAs, miR-4433b-3p and miR-509-3-5p, were identified among both 30TMZ-, and 900TMZ-treated cells (**Table 8**).

Table 8. Benjamini-Hochberg adjusted p-values of DE miRNAs

	DMSO vs. 30TMZ			DMSO vs. 900TMZ		
	4 h	18 h	36 h	4 h	18 h	36 h
hsa-miR-4433b-3p			<0.001		<0.001	<0.001
hsa-miR-485-3p					<0.001	<0.001
hsa-miR-937-5p						<0.001
hsa-miR-197-5p					<0.001	<0.001
hsa-miR-345-3p						<0.001
hsa-miR-7161-3p					0.009	<0.001
hsa-miR-29b-3p		0.046				
hsa-miR-16-1-3p						<0.001
hsa-miR-181d-3p						<0.001
hsa-miR-377-5p						<0.001
hsa-miR-509-3-5p		0.046				<0.001
hsa-miR-942-3p						<0.001
hsa-miR-598-5p						0.003
hsa-miR-376b-3p						0.006
hsa-miR-375-5p		<0.001				
hsa-miR-2110						0.005
hsa-miR-323a-5p						<0.001
hsa-miR-493-5p		<0.001				
hsa-miR-548ay-5p	0.025					
hsa-miR-363-5p		0.019				
hsa-miR-597-5p						0.004
hsa-miR-323b-5p						0.027
hsa-miR-188-3p	<0.001					
hsa-miR-216a-3p						0.012
hsa-miR-542-3p						0.006
hsa-miR-589-5p						0.045
hsa-miR-224-5p						0.003
hsa-miR-532-3p						0.036
hsa-miR-491-5p						0.047
hsa-miR-150-5p		0.046				
hsa-miR-483-3p	0.025					

To further confirm the existence of unique miRNA expression profiles among 30TMZ-, and 900TMZ-treated cells, log2(CPM) of DMSO-, 30TMZ-, and 900TMZ-treated cells at 4 h, 18 h, and 36 h post-exposure were z-score scaled and clustered based on Euclidean distance (**Fig. 12**). Indeed, distinct patterns of miRNA expression were observed that can be organised into 6 clusters: 1) Pre (untreated); 2) DMSO 4 h, 900TMZ 4 h; 3) DMSO 18 h and 30TMZ 4 h; 4) 30TMZ 18 h and DMSO 36 h; 5) 30TMZ 36 h and 900TMZ 18 h; 6) 900TMZ 36 h. Perhaps the most striking miRNA expression pattern was observed for 900TMZ-treated cells 36 h post-exposure, which corresponds with our observations that the most DE miRNAs were observed among this group of cells as determined by LPEseq (**Table 8**). This clearly suggests that 30TMZ-, and 900TMZ-treated cells have different miRNA expression profiles, and indicates 36 h post-exposure as a potential critical time-point for comparison. Moreover, the stark contrast between 900TMZ-treated cells 36 h post-exposure, and the time-matched DMSO control clearly indicates these miRNAs to be DNA damage-, and more specifically, TMZ-responsive.

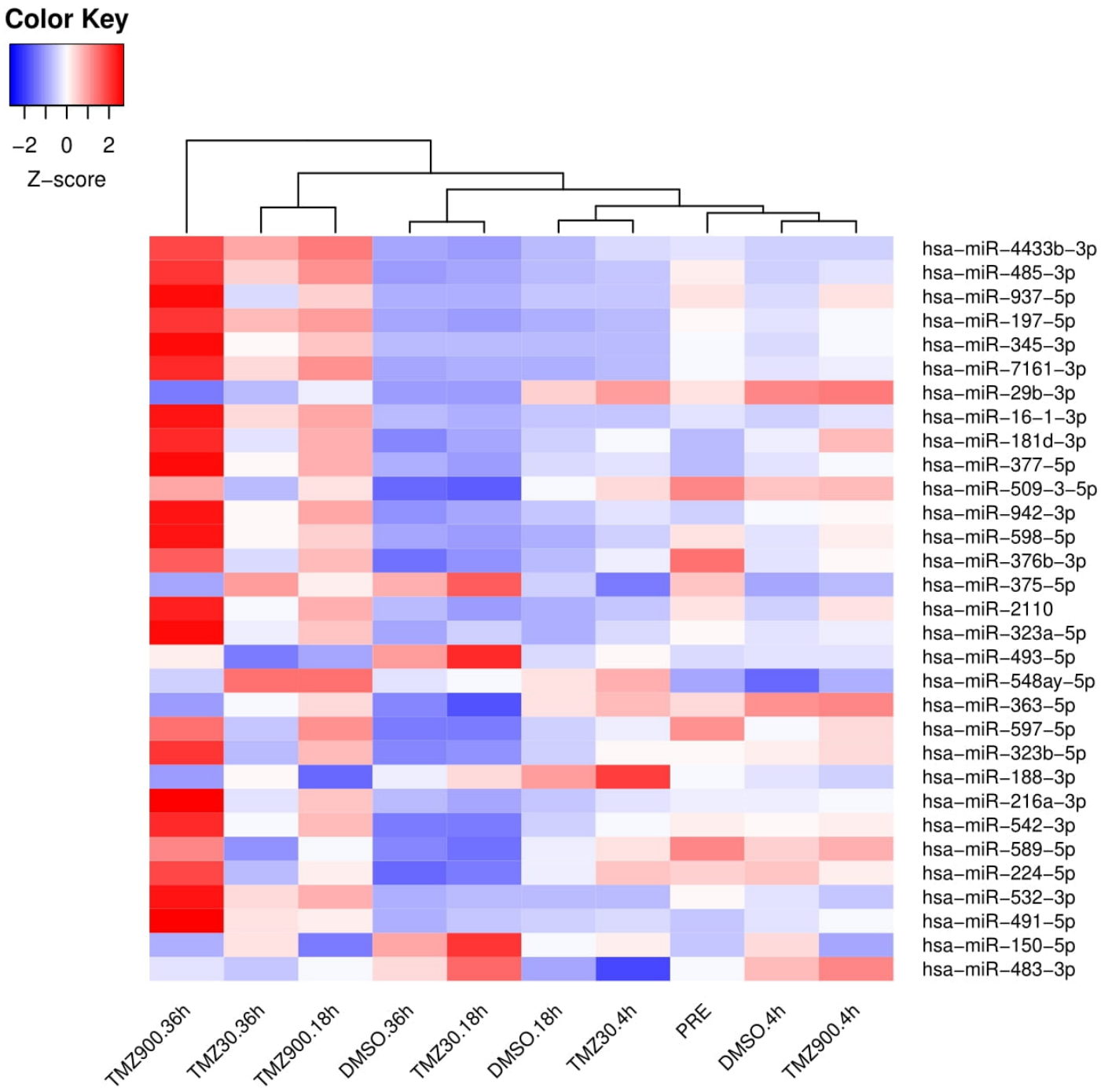

Figure 12. Heatmap representing log2(CPM) of DE miRNAs.

Log2(CPM) of DE miRNAs were scaled based on z-score which is derived from the row mean and standard deviation. Dendrogram indicates the relatedness in miRNA expression between samples. Specifically, six unique miRNA expression clusters are apparent: 1) Pre (untreated); 2) DMSO 4 h, 900TMZ 4 h; 3) DMSO 18 h and 30TMZ 4 h; 4) 30TMZ 18 h and DMSO 36 h; 5) 30TMZ 36 h and 900TMZ 18 h; 6) 900TMZ 36 h.

2.3.2. Selecting and validating miRNA expression among sub-lethal-, and lethal-treated TK6 cells

Originally, seven miRNAs were selected as representative of distinct expression patterns between DMSO-, and TMZ-treated, or 30TMZ-, and 900TMZ-treated cells (**Appendix E**). However, based on overall expression abundance, availability of validated primers, and detectability within our system, only miR-29b-3p, miR-363-5p, and miR-485-3p were retained for validation and further analysis. qRT-PCR analysis confirmed the expression of these miRNAs (**Fig. 13**). Strikingly, miR-29b-3p, miR-363-5p, and miR-485-3p showed a significant decrease from 4 h to 36 h post-exposure to 900TMZ (**p = 0.043**, **p = 0.002**, **p = 0.002**, respectively). A similar pattern was observed for miR-363-5p among 30TMZ-treated cells, showing a significant decrease (**p = 0.021**) from 4 h to 36 h post-exposure, however no significant differences were seen for miR-29b-3p or miR-485-3p. Pair-wise comparisons revealed miR-29b-3p, miR-363-5p, and miR-485-3p to be significantly decreased among 900TMZ-treated cells, 36 h post-exposure as compared to time-matched 30TMZ-treated cells (**p = 0.007, p = 0.022**, **p = 0.029**, respectively). This data confirms miR-29b-3p, miR-363-5p, and miR-485-3p to be DE when comparing sub-lethal and lethal TMZ doses, and aligns with our assertion that 36 h post-exposure is a critical time-point of distinct miRNA expression.

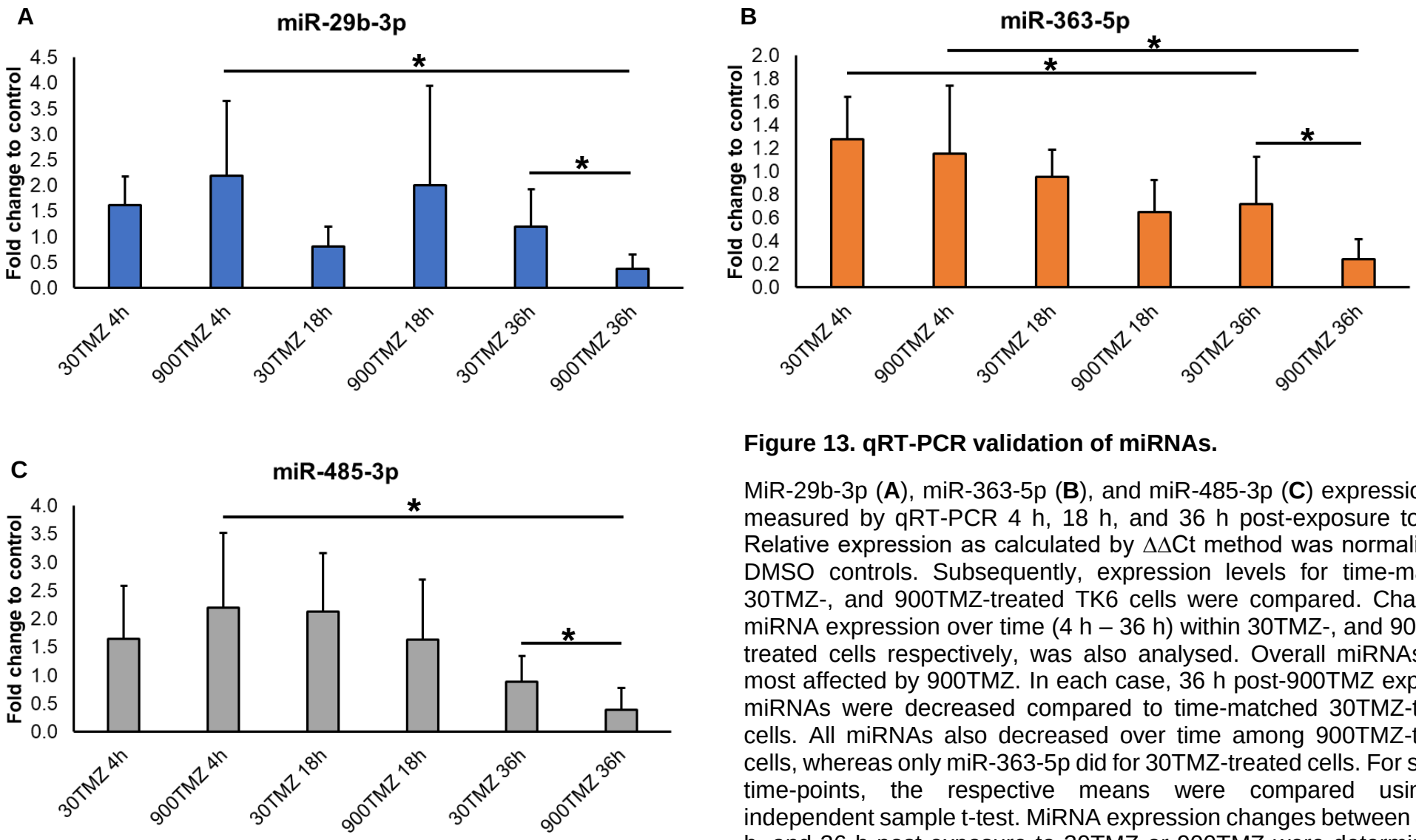

Figure 13. qRT-PCR validation of miRNAs.

MiR-29b-3p (**A**), miR-363-5p (**B**), and miR-485-3p (**C**) expression was measured by qRT-PCR 4 h, 18 h, and 36 h post-exposure to TMZ. Relative expression as calculated by ΔΔCt method was normalised to DMSO controls. Subsequently, expression levels for time-matched 30TMZ-, and 900TMZ-treated TK6 cells were compared. Change of miRNA expression over time (4 h – 36 h) within 30TMZ-, and 900TMZ-treated cells respectively, was also analysed. Overall miRNAs were most affected by 900TMZ. In each case, 36 h post-900TMZ exposure, miRNAs were decreased compared to time-matched 30TMZ-treated cells. All miRNAs also decreased over time among 900TMZ-treated cells, whereas only miR-363-5p did for 30TMZ-treated cells. For specific time-points, the respective means were compared using an independent sample t-test. MiRNA expression changes between 4 h, 18 h, and 36 h post-exposure to 30TMZ or 900TMZ were determined by one-way ANOVA and Tukey's post-hoc test, Welch's ANOVA and Dunnett's T3 post-hoc test, or Kruskal-Wallis with Bonferroni correction. Data normality was assessed with Shapiro-Wilk test. * represents significant ($p < 0.05$) differences. Data represents mean + SD (error bars). Data represents at least three biological repeats (**n = 3**).

2.3.3. Functional enrichment analysis of DE miRNAs

To identify specific biological processes associated with DE miRNAs, functional enrichment analysis was performed and the top ten most significantly enriched (lowest q-values) biological processes are displayed for each time-point and comparison where DE miRNAs were identified (**Figs. 14 - 17**). Comparing DMSO vs. 30TMZ at 4 h, the *cell population proliferation* term that was significantly enriched (**q = 0.01**) is of note, as this has a direct bearing on cell survival (**Fig. 14**). Furthermore, significant enrichment (**q = 0.013**) of the *activation of cysteine-type endopeptidase activity involved in apoptotic process* term is of particular relevance as it pertains to caspase activity. At the 18 h time-point within the same group, three significantly enriched GO:BP terms were of interest. The *negative regulation of transcription by RNA polymerase II* (**q < 0.001**) and *positive regulation of transcription by RNA polymerase II* (**q < 0.001**) are of interest as these could relate to miRNA transcription, whereas *positive regulation of cell population proliferation* (**q < 0.001**) relates to the cell cycle (**Fig. 15**). It is worth noting that at the 36 h time-point within the same group, only hsa-miR-4433b-3p was identified as DE, but functional enrichment could not be performed as it did not match any annotations within the databases used. Regarding DMSO vs. 900TMZ, at the 18 h time-point, *negative regulation of smooth muscle cell proliferation* (**q = 0.005**) and *type B pancreatic cell proliferation* (**q = 0.008**) were significantly functionally enriched, both having a bearing on cell survival (**Fig. 16**). Additionally, the significantly enriched (**q = 0.01**) term *positive regulation of transcription by RNA polymerase II* could pertain to miRNA transcription. Perhaps not surprisingly, at the 36 h time-point several GO:BP terms relevant to cell fate were significantly functionally enriched (**Fig. 17**). Among these, *protein phosphorylation* (**q < 0.001**), *positive regulation of protein phosphorylation* (**q < 0.001**), and *phosphorylation* (**q < 0.001**) are of note as it relates to DDR protein kinetics.

Moreover, *negative regulation of apoptotic process* (**q < 0.001**), *apoptotic process* (**q < 0.001**), and *positive regulation of cell population proliferation* (**q < 0.001**) has a bearing on cell fate, whereas *positive regulation of transcription by RNA polymerase II* (**q < 0.001**) relates to miRNA transcription. It is important to realise that miRNAs typically have a transcriptional repressive role, which implies, any functionally enriched terms resulting from the gene targets of increased DE miRNAs should be interpreted in an opposing sense. For example, the aforementioned *positive regulation of cell population proliferation* term may be interpreted as miRNAs facilitating the *negative* regulation of cell population proliferation. Thus, it is interesting to note that only 36 h post-900TMZ exposure had the *negative regulation of apoptotic process* term among the top ten functionally enriched biological processes, that ultimately implies a pro-apoptotic outcome and thus, reaffirming the lethal nature of 900TMZ. Admittedly, the expression pattern of all the DE miRNAs in **Fig. 12** have not been validated, and miRNAs are increasingly reported to also have a positive regulatory role in gene expression (Vasudevan, 2012; Xiao *et al*., 2017; Xu *et al*., 2022). Thus, our assumptions regarding the role of DE miRNAs mentioned in this thesis in context of the identified functionally enriched terms remains speculative. Nevertheless, with particular emphasis on the pattern of mostly increased DE miRNAs observed 36 h post-900TMZ exposure, and its corresponding functional enrichment of *negative regulation of apoptotic process*, it seems sensical that, at least at this time-point, our assertion of interpreting these terms in an opposing manner holds true.

Top 10 significantly (q < 0.05) enriched GO:BP terms for DMSO vs. 30TMZ at 4 hours.

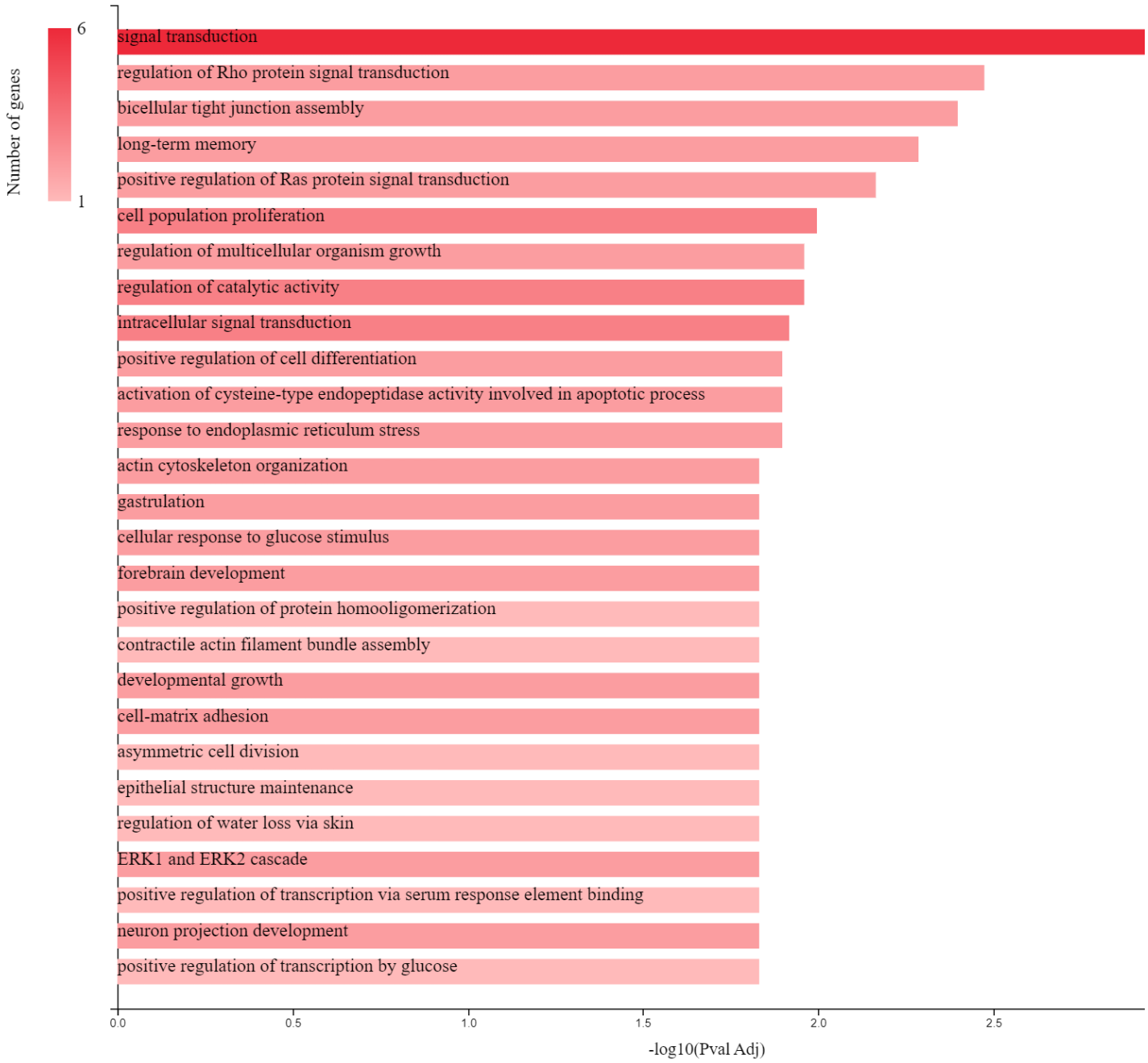

Figure 14. Functional enrichment of DE miRNAs when comparing DMSO-, and 30TMZ-treated TK6 cells 4 h post-exposure.

DE miRNAs resulting from comparison between DMSO-, and 30TMZ-treated cells 4 h post-exposure were arranged in descending order of significance (q-value), and functional enrichment was derived from the GO:BP database using GeneCodis 4. The length of the bars represents greater statistical significance and is arranged in descending order of significance. Bar colour intensity increases with the number of miRNA gene targets associated with respective biological processes. Top 10 enriched terms were included based on q-value, however, if the last term q-value was tied, subsequent terms were included until the tie was broken.

Top 10 significantly (q < 0.05) enriched GO:BP terms for DMSO vs. 30TMZ at 18 hours.

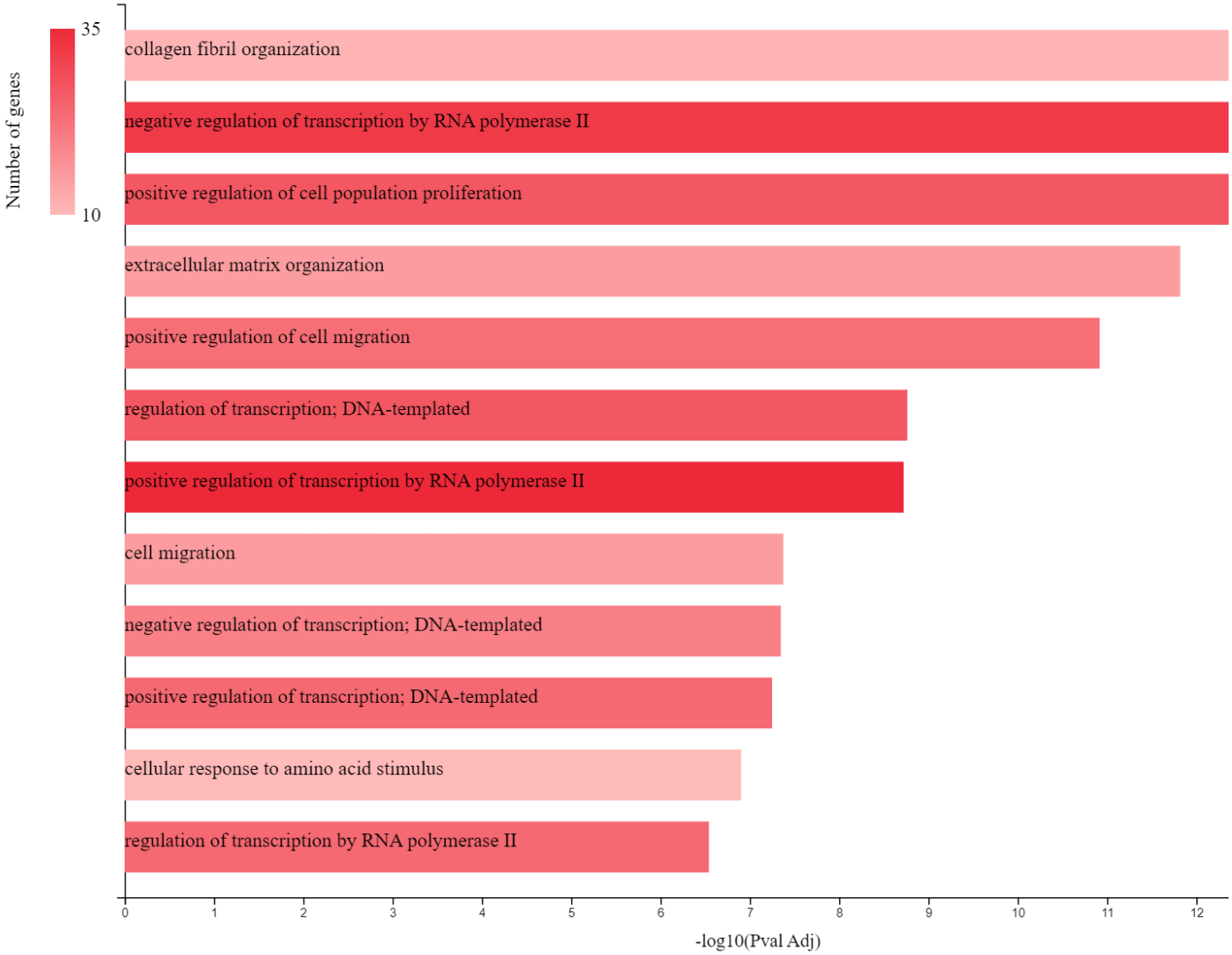

Figure 15. Functional enrichment of DE miRNAs when comparing DMSO-, and 30TMZ-treated TK6 cells 18 h post-exposure.

DE miRNAs resulting from comparison between DMSO and 30TMZ-treated cells 18 h post-exposure were arranged in descending order of significance (q-value), and functional enrichment was derived from the GO:BP database using GeneCodis 4. The length of the bars represents greater statistical significance and is arranged in descending order of significance. Bar colour intensity increases with the number of miRNA gene targets associated with respective biological processes. Top 10 enriched terms were included based on q-value, however, if the last term q-value was tied, subsequent terms were included until the tie was broken.

Top 10 significantly (q < 0.05) enriched GO:BP terms for DMSO vs. 900TMZ at 18 hours.

Figure 16. Functional enrichment of DE miRNAs when comparing DMSO-, and 900TMZ-treated TK6 cells 18 h post-exposure.

DE miRNAs resulting from comparison between DMSO and 900TMZ-treated cells 18 h post-exposure were arranged in descending order of significance (q-value), and functional enrichment was derived from the GO:BP database using GeneCodis 4. The length of the bars represents greater statistical significance and is arranged in descending order of significance. Bar colour intensity increases with the number of

miRNA gene targets associated with respective biological processes. Top 10 enriched terms were included based on q-value, however, if the last term q-value was tied, subsequent terms were included until the tie was broken.

Top 10 significantly (q < 0.05) enriched GO:BP terms for DMSO vs. 900TMZ at 36 hours.

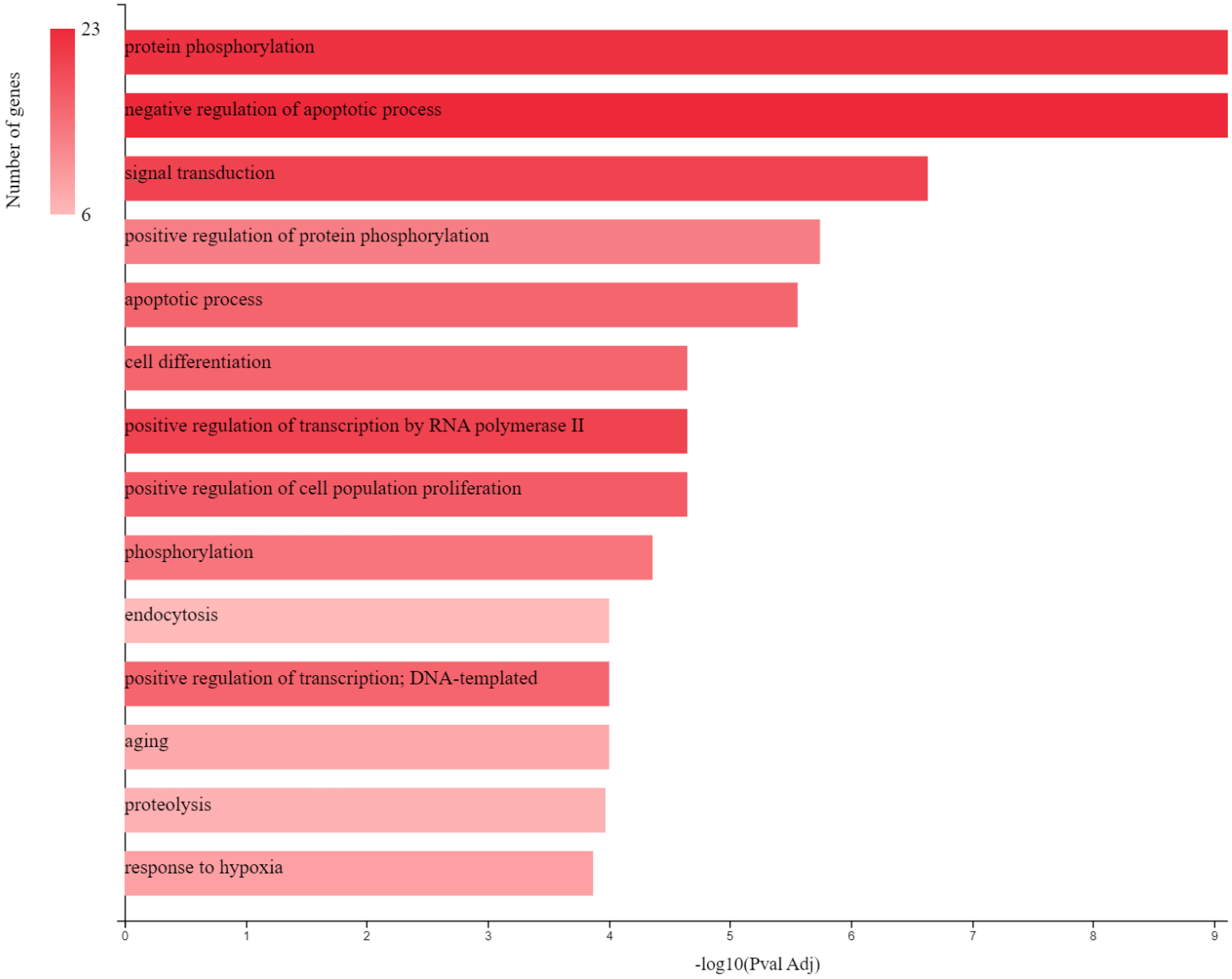

Figure 17. Functional enrichment of DE miRNAs when comparing DMSO-, and 900TMZ-treated TK6 cells 36 h post-exposure.

DE miRNAs resulting from comparison between DMSO and 900TMZ-treated cells 36 h post-exposure were arranged in descending order of significance (q-value), and functional enrichment was derived from the GO:BP database using GeneCodis 4. The length of the bars represents greater statistical significance and is arranged in descending order of significance. Bar colour intensity increases with the number of miRNA gene targets associated with respective biological processes. Top 10 enriched terms were included based on q-value, however, if the last term q-value was tied, subsequent terms were included until the tie was broken.

2.3.4. Correlating DDR protein and miRNA expression

To explore the possibility that miRNAs may be DDR-responsive, the expression of miR-29b-3p, miR-363-5p, and miR-485-3p was correlated with time (4 h, 18 h, and 36 h) post-exposure to 30TMZ or 900TMZ, respectively. Likewise, p53 protein levels were correlated with these time-points in 30TMZ-, and 900TMZ-treated cells, respectively. P53 was selected as it is a transcription factor and has been demonstrated to both repress and upregulate miRNAs (Liu *et al*., 2016). Our theory was that if these miRNAs are DDR-responsive, it would be reflected in the resulting correlation coefficients. Specifically, the direction of the correlation can inform if p53 has a potential regulatory function toward miR-29b-3p, miR-363-5p, and miR-485-3p. Indeed, the level of p53 showed a significant positive association with time (4 h, 18 h, and 36 h) in both 30TMZ-, and 900TMZ-treated cells (**p = 0.003**; **p = 0.004**, respectively) (**Fig. 18**). Importantly, the expression of miR-29b-3p, miR-363-5p, and miR-485-3p was consistently negatively associated with the same time-points in both TMZ-treated groups, respectively (**Figs. 19** and **20**). Although, among 30TMZ-treated cells, only miR-363-5p was significantly (**p = 0.004**) associated with time post-exposure (**Fig. 19B**). Contrarily, miR-29b-3p (**p = 0.008**), miR-363-5p (**p < 0.001**), and miR-485-3p (**p = 0.007**) were all significantly associated with time post-900TMZ exposure (**Figs. 20A - C**). To strengthen our assertion that these miRNAs might be regulated by p53, we sought to correlate p53 and miRNA levels over time, among 30TMZ-, and 900TMZ-treated cells directly. Unfortunately, the nature of our data limits the statistical appropriateness of such a correlation. Nonetheless, statistical appropriateness aside, an approximation of the relationship between p53 and respective miRNAs can be seen in **Appendix D**. For 30TMZ-treated cells, no significant correlation was observed between p53 and miRNAs (**Appendix D Fig. 37**). It should be noted that while our overall assertion is that no

correlation exists between p53 and miRNA expression among 30TMZ-treated cells, there were instances when a statistically significant correlation was observed. However, this was only observed for two of nine combinations when correlating p53 with miR-485-3p levels and was thus regarded as spurious (**Appendix D Table 11**). Among 900TMZ-treated cells, p53 showed a significant negative correlation with miR-363-5p (**p = 0.022**) (**Appendix D Fig. 38**). However, it should be noted that a significant correlation was also observed for 7 of 9 combinations when correlating p53 with miR-29b-3p, and 2 of 3 combinations when correlating p53 with miR-485-3p (**Appendix D Table 11**). While these findings are regarded as not having a significant correlation, it is appreciated that our classification of a significant correlation may be, necessarily, overly conservative.

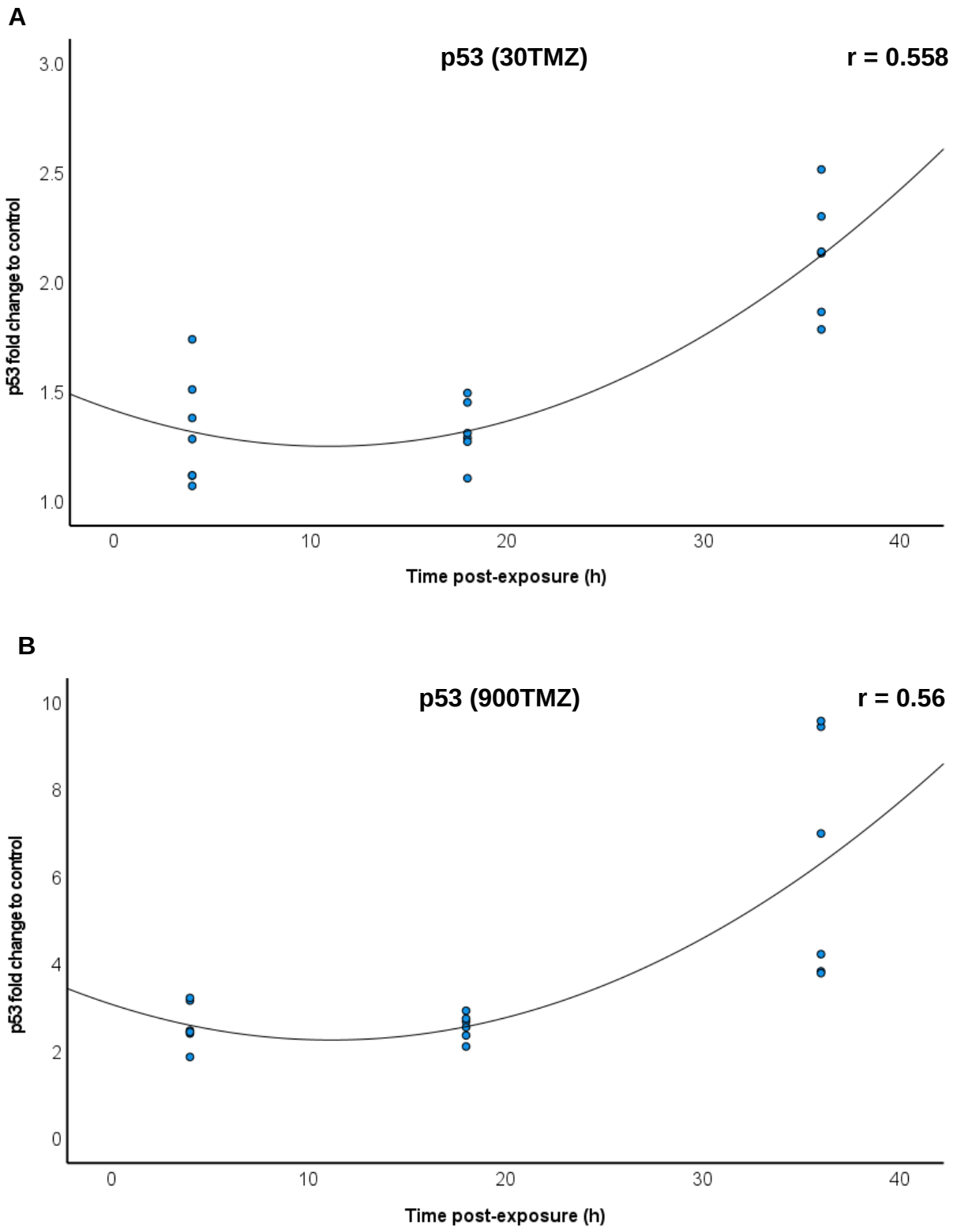

Figure 18. Correlation of p53 protein levels with time post-TMZ exposure.

Fold changes of p53 measured 4 h, 18 h, 36 h post-exposure to 30TMZ (**A**) and 900TMZ (**B**) were correlated with time (4 h, 18 h, and 36 h) post-exposure. A significant ($p < 0.05$) positive correlation between p53 levels and time post-exposure is seen for both 30TMZ-, and 900TMZ-treated cells, as determined with Kendall's tau-b. Scatter plots represent the individual data points of at least six (**n = 6**) biological replicates.

A

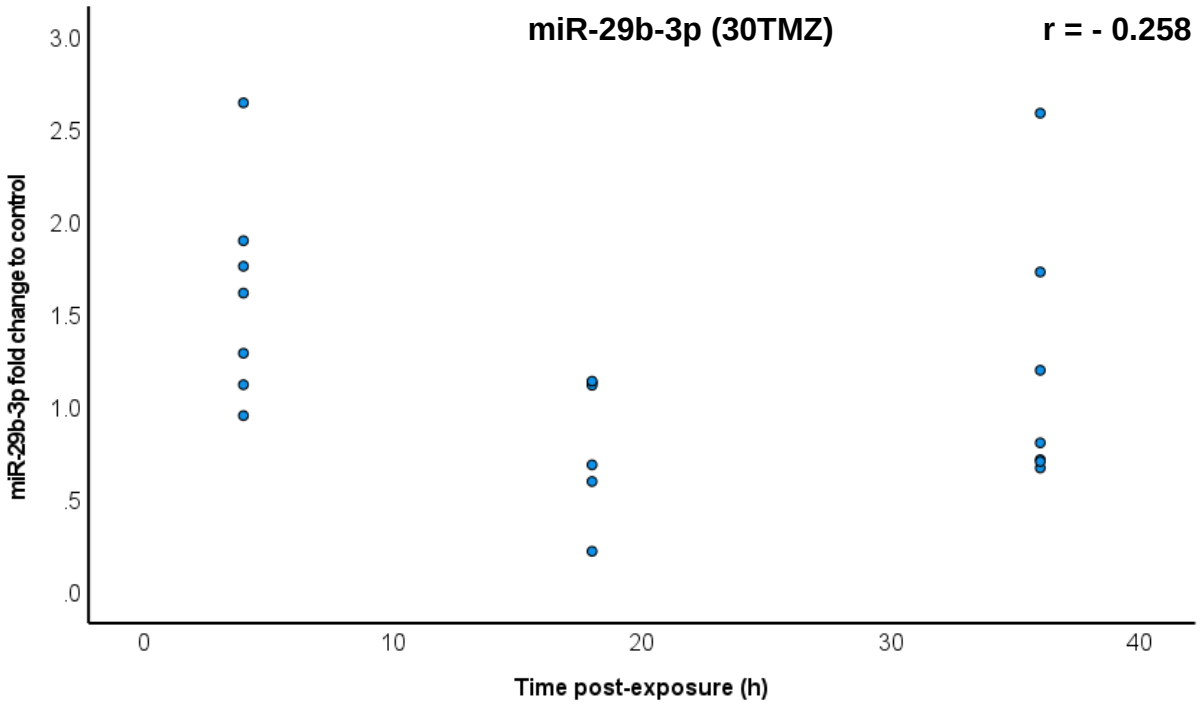
miR-29b-3p (30TMZ)
r = - 0.258
miR-29b-3p fold change to control
3.0
2.5
2.0
1.5
1.0
.5
.0
0
10
20
30
40
Time post-exposure (h)

B

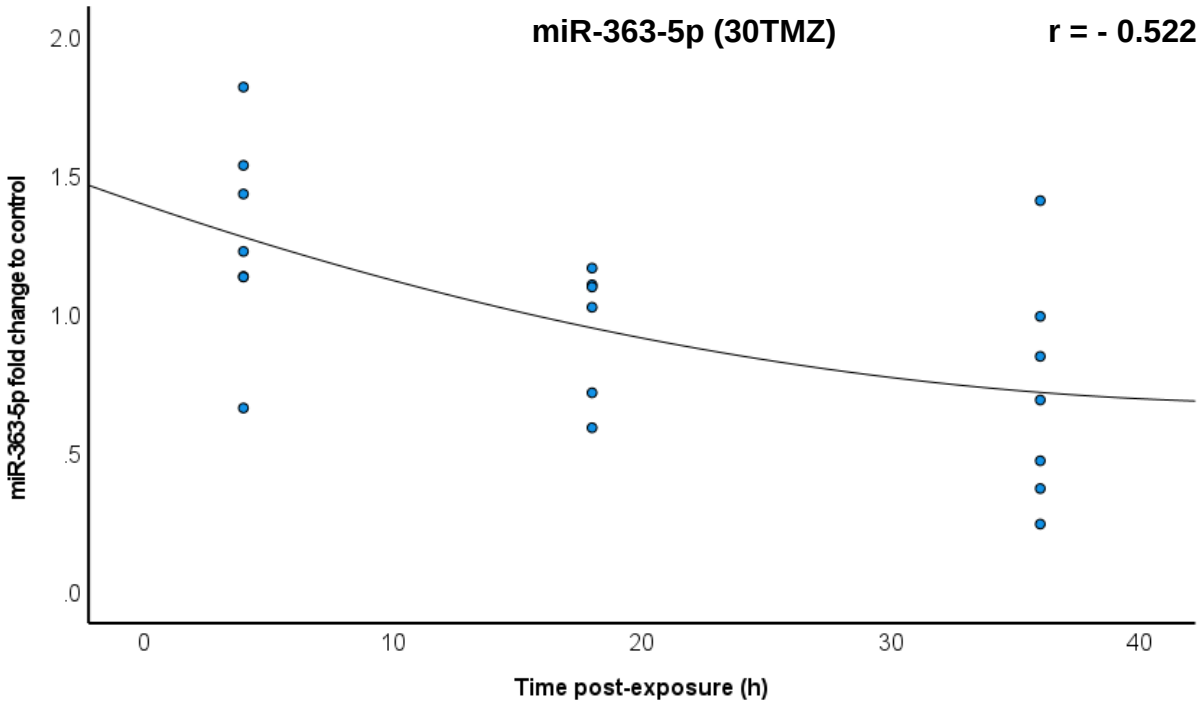
miR-363-5p (30TMZ)
r = - 0.522
miR-363-5p fold change to control
2.0
1.5
1.0
.5
.0
0
10
20
30
40
Time post-exposure (h)

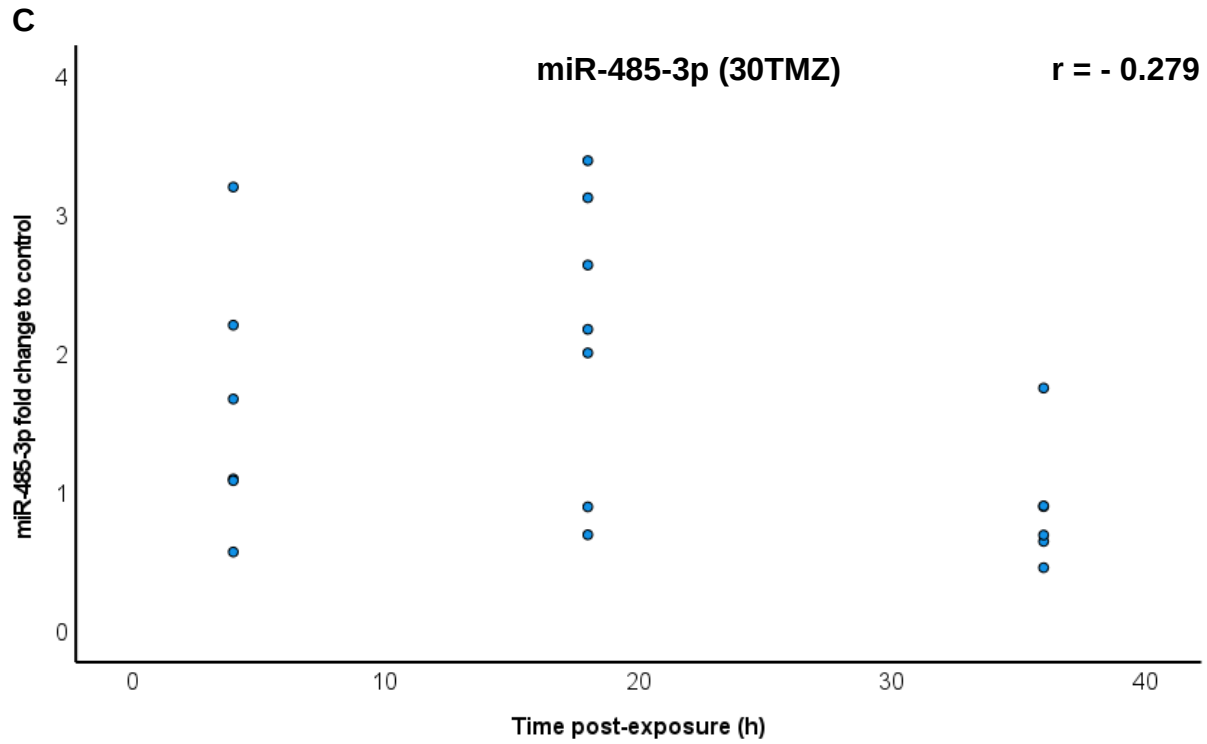

Figure 19. Correlation between miRNA levels and time post-30TMZ exposure.

Fold changes of miR-29b-3p (**A**), miR-363-5p (**B**), miR-485-3p (**C**) were correlated with time (4 h, 18 h, 36 h) post-exposure to 30TMZ. A significant ($p < 0.05$) negative correlation is only observed between miR-363-5p levels and time post-exposure, as determined with Kendall's tau-b. Scatter plots represent the individual data points of at least six (**n = 6**) biological replicates.

A

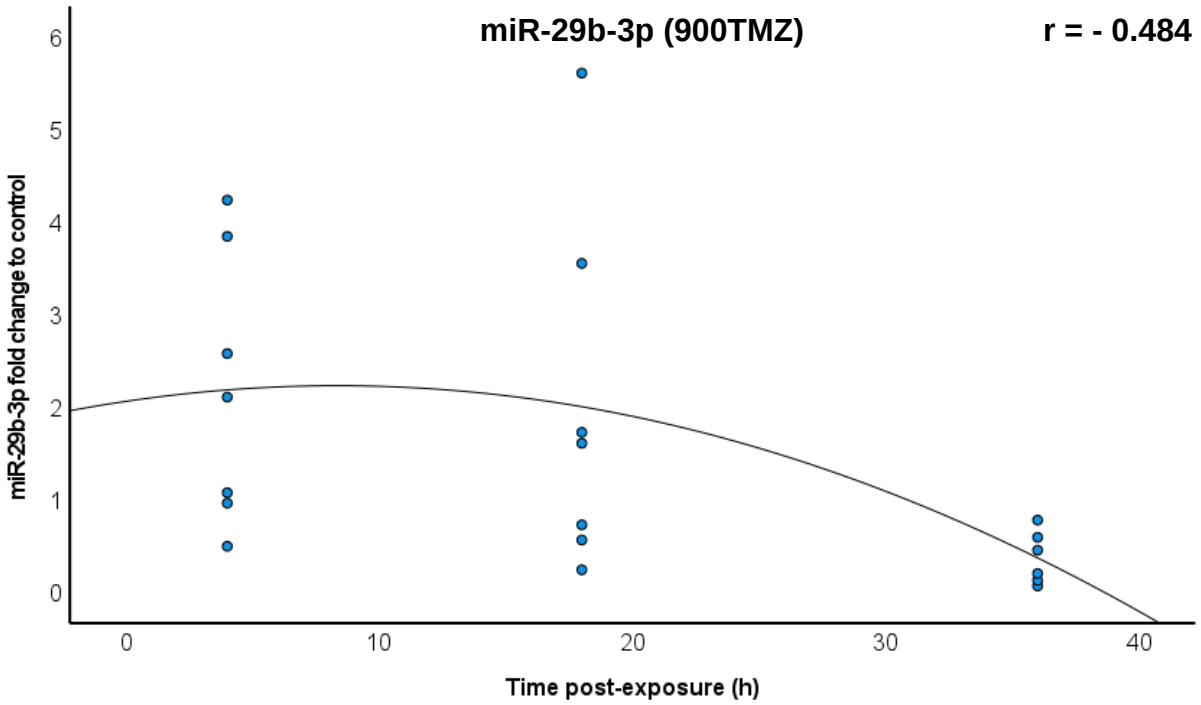
miR-29b-3p (900TMZ)
r = - 0.484
miR-29b-3p fold change to control
Time post-exposure (h)

B

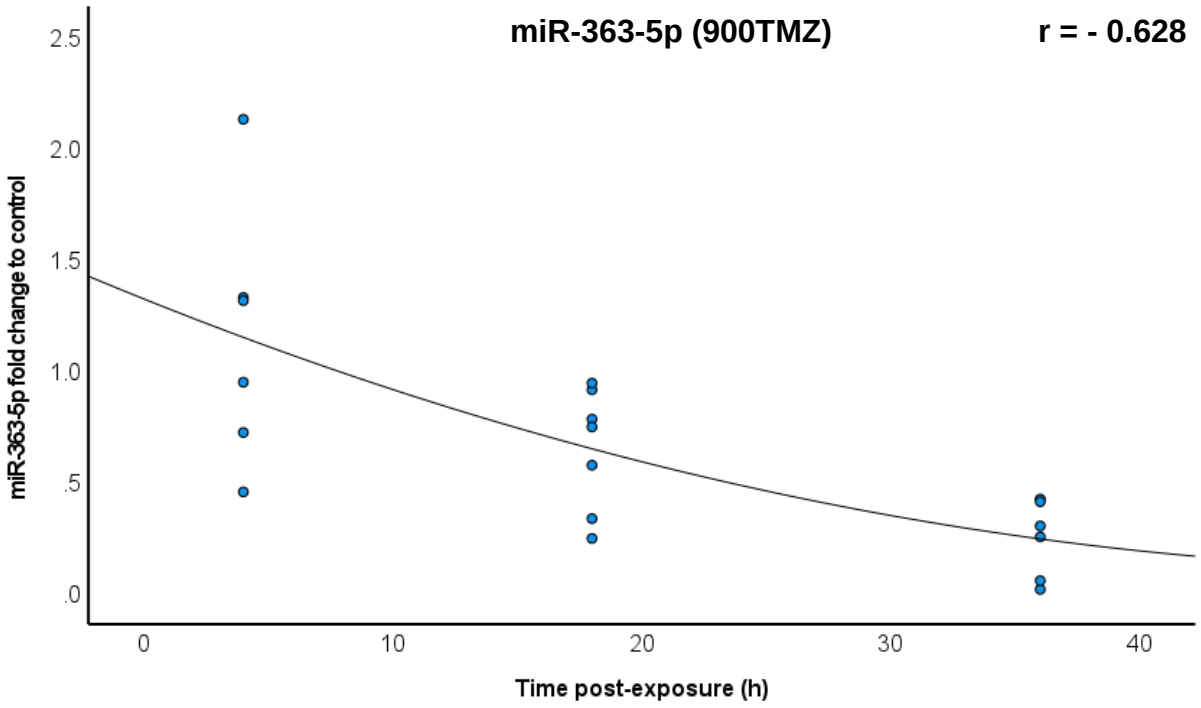
miR-363-5p (900TMZ)
r = - 0.628
miR-363-5p fold change to control
Time post-exposure (h)

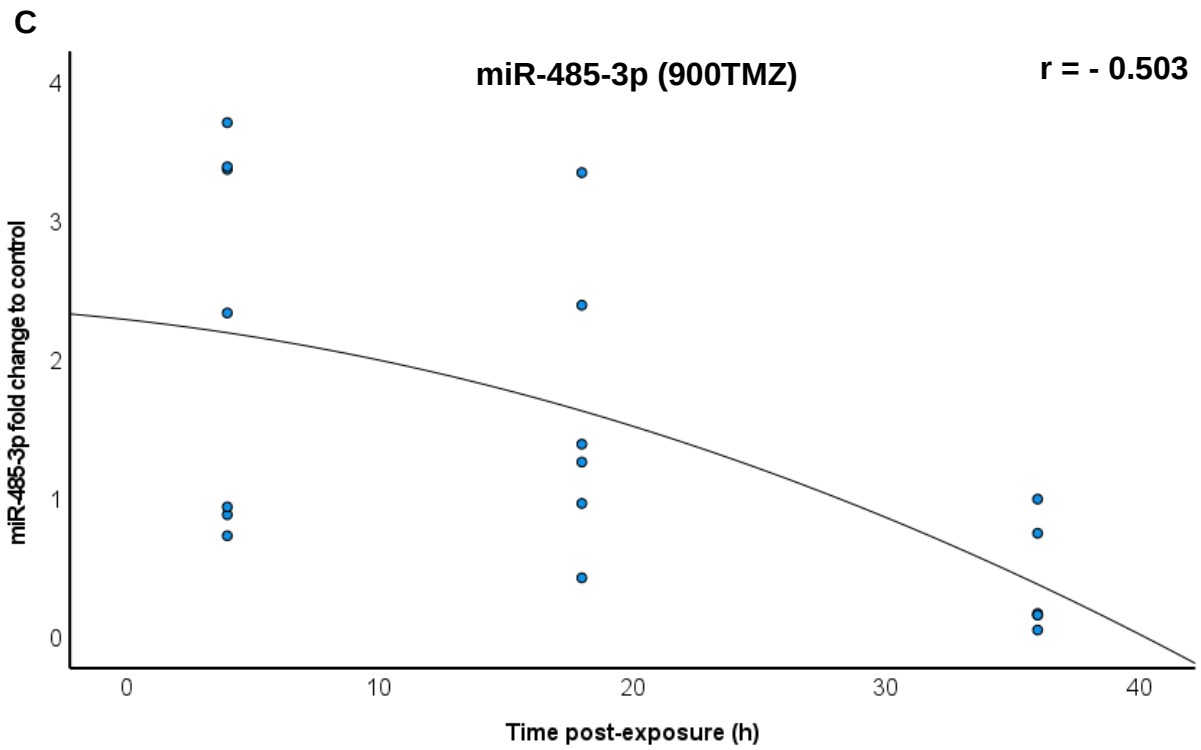

Figure 20. Correlation between miRNA levels and time post-900TMZ exposure.

Fold changes of miR-29b-3p (**A**), miR-363-5p (**B**), miR-485-3p (**C**) were correlated with time (4 h, 18 h, 36 h) post-exposure to 900TMZ. A significant ($p < 0.05$) negative correlation is observed between all miRNA levels and time post-exposure, as determined with Kendall's tau-b. Scatter plots represent the individual data points of at least six (**n = 6**) biological replicates.

2.4. Discussion

Exposure to genotoxicants can result in different cell fates, e.g., cell cycle arrest, DNA repair and subsequent survival, or apoptosis. How the distinction is made to follow a specific DDR continues to be a conundrum. Our research addressed this by investigating the existence of differential miRNA 'signatures' that may underpin a finely tuned DDR toward a specific cell fate. Indeed, 31 miRNAs were found to be differentially expressed in TK6 cells when exposed to sub-lethal and lethal doses of TMZ, and compared with DMSO controls. To the best of our knowledge, at the time of writing, this is the first report that identifies miR-29b-3p, miR-363-5p, and miR-485-3p to be DNA damage responsive, and differentially regulated in TK6 cells in response to TMZ.

Identifying molecular signatures that underpin the cellular response to DNA damage presents a multitude of treatment and diagnostic opportunities. Specifically, a miRNA profile indicative of apoptosis could inform successful chemotherapy, whereas the reverse is true for signatures indicative of survival outcomes such as cell cycle arrest and DNA repair. Additionally, identifying DE miRNAs in either cell fate creates potential druggable targets, or could identify miRNAs that may become treatment options themselves. Based on our observations, it is clear that miRNAs are intimately involved with DDR regulation. Given that the DDR directs cell fate, it is reasonable to assume a corresponding alteration in those miRNAs involved with different cell fates. Indeed, different miRNA profiles were observed when comparing DMSO-, and TMZ-treated TK6 cells (**Table 8; Figs. 12** and **13**). Particularly, 900TMZ-treated cells showed 23 DE miRNAs at 36 h post-exposure while only 1 miRNA was DE for the same time-point among 30TMZ-treated cells. Recall (**Chapter 1**), at this time-point, 900TMZ-treated cells preferentially underwent apoptosis, whereas 30TMZ-treated cells arrested in G_2-phase. Consequently, it is likely that at least some of the DE miRNAs observed 36 h

post-900TMZ exposure is in response to DNA damage and/or apoptosis. Thus, the lack of these same DDR-responsive miRNAs among 30TMZ-treated cells might suggest that the DNA damage induced by 30TMZ is either resolved within 36 h post-exposure, or tolerated to an extent that does not provoke significantly altered miRNA expression.

Considering the distribution of the primary TMZ-induced adduct spectrum (*N*7-meG (> 70%), *N*3-meA (≈ 9%), O^6-meG (5%)) (Newlands *et al*., 1997), it is not unreasonable to assume that at sub-lethal doses, like 30TMZ, the primary source of DNA damage results from *N*3-meA and *N*7-meG adducts, as they constitute ≈ 80% of TMZ-induced lesions. However, these lesions are efficiently repaired by BER (Zhang, Stevens, and Bradshaw, 2012), and may thus explain why the same DDR-responsive miRNAs that are observed 36 h post-900TMZ exposure, is not observed for time-matched 30TMZ-treated cells. Turning attention to O^6-meG, these lesions are not resolved in TK6 cells as they are MGMT deficient (Chapman, Doak, and Jenkins, 2015). In spite of this, it is possible that 30TMZ might not result in sufficient O^6-meG accumulation within our investigated time-frame to elicit altered miRNA expression, especially considering it only constitutes ≈ 5% of the TMZ-induced damage spectrum. Nonetheless, even at low levels, O^6-meG remains an adduct to be repaired, and thus retains genotoxic potential. This implies an underlying tolerance to O^6-meG adducts induced by sub-lethal TMZ doses in TK6 cells. Thus, the question becomes, by what means do TK6 cells undermine O^6-meG genotoxicity? Recall (**Chapter 1**), the genotoxic potential of O^6-meG is underpinned by the MMR futile cycle. Specifically, it has been suggested that MMR precipitates stalled replication forks, which can lead to DSBs (Feitsma, Akay, and Cuppen, 2008; Gupta *et al*., 2018). Thus, it is reasonable to assume that mechanisms that can prevent stalled replication forks may contribute to a tolerance of O^6-meG adducts. One such mechanism is DNA translesion synthesis (TLS), a mechanism known to be active in

TK6 cells (Tsuda *et al*., 2019; Inomata *et al*., 2021), and thus, could be its means of undermining low levels of O^6-meG adducts. Consequently, this could explain why 30TMZ-treated cells do not display a similarly altered miRNA expression profile as 900TMZ-treated cells, 36 h post-exposure.

Further supporting distinct miRNA profiles in TK6 cells exposed to sub-lethal and lethal TMZ doses, hierarchical clustering of log2(CPM) derived z-scores from different treatment groups revealed distinct miRNA expression patterns as indicated by a dendrogram (**Fig. 12**). Specifically, 36 h post-exposure to 900TMZ emerged as a distinct miRNA profile, suggesting 36 h post-exposure as an important time-point in the cellular response to lethal DNA damage. Admittedly, the nature of this data set does not allow resolution of absolute directional changes in miRNA expression, and thus, was regarded a largely qualitative representation of the *presence* of distinct miRNA expression patterns, thereby informing subsequent analyses. To that end, miR-29b-3p, miR-363-5p, and miR-485-3p were selected, and expression patterns were validated with qRT-PCR (**Fig. 13**). Indeed, these miRNAs were found to be differentially expressed between 30TMZ and 900TMZ, specifically at 36 h post-exposure, thereby confirming our earlier suggestion based on hierarchical clustering of log2(CPM) derived z-scores, that 36 h post-exposure is an important time-point in response to lethal and sub-lethal DNA damage. Importantly, 900TMZ-treated cells did not only have significantly lower expression of each of these miRNAs when compared to 30TMZ-treated cells at 36 h post-exposure, but it also decreased significantly over time (4 h – 36 h), suggesting these miRNAs to be both dose-, and time-responsive. Similarly, miR-363-5p decreased significantly with time among 30TMZ-treated cells, thus suggesting miR-363-5p to be both dose-, and time-responsive among sub-lethal and lethal TMZ doses.

The concept of differential miRNA expression patterns in response to varying degrees of DNA damage is gaining traction, and our results fit well within the reported dose responsive miRNA landscape. For example, mice exposed to sub-lethal or lethal doses of radiation exhibit different serum miRNA profiles (Acharya *et al*., 2015). While miR-187-3p, miR-194-5p, and miR-27a-3p were significantly downregulated 24 h after lethal radiation exposure, miR-30c-5p and miR-30a-3p were significantly upregulated when compared to sub-lethal doses. Another example is reported by Kumar, Ghosh, and Chandna (2015) that observed miR-31 upregulation in response to lethal radiation and likewise, downregulation in response to sub-lethal radiation in insect cells with an apoptotic mechanism, and miR-31, that is conserved between insects and mammals. MiR-31 upregulation corresponded to increased apoptosis, as indicated by caspase-3 activity. Moreover, the authors suggested miR-31 to promote apoptosis, at least in part, by promoting mitochondrial translocation of BAX in a BIM-dependent manner. Strikingly, miR-31 transfection maintained a pro-apoptotic phenotype even in the absence of radiation. MiR-96 expression has also been demonstrated to be dose-dependent as 1 – 2 µg/mL cisplatin, or 1 – 2 µM dox can significantly induce its expression after 24 h, whereas higher doses (up to 10 µg/mL or 10 µM respectively) were either unable to do so, or to a lesser extent than that of the lower doses (Lang *et al*., 2018). The authors suggested miR-96 to inhibit FOXO1, which in turn caused p21 repression, thereby supporting a pro-survival phenotype. Moreover, although not explicitly measuring apoptosis, miR-96 over-expression decreased cell death rate based on the fraction of PI positive cells. These findings are supported by that of Wang *et al*. (2020) that demonstrated miR-3174 to inhibit apoptosis by antagonising FOXO1 in hepatocellular carcinoma cells. Another example is described by Leslie *et al*. (2018) that showed miR-103 and miR-107 are significantly upregulated by lethal doses of dox, whereas sub-

lethal doses were less/unable to do so. In turn, miR-103 and miR-107 inhibited low-density lipoprotein receptor-related protein (LRP1), thereby promoting apoptosis. LRP1 is known to mediate anti-apoptotic functions by promoting AKT pathway activation (Fuentealba *et al*., 2009). Although, the association between lethal doses and LRP1 may be more applicable to miR-103, as miR-107 was also significantly upregulated after sub-lethal doses, albeit less than at lethal doses. Although these studies indicate differential miRNA expression at varying treatment doses (and by extension, DNA damage), interpretations should be made with caution as 'lethal' and 'sub-lethal' doses may be context-dependent descriptors likely to differ between studies.

The question becomes, 1) Why are miRNAs differentially expressed in response to different levels of genotoxicity? 2) How is this related to cell fate? While the aforementioned studies implicate some miRNAs in a DNA damage responsive context, our study provides an expansive extrapolation of DE miRNAs in a dose-, and time-dependent context. Consequently, we were able to perform functional enrichment and identify dose-, and time-dependent changes in biological processes (**Figs. 14 – 17**). Perhaps the most telling observation is the disparity between functionally enriched terms of 30TMZ-, and 900TMZ-treated cells, 36 h post-exposure. Specifically, 900TMZ-treated cells 36 h post-exposure had the *negative regulation of apoptotic process* term among the top ten functionally enriched biological processes, that ultimately implies a pro-apoptotic outcome (**Fig. 17**). This is not unexpected given our previous observations that 900TMZ-treated cells have a predominantly apoptotic phenotype 36 h post-exposure (**Chapter 1**). Moreover, enrichment of *protein phosphorylation* and *positive regulation of protein phosphorylation* fits well within the context of DDR signalling. Recall that the DDR is driven by a cascade of phosphorylations and dephosphorylations to effect specific cell fates. Regarding 30TMZ-treated cells at the same time-point, no

functionally enriched terms were identified, and thus, could be construed as confirmation of its sub-lethal status (**Chapter 1**). Moreover, the absence of any enriched pathways among these cells could also suggest that 36 h post-exposure, 30TMZ-treated cells have largely recovered from the TMZ-induced insult, and now approximates homeostasis. However, this contrasts our earlier observations (**Chapter 1**), that 36 h post-30TMZ exposure, cells are still predominantly arresting in G_2-phase. It is plausible that the changes in miRNA expression that might have brought about the G_2-arrest occurred 18 h post-30TMZ exposure, acting as initiators to set in motion the molecular mechanisms that facilitate cell cycle arrest. In this capacity as initiators, it makes sense that continuous altered miRNA expression is not required, and thus explains the absence of functionally enriched terms related to cell cycle arrest, 36 h post-30TMZ exposure. This assumption is supported by the functionally enriched terms identified 18 h post-exposure to 30TMZ (**Fig. 15**). Particularly, *positive regulation of cell population proliferation*, which could imply a cell cycle arrest phenotype, given the primarily repressive role of miRNAs on the target genes from which these GO:BP terms are derived. However, miRNAs are increasingly reported to also have a positive regulatory role in gene expression, and thus, this assumption remains speculative (Vasudevan, 2012; Xiao *et al*., 2017; Xu *et al*., 2022). It is also interesting to note that 18 h post-exposure to 30TMZ and 36 h post-exposure to 900TMZ, terms related to transcriptional regulation by RNA polymerase II were functionally enriched. Although this could just be indicative of transcriptomic changes, it is tempting to speculate that it stems from the regulation of miRNA transcription at these time-points, particularly as the most DE miRNAs were observed at these time-points within respective treatment groups. Admittedly, *positive regulation of transcription by RNA polymerase II* was also significantly enriched 18 h post-900TMZ exposure, though, to a much lesser extent than

that observed 36 h post-900TMZ exposure (**q = 0.01** vs. **q < 0.001**). It is possible that the enrichment of this term 36 h post-900TMZ exposure is a continuation of the one observed 18 h post-exposure and may be required to precipitate the significant downregulation of miR-29b-3, miR-363-5p, and miR-485-3p that is seen when expression levels are compared between 30TMZ-, and 900TMZ-treated cells, 36 h post-exposure.

It is telling that significant differences in miR-29b-3p, miR-363-5p, and miR-485-3p expression occurred 36 h post-exposure when comparing 30TMZ and 900TMZ. Specifically, the expression of these miRNAs were significantly repressed among 900TMZ-treated cells, as compared to those treated with 30TMZ (**Fig. 13**). This time-point corresponds with the previously reported assertion that TMZ requires at least two replicative cycles to exert its full genotoxic potential (Quiros, Roos, and Kaina, 2010). Thus, it is tempting to speculate that these miRNAs are pro-survival/anti-apoptotic e.g., promoting DNA repair and cell cycle progression, and thus need to be repressed when DNA damage occurs to maintain DNA replicative fidelity. Indeed, miR-29b-3p has been reported to be anti-apoptotic. For example, miR-29b-3p transfected human cardiomyocytes are protected against hypoxic-induced apoptosis by directly targeting TRAF5 (Cai and Li, 2019). Similarly, miR-29b-3p has been demonstrated to inhibit apoptosis and promote proliferation in breast cancer cells in a NF-κβ-dependent manner by directly targeting TRAF3 (Zhang *et al*., 2019). However, miR-29b-3p can also be pro-apoptotic, as miR-29b-3p transfected NSCLC cells showed increased sensitivity to cisplatin as indicated by increased apoptosis and BAX expression, and decreased proliferation. The authors attributed this to miR-29b-3p directly targeting COL1A1 (Jia and Wang, 2020). Incidentally, COL1A1 was also identified as a putative target for both miR-29b-3p, and miR-363-5p in our bioinformatics analysis (discussed in **Chapter 3**).

Showing similar duality in effecting cell fates, miR-485-3p has been reported to be both pro-, and anti-apoptotic. For example, miR-485-3p has been reported to upregulate BAX and caspase-3, and downregulate Bcl-2 in renal carcinoma cells, an effect that was partially reversed by circHIPK3-mediated sponging of miR-485-3p (Lai *et al*., 2020). Contrarily, miR-485-3p can promote proliferation and inhibit apoptosis in chondrocytes by targeting NOTCH2, thereby negatively impacting the NF-κβ pathway (Zhou *et al*., 2021). The involvement of miR-363-5p in cell fate determination is not well described. It has been reported that miR-363-5p has no detectable effect on apoptosis in transfected squamous carcinoma cells, however, it is reportedly anti-proliferative, despite having caused marked upregulation of EGFR (Khuu *et al*., 2014), a proto-oncogene with proliferative and anti-apoptotic functions (Wee and Wang, 2017). These examples demonstrate the molecular ambivalence of miRNA-mediated regulation that underpins the complexity of cell fate determination.

Notwithstanding the molecular ambivalence of miRNAs, unravelling its involvement in cell fate determination is further complicated by miRNA-DDR protein cross-talk. Our data demonstrated p53 protein levels to be significantly positively correlated with time post-exposure to both 30TMZ and 900TMZ (**Fig. 18**). Moreover, all miRNAs tested were negatively correlated with time post-exposure to both 30TMZ and 900TMZ (**Figs. 19** and **20**). However, among 30TMZ-treated cells, only miR-363-5p showed a significant negative correlation with time, whereas all miRNAs among 900TMZ-treated cells showed a significant negative correlation with time. Given the opposing directions in which p53 and the miRNAs are regulated in response to TMZ could be suggestive of a miRNA-regulatory role for p53. Supporting this assertion is our previous observations that p53 protein levels are significantly increased among 900TMZ-treated cells, as compared to 30TMZ-treated cells at 4 h, 18 h, and 36 h post-exposure (**Chapter 1**).

Thus, it is tempting to speculate that among 30TMZ-treated cells, miR-29b-3p and miR-485-3p did not show a significant negative correlation with time, because this dose does not facilitate sufficient p53 accumulation. Contrastingly, among 900TMZ-treated cells in which p53 levels were significantly increased at every time-point as compared to 30TMZ-treated cells (**Chapter 1**), a significant negative correlation of all miRNAs with time post-exposure was observed. This further implicates p53 as a potential negative regulator of miR-29b-3p, miR-363-5p, and miR-485-3p.

Admittedly, a direct correlation between miRNA and p53 levels would provide more insight regarding any existing relationship. However, the nature of our data limits the statistical appropriateness of such a correlation. Nonetheless, an approximation of what such a correlation might look like can bee seen in **Appendix D**. Indeed, our data demonstrated a significant negative correlation between p53 protein levels and miR-363-5p expression among 900TMZ-treated cells. Specifically, as p53 levels increased, the level of miR-363-5p decreased (**Appendix D Fig. 38**). Moreover, while our classification of a significant correlation deemed the relationship between p53 and miR-29b-3p, and miR-485-3p to be respectively non-significant, it is likely a consequence of an overly conservative, but necessary, approach. Specifically, 7 of 9 correlation combinations between p53 and miR-29b-3p showed a significant negative correlation. Similarly, 2 of 3 correlation combinations between p53 and miR-485-3p showed a significant negative correlation. Contrastingly, no correlation was observed between p53 and miRNAs among 30TMZ-treated cells. Admittedly, it could be argued that the seemingly random distribution of the data (**Appendix D Fig. 37**) does not lend itself well to a Spearman correlation test. However, the absence of a clear monotonic relationship between p53 and miRNAs among 30TMZ-treated cells is, in itself, indicative of a differential response as compared to 900TMZ-treated cells. While correlation does not

presume causation, it is tempting to speculate that the expression of miRNAs is tied to DDR protein levels. Specifically, p53 has been known to regulate, and be regulated by miRNAs.

P53 can regulate miRNAs both transcriptionally, and post-transcriptionally. Mechanistically, this entails direct or indirect interaction of p53 with miRNA promoters or their host genes, or with miRNA biogenesis machinery respectively (**Fig. 22**, **Chapter 3**). For example, p53 is well-known to directly transactivate miR-34 (Bommer *et al*., 2007; Chang *et al*., 2007). Specifically, miR-34a is a transcriptional target of p53 and promotes p53 functions either by positive regulation, or in support of a specific phenotype, e.g., apoptosis. This was observed by Bommer *et al*. (2007) that demonstrated Bcl-2 as a target of miR-34a.

Furthermore, miR-22 has been demonstrated as pro-apoptotic as evidenced by upregulated BAX and caspase-3 in miR-22 transfected, lipopolysaccharide (LPS)-treated human glial cells (Yu, Zeng, and Sun, 2018). Importantly, the authors suggested miR-22 to be regulated by p53, as p53 inhibition resulted in significant miR-22 inhibition. Another example is that of miR-145 that has pro-apoptotic functions. In addition to promoting extrinsic apoptosis (discussed in **Chapter 3**) (Zaman *et al*., 2010), miR-145 can also induce apoptosis in several breast cancer cell lines, even in the absence of DNA damage (Spizzo *et al*., 2010). Mechanistically, miR-145 augments the transcriptional capabilities of p53 as evidenced by induced PUMA and p21 following miR-145 transfection. Additionally, p53 induction corresponded with miR-145 expression, suggesting a positive feedback loop. Similarly, p53 is suggested to transcriptionally regulate miR-192, miR-194, and miR-215 in multiple myeloma cells, as p53 upregulation corresponded with concomitant upregulation of the respective miRNAs. Subsequently, these miRNAs promote p53 stabilisation by antagonising

MDM2, thus forming a positive feedback loop. Noteworthy is that miR-192 and miR-215 can be classified as pro-apoptotic as they were demonstrated to target both insulin-like growth factor (IGF-1) and IGF-1R (Pichiorri *et al*., 2010), which are components of the pro-survival IGF-1/PI3K/AKT pathway (Zhang *et al*., 2018).

MiR-605 has also been suggested to promote apoptosis indirectly by disrupting the p53-MDM2 interaction. Interestingly, the authors demonstrated miR-605 to promote apoptosis, comparable to the effect of dox. Though, this effect is likely a result of miR-605 supporting p53 liberation from MDM2, rather than direct participation in the apoptotic pathway. Moreover, miR-605 is also reportedly under the transcriptional control of p53 that interacts with its host gene, protein kinase CGMP-dependent 1 (PRKG1), thus forming a positive feedback loop (Xiao *et al*., 2011). This exemplifies how p53 can promote miRNA expression by host gene upregulation in its capacity as a transcription factor. This relates to the observations of Barsotti *et al*. (2012) that identified plasmacytoma variant translocation 1 (PVT1) as a transcriptional target of p53. Importantly, PVT1 hosts miR-1204, which was demonstrated to increase the sub-G_1 fraction among untreated, transfected colorectal cancer cells. Although sub-G_1 is often used to indicate cell death, this approach is fallible as sub-G_1 denotes DNA fragmentation which can also result from mechanical stresses during sample processing, or non-apoptotic chromosomal fragmentation (Darzynkiewicz *et al*., 1997). Nonetheless, miR-1204 was capable of upregulating p53 protein levels following transfection, thus suggesting a p53-miR-1204 positive feedback loop.

Another pro-apoptotic miRNA is described by Yang *et al*. (2017), showing miR-15a to antagonise anti-apoptotic, neuronal apoptosis inhibitory protein (NAIP), *in vitro*. Although miR-15a expression was induced by p53 upregulation, the authors suggest p53 to regulate miR-15a post-transcriptionally, as only pre-miRNA-15a was induced by

p53 upregulation, and not pri-miR-15a. Furthermore, while miRNA (or miRNA host gene) promoter transactivation constitutes transcriptional regulation, the observations by Yang *et al*. suggests p53 can extend miRNA induction post-transcriptionally. For example, p53 promotes pri-, to pre-miRNA maturation of miR-16-1, miR-143, and miR-145 by interacting with DROSHA through DDX5 (Suzuki *et al*., 2009). Incidentally, each of these miRNAs have pro-apoptotic tendencies. While miR-16 and miR-145 have been discussed previously, miR-143 contributes toward apoptosis by inhibiting Bcl-2 (Li *et al*., 2016). Of note, miR-16-1-3p was found to be differentially expressed in our study, 36 h post-exposure to 900TMZ (**Table 8**). This makes sense given the predominantly apoptotic phenotype observed among these cells at this time-point.

While all the aforementioned examples portray a stimulatory role for p53 in the context of miRNA upregulation, p53 can also repress miRNA levels. For example, p53 competent colorectal cancer cells treated with either, etoposide, hydrogen peroxide, or UV, caused a significant reduction in let-7a and let-7b, while this was not observed in p53 depleted cells. Additionally, the authors suggested this p53-mediated repression of let-7a and let-7b to be ATM dependent, as repression of these miRNAs were not observed in $ATM^{-/-}$ fibroblasts (Saleh *et al*., 2011). However, it should be noted that this ATM dependence may be contingent on DNA damage that is preferentially detected by ATM. It could be argued that it is less about the upstream DNA damage detecting kinase, and more about the resulting stabilisation of p53, which can also be achieved by ATR. Consequently, while let-7a and let-7b repression is p53-dependent, p53 stabilisation is facilitated by both ATM and ATR, and is thus DNA damage dependent. Another example of p53-mediated miRNA repression is described by Liang *et al*. (2013). The authors describe p53 and the NF-κβ p65 subunit to individually and co-operatively bind and repress the miR-224 host gene, *GABRE*, in murine granulosa cells. Individual

or combined inhibition of p53 and p65 caused a significant increase in pri-miR-224, which resulted in miR-224-mediated repression of *SMAD4*, causing increased proliferation. Incidentally, miR-224-5p is among the DE miRNAs identified in 900TMZ-treated cells, 36 h post-exposure (**Table 8**).

Another example pertains to the miRNA cluster, miR-17-92, that is directly repressed by p53 in colorectal cancer cells during hypoxic conditions (Yan *et al*., 2009). Importantly, miR-17-92 is a paralogue of the miR-106a-363 cluster that contains miR-363-5p (Mogilyansky and Rigoutsos, 2013), an miRNA relevant to our study. Interestingly, this p53-mediated repression was not limited to hypoxic conditions, but was also observed in response to DNA damage following 0.3 μM dox treatment. Moreover, over-expression of the miR-17-92 cluster in p53 competent colorectal cancer cells significantly reduced apoptosis, suggesting the miR-17-92 cluster to be anti-apoptotic. Similarly, miR-18a, a constituent of the miR-17-92 cluster, is inhibited by p53 as demonstrated in rat cardiac cells and tissue (Huang *et al*., 2017). At this point it is worth noting that the aforementioned p53-mediated miRNA repression is observed in human, mouse, and rat cells, suggesting it to be a p53-mediated process that is conserved across multiple species.

Notwithstanding statistical appropriateness, the literature clearly provides a basis for our observations of a significant negative correlation between p53 protein levels and miR-363-5p tested among 900TMZ-treated cells. Particularly considering that miR-363-5p is a constituent of the miR-106a-363 cluster, which is a paralogue of the aforementioned miR-17-92 cluster. In addition to its ability to interact with DNA directly, p53 can also regulate intermediary proteins to effect a miRNA repressing response. For example, representative miRNAs of the miR-17-92, miR-106b-25, and miR-106a-363 clusters have been shown to be transcriptionally upregulated by E2F1 in human

fibroblasts (Brosh *et al*., 2008). Importantly, the authors showed that E2F1 is transcriptionally and post-transcriptionally inhibited by p53, thereby repressing the expression of the aforementioned miRNAs. Further supporting the notion that E2F1 transactivates miRNAs, Luo *et al*. (2016) showed quail muscle cells transfected with an E2F1-expressing construct to have significantly increased expression of pri-miR-17-92 and pri-miR-106a-363 while the reverse was true when transfected with si-E2F1. Of note, while research regarding the transactivation of miR-485-3p is limited, E2F1 is one of its predicted transcription factors (TransmiR v2.0 (https://www.cuilab.cn/transmir); Wang *et al*., 2010; Tong *et al*., 2019). Another transcription factor influencing miRNA expression is SOX2. SOX2 has been demonstrated to directly upregulate miR-29b in SOX2-transduced murine embryonic fibroblasts (Guo *et al*., 2013). Furthermore, p21, a well-known product of p53 activation, has been shown to bind and repress the SOX2 enhancer, SRR2 in murine neuronal stem cells, resulting in SOX2 inhibition (Marqués-Torrejón *et al*., 2013). Interestingly, canonical E2F1 repression during cell cycle arrest is also facilitated by p21. Taken together, it is clear that p53 has a role in the positive and negative regulation of miRNA expression, which can be direct (e.g., interacting with miRNA promotors) or indirect (e.g., transcriptional activation of intermediary proteins capable of miRNA regulation). In context of our findings, it is tempting to speculate a causal relationship between increased p53 expression and decreased miR-29b-3p, miR-363-5p, and miR-485-3p expression, considering that each of these are empirically determined, or predicted to be transactivated by E2F1 or SOX2, both of which are directly or indirectly repressed by p53. Therefore, we propose ATR-Chk1-p53 as a novel regulatory pathway of miR-29b-3p, miR-363-5p, and miR-485-3p.

Chapter 3

Functional assessment of miR-363-5p and miR-29b-3p in response to sub-lethal and lethal TMZ doses

3.1. Introduction

3.1.1. Overview of apoptosis

Thus far, we have discussed the DDR and how it might relate to specific DNA damage responsive miRNAs. Equally important, however, is the exact role of miRNAs in promoting or impairing specific cell fates. Of particular importance to this thesis is how DNA damage responsive miRNAs might influence apoptosis. In order to appreciate how miRNAs can impact apoptosis, the apoptotic landscape and its individual components needs to be discussed. Recall (**Chapter 1; Fig. 21**) that apoptosis comprises two main pathways, intrinsic (mitochondrial) and extrinsic (receptor-mediated). The intrinsic pathway relies on pro-apoptotic proteins to compromise the mitochondrial outer membrane. Perhaps the most extensively researched regulators of the intrinsic apoptotic pathway are the Bcl-2 family of apoptosis regulating proteins. Broadly, these are classified as either pro-apoptotic (e.g., BOK, BAK, and BAX) or anti-apoptotic (e.g., Bcl-2, Bcl-xL, and Mcl-1). Moreover, BH3-only proteins (e.g., BAD, BID, BIM, PUMA, and NOXA) are a subset of pro-apoptotic regulators that, as the name suggests, only contains a BH3 domain. This domain allows BH3-only proteins to interact with both pro-, and anti-apoptotic regulators. While interactions with anti-apoptotic proteins are inhibitory, those with pro-apoptotic proteins can be activating. Thus, BH3-only proteins both directly and indirectly promote apoptosis (Elmore, 2007; Edlich, 2018; Galluzzi *et al*., 2018).

Among pro-apoptotic Bcl-2 proteins, BOK, BAX, and BAK are the only ones demonstrated to be capable of mitochondrial outer membrane permeabilisation (MOMP) (Galluzzi *et al*., 2018). BAX and BAK are antagonised by anti-apoptotic Bcl-2 proteins. It has been suggested that BAX and BAK have differential binding specificities

to anti-apoptotic Bcl-2 proteins. For example, while Bcl-xL binds both BAX and BAK, Bcl-2 preferentially interacts with BAX, whereas Mcl-1 interacts with BAK (Chen *et al*., 2015; Einsele-Scholz *et al*., 2016; Galluzzi *et al*., 2018). Unlike BAX and BAK, BOK is impervious to Bcl-2 inhibition. Rather, BOK is degraded in a glycoprotein 78 (GP78)-dependent manner as part of ER-associated degradation (ERAD) (Llambi *et al*., 2016). GP78 is an E3-ubiquitin ligase that ubiquitinates BOK, thus facilitating proteasomal degradation (Joshi *et al*., 2017). The activity of BAX and BAK is governed by BH3-only proteins that induces a conformational change through direct interaction, and ultimately facilitates hetero-, and homo-oligomerisation required for MOMP (Galluzi *et al*., 2018). Of note, only certain BH3-only proteins serve in this direct capacity to activate BAX and BAK, including BID, BIM, PUMA, and NOXA (Kim *et al*., 2009; Galluzi *et al*., 2018). However, other BH3-only proteins, including BAD and NOXA, indirectly promote BAX and BAK activation by sequestering anti-apoptotic proteins. In contrast to BAX and BAK, BOK exists in a less stable conformation and thus does not require BH3-only proteins to induce a conformational change and subsequent activation (Zheng *et al*., 2018).

Following MOMP, pro-apoptotic proteins are leaked from the intermembrane space, including cytoC, endonucleases (e.g., CAD), and second mitochondrial activator of caspases (SMAC). Arguably, cytoC is the principal pro-apoptotic component as it serves as a molecular signal to continue with apoptosis, forming the apoptosome. Incidentally, miR-34a has been suggested to target cytoC in cerebrovascular endothelial cells, causing mitochondrial dysfunction (Bukeirat *et al*., 2016). However, whether cytoC is a direct target of miR-34a remains speculative, as the authors did not experimentally confirm miR-34a-cytoC interaction, but rather inferred interaction based on reduced cytoC levels. The apoptosome is a multimeric construct of cytoC, APAF1, and pro-caspase-9. This structural arrangement allows for pro-caspase-9-pro-caspase-9 and

pro-caspase-9-APAF1 dimerisation, which cleaves pro-caspase-9, forming active caspase-9. Subsequently, caspase-9 activates executioner caspases (e.g., caspase-3/7) that digests cellular components. SMAC promotes apoptosis by antagonising inhibitors of apoptosis (IAP), foremost of which is X-linked IAP (XIAP). XIAP impedes apoptosis by inhibiting caspase activity. Regarding leaked endonucleases, this is a 'late stage' event that serves to digest DNA and may be construed as a commitment to apoptosis. Particularly, caspase-3 activates CAD by cleaving it from its inhibitory dimer complex, ICAD-CAD. Subsequently, CAD serves as the predominant facilitator of DNA fragmentation (Nagata *et al*., 2003). The final stage of apoptosis involves phagocytic uptake of the dead cell in a process known as efferocytosis. This is achieved by externalisation of phosphatidylserine from the membrane of apoptotic cells, which serves as a cue to phagocytes (e.g., macrophages) to phagocytose the cell (Elmore, 2007; Kim *et al*., 2009; Einsele-Scholz *et al*., 2016; Llambi *et al*., 2016; Galluzzi *et al*., 2018; Zheng *et al*., 2018).

Similar to the intrinsic pathway, the extrinsic apoptotic pathway relies on caspase activation, though mediated through death receptors. Perhaps best described are the receptors of the TNF superfamily and their respective ligands. These include FAS, TNFR1, DR4, and DR5 receptors with corresponding ligands FASL, TNF-α, and TNF-related apoptosis-inducing ligand (TRAIL), respectively. In the context of apoptosis induction, some variability exists between these death receptor pathways, particularly regarding TNF-α-TNFR1, which primarily functions in an immunological context (Wayant, Pfizenmaier, and Scheurich, 2003). Therefore, only FAS, DR4, and DR5 will be discussed as 'canonical' extrinsic apoptosis pathways. Upon stimulation by their cognate ligands, these transmembrane receptors undergo a conformational change that facilitates recruitment of adapter proteins to their intracellular (cytoplasmic) death

domains. One such adapter protein is Fas-associated death domain containing protein (FADD). Adapter recruitment is required as it contains a death effector domain (DED) that facilitates recruitment of initiator pro-caspases-8/10, thereby forming the death induced signalling complex (DISC). The DISC allows pro-caspases-8/10 to become active caspases-8/10. Analogous to the function of anti-apoptotic Bcl-2 proteins in the intrinsic pathway, DED-containing proteins can impede initiator caspase function (Elmore, 2007; Galluzzi *et al*., 2018). Primarily, cFLIP can inhibit caspase-8/10 at the level of the DISC (Safa, 2013).

Following caspase-8/10 activation, signalling can proceed in two ways, dependent on whether mitochondrial-independent or dependent mechanisms will subsequently be used to facilitate apoptosis. This distinction was described by Scaffidi *et al*. (1998), classifying mitochondrial-independent mechanisms as ‘type 1’ cells, while cells relying on mitochondrial-dependent mechanisms were termed ‘type 2’. This classification has since been extended by Özören and El-Deiry (2002), suggesting the ability of cells to cleave BID (into tBID) as a determinant of being type 1 or type 2. This stems from the ability of tBID to activate BAK and BAX in its capacity as a BH3-only protein, and thereby co-opting the intrinsic pathway as part of the extrinsic pathway. On the other hand, type 1 cells are capable of directly activating subsequent executioner caspases (e.g., caspase-3) to induce apoptosis.

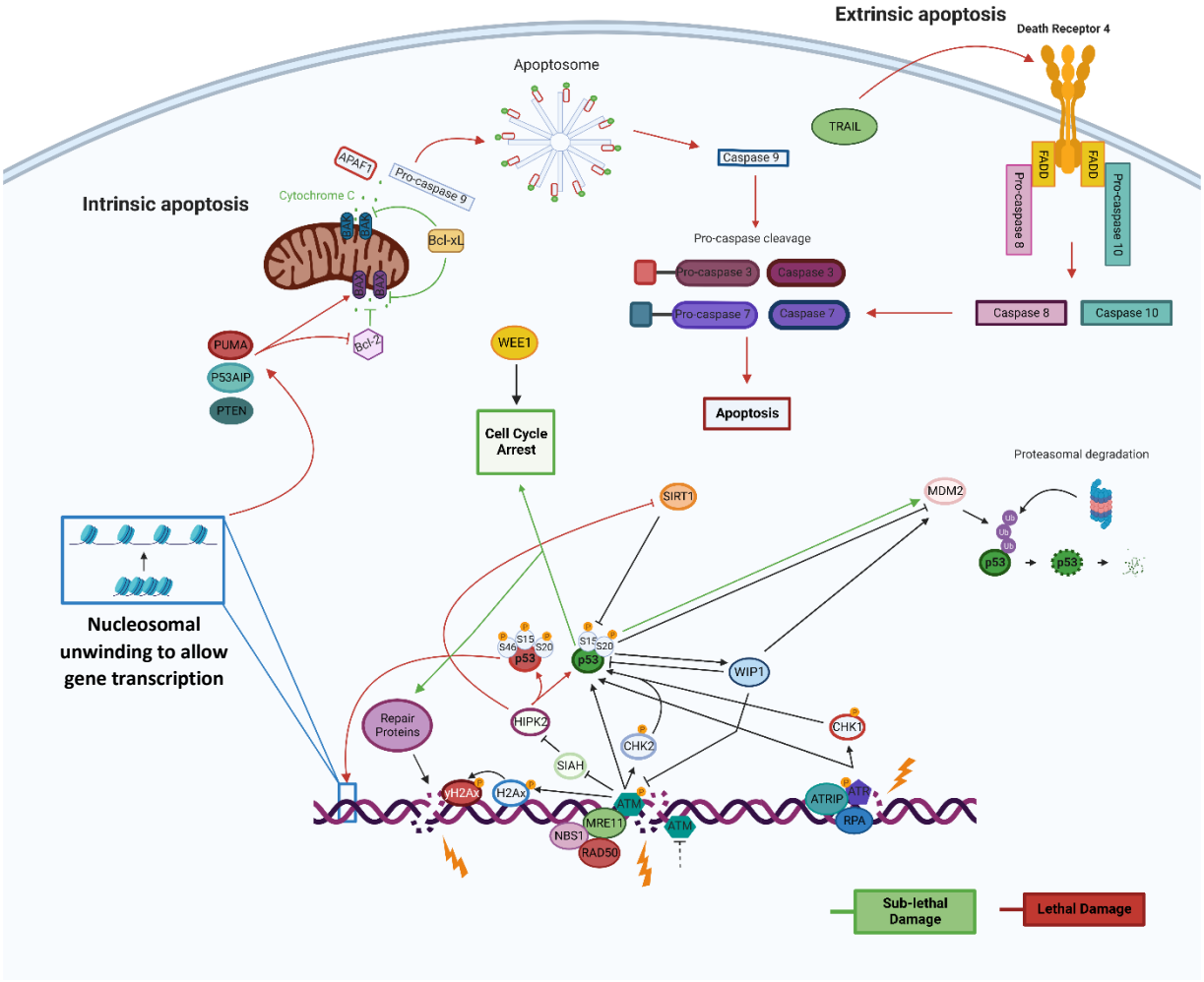

Figure 21. Overview of the apoptosis pathway in context of sub-lethal and lethal DNA damage.

DNA damage is detected by ATM, or ATR that propagate ‘damage signals’ to Chk1/2 by means of phosphorylation. In turn, pChk1/2 further propagate the signal, resulting in p53 activation. Depending on the severity of the DNA damage, signalling may follow the ‘sub-lethal damage’ route, if the damage is tolerable/repairable, resulting in cell cycle arrest, DNA repair, and ultimately survival. However, if DNA damage is too severe, signalling may follow the ‘lethal damage’ route resulting in transcriptional activation of pro-apoptotic proteins, eventuating in apoptosis which can be mitochondrial (intrinsic), or receptor-mediated (extrinsic). Arrows represent activation whereas blunted ends indicate inhibition. Created on license from BioRender.com.

3.1.2. Pro-apoptotic miRNAs

In **Chapter 2**, many pro-apoptotic miRNAs were discussed, particularly those regulated by p53 (**Fig. 22**). This section adds to that information and discusses pro-apoptotic miRNAs in the context of specific apoptotic pathways (i.e., intrinsic or extrinsic). For example, several miRNAs are known to regulate Bcl-2 proteins (directly and indirectly). Specifically, miR-1 inhibition decreases BAX and increase Bcl-2, conferring an anti-apoptotic phenotype in a liver X-receptor (LXRα)-dependent manner (Cheng *et al*., 2018). It was not clear whether LXRα is a direct target of miR-1, thus the pro-apoptotic capability of miR-1 requires mechanistic elaboration. These observations are reminiscent of the findings by Valledor *et al*. (2004) that reported LXR agonists to counteract Bcl-2 downregulation and BAX upregulation in response to LPS treatment of murine macrophages. Bcl-2 proteins are also substrates for miR-15a and miR-16-1, causing apoptosis *in vitro* (Cimmino *et al*., 2005). The authors confirmed induction of the intrinsic apoptotic pathway through increased APAF1 expression in miR-15a/16-1 transfected chronic myelogenous leukaemia (CML) cells. MiRNA regulation also extends to extrinsic apoptosis. For example, miR-145 can upregulate TRAIL, *in vitro* (Zaman *et al*., 2010). Recall, TRAIL is part of a family of ligands that induce extrinsic apoptosis by dimerising with death receptors. Ultimately, this interaction facilitates caspase-8/10 activation, which in turn activates executioner caspases (Wang and El-Deiry, 2003).

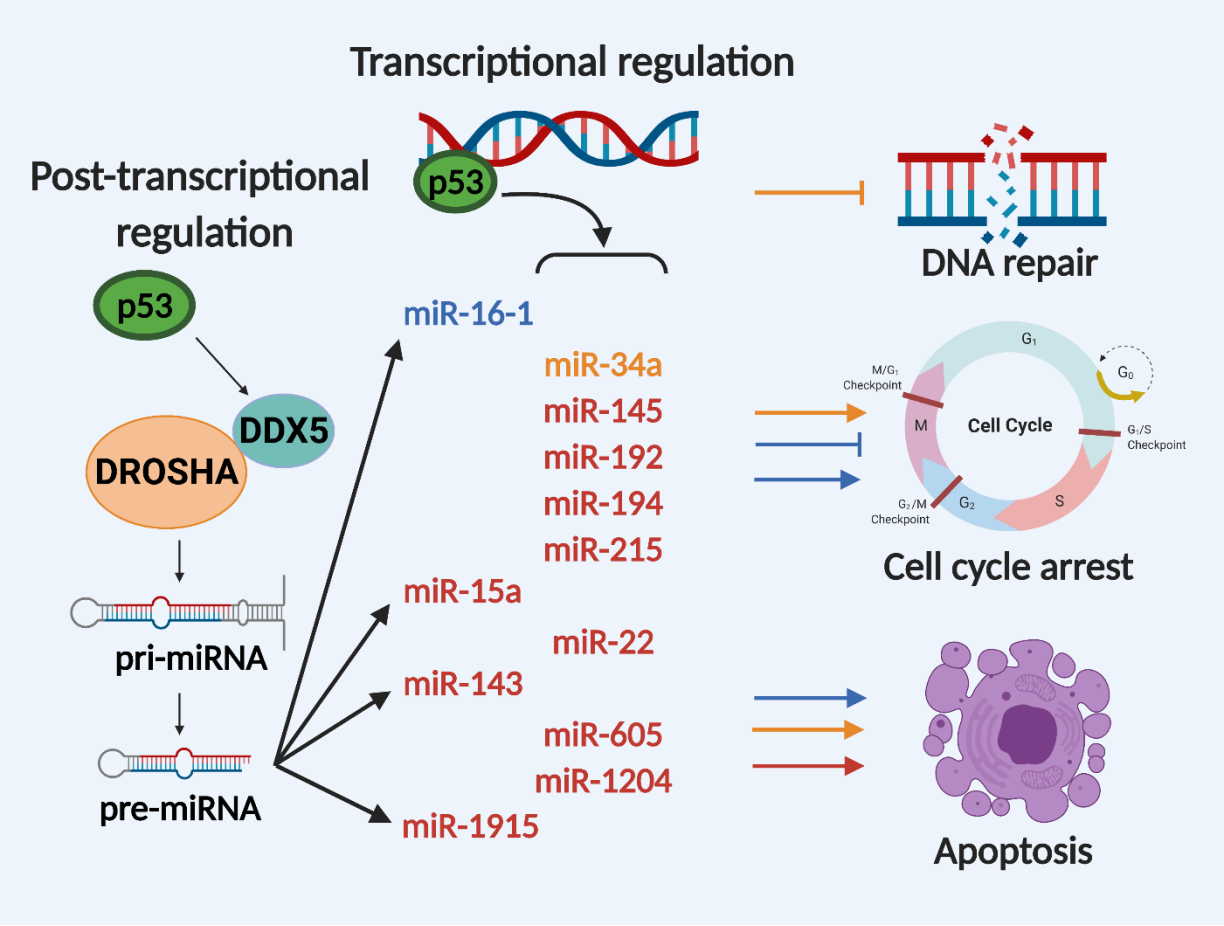

Figure 22. Transcriptional and post-transcriptional regulation of miRNAs by p53.

Several miRNAs are under the direct transcriptional control of p53, whereas miR-16-1, miR-15a, miR-143, and miR-1915 are indirectly regulated by p53-mediated pri-to-pre-miRNA maturation. While certain p53-regulated miRNAs can have dual contributions (orange), others (red) are apparently dedicated to apoptosis. Pointed arrows (activation), blunt arrows (inhibition). Note: Image adapted from Visser and Thomas (2021) and used with permission. Created on license from BioRender.com.

3.1.3. Anti-apoptotic miRNAs

Given the multitude of pro-apoptotic miRNAs that has been discussed thus far, it is not unexpected that several anti-apoptotic miRNAs exist that likely function to maintain a physiological balance in uninjured cells, or when DNA damage is tolerable. Cao *et al*. (2017) demonstrated miR-504 to be anti-apoptotic in transfected smooth muscle cells as evidenced by significantly reduced levels of apoptosis and caspases-3/9. Furthermore, Bcl-2 was significantly upregulated in these cells. These observations were reversed upon transfection with a miR-504 inhibitor. Importantly, the anti-apoptotic capability of miR-504 is facilitated by directly targeting the 3' UTR of p53, causing, amongst others, a significant reduction in BAX and p21 expression. Similarly, Li *et al*. (2011b) showed that miR-886-5p inhibited BAX in transfected non-cancerous cervical cells, whereas miR-886-5p inhibition promoted BAX and apoptosis in cervical cancer cells. MiR-183-5p also has anti-apoptotic and pro-proliferative functions in breast cancer cells, which has been suggested to involve direct inhibition of programmed cell death protein (PDCD4) (Cheng *et al*., 2016). PDCD4 inhibition was shown to reduce p21 and, to a lesser extent, p27 expression. While this observation supports the pro-proliferative effect of miR-183-5p, the authors did not elaborate on the observed anti-apoptotic effect. Nonetheless, PDCD4 has been reported to promote apoptosis by upregulating BAX and inhibiting Bcl-2 in colorectal cancer cells (Wang *et al*., 2019). This suggests that the anti-apoptotic effect of miR-183-5p may result from PDCD4 inhibition. However, Eto *et al*. (2012) suggests PDCD4 to be inherently anti-apoptotic by inhibiting pro-caspase-3 translation. Therefore, the underlying anti-apoptotic mechanism of miR-183-5p requires further exploration.

MiR-24-3p can also impair p27 levels, though, unlike the observations of Cheng *et al*. (2016), this is through direct 3' UTR interaction. MiR-24-3p was also capable of reducing

apoptosis as indicated by significantly elevated apoptotic levels when miR-24-3p was antagonised. Although p27 inhibition augments a pro-survival phenotype, it does not fully explain reduced apoptosis. However, miR-24a can inhibit APAF1 and caspase-9 (Walker and Harland, 2009), which could potentially clarify the anti-apoptotic effect of miR-24-3p. Walker and Harland (2009) demonstrated that miR-24a can directly inhibit APAF1 and caspase-9, thus manifesting an anti-apoptotic phenotype, as evidenced by significantly less frog embryos undergoing apoptosis following miR-24a and hydroxyurea treatment. Relatedly, caspase-9 is also directly inhibited by miR-378 in murine tissues, thereby attenuating intrinsic apoptosis (Li *et al*., 2018). Furthermore, APAF1 is also suggested to be a substrate for miR-155**,** *in vitro*, thus exerting an anti-apoptotic effect (Zang *et al*., 2012). MiR-155 and APAF1 exhibited an inverse relationship in lung cancer patient samples, with miR-155 expression being significantly elevated while APAF1 was significantly downregulated. Moreover, normal lung patient samples displayed significantly less miR-155, and significantly higher APAF1 levels than lung cancer samples. This relationship was further supported by similar apoptotic rate responses being obtained following either APAF1 or miR-155 inhibitor transfection into lung cancer cells, with and without cisplatin treatment. Of note, miR-155 inhibition increased apoptotic rate with and without cisplatin treatment. This exemplifies how miRNAs can be manipulated to coerce cell fate, both in the presence and absence of exogenous DNA damage.

An miRNA-mediated anti-apoptotic effect is also described by Grieco *et al*. (2017) that demonstrated several BH3-only proteins to be targets of miR-23a-3p, miR-23b-3p, and miR-149-5p. The authors identified these miRNAs as pro-inflammatory cytokine responsive, noting an inverse relationship between miRNA and BH3-only mRNA expression. Specifically, these miRNAs were downregulated in response to pro-

inflammatory cytokine, interleukin-1β (IL-1β) and interferon-γ (IFN-γ), treatment while BH3-only expression was upregulated in both human pancreatic β-cells, and primary pancreatic islets. Main targets of these miRNAs were reportedly death protein (DP5) and PUMA. However, miR-23a-3p inhibition also upregulated BAX and BIM, and miR-149-5p inhibition upregulated BAX. Moreover, c-Jun upregulation was observed following miR-23a/b-3p inhibition. Upregulation of BAX, BIM, and c-Jun upon inhibition of the respective miRNAs emphasises a larger role in the apoptotic network. Inhibition of these miRNAs and consequent caspase-3 cleavage led the authors to conclude intrinsic apoptosis pathway activation. However, this does not preclude involvement of the extrinsic apoptosis pathway, as this also results in caspase-3 cleavage. Additionally, c-Jun is part of the c-Jun N-terminal kinase (JNK) pathway which is known to participate in both intrinsic and extrinsic apoptosis pathways (Roos, Thomas, and Kaina, 2016; Dhanasekaran and Reddy, 2017). Importantly, miR-23a/b-3p inhibition was able to significantly increase apoptosis in both pancreatic β-cells and primary pancreatic islets, even without cytokine treatment. These findings suggest that these miRNAs may be part of an inherent regulatory network that serves to suppress apoptosis during homeostasis, but becomes downregulated when cells are fated for apoptosis.

A pro-survival phenotype has also been observed in murine embryonic stem cells (mESC), owing to BIM inhibition by miR-20a, miR-92a, and miR-302a, impairing intrinsic apoptosis (Pernaute *et al*., 2014). Transfection of DICER-depleted mESCs with these miRNAs resulted in decreased BIM levels. Importantly, DICER depletion increased apoptosis in these cells, and BIM inhibition partially alleviated it. Furthermore, while DICER depletion manifested an apoptotic phenotype, BIM $^{-/-}$ murine embryos resembled wild-type controls. These findings allude to BIM being the causative agent of apoptosis in mESCs, and miR-20a, miR-92a, and miR-302a can alleviate this by targeting BIM.

However, it is not clear whether these miRNAs target BIM directly. Thus miRNA-regulated intermediary molecules (including other miRNAs) may exist that enacts BIM inhibition. To this end, BIM has been described as a target for several miRNAs. For example, Floyd *et al*. (2014) demonstrated miR-363 and miR-582-5p to be anti-apoptotic in transfected glioblastoma cells by directly targeting BIM and caspase-3, and caspases-3/9, respectively. Similarly, Zhang *et al*. (2014b) showed miR-214 to be anti-apoptotic by targeting BIM in nasopharyngeal carcinoma cells.

Many of the anti-apoptotic miRNAs described thus far regulate intrinsic apoptosis, however, anti-apoptotic miRNAs are also described for the extrinsic apoptosis pathway. For example, both caspase-8 and -3 are direct targets of miR-24 and miR-221 respectively, *in vitro* (Jin *et al*., 2018). Consequently, when transfected into hepatocarcinoma cells, these miRNAs can significantly decrease apoptosis in response to TRAIL treatment. Moreover, miR-25 is capable of inhibiting TRAIL-induced (extrinsic) apoptosis, by directly targeting its death receptor, DR4 (Razumilava *et al*., 2012). Recall, death receptors require adapter proteins to recruit and subsequently activate caspase-8/10. FADD is such an adapter protein that couples intracellularly with death receptors (Schulze-Osthoff *et al*., 1998). Importantly, FADD and caspase-3 are direct targets of miR-155, which can result in impaired extrinsic apoptosis (Wang *et al*., 2011). Extrinsic apoptosis can also be impaired by inhibiting the recruitment of adapter proteins to the death receptor. PTEN facilitates FADD recruitment by mediating the displacement of the inhibitory protein, mitogen-activated kinase activating death domain containing protein (MADD), attached to the death receptor. Interestingly, displaced MADD can, in turn, displace pro-apoptotic BAX from inhibitory 14-3-3 proteins. Thus, PTEN can facilitate both intrinsic and extrinsic apoptosis (Jayarama *et al*., 2014). Incidentally, miR-498 can suppress PTEN in miRNA-transfected/transduced breast cancer cells,

implicating it as a therapeutic target to promote both, intrinsic and extrinsic apoptosis pathways (Chai *et al*., 2018).

3.1.4. MiRNAs in a clinical context

MiRNAs are becoming well-established as regulators of cellular function. In particular, the expression pattern of miRNAs has proven useful as biomarkers of certain disease phenotypes (Bonneau *et al*., 2019). Perhaps best known is miR-34a in its role as a tumour-suppressor miRNA, or diagnostic/prognostic biomarker for cancers e.g., breast cancer (Imani *et al*., 2017), colorectal cancer (Rapti *et al*., 2017), and cervical cancer (Chen *et al*., 2017). From a clinical perspective, it is imperative to investigate the physiological relevance of miRNAs. Not only does this promote our understanding of endogenous regulatory networks, it also provides a plethora of avenues to explore that can lead to the development of novel cancer therapies. Particularly, the extensive involvement of miRNAs in both pro-survival and apoptosis pathways identifies them as candidate therapeutic targets, or treatment options in itself (**Fig. 23; Table 9**). Indeed, miRNA dysregulation among these pathways have sparked much research into the use of miRNA mimics or inhibitors as therapeutic options. For example, MRX34, a liposomal miR-34a mimic has recently entered a phase I clinical trial in patients with advanced solid tumours (Beg *et al*., 2017; Hong *et al*., 2020). However, the study was terminated due to severe adverse effects. Notwithstanding this, several other clinical trials are investigating the therapeutic application of miRNAs, e.g., MesomiR-1, a miR-16 mimic intended to treat mesothelioma and lung cancer that has completed phase I clinical trials (Hanna, Hossain, and Kocerha, 2019). Importantly, the use of miRNA mimics/inhibitors is not limited to oncology and may be useful in the remediation of diseases characterised by excessive cell death, e.g., Alzheimer's disease (Behl, 2000), by impeding a switch from cell cycle arrest and DNA repair to apoptosis.

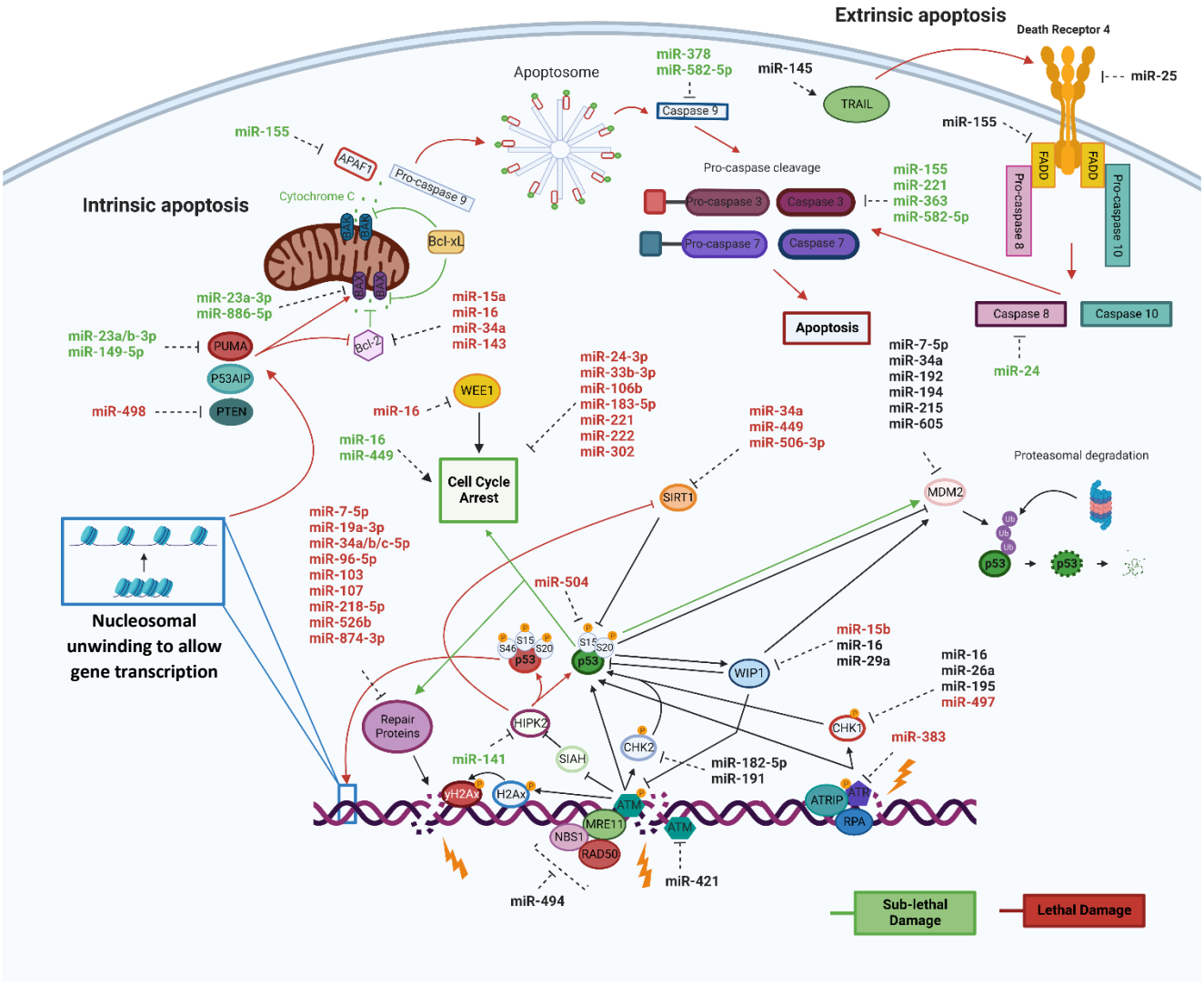

Figure 23. MiRNA regulation of the DDR.

MiRNA-mediated regulation of the DDR at sub-lethal and lethal DNA damage. The canonical DDR pathway consisting of MRN, ATRIP-RPA, ATM, ATR, Chk1/2, and p53 (solid black lines) to facilitate DNA repair, cell cycle arrest, or apoptosis, and the hypothesised signalling cascade that results from sub-lethal (green) and lethal DNA damage (red). The influence of miRNAs (dashed lines) is also presented, and classified according to the likely cell fate that it facilitates, based on empirical evidence of their role in DNA damage sensitisation or resistance (survival (green), cell death (red), or unresolvable (black)). Note: Image taken from Visser and Thomas (2021) and used with permission. Created on license from BioRender.com.

Table 9. Examples of miRNAs as regulators of apoptosis

Pro-death

miRNA	Tissue/Cell type	Target	Cell fate	Reference
miR-7–5p	Lymphoblastoid cells	NR	Pro-apoptotic	Luo *et al*. (2018)
miR-15b/16–2	Human bronchial epithelial cells	WIP1	Pro-apoptotic	Rahman *et al*. (2014)
miR-15a/16-1	Chronic myelogenous leukaemia cells	Bcl-2	Pro-apoptotic	Cimmino *et al*. (2005)
miR-16	Glioma cells	WIP1	Pro-apoptotic	Zhan *et al*. (2017)
miR-22	Glial cells	NR	Pro-apoptotic	Yu, Zeng, and Sun (2018)
miR-34a	Colorectal cancer cells	SIRT1	Pro-apoptotic	Lizé, Pilarski, and Dobbelstein (2009)
miR-34a/b/c-5p	Colon cancer cells	RAD51	Pro-apoptotic	Chen *et al*. (2019)
miR-126	Hepatocellular carcinoma cells	PLK-4	Pro-apoptotic	Bao *et al*. (2018)
miR-143	Osteosarcoma cells	Bcl-2	Pro-apoptotic	Li *et al*. (2016)
miR-145	Prostate cancer cells	NR	Pro-apoptotic	Zaman *et al*. (2010)
miR-185	Renal cell carcinoma cells	ATR	Pro-apoptotic	Wang *et al*. (2013)
miR-194–5p	Glioblastoma cells	IGF1R	Pro-apoptotic	Zhang *et al*. (2017)
miR-421	Cervical carcinoma cells	ATM	Anti-survival	Hu *et al*. (2010)
miR-449	Colorectal cancer cells	SIRT1	Pro-apoptotic	Lizé, Pilarski, and Dobbelstein (2009)
miR-506–3p	Ovarian cancer cells	SIRT1	Pro-apoptotic	Xia *et al*. (2020)
miR-526b	Non-small cell lung cancer cells	XRCC5	Pro-apoptotic	Zhang *et al*. (2014a)
miR-623	Breast cancer cells	XRCC5	Pro-apoptotic	Li *et al*. (2020)

Pro-survival

miR-23a-3p	Pancreatic cells	DP5 PUMA	Anti-apoptotic	Grieco *et al*. (2017)
miR-23b-3p	Pancreatic cells	DP5 PUMA	Anti-apoptotic	Grieco *et al*. (2017)
miR-24–3p	Breast cancer cells	p27	Anti-apoptotic	Lu *et al*. (2015)
	Hepatocarcinoma cells	Caspase-8		Jin *et al*. (2018)
miR-25	Cholangiocarcinoma cells	DR4	Anti-apoptotic	Razumilava *et al*. (2012)
miR-33b-3p	Non-small cell lung cancer cells	p21	Pro-survival	Xu *et al*. (2016)
miR-149–5p	Pancreatic cells	DP5 PUMA	Anti-apoptotic	Grieco *et al*. (2017)
miR-155	Lung cancer cells	APAF1	Anti-apoptotic	Zang *et al*. (2012)
	Nucleus pulposus cells			Wang *et al*. (2011)
miR-183–5p	Breast cancer cells	PDCD4	Anti-apoptotic	Cheng *et al*. (2016)
miR-214	Nasopharyngeal carcinoma cells	BIM	Anti-apoptotic	Zhang *et al*. (2014b)
miR-221	Hepatocarcinoma cells	Caspase-3	Anti-apoptotic	Jin *et al*. (2018)

miR-363	Glioblastoma cells	BIM Caspase-3	Anti-apoptotic	Floyd *et al*. (2014)
miR-504	Smooth muscle cells	p53	Anti-apoptotic	Cao *et al*. (2017)
miR-582–5p	Glioblastoma cells	Caspase-3 Caspase-9	Anti-apoptotic	Floyd *et al*. (2014)
miR-886–5p	Cervical cells	BAX	Anti-apoptotic	Li *et al*. (2011b)

Note - table adapted from Visser and Thomas (2021) and used with permission. NR – not reported

3.1.5. Functional ambivalence of miRNAs

Clearly, functional characterisation of miRNAs is clinically imperative. However, functional characterisation is no small feat given the dynamic nature of miRNAs in the context of the DDR and cell fate. In addition to our observations (**Chapter 2**), DE miRNA profiles have been described. As previously mentioned (**Chapter 2**), mice exposed to sub-lethal or lethal doses of radiation exhibit different serum miRNA profiles (Acharya *et al*., 2015). Recall, miR-187-3p, miR-194-5p, and miR-27a-3p were significantly downregulated 24 h after lethal radiation exposure, whereas miR-30c-5p and miR-30a-3p was significantly upregulated when compared to sub-lethal doses. Interestingly, this was not a static change, as most miRNAs that were initially downregulated following lethal irradiation either became upregulated, beyond that observed at sub-lethal doses, or approached that of sub-lethal doses, beyond 3 days after irradiation. Moreover, miRNAs initially upregulated mainly remained elevated, though not always reaching significance.

The aforementioned miRNA profiles embody the complexity of miRNA-mediated regulation, given the seemingly ambivalent function of the miRNAs involved. For example, as miR-187-3p, miR-194-5p, and miR-27a-3p were downregulated following lethal radiation, it is reasonable to assume that these miRNAs might be involved in certain cellular survival strategies, or are otherwise anti-apoptotic. Indeed, miR-187-3p can inhibit apoptosis by targeting the tumour suppressor, collapsin response mediator protein (CRMP1) (Ren *et al*., 2017). However, miR-187-3p can also inhibit HIPK3 (Hu *et al*., 2020), which is known to inhibit Fas-mediated apoptosis by phosphorylating FADD, thereby disrupting extrinsic apoptosis (Curtin and Cotter, 2004). Thus, miR-187-3p may facilitate both apoptotic and anti-apoptotic outcomes. Moreover, HIPK3 houses circular RNA HIPK3 (circHIPK3) which has ambivalent functions in the context of

apoptosis. CircHIPK3 serves to ‘mop up’ miRNAs to exert an effect. For example, both miR-149-5p (Zhang *et al*., 2021) and miR-485-3p (Lai *et al*., 2020) are targets of circHIPK3. However, the outcomes may be contradictory as miR-149-5p inhibition can upregulate BAX, PUMA, and BIM, thus promoting apoptosis (Grieco *et al*., 2017), whereas inhibition of miR-485-3p inhibits apoptosis as miR-485-3p has been reported to upregulate BAX and caspase-3, and downregulate Bcl-2 (Lai *et al*., 2020). MiR-27a-3p displays a similar duality in that, it has anti-apoptotic functions by inhibiting tumour suppressor, B-cell translocation gene (BTG1) (Su *et al*., 2019), but can also increase apoptosis in transfected hepatocellular carcinoma cells (Yang *et al*., 2021). Furthermore, miR-194-5p can induce apoptosis by targeting IGF1R (Zhang *et al*., 2017), but may also adopt an anti-apoptotic role in rat cardiomyocytes by attenuating AKT signalling (Zhang, Wu, Yang, 2021).

Regarding miR-30c-5p and miR-30a-3p that were upregulated following lethal radiation (Acharya *et al*., 2015), no clear functional significance can be assigned. As with those miRNAs downregulated after lethal radiation, miR-30c-5p exhibits functional duality. MiR-30c-5p has been demonstrated to inhibit apoptosis in a hypoxia-inducible factor (HIF1)-mediated manner. HIF1 is a transcription factor known to combat apoptosis in hypoxic conditions (Flamant *et al*., 2010; Zou *et al*., 2017). Contrastingly, miR-30c-5p can promote apoptosis in transfected glioma cells by directly targeting Bcl-2 (Yuan *et al*., 2021). Literature predominantly portrays miR-30a-3p as pro-apoptotic as it has been shown to induce apoptosis by increasing the BAX:Bcl-2 ratio (Wei, Yu, and Zhao, 2019). Thus, miR-30a-3p may not necessarily display functional ambivalence, but its pro-apoptotic tendencies could oppose the actions of miR-30c-5p, if it were to function in an anti-apoptotic capacity.

In context of the observations by Acharya *et al*., it is curious that miRNAs with potentially opposing functions were regulated in the same direction. For example, upregulation of pro-apoptotic miR-30a-3p and potentially anti-apoptotic miR-30c-5p appears counterintuitive. However, it is tempting to speculate a scenario in which these opposing miRNAs are co-regulated to form an inherent regulatory feedback network in which they counteract each other in an attempt to maintain a balance that is in line with the ensuing cell fate. Though plausible, this suggestion is based on miRNA functions observed in various biological contexts, and thus do not accommodate tissue-specific functions. Nonetheless, it provides insight to the complexity that underlies miRNA-mediated regulation of cell fate.

3.1.6. Rationale

MiRNA research began ≈ 30 years ago with the discovery of lin-4 (Rosalind, Feinbaum, and Ambros, 1993). Since then, our understanding of miRNAs have developed substantially, though, as evident from this chapter, much requires clarification. MiRNAs add another dimension to the clinical research landscape, extending it beyond genes and proteins as therapeutic avenues. While miRNAs are promising candidates for diagnostic and therapeutic application, their intricate involvement in homeostasis and the DDR creates both opportunities and challenges. Specifically, the ubiquitous involvement of miRNAs in a host of cellular responses and disease pathologies provide, in turn, a wide range of miRNAs that may be of diagnostic or therapeutic benefit. However, this requires functional characterisation of these miRNAs, which is not a ‘one size fits all’ approach, as these functions may be context-dependent. Particularly, the function of specific miRNAs within a network of miRNAs needs extrapolation, to account for (among others) miRNA-miRNA cross-talk (e.g., synergism). In an apoptotic context, miRNAs have been known to co-operate (synergise). For example, miR-34a and miR-

34c co-operate to induce apoptosis, while individually they cannot (Rokhlin *et al*., 2008). Similarly, miR-30c and miR-181a co-expression yielded a more pronounced inhibition of apoptosis, by synergistically targeting the p53-p21 pathway (Raut *et al*., 2016). Additionally, miRNAs can also regulate each other, for example, ectopic miR-29c can significantly upregulate miR-34c and miR-449a in transfected nasopharyngeal carcinoma cells (Niu *et al*., 2016). Therefore, miR-29c may be regarded pro-apoptotic as both miR-34c (Li, Zhang, and Zheng, 2018) and miR-449a (Ye *et al*., 2014) contribute towards an apoptotic cell fate.

Another consideration is cell state, that is, any condition that influences the homeostatic state of a cell and might influence miRNA expression. In **Chapter 2**, we showed that DNA damage can influence miRNA expression. In light of this, and considering miRNAs can influence each other (as discussed above), it is clear that the function of certain miRNAs may be contingent on cell state. Functional annotation of miRNAs in the context of cell state and miRNA-miRNA interaction could facilitate the identification of novel druggable targets, and/or miRNAs that may be suitable treatment options. While this requires expansive research, a logical starting point is defining the role of miRNAs within specific cellular contexts. In **Chapter 2**, we identified miR-29b-3p, miR-363-5p, and miR-485-3p as DNA damage responsive. Specifically, these miRNAs were significantly downregulated among 900TMZ-treated TK6 cells as compared to 30TMZ-treated cells. Given the respective lethal and sub-lethal nature (as empirically determined here) of these doses, it is not unreasonable to speculate that these miRNAs might have been downregulated because they function to inhibit apoptosis. Literature regarding miR-363-5p in the context of the DDR and cell fate determination is extremely limited. In fact, the only substantive evidence that could be related to the DDR and cell fate, suggests miR-363-5p to have an anti-proliferative function (Khuu *et al*., 2014; Chen *et al*., 2018; Hou,

Wang, and Du, 2020; Yin *et al*., 2021). Not only does this identify a knowledge-gap, but it also contrasts our hypothesis that miR-363-5p might be anti-apoptotic. Consequently, the function of miR-363-5p will be investigated in the context of the DDR and cell fate. Additionally, miR-29b-3p will be investigated, as it has been reported to both, promote apoptosis (Jia and Wang, 2020; Tang *et al*., 2022) and inhibit it (Cai and Li, 2019; Zhang *et al*., 2019; Xiao *et al*., 2022), thus implying its function to be context-dependent. While functional analysis of miR-485-3p is also warranted, logistical limitations only allowed miR-363-5p and miR-29b-3p to be investigated in the first instance.

Aim:

1. Manipulate miR-363-5p and miR-29b-3p levels in TK6 cells and observe its effect on cell fate.

3.2. Methods

3.2.1. Determining the effect of miRNAs on TK6 cell fate

3.2.1.1. Transfection with miRNA mimics

All reagents used for transfection were purchased from Qiagen (Manchester, UK). To determine the influence of selected miRNAs on cell fate, TK6 cells were transfected with 100 nM miR-363-5p (cat. YM00472894-AGA) or miR-29b-3p (cat. YM00473486-AGA), or a combination of 50 nM miR-363-5p and miR-29b-3p using HiPerfect™ transfection reagent. A scramble miRNA (YM00479902-AGA) was used as negative control at the same concentrations as miR-363-5p or miR-29b-3p. To determine transfection efficiency, TK6 cells were transfected with 100 nM AllStars™ Alexa Fluor 647 (AF647)-labelled negative control siRNA and the proportion of positively transfected cells were determined by flow cytometry. Briefly, ≈ 1 x 10^6 transfected or untransfected cells were sampled, washed with PBS, and resuspended in PBS. Subsequently, flow cytometric analysis was performed as described in **Chapter 1** (**1.2.2.3**) with the only exception being that the FL4-A channel was used to detect AF647 positive cells, as opposed to the FL1-A channel. Additionally, miR-363-5p transfected cells were assessed by qRT-PCR as described in **Chapter 2** (**2.2.4**) as a further indicator of successful transfection.

Transfections were performed on ≈ 1 x 10^6 TK6 cells in complete RPMI by dropwise adding an equal volume of HiPerfect™-miRNA/siRNA transfection complex (prepared in serum-free RPMI according to manufacturer specifications). Subsequently, samples were topped up with a volume of complete RPMI that was 25% of the suspension volume (e.g., if 1 ml 1 x 10^6 TK6 cells were transfected with 1 ml transfection complexes, then 0.5 ml complete RPMI was added). Following this, cells were incubated under normal conditions for 12 h for transfection. After 12 h, the culture medium was replaced

with fresh complete RPMI and further incubated (≈ 22 h) until TMZ treatments were performed. Cells, transfected with AF647-labelled siRNA, to determine transfection efficiency, were sampled immediately after transfection, and samples used to validate transfection with qRT-PCR were collected 36 h post-transfection. This was done to determine whether the miRNA mimics would still be present at the time of TMZ treatment.

3.2.1.2. Measuring DDR proteins in TMZ-treated transfected cells

Transfected TK6 cells were treated with 30TMZ and 900TMZ and sampled 36 h post-TMZ exposure. Subsequently, proteins were extracted and immunoblotted for key DDR proteins as described in **Chapter 1** (**1.2.3**).

3.2.1.3. Determining the influence of transfected miRNAs on the cell fate of TMZ-treated cells

Transfected TK6 cells were treated with 30TMZ and 900TMZ and sampled 36 h post-TMZ exposure. Subsequently, samples were processed as described in **Chapter 1** (**1.2.4**; **1.2.5**).

3.2.1.4. Identification of putative targets for miR-363-5p and miR-29b-p

To identify putative mRNA targets for miR-363-5p and miR-29b-3p, miRNet 2.0 (https://www.mirnet.ca) (Chang *et al*., 2020) was used. MiRBase identifiers of miR-363-5p and miR-29b-3p were entered into the online platform. Subsequently, miRTarBase (v.8) and TarBase (v.8) were selected to generate an interaction network. To reduce the density of the network, the ‘shortest path filter’ was applied.

3.2.2. Statistical analysis

Statistical analyses were performed using IBM SPSS Statistics v.28. Normality was assessed using Shapiro-Wilk test. Parametric data was analysed with either independent sample t-test or one-way ANOVA with Tukey's test or Dunnett's test as a post-hoc test depending on the type and number of comparisons made. Non-parametric data was assessed with either Mann-Whitney U test or Kruskal-Wallis test with Bonferroni test as a post-hoc test depending on the number of comparisons made and nature of the data. For all statistics $p < 0.05$ was considered statistically significant.

3.3. Results

3.3.1. Validating miRNA transfection of TK6 cells

To validate our suspension cell transfection protocol and determine if TK6 cells can be successfully transfected, the efficiency of TK6 cell transfection was measured using an AF647 tagged siRNA. Following transfection for 12 h, transfected viable TK6 cells expressed significantly (**$p < 0.001$, ≈ 73%**) more AF647 positive cells when compared to untransfected cells (**0.01%**) (**Fig. 24**). Additionally, untransfected TK6 cells had a significantly (**$p < 0.001$, ≈ 92%**) greater proportion of AF647 negative cells as compared to transfected cells (**≈ 18%**). Thus, transfection efficiency is estimated at ≈ 73%, using the protocol described. To further validate our transfection protocol, TK6 cell were transfected with 50 nM or 200 nM miR-363-5p or scramble miRNA (negative control) (**Fig. 25**). Total RNA was extracted from transfected TK6 cells 36 h post-transfection as a means to confirm that transfected miRNAs would still be present at the time of TMZ treatment. As expected, transfected cells expressed significantly (**$p = 0.03$** (50 nM), **$p = 0.013$** (200 nM)) more miR-363-5p as compared to negative controls.

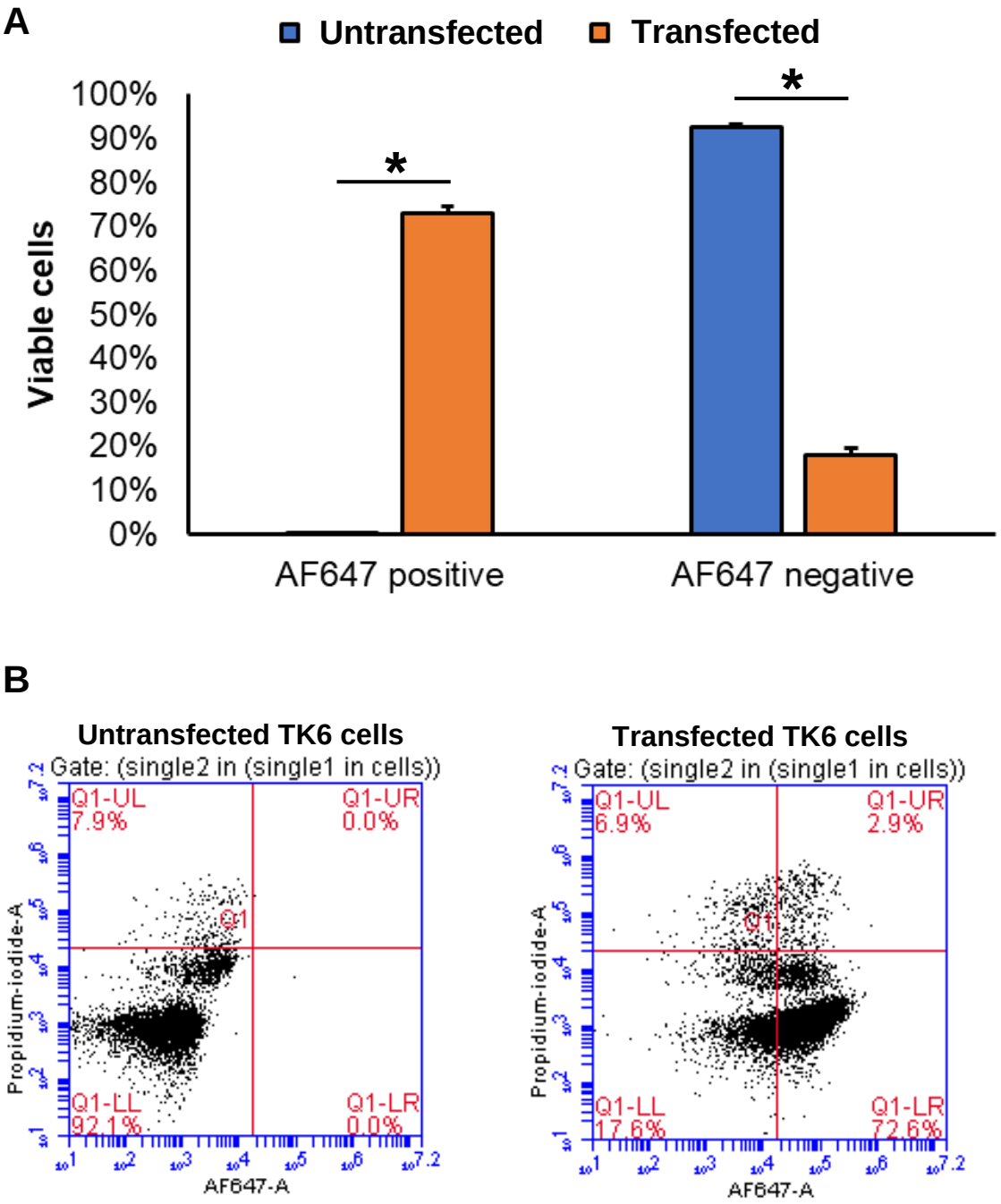

Figure 24. Validating TK6 cell transfection efficiency.

TK6 cells were transfected with 100 nM AF647 tagged scramble siRNA for 12 h. Subsequently, siRNA was removed and TK6 cells were flow cytometrically assessed. Transfected cells had significantly more AF647 positive cells compared to untransfected cells, indicating successful transfection. Data represents mean + SD (error bars) of three (**n = 3**) biological replicates. Percentage AF647 positive or negative viable TK6 cells (**A**). Flow cytometry gating strategy (**B**). * Indicates statistical significance ($p < 0.05$) between comparisons (indicated by connecting lines), as determined by independent sample t-test.

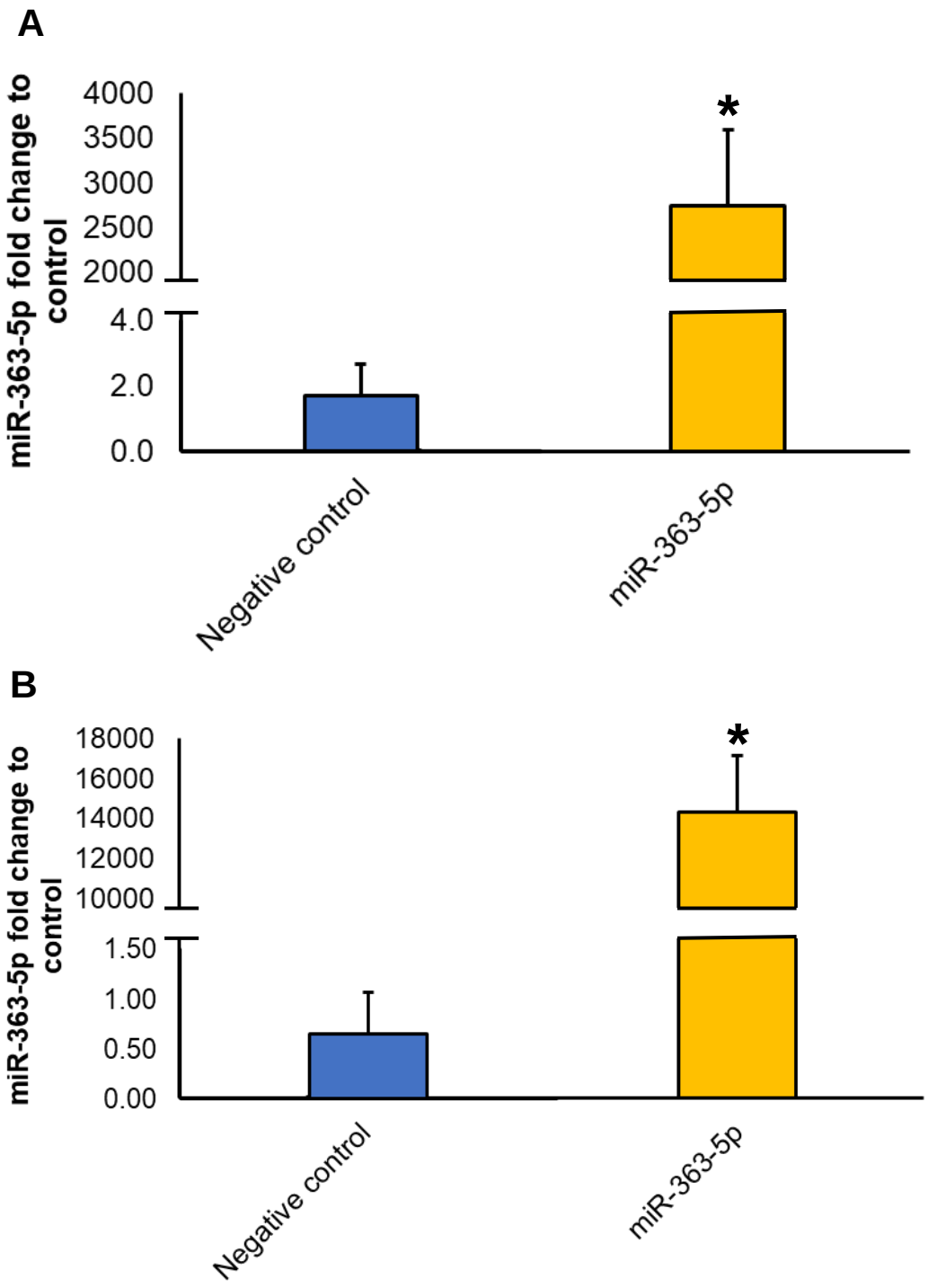

Figure 25. Assessing TK6 cell transfection with miR-363-5p.

TK6 cells were transfected with 50 nM (**A**) or 200 nM (**B**) miRNA negative control or miR-363-5p for 12 h. Subsequently, RPMI was replaced and TK6 cells were further incubated for 36 h, after which RNA was extracted and assessed by qRT-PCR for miR-363-5p expression. Negative control samples were normalised against untreated controls, while miR-363-5p was normalised against negative controls. In each case, mimic transfected samples had significantly higher miR-363-5p expression compared to negative controls, indicating successful transfection. Data represents mean + SD (error bars) and is from three (**n = 3**) biological replicates. * Indicates statistical significance ($p < 0.05$) when compared to the negative control, as determined by independent sample t-test.

3.3.2. Assessing the effect of miR-29b-3p, miR-363-5p, and a combination of both on TK6 cell fate, 36 h post-exposure to 30TMZ or 900TMZ.

To determine if miR-363-5p or miR-29b-3p can influence cell fate, TK6 cells were transfected with 100 nM of either miRNA, or 50 nM of each in combination and treated with DMSO or TMZ. Sampling 36 h post-exposure, no effect on apoptosis was observed for any miRNA, alone or in combination, when comparing negative control and transfected counterparts (**Fig. 26**). Following the same procedure, TK6 cells were analysed to determine if these miRNAs influence cell cycle distribution (**Fig. 27**). DNA content analysis did not reveal any significant changes when comparing negative controls to transfected counterparts. To determine if these miRNAs influence individual DDR proteins that may not be reflected in functional end-points (i.e., apoptosis and cell cycle), key DDR proteins were assessed following miRNA transfection. As a representative, miR-363-5p was selected to investigate this notion. However, none of the DDR proteins assessed were significantly influenced by miR-363-5p transfection (**Figs. 28 - 31**). In an attempt to identify putative targets that may influence cell fate, bioinformatic analysis was performed. Interestingly, caspase-2 was predicted as a shared target between miR-363-5p and miR-29b-3p (**Fig. 32**). Indeed, further analysis revealed three putative binding sites for miR-363-5p in the 3' UTR of caspase-2. However, miR-363-5p did not significantly influence caspase-2 in transfected TK6 cells (**Fig. 33**). Incidentally, 900TMZ-treated TK6 cells showed significantly decreased caspase-2 protein levels among both negative control (**$p < 0.001$**) and miR-363-5p transfected (**$p = 0.006$**) cells, as compared to respective 30TMZ-treated counterparts.

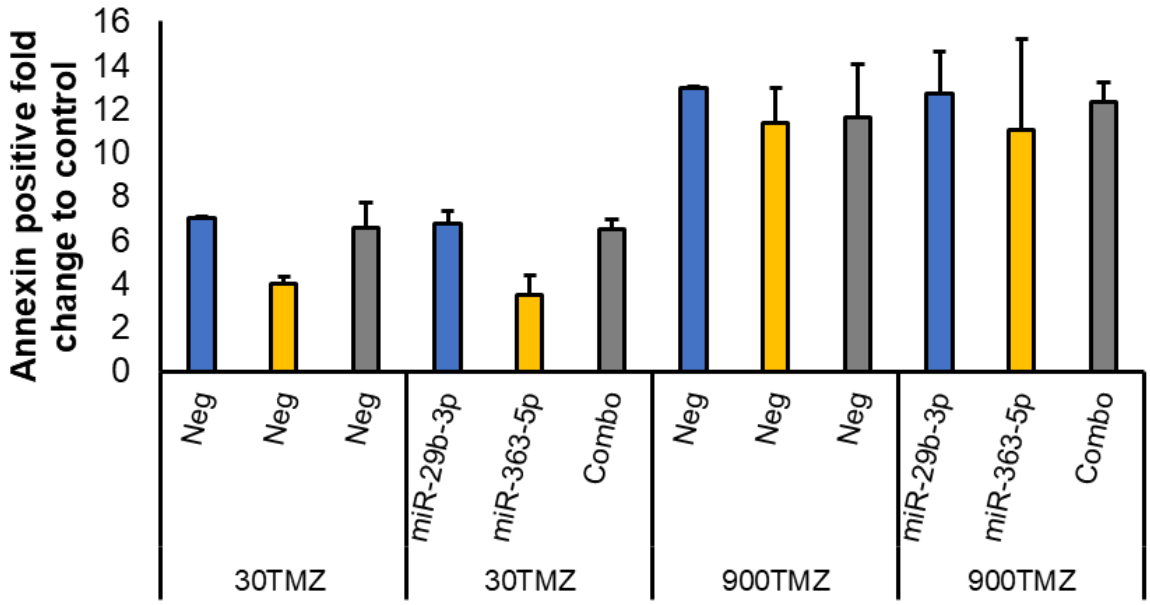

Figure 26. The influence of miR-363-5p and miR-29b-3p on TK6 cell apoptosis.

TK6 cells were transfected with 100 nM miR-363-5p or miR-29b-3p, or 50 nM miR-363-5p and miR-29b-3p for 12 h. Subsequently, RPMI was replaced with fresh complete RPMI, and cells were further incubated ≈ 22 h before treating with DMSO, 30TMZ, or 900TMZ for 1 h. Subsequently, medium was replaced with fresh RPMI and incubated another 36 h, after which cells were flow cytometrically assessed for apoptosis levels using annexin V/PI double staining. Overall, neither miR-363-5p or miR-29b-3p (individually or combined) significantly influenced apoptosis as compared to respective negative control samples. Data represents mean + SD (error bars) of three (**n = 3**) biological replicates.

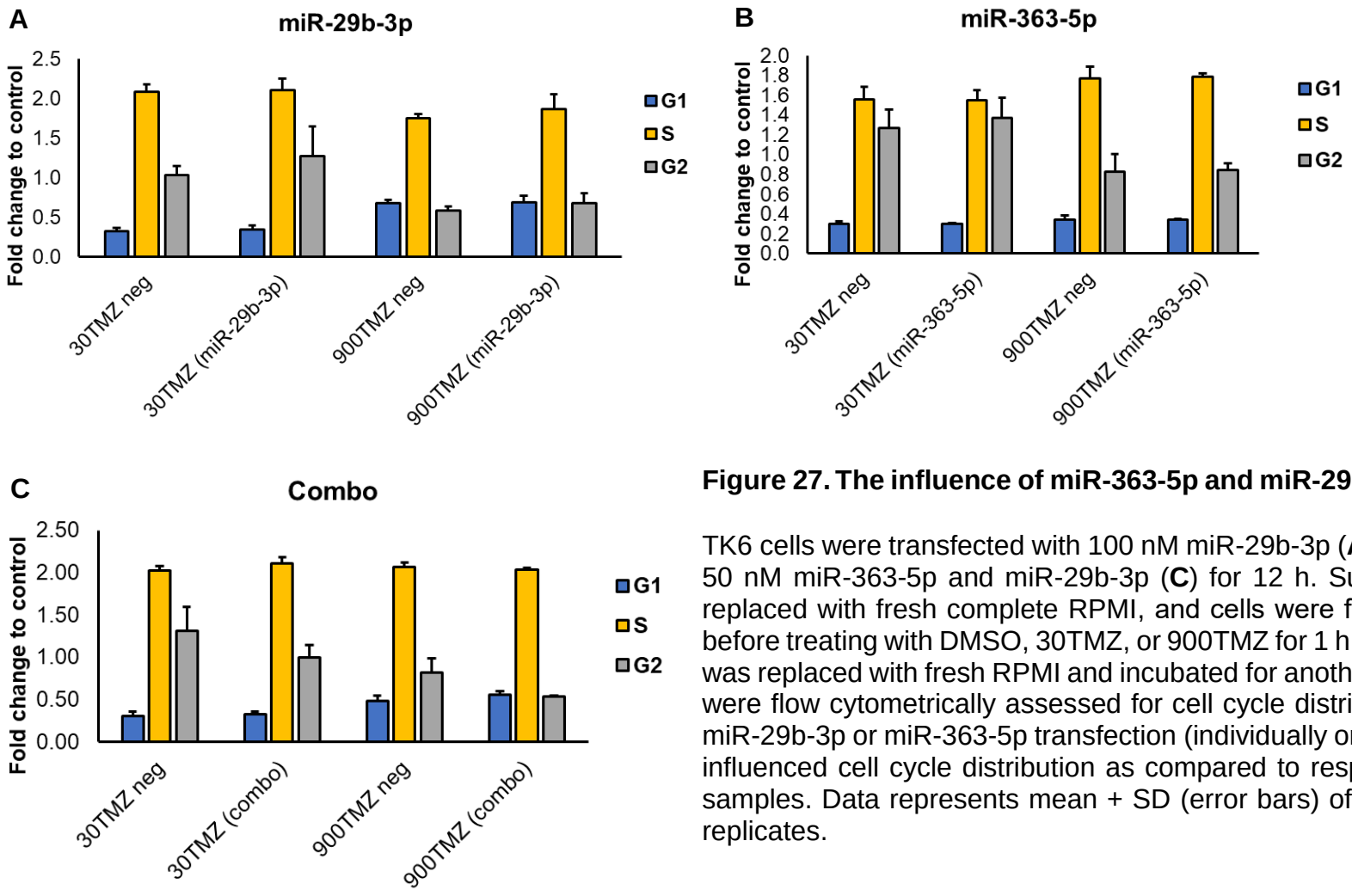

Figure 27. The influence of miR-363-5p and miR-29b-3p on TK6 cell cycle.

TK6 cells were transfected with 100 nM miR-29b-3p (**A**) or miR-363-5p (**B**), or 50 nM miR-363-5p and miR-29b-3p (**C**) for 12 h. Subsequently, RPMI was replaced with fresh complete RPMI, and cells were further incubated ≈ 22 h before treating with DMSO, 30TMZ, or 900TMZ for 1 h. Subsequently, medium was replaced with fresh RPMI and incubated for another 36 h, after which cells were flow cytometrically assessed for cell cycle distribution. Overall, neither miR-29b-3p or miR-363-5p transfection (individually or combined) significantly influenced cell cycle distribution as compared to respective negative control samples. Data represents mean + SD (error bars) of three (**n = 3**) biological replicates.

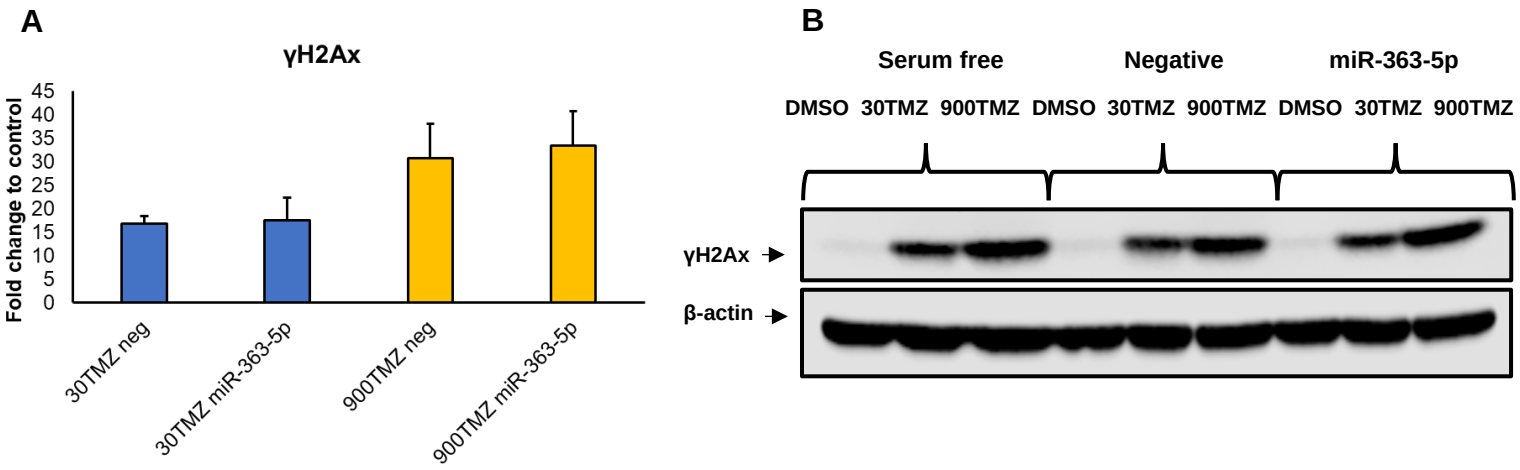

Figure 28. The influence of miR-363-5p on γH2Ax.

TK6 cells were transfected with 100 nM miR-363-5p for 12 h. Subsequently, RPMI was replaced with fresh complete RPMI, and cells were further incubated ≈ 22 h before treating with DMSO, 30TMZ, or 900TMZ for 1 h. Subsequently, medium was replaced with fresh RPMI and incubated for another 36 h. Following this, protein was extracted of which 13 µg – 20 µg was analysed by immunoblotting. Overall, miR-363-5p did not significantly influence γH2Ax protein levels (**A** and **B**) as compared to respective negative control samples. Data represents mean + SD (error bars) of three (**n = 3**) biological replicates.

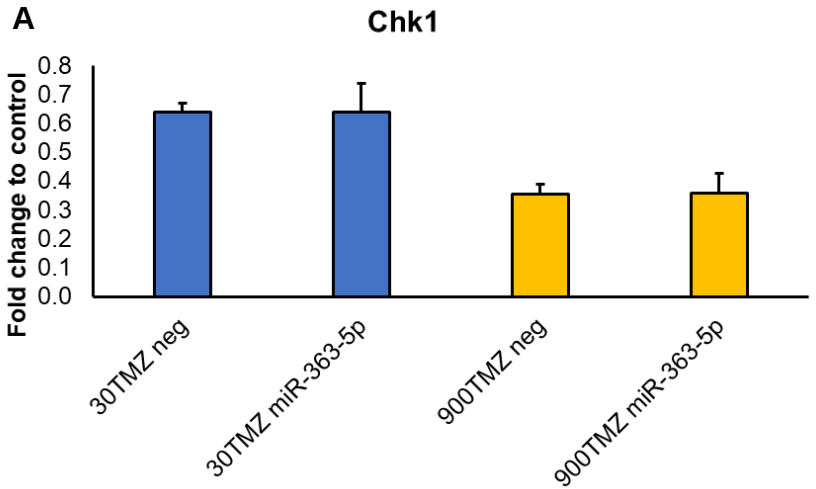

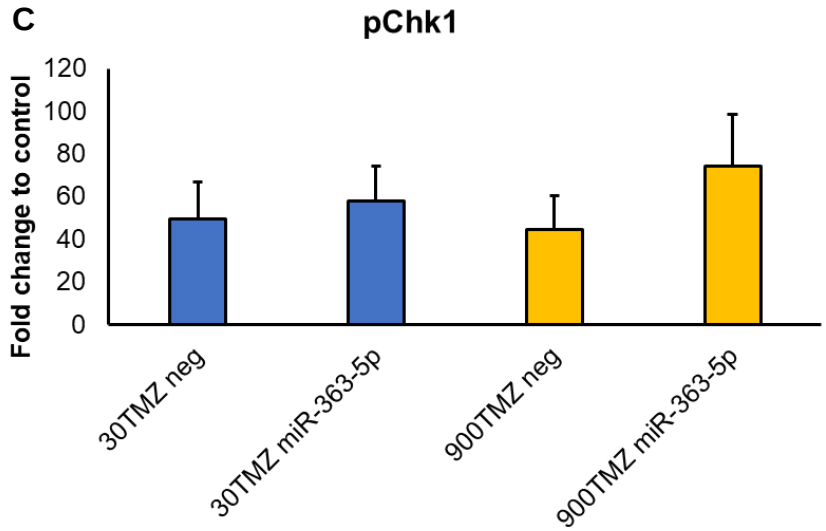

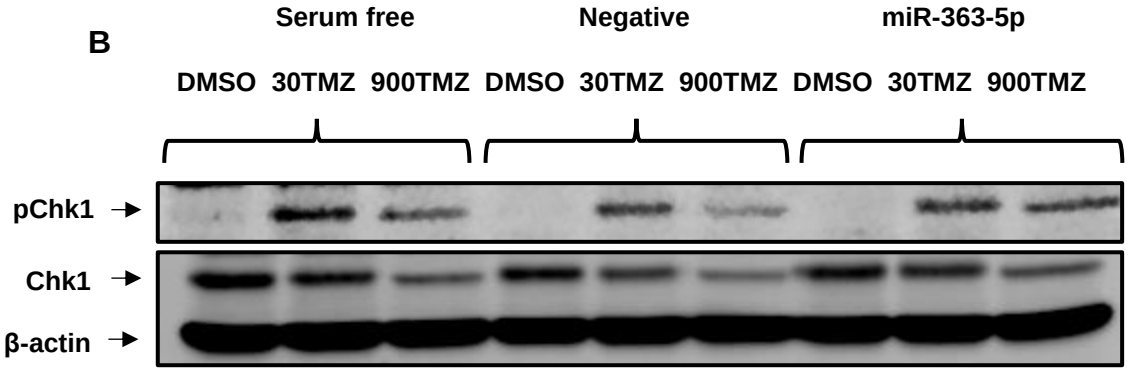

Figure 29. The influence of miR-363-5p on Chk1/pChk1.

TK6 cells were transfected with 100 nM miR-363-5p for 12 h. Subsequently, RPMI was replaced with fresh complete RPMI, and cells were further incubated ≈ 22 h before treating with DMSO, 30TMZ, or 900TMZ for 1 h. Subsequently, medium was replaced with fresh RPMI and incubated for another 36 h. Following this, protein was extracted of which 13 µg – 20 µg was analysed by immunoblotting. Overall, miR-363-5p did not significantly influence Chk1 (**A** and **B**) or pChk1 (**C** and **B**) protein levels as compared to respective negative control samples. Data represents mean + SD (error bars) of three (**n = 3**) biological replicates.

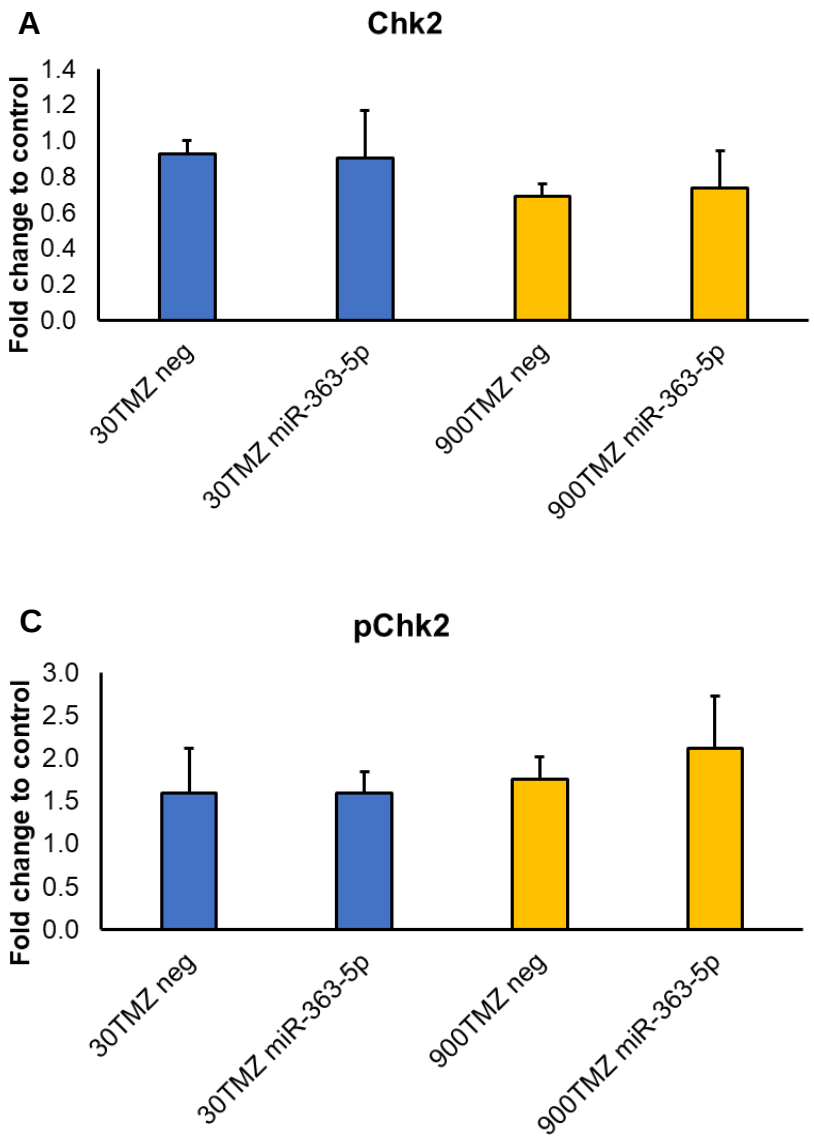

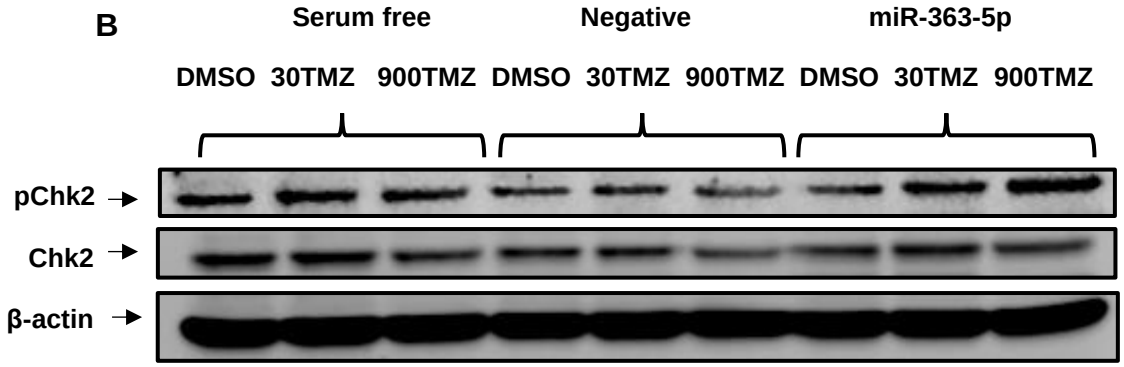

Figure 30. The influence of miR-363-5p on Chk2/pChk2.

TK6 cells were transfected with 100 nM miR-363-5p for 12 h. Subsequently, RPMI was replaced with fresh complete RPMI, and cells were further incubated ≈ 22 h before treating with DMSO, 30TMZ, or 900TMZ for 1 h. Subsequently, medium was replaced with fresh RPMI and incubated for another 36 h. Following this, protein was extracted of which 13 µg – 20 µg was analysed by immunoblotting. Overall, miR-363-5p did not significantly influence Chk2 (**A** and **B**) or pChk2 (**C** and **B**) protein levels as compared to respective negative control samples. Data represents mean + SD (error bars) of three (**n = 3**) biological replicates.

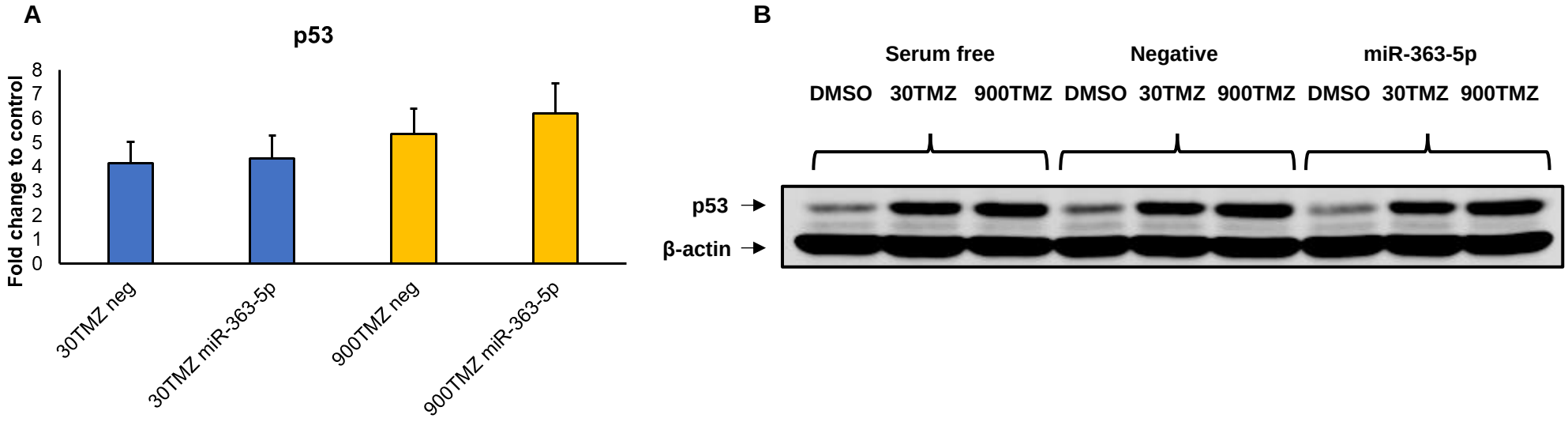

Figure 31. The influence of miR-363-5p on p53.

TK6 cells were transfected with 100 nM miR-363-5p for 12 h. Subsequently, RPMI was replaced with fresh complete RPMI, and cells were further incubated ≈ 22 h before treating with DMSO, 30TMZ, or 900TMZ for 1 h. Subsequently, medium was replaced with fresh RPMI and incubated for another 36 h. Following this, protein was extracted of which 13 µg – 20 µg was analysed by immunoblotting. Overall, miR-363-5p did not significantly influence p53 protein levels (**A** and **B**) as compared to respective negative control samples. Data represents mean + SD (error bars) of three (**n = 3**) biological replicates.

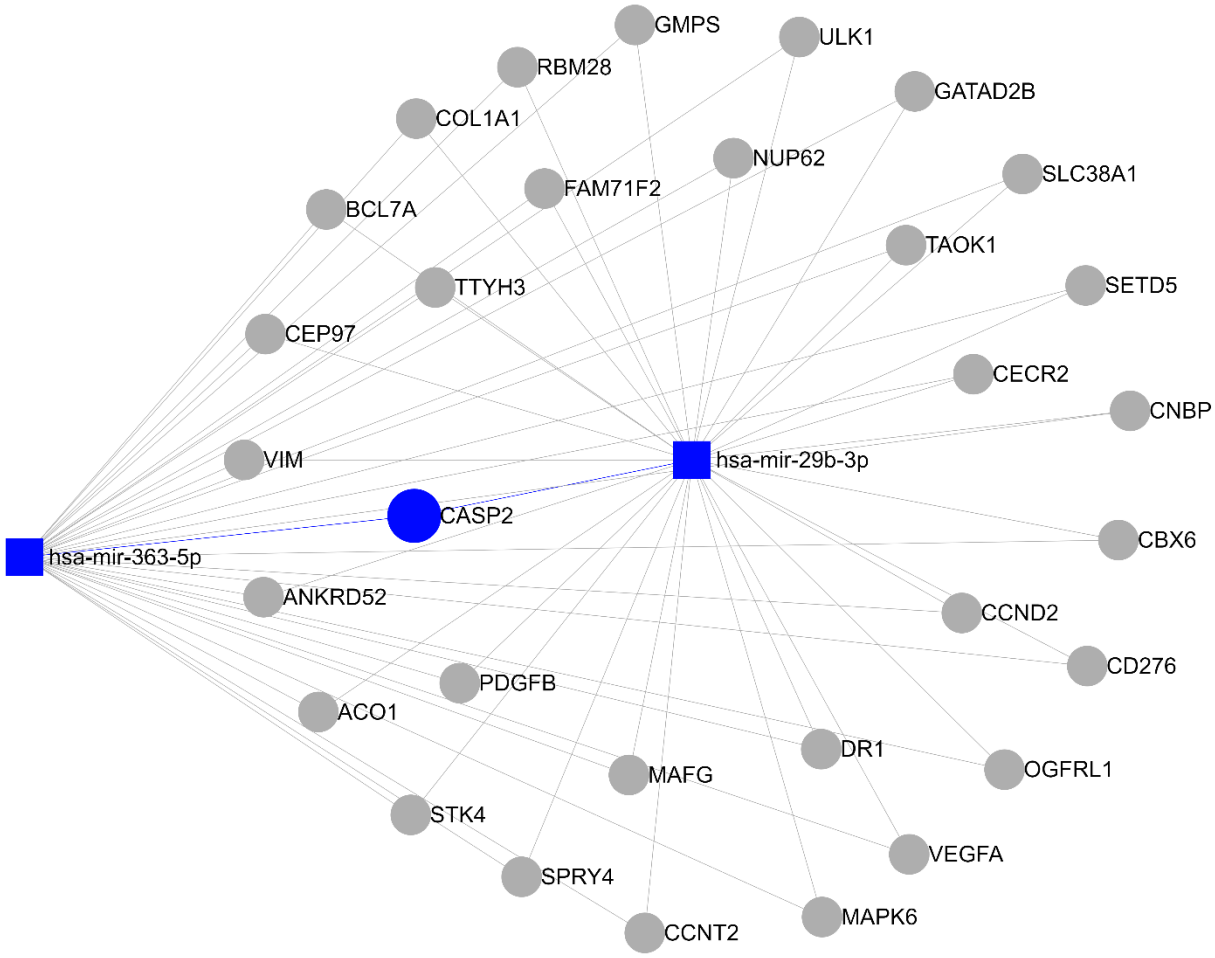

Figure 32. Caspase-2 is a shared target between miR-29b-3p and miR-363-5p.

Using miRNet 2.0, an interaction network for miR-363-5p and miR-29b-3p based on miRTarbase (v.8) and TarBase (v.8) databases was generated, and showed caspase-2 as a shared putative target between both miRNAs.

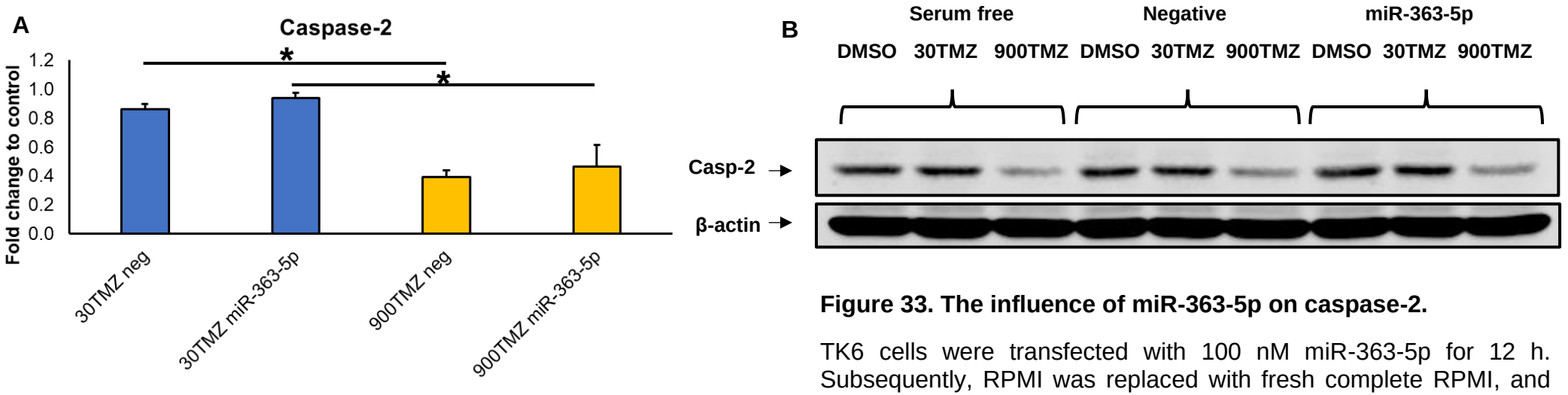

Figure 33. The influence of miR-363-5p on caspase-2.

TK6 cells were transfected with 100 nM miR-363-5p for 12 h. Subsequently, RPMI was replaced with fresh complete RPMI, and cells were further incubated ≈ 22 h before treating with DMSO, 30TMZ, or 900TMZ for 1 h. Subsequently, medium was replaced with fresh RPMI and incubated for another 36 h. Following this, protein was extracted of which 13 µg – 20 µg was analysed by immunoblotting. Overall, miR-363-5p transfection did not significantly influence caspase-2 protein levels (**A** and **B**) as compared to respective negative control samples, despite having putative binding sites within the caspase-2 3'UTR (**C**). Importantly, however, caspase-2 was significantly decreased among 900TMZ-treated cells, as compared to 30TMZ-treated counterparts. Data represents mean + SD (error bars) of three (**n = 3**) biological replicates. ***** Indicates statistical significance ($p < 0.05$) as determined by independent sample t-test when comparing miR-363-5p transfected to dose-matched negative control samples.

3.4. Discussion

MiRNAs are becoming well-established as regulators of cellular function, disease biomarkers, and potential therapeutic options/targets. As diagnostic tools, miRNA products are available and changing the diagnostic landscape for many diseases. However, as therapeutic options, miRNAs have been less successful and none, to our knowledge, are currently available as approved therapies (Bonneau *et al*., 2019). Nevertheless, albeit for diagnostic or therapeutic purposes, the identification and functional annotation of candidate miRNAs could have significant implications. To this end, our study investigated the influence of miR-363-5p and miR-29b-3p on TK6 cell fate, following exposure to TMZ. Having previously shown significant downregulation in response to 30TMZ (miR-363-5p) and 900TMZ (miR-29b-3p and miR-363-5p) treatment (**Chapter 2**), we investigated the possibility that these miRNAs may be anti-apoptotic and are downregulated in response to DNA damage to prevent mutant propagation. Interestingly, transfection with these miRNAs, individually or combined, had no observable effect on cell fate as measured by cell cycle distribution and apoptosis functional assays. One possible explanation for this could be that the miRNA-regulating mechanisms that suppressed these miRNAs in response to TMZ in the first instance, was sufficient to overpower the transfected miRNAs. Thus, it becomes a matter of dose, as this assertion is dependent on prevailing TMZ adducts, and consequent DNA damage, that continuously suppress newly introduced miRNAs. This makes sense given that the most genotoxic lesion, O^6-meG, induced by TMZ is not repaired in TK6 cells, as they are MGMT deficient (Goldmacher, Cuzick Jr, and Thilly, 1986; Kaina *et al*., 2007). It follows that these adducts continuously activate a miRNA-suppressive mechanism that is DNA damage responsive. Indeed, we have previously observed an inverse relationship between p53 stabilisation, and miR-363-5p and miR-29b-3p

expression, suggesting p53 to be, or possibly regulate, the miRNA-suppressive mechanism. This theory is supported by our previous observations that 900TMZ results in a more pronounced downregulation of these miRNAs (**Chapter 2**).

It is possible that at this lethal dose, O^6-meG, constituting the smallest portion of the TMZ-induced DNA damage spectrum (≈ 5 - 6%) (Newlands *et al*., 1997; Bouzinab *et al*., 2019), accumulates and causes DNA damage that ultimately upregulates p53 to a level capable of undermining even miRNA-363-5p and miR-29b-3p over-expression. Recall (**Chapter 2**), p53 has been implicated in the repression of let-7a and let-7b (Saleh *et al*., 2011), miR-224 (Liang *et al*., 2013), and the miR-17-92 cluster (Yan *et al*., 2009), thus clearly underpinning a miRNA-repressive role for p53. This might also explain why suppression of these miRNAs were less pronounced among 30TMZ-treated cells. In this case, the O^6-meG lesion burden is likely less than for 900TMZ-treated cells and may even be overcome by DNA damage tolerance mechanisms such as TLS (Peng *et al*., 2016; Kaina and Christmann, 2019). Interestingly, ATR signalling has been associated with TLS, as inhibition of DNA polymerase κ, known to participate in DNA TLS, has been shown to impair ATR and Chk1 phosphorylation in glioblastoma cells (Peng *et al*., 2016). Furthermore, ATR has been shown to directly phosphorylate DNA polymerase η (pol η) in human fibroblasts (Göhler *et al*., 2011), which is required for pol η-mediated TLS (Peddu *et al*., 2018). Thus, TLS is likely a mechanism of DNA damage tolerance in both 30TMZ-, and 900TMZ-treated cells, but differs in magnitude of activation, in favour of 900TMZ-treated cells. Again, this is supported by the significantly increased pATR levels observed among 900TMZ-treated cells when compared to those treated with 30TMZ at 4 h, 18 h, and 36 h post-exposure (**Chapter 2**). However, the fact that miRNA over-expression did not influence cell fate at either TMZ dose cannot be reconciled. On one hand, it is possible that 36 h post-exposure even 30TMZ induces a

sufficient miRNA-suppressive response capable of impeding phenotypic changes that might otherwise occur following miRNA over-expression. Although, this does not agree with our assertion that p53 might facilitate miRNA suppression, as p53 levels were not significantly correlated with miRNA expression among 30TMZ-treated cells (**Appendix D Fig. 37**). Moreover, only miR-363-5p showed a significant negative correlation with time post-30TMZ exposure. On the other hand, it is possible that the effect of miRNA over-expression is also influenced by the overall state of the cell. Particularly, a significant proportion of cells became apoptotic between 4 h – 36 h post-exposure to 900TMZ, whereas 30TMZ-treated cells did not. This implies that potential targets of miR-363-5p and miR-29b-3p might be upregulated during an apoptotic cell fate and are required to effect phenotypic changes caused by these miRNAs. Indeed, both miRNAs are predicted to converge on caspase-2 (**Fig. 32**). Among miR-363-5p and miR-29b-3p, only miR-363-5p is predicted to directly target the caspase-2 3' UTR at two 7-mer and one 6-mer complimentary binding sites (TargetScan (v.8); Agarwal *et al*., 2015; McGeary *et al*., 2019). However, miR-363-5p transfection did not influence caspase-2 levels (**Fig. 33**).

Given that miR-29b-3p is predicted to converge on caspase-2 with miR-363-5p, it is possible that both are required to inhibit caspase-2 protein levels. Since miR-29b-3p has no predicted binding sites within the caspase-2 3' UTR (TargetScan (v.8); Agarwal *et al*., 2015; McGeary *et al*., 2019), it is possible that miR-29b-3p targets caspase-2 regulatory proteins. Caspase-2 is an initiator caspase with pro-apoptotic functions. Activation of caspase-2 remains a topic of debate but there are three prevailing models for caspase activation i.e., pro-caspase recruitment and dimerisation with protein complexes and subsequent cleavage; autocleavage; or transactivation by other caspases. These mechanisms are reviewed in detail elsewhere (Vigneswara and

Ahmed, 2020), and is beyond the scope of this thesis. However, it is worth noting that caspase-2 activation includes a death receptor-mediated pathway and an oligomeric structure, PIDDosome-, mediated pathway. These activating mechanisms involve various non-communal proteins and thus, it is reasonable to conclude that inhibiting a single protein might not always be sufficient to completely undermine caspase-2 activation.

Consider, for example, TRAF3, a protein that has been shown to interact with, and promote caspase-2 dimerisation and activation (Robeson *et al*., 2018). Inhibition of TRAF3 reduced both, caspase-2 dimerisation and subsequent apoptosis by only ≈ 15%, following 20 μM cisplatin treatment. While this decrease was statistically significant, the authors also showed siTRAF3-transfection into HeLa cells to have no significant effect on caspase-2 dimerisation following 20 μM cisplatin treatment, as compared with control-transfected cells. This implies that TRAF3 inhibition may not always be sufficient to abrogate caspase-2 activity. Herein lies the underpinning of our previous assertion that inhibition of a single protein may not always suffice to prevent protein activation. In relation to our study, it is important to note that miR-29b-3p has been shown to directly target the 3' UTR of TRAF3 in breast cancer cells (Zhang *et al*., 2019). However, in our study, miR-29b-3p transfection was unable to rescue the apoptotic phenotype observed following TMZ treatment (**Fig**. **26**), possibly due to insufficient suppression of caspase-2 levels. It is possible that, along with miR-29b-3p, miR-363-5p is also required to sufficiently inhibit caspase-2 protein levels, given its caspase-2 3' UTR complementarity. This might explain why we did not observe individual miR-363-5p transfection to influence caspase-2 protein levels (**Fig. 33**), as co-operation between miR-29b-3p and miR-363-5p might be required to repress caspase-2 levels at both a

transcriptional (miR-363-5p binds 3' UTR of capase-2) and post-transcriptional (e.g., miR-29b-3p inhibits caspase-2 activity by inhibiting TRAF3) level.

This is a reasonable assertion as miRNAs have been reported to co-operatively facilitate or augment various cellular outcomes. For example, co-transfection with miR-125a-5p and miR-145 increased lung carcinoma cell sensitivity to erlotinib as compared with either miRNA individually (Amri *et al*., 2021). Another example is that of miR-381 and miR-424 that significantly increased the apoptotic fraction of renal carcinoma cells when co-transfected, and compared with individually transfected cells (Chen *et al*., 2013b). Furthermore, prostate cancer cells transfected with either miR-34a or miR-34c was not sensitised to the effects of dox as indicated by caspase activity, whereas combined transfection significantly increased caspase activity, even in the absence of dox (Rokhlin *et al*., 2008). Notwithstanding overall cell fate, miRNAs also co-operate to target specific proteins. For example, miR-26a is incapable of inhibiting WEE1 when individually transfected into lung cancer cells but can augment the inhibitory effect of miR-16 when co-transfected. Furthermore, the inhibitory effect of miR-26a and miR-16 on Chk1 is strengthened when co-transfected into lung cancer cells (Lezina *et al*., 2013). Similarly, the inhibitory effect of miR-205 and miR-342 on E2F1 is augmented when co-transfected in lung carcinoma or melanoma cells (Lai *et al*., 2018).

Surprisingly, dual transfection of miR-363-5p and miR-29b-3p was unable to rescue the TMZ-induced apoptotic phenotype observed in our study (**Fig. 26**). It is possible that caspase-2 was sufficiently inhibited by these miRNAs, but did not alter the apoptotic cell fate as caspase-2 is known to have redundant functions in apoptosis induction. Moreover, it has been demonstrated that caspase-2 inhibition does not always alleviate apoptosis (Kumar, 2009; Bouchier-Hayes and Green, 2012, Puccini, Dorstyn, and Kumar, 2013, Brown-Suedel and Bouchier-Hayes, 2020). Consequently, apoptosis may

not be a suitable metric for successful caspase-2 inhibition. Another possible explanation could be that the miRNA concentration used for dual-transfection was insufficient for effective caspase-2 inhibition, as these were only 50 nM (each), while the recommended concentration for suspension cells is 100 nM (Qiagen). However, increasing each miRNA to 100 nM runs the risk of endogenous miRNA dysregulation, resulting from competition with RISC machinery (Khan *et al*., 2009), thereby causing confounding effects.

Despite miRNA-transfection having no observable effect, caspase-2 levels were significantly decreased when comparing 900TMZ to 30TMZ-treated samples, suggesting a greater proportion of cleaved, and thus potentially active, caspase-2 among 900TMZ-treated cells (Fava *et al*., 2012; Bronner, O'Riordan, and He, 2013). Coupled with our observations of miR-29b-3p and miR-363-5p downregulation in response to TMZ treatment, and the predicted negative regulation of caspase-2 by these miRNAs, caspase-2 appears to be part of the TMZ-induced apoptotic response in TK6 cells. Therefore, it is tempting to speculate that miR-363-5p and miR-29b-3p is downregulated in response to TMZ as part of an endogenous mechanism to facilitate apoptosis that may, at least partly, be facilitated by caspase-2. This expands our observed TMZ induced DDR response pathway in TK6 cells i.e., ATR-Chk1-p53-Caspase-2.

4.1. Final Discussion

DNA is constantly exposed to a genotoxic environment. Albeit endogenous (e.g., cellular respiration) or exogenous (e.g., chemotherapeutic agents), DNA damage must be resolved to prevent its propagation and subsequent manifestation of mutations that can give rise to a host of pathologies (Auten and Davies, 2009; Tubbs and Nussenzweig, 2017). The DDR functions to resolve DNA damage through DNA repair mechanisms. However, severe DNA damage that exceeds repair capabilities trigger programmed cell death e.g., apoptosis (Surova and Zhivotovsky, 2013; Tubbs and Nussenzweig, 2017). The dynamics of the DDR has been well-studied but numerous aspects remain enigmatic. For example, the same DDR is triggered to facilitate both DNA repair, implying a survival strategy, and apoptosis. This suggests the existence of endogenous mechanisms capable of quantifying DNA damage that needs to surpass a stochastic threshold that directs the DDR to a specific cell fate. Prevailing theories include: 1) the existence of DDR pulses in response to DNA damage that differs in frequency and amplitude depending on the nature of the DNA damage, which drives differential cell fates (Loewer *et al*., 2010; Batchelor *et al*., 2011; Li *et al*., 2011a; Loewer *et al*., 2013; Porter, Fisher, and Batchelor, 2016); 2) the status of p53 phosphorylation modifies its transcriptional activities to facilitate different cell fates (Jabbur, Huang, and Zhang, 2000; Mayo *et al*., 2005; Smeenk *et al*., 2011; Loughery *et al*., 2014). Additionally, both these theories are contingent on the level of DNA damage.

Our study shows 30TMZ to preferentially direct cell fate toward cell cycle arrest, whereas 900TMZ induces significant apoptosis. Consequently, differences in the DDR observed in TK6 cells following exposure to these doses could identify underlying molecular signatures that exemplify different cell fates. Indeed, our data identified distinct DDR protein levels among 900TMZ-treated cells from as early as 4 h post-

exposure. At most time-points, pATR, γH2Ax, pChk1, and p53 were significantly increased, suggesting this to be the predominant DDR pathway in response to lethal TMZ doses in TK6 cells. This is unexpected as TMZ induces DSBs, as indicated by significantly increased levels of γH2Ax, which is quintessentially detected by ATM, whereas ATR preferentially detects SSBs and replication fork stalling (Cimprich and Cortez, 2008; Maréchal and Zou, 2013; Zeman and Cimprich, 2014). It is possible that both ATM and ATR is involved, exhibiting a switching behaviour in a time-dependent manner. This might explain why pATR increased in a time-, and dose-dependent manner, as pATM presumably directed an early response to TMZ-induced damage. Indeed, ATM has been suggested to be the initial response to DNA damage, eventually being succeeded by ATR (Shiotani and Zou, 2009; Loughery and Meek, 2013). However, we were unable to confirm the early involvement of ATM. Nonetheless, pATR appears to be the principal driver of TMZ-induced damage within the investigated time-frame. This is further supported by the observation that pChk1, a known downstream effector of pATR, was consistently significantly increased among 900TMZ-treated cells as compared to 30TMZ-treated cells, at a magnitude that far exceeded the levels of pChk2, the typical downstream effector of pATM.

A principal role for pATR in response to TMZ could stem from the resulting DNA repair mechanisms. As previously discussed, the underlying genotoxicity of TMZ is proposed to be driven by the MMR futile cycle. During this reaction single stranded DNA (ssDNA) is produced that triggers ATR signalling. Further compounding ATR involvement is the imminent uncoupling/stalling of DNA replication machinery as a result of MMR. Thus, the MMR futile cycle causes an accumulation of ssDNA, eventually forming DSBs (De Zio, Cianfanelli, Cecconi, 2013; Li, Pearlman, and Hsieh, 2016; Gupta *et al*., 2018). Further validating the pATR signalling cascade as the predominant response to TMZ-

induced DNA damage is our observation of tandem increases in downstream proteins, γH2Ax, pChk1, and p53. Thus, it is possible that the differential cell fates observed between 30TMZ and 900TMZ stems from within this pathway. Given its function as a transcription factor, p53 is a likely candidate.

It is known that upon DNA damage, p53 becomes stabilised through PTMs (**Chapter 1**). Though, the exact contribution that these PTMs play in p53 functionality is an ongoing question. Perhaps the most extensively researched is phosphorylation of p53, which has been proven to uncouple the interaction between p53 and its inhibitor MDM2, thereby promoting its transcriptional activity (Moll and Petrenko, 2003). In recent years, it has been proposed that cell cycle arrest and ultimately DNA repair is accompanied by a p53 phosphorylation status distinct from what is observed during apoptosis. It has been proposed that this “pro-death” phosphorylation status shifts the transcriptional directive of p53 to preferentially upregulate pro-apoptotic genes (Jabbur, Huang, and Zhang, 2000; Oda *et al*., 2000; Mayo *et al*., 2005; Smeenk *et al*., 2011; Loughery *et al*., 2014). However, the range of genes fostered by this pro-apoptotic p53 phosphorylation status requires elaboration. Moreover, the involvement of other molecular regulators that may be under transcriptional control of p53 requires investigation. Our results clearly demonstrate a predominantly apoptotic cell fate among 900TMZ-treated cells 36 h post-exposure, but not 30TMZ. Thus, it is reasonable to assume that the phosphorylation, and thus transcriptional selectivity, of p53 is distinct between 30TMZ-, and 900TMZ-treated cells 36 h post-exposure.

In line with this, we sought to determine if 30TMZ and 900TMZ exhibited distinct changes in miRNA expression. MiRNAs are known regulators of a wide range of cellular functions, and many have been reported to be transcriptionally controlled by p53 (**Fig. 22**). Indeed, we identified a total of 31 DE miRNAs at different time-points following

30TMZ or 900TMZ treatment, as compared to DMSO controls (**Table 8**). The majority of DE miRNAs were observed 36 h post-exposure to 900TMZ, as compared to time-matched DMSO controls. Incidentally, at this time-point, the highest overall levels of DNA damage, DDR proteins, and apoptosis was observed for 900TMZ-treated cells, along with showing the greatest disparity when compared with 30TMZ-treated cells. Thus, it is not unreasonable to assume that cell fate observed for these doses 36 h post-exposure is inextricably linked to the distinct miRNA profiles. It is telling that only one miRNA was DE when comparing DMSO and 30TMZ-treated cells 36 h post-exposure, as we also observed no significant change in apoptosis when comparing 30TMZ-treated cells 4 h post-exposure to those 36 h post-exposure. This further alludes to the DE miRNA patterns between 30TMZ and 900TMZ to be the regulator between different cell fates, perhaps specifically, apoptosis. In support of this, functional enrichment analysis of all DE miRNAs 36 h post-exposure to 900TMZ revealed *protein phosphorylation* and *negative regulation of the apoptotic process* to be the most significantly enriched terms. This makes sense given the critical role phosphorylation plays in the DDR cascade. Moreover, given the inhibitory role of miRNAs, it can be concluded that enrichment of the *negative regulation of the apoptotic process* amounts to positive regulation of apoptosis, as the DE miRNAs would function to repress transcripts involved in the negative regulation of the apoptotic process.

To further confirm miRNA involvement in TK6 cell fate following TMZ exposure, the expression of selected DE miRNAs, miR-29b-3p, miR-363-5p, and miR-485-3p were determined, and all were found to be significantly repressed 36 h post-exposure to 900TMZ, when compared to 30TMZ-treated cells. Additionally, each of these miRNAs decreased significantly when comparing expression levels 4 h post-exposure, to those at 36 h post-exposure to 900TMZ, whereas this was only observed for miR-363-5p

among 30TMZ-treated cells. This suggests the expression of these miRNAs to be both time-, and dose-responsive. Additionally, at the time of writing, none of these miRNAs had been reported in TK6 cells in the context of the DDR. In line with our previous assertion that the molecular determinant of the differential cell fates observed between 30TMZ-, and 900TMZ-treated TK6 cells stems from within the ATM-γH2Ax-Chk1-p53 pathway, we observed p53 and miRNA levels to be regulated in opposing directions following TMZ exposure. Specifically, p53 levels had a significant positive correlation with time post-900TMZ exposure, while miR-29b-3p, miR-363-5p, and miR-485-3p were each significantly negatively correlated with time post-900TMZ exposure. Contrastingly, while p53 levels among 30TMZ-treated cells also had a positive correlation with time post-exposure, only miR-363-5p was significantly negatively correlated with time post-30TMZ exposure. However, though not significant, miR-29b-3p and miR-485-3p were also negatively correlated with time post-30TMZ exposure, suggesting that p53 levels might be driving the differential miRNA-response between 30TMZ-, and 900TMZ-treated cells. Recall from **Chapter 1** that p53 levels of 900TMZ-treated cells were significantly greater than that of 30TMZ-treated cells, at each time-point. Thus, it is possible that among 900TMZ-treated cells, p53 levels are sufficiently elevated to facilitate miRNA-repression, whereas among 30TMZ-treated cells, only a partial miRNA-repressive effect is observed as the levels of p53 is not elevated to the same extent as in 900TMZ-treated cells.

Given the distinct PTMs that p53 undergoes to change its transcriptional selectivity and effect specific cell fates, it is not unreasonable to suspect p53 as the driving force for the observed miRNA repression following TMZ exposure. However, typical examples of p53 mediated transcriptional regulation involves upregulation, as is seen with p21 or PUMA (**Chapter 1; Table 1**). Nonetheless, p53 has been reported to repress miRNAs

both directly and indirectly (Yan *et al*., 2009; Saleh *et al*., 2011; Liang *et al*., 2013). Thus, we postulate that in lethally damaged cells, p53 is upregulated in response to DNA damage and ultimately represses miR-29b-3p, miR-363-5p, and miR-485-3p. However, while it is tempting to speculate that these miRNAs are repressed as part of an inherent mechanism to induce apoptosis, thereby suggesting an anti-apoptotic role for these miRNAs, their exact role in TK6 cells in response to DNA damage remains elusive.

To investigate the biological significance of these DNA damage responsive miRNAs in cell fate, miR-363-5p and miR-29b-3p was ectopically over-expressed in TK6 cells. Notwithstanding their individual physiological relevance, miR-29b-3p and miR-363-5p are predicted to converge on caspase-2. This fits well with our assumption that miR-29b-3p and miR-363-5p are anti-apoptotic as caspase-2 has known pro-apoptotic functions (Vigneswara and Ahmed, 2020). This would also explain their repression in 900TMZ-treated cells, as we demonstrated TK6 cells at this dose to be fated for apoptosis. Surprisingly, miRNA over-expression did not significantly alter cell fate, nor caspase-2 protein levels (**Figs. 26, 27,** and **33**). It is possible that miRNA-mediated functions in cell fate determination is a concerted effort by a host of miRNAs cooperating in tandem, or relaying cascades to effect biological change. MiRNAs are known to synergise and converge on the same, or multiple targets within the same pathway to facilitate specific changes (**Fig. 23**; **Table 9**; Rokhlin *et al*., 2008; Niu *et al*., 2016; Raut *et al*., 2016). It is also possible that over-expression disrupted other endogenous mechanisms by saturating RISC machinery and thereby altering miRNA homeostasis (Khan *et al*., 2009). Another possibility is that the TMZ-induced damage can overcome our attempts at miRNA over-expression. This may result from O^6-MeG adducts that is not resolved in TK6 cells as they are MGMT deficient (Chapman, Doak, and Jenkins,

2015). Thus, these unresolved lesions would continuously activate the endogenous mechanism responsible for miRNA repression.

4.2. Concluding remarks and broader scientific impact

Despite a plethora of research surrounding the DDR, a complete understanding regarding the DDR signalling cascade remains enigmatic. Even more so is the response variability associated with varying levels of genotoxicity and ultimately, different cell fates. Our work identifies a sub-lethal and lethal TMZ dose and extends the TMZ-induced DDR mechanism in TK6 cells. We identify ATR-γH2Ax-Chk1-p53 as the principal differentially regulated DDR pathway in TK6 cells in response to sub-lethal and lethal TMZ doses. Additionally, we suggest a role for caspase-2 in TMZ-induced apoptosis of TK6 cells. A firm understanding of the DDR mechanism involved in specific cells and in response to specific chemotherapeutic agents is critically important to measure chemotherapeutic efficacy. Moreover, unravelling the TMZ-induced DDR pathway can lead to the discovery of druggable targets in TMZ-resistant cancers. Beyond this, understanding what drives the decision to survive or undergo apoptosis in response to DNA damage can improve the therapeutic landscape. In this regard, our study bridges the current, incomplete, understanding of DDR regulation by providing 31 candidate miRNAs that appear to be DNA damage responsive and may be useful as treatments or targets in future cancer therapies. Moreover, these DNA damage responsive miRNAs may serve as specific biomarkers of genotoxic damage. As a principle finding of this study, we identify miR-29b-3p, miR-363-5p, and miR-485-3p as time-, and dose-responsive, and we implicate p53 as the potential repressor of these miRNAs (**Fig. 34**). While we could not determine the physiological importance of suppressing these miRNAs in response to lethal DNA damage, the dynamic nature of endogenous miRNAs prevent their exclusion as contributors to cell fate in response to

DNA damage. Thus, this study demonstrates DNA damage responsive miRNAs that are dose-, and time-dependent, and provides a platform to begin unravelling exactly which miRNAs and in which combinations they may regulate cell fate decisions. While this could form the basis for developing rapid screening panels used in a therapeutic setting to inform chemotherapeutic efficacy *en masse*, an ideal outcome stemming from the cell-fate-associated miRNAs identified in our research would be the harnessing of these miRNAs to 'manipulate' cancerous cells into an apoptotic cell fate without the requirement for toxic chemotherapeutic regimens, thereby improving patient quality of life.

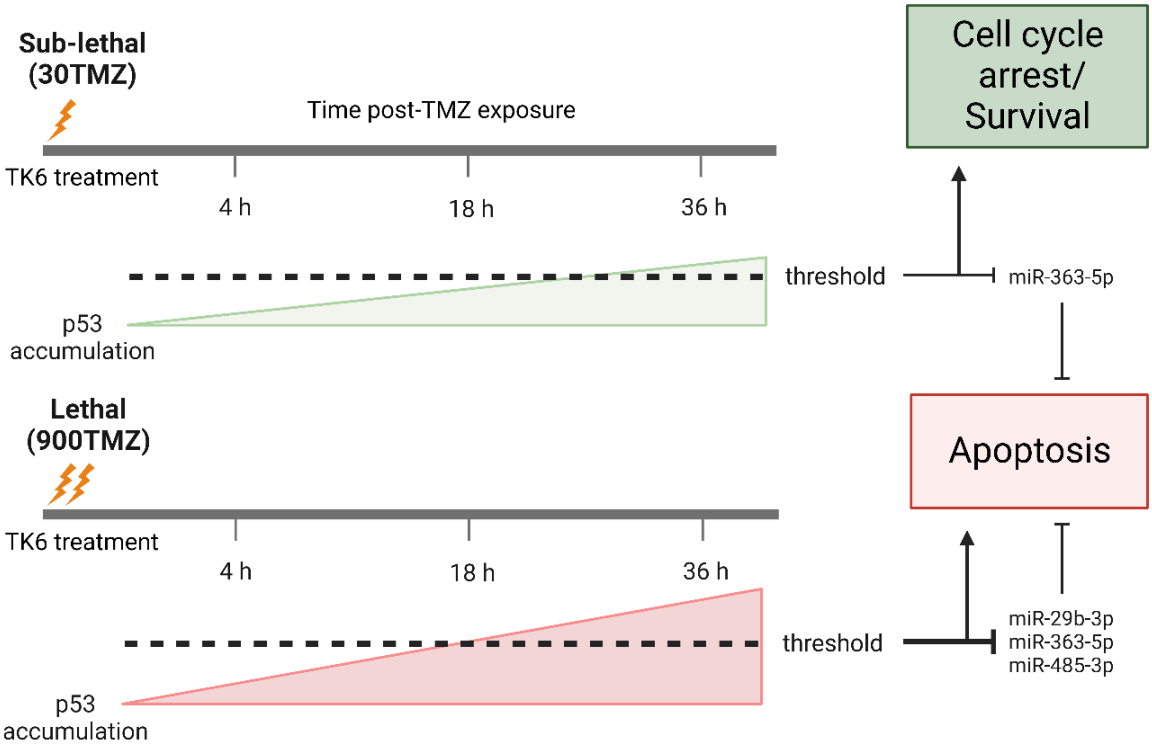

Figure 34. Proposed mechanism for miRNA inhibition and its relation to cell fate.

TK6 cells exposed to sub-lethal (30TMZ) and lethal (900TMZ) TMZ doses variably influence miRNA levels. At 30TMZ, the kinetics of p53 protein accumulation is slower and less pronounced compared with 900TMZ-treated TK6 cells. Consequently, 900TMZ-treated cells surpasses a proposed stochastic threshold of p53 protein levels (dashed line) earlier, and more substantially when compared with that of 30TMZ-treated cells. This results in limited capability of 30TMZ-treated cells to inhibit miRNAs, with only miR-363-5p demonstrating significant inhibition 36 h post-30TMZ exposure. Contrastingly, 900TMZ-treated cells significantly inhibit miR-29b-3p, miR-363-5p, and miR-485-3p 36 h post-exposure, suggesting a potential anti-apoptotic function for these miRNAs. Arrows – promotion; blunt ends – inhibition. Created on license from BioRender.com.

4.3. Future directions

1. While this study followed an in-depth line of enquiry, it could benefit from expansion. Foremost, it would be interesting to determine if the observed DE miRNA profile is also present in other cell lines and in response to different types of DNA damage. Not only could this provide validation of our findings, but also determine if the involvement of miRNAs in the DDR is conserved, or cell-specific.
2. As our study only investigated over-expression of certain miRNAs, it is worth identifying miRNAs that are endogenously upregulated in response to DNA damage, and subsequently inhibit these to ascertain its influence on cell fate.
3. Our study provided a broad range of dose-responsive DE miRNAs, each requires investigation in the context of the DDR and cell fate regulation.
4. Given the involvement of ATR-γH2Ax-Chk1-p53 in response to TMZ, it would be worth selectively inhibiting individual proteins, particularly p53, to determine exactly which proteins regulate miRNA expression.
5. The effects of miRNA over-expression and knock-down in TK6 cells could also be performed under basal conditions.
6. It could be useful to extend the sampling time of TK6 cells exposed to 30TMZ to determine if it eventually mimics the response of 900TMZ exposed cells, or returns to basal levels.
7. Beyond miRNAs, exploration of transcriptomic changes that define different cell fates could extend our findings.

4.4. Limitations

1. The breadth of our study only allowed investigation of TK6 cells. Admittedly, TK6 cells are well-established for genotoxicity assessment. However, expansion to different or isogenic cell lines could inform conserved or cell-specific mechanisms.
2. While 30TMZ represents a physiologically achievable dose, 900TMZ is excessive (barring TMZ resistant cells) and may have limited time-dependent observations that would occur with lower, but still lethal, TMZ doses. This was not possible for 900TMZ as beyond 36 h post-exposure, apoptosis rises sharply, limiting the amount of nucleic acid or protein that can be harvested.
3. Our sampling time-frame was sufficient to address our aim, but a more finely tuned experiment could refine subtle shifts in DDR protein dynamics that could further elucidate when key cell fate decisions are made and identify contributing molecular constituents.
4. TMZ is an alkylating chemotherapy that induces DSBs to cause apoptosis, and is used as a first-line treatment against gliomas. However, TMZ-resistance does occur, thus warranting investigation of TMZ-induced pathways. Nonetheless, it only represents one type of DNA damage and thus, therapies that can induce DNA damage with different modes of action require exploration.
5. Our study investigated DDR protein activation in the form of phosphorylation, however, not all DDR proteins are sufficiently phosphorylated during basal conditions. Consequently, relative fold change of phospho-protein levels among TMZ-treated cells in relation to those treated with DMSO may be distorted. Upscaling the experiment to increase the concentration of extracted proteins is one possible solution.

6. Cell synchronisation does not represent physiological conditions and is achieved by inducing a stress response, which is counterintuitive in genotoxicity assessment. However, using unsynchronised cells creates variability, particularly as DNA damage is detected during DNA replication. Consequently, cells replicating out of sync might mask time-dependent changes in DDR protein or miRNA expression. Performing a tandem experiment with synchronised and unsynchronised cells might resolve subtle DDR protein or miRNA expression changes.
7. Due to the nature of our data and experimental setup, we could only provide, what we deem to be, an approximation of a direct correlation between p53 and miRNA levels, and likewise γH2Ax and apoptosis levels.
8. Due to limited funding, this project was limited to a single RNAseq experiment. It would be worth-while to conduct more RNAseq repeats, which will increase reliability of the data and might refine our list of DE miRNAs.
9. This project was conducted in the midst of the COVID-19 pandemic, which resulted in months of disruption and delays/unavailability of research products and materials.

References

Abbas, T., & Dutta, A. (2009). p21 in cancer: Intricate networks and multiple activities. *Nature Reviews Cancer*, *9*(6), 400–414. https://doi.org/10.1038/nrc2657

Abbastabar, M., Kheyrollah, M., Azizian, K., Bagherlou, N., Tehrani, S. S., Maniati, M., & Karimian, A. (2018). Multiple functions of p27 in cell cycle, apoptosis, epigenetic modification and transcriptional regulation for the control of cell growth: A double-edged sword protein. *DNA Repair*, *69*, 63–72. https://doi.org/10.1016/j.dnarep.2018.07.008

Acharya, S. S., Fendler, W., Watson, J., Hamilton, A., Pan, Y., Gaudiano, E., Moskwa, P., Bhanja, P., Saha, S., Guha, C., Parmar, K., & Chowdhury, D. (2015). Serum microRNAs are early indicators of survival after radiation-induced hematopoietic injury. *Science Translational Medicine*, *7*(287), 287ra69. https://doi.org/10.1126/scitranslmed.aaa6593

Adams, J. M., & Cory, S. (2007). The Bcl-2 apoptotic switch in cancer development and therapy. *Oncogene*, *26*(9), 1324–1337. https://doi.org/10.1038/sj.onc.1210220

Afgan, E., Baker, D., Batut, B., van den Beek, M., Bouvier, D., Čech, M., Chilton, J., Clements, D., Coraor, N., Grüning, B. A., Guerler, A., Hillman-Jackson, J., Hiltemann, S., Jalili, V., Rasche, H., Soranzo, N., Goecks, J., Taylor, J., Nekrutenko, A., & Blankenberg, D. (2018). The Galaxy platform for accessible, reproducible and collaborative biomedical analyses: 2018 update. *Nucleic Acids Research*, *46*(W1), W537–W544. https://doi.org/10.1093/nar/gky379

Agarwal, V., Bell, G. W., Nam, J.-W., & Bartel, D. P. (2015). Predicting effective microRNA target sites in mammalian mRNAs. *ELife*, *4*, e05005. https://doi.org/10.7554/eLife.05005

Ahmed, M., & Jamil, K. (2011). Cytotoxicity of neoplastic drugs Gefitinib, Cisplatin, 5-FU, Gemcitabine, and Vinorelbine on human cervical cancer cells (HeLa). *Biology and Medicine*, *3*(5), 60-71.

Amri, J., Molaee, N., Karami, H., & Baazm, M. (2022). Combination of two miRNAs has a stronger effect on stimulating apoptosis, inhibiting cell growth, and increasing erlotinib sensitivity relative to single miRNA in A549 lung cancer cells. *Biotechnology and Applied Biochemistry*, *69*(4), 1383–1394. https://doi.org/10.1002/bab.2211

Arias-Lopez, C., Lazaro-Trueba, I., Kerr, P., Lord, C. J., Dexter, T., Iravani, M., Ashworth, A., & Silva, A. (2006). P53 modulates homologous recombination by transcriptional regulation of the RAD51 gene. *EMBO Reports*, *7*(2), 219–224. https://doi.org/10.1038/sj.embor.7400587

Auten, R. L., & Davis, J. M. (2009). Oxygen Toxicity and Reactive Oxygen Species: The Devil Is in the Details. *Pediatric Research*, *66*(2), 121–127. https://doi.org/10.1203/PDR.0b013e3181a9eafb

Avondoglio, D., Scott, T., Kil, W. J., Sproull, M., Tofilon, P. J., & Camphausen, K. (2009). High throughput evaluation of gamma-H2AX. *Radiation Oncology*, *4*(1), 31. https://doi.org/10.1186/1748-717X-4-31

Bao, J., Yu, Y., Chen, J., He, Y., Chen, X., Ren, Z., Xue, C., Liu, L., Hu, Q., Li, J., Cui, G., & Sun, R. (2018). MiR-126 negatively regulates PLK-4 to impact the development of hepatocellular carcinoma via ATR/CHEK1 pathway. *Cell Death & Disease*, *9*(10), 1045. https://doi.org/10.1038/s41419-018-1020-0

Barr, M. P., Gray, S. G., Hoffmann, A. C., Hilger, R. A., Thomale, J., O'Flaherty, J. D., Fennell, D. A., Richard, D., O'Leary, J. J., & O'Byrne, K. J. (2013). Generation and Characterisation of Cisplatin-Resistant Non-Small Cell Lung Cancer Cell Lines

Displaying a Stem-Like Signature. *PLoS ONE*, *8*(1), e54193. https://doi.org/10.1371/journal.pone.0054193

Barsotti, A. M., Beckerman, R., Laptenko, O., Huppi, K., Caplen, N. J., & Prives, C. (2012). P53-dependent Induction of PVT1 and miR-1204. *Journal of Biological Chemistry*, *287*(4), 2509–2519. https://doi.org/10.1074/jbc.M111.322875

Bartek, J., & Lukas, J. (2003). Chk1 and Chk2 kinases in checkpoint control and cancer. *Cancer Cell*, *3*(5), 421–429. https://doi.org/10.1016/S1535-6108(03)00110-7

Batchelor, E., Loewer, A., Mock, C., & Lahav, G. (2011). Stimulus-dependent dynamics of p53 in single cells. *Molecular Systems Biology*, *7*(1), 488. https://doi.org/10.1038/msb.2011.20

Beg, M. S., Brenner, A. J., Sachdev, J., Borad, M., Kang, Y.-K., Stoudemire, J., Smith, S., Bader, A. G., Kim, S., & Hong, D. S. (2017). Phase I study of MRX34, a liposomal miR-34a mimic, administered twice weekly in patients with advanced solid tumors. *Investigational New Drugs*, *35*(2), 180–188. https://doi.org/10.1007/s10637-016-0407-y

Behl, C. (2000). Apoptosis and Alzheimer's disease. *Journal of Neural Transmission*, *107*, 1325-1344. https://doi.org/10.1007/s007020070021

Beltran, H. (2014). The N-myc Oncogene: Maximizing its Targets, Regulation, and Therapeutic Potential. *Molecular Cancer Research*, *12*(6), 815–822. https://doi.org/10.1158/1541-7786.MCR-13-0536

Beltzig, L., Stratenwerth, B., & Kaina, B. (2021). Accumulation of Temozolomide-Induced Apoptosis, Senescence and DNA Damage by Metronomic Dose Schedule: A Proof-of-Principle Study with Glioblastoma Cells. *Cancers*, *13*(24), 6287. https://doi.org/10.3390/cancers13246287

Berte, N., Lokan, S., Eich, M., Kim, E., & Kaina, B. (2016). Artesunate enhances the therapeutic response of glioma cells to temozolomide by inhibition of homologous recombination and senescence. *Oncotarget*, *7*(41), 67235–67250. https://doi.org/10.18632/oncotarget.11972

Biswas, A. K., & Johnson, D. G. (2012). Transcriptional and Nontranscriptional Functions of E2F1 in Response to DNA Damage. *Cancer Research*, *72*(1), 13–17. https://doi.org/10.1158/0008-5472.CAN-11-2196

Blomberg, I., & Hoffmann, I. (1999). Ectopic Expression of Cdc25A Accelerates the G $_1$ /S Transition and Leads to Premature Activation of Cyclin E- and Cyclin A-Dependent Kinases. *Molecular and Cellular Biology*, *19*(9), 6183–6194. https://doi.org/10.1128/MCB.19.9.6183

Blough, M. D., Beauchamp, D. C., Westgate, M. R., Kelly, J. J., & Cairncross, J. G. (2011). Effect of aberrant p53 function on temozolomide sensitivity of glioma cell lines and brain tumor initiating cells from glioblastoma. *Journal of Neuro-Oncology*, *102*(1), 1–7. https://doi.org/10.1007/s11060-010-0283-9

Bolger, A. M., Lohse, M., & Usadel, B. (2014). Trimmomatic: A flexible trimmer for Illumina sequence data. *Bioinformatics*, *30*(15), 2114–2120. https://doi.org/10.1093/bioinformatics/btu170

Bommer, G. T., Gerin, I., Feng, Y., Kaczorowski, A. J., Kuick, R., Love, R. E., Zhai, Y., Giordano, T. J., Qin, Z. S., Moore, B. B., MacDougald, O. A., Cho, K. R., & Fearon, E. R. (2007). P53-Mediated Activation of miRNA34 Candidate Tumor-Suppressor Genes. *Current Biology*, *17*(15), 1298–1307. https://doi.org/10.1016/j.cub.2007.06.068

Bonneau, E., Neveu., B., Kostantin., E., Tsongalis, G. J., De Guire, V. (2019). How close are miRNAs from clinical practice? A perspective on the diagnostic and therapeutic market.

The Journal of the International Federation of Clinical Chemistry and Laboratory Medicine, *30*(2), 114-127.

Bouchier-Hayes, L., & Green, D. R. (2012). Caspase-2: The orphan caspase. *Cell Death & Differentiation*, *19*(1), 51–57. https://doi.org/10.1038/cdd.2011.157

Bouras, T., Fu, M., Sauve, A. A., Wang, F., Quong, A. A., Perkins, N. D., Hay, R. T., Gu, W., & Pestell, R. G. (2005). SIRT1 Deacetylation and Repression of p300 Involves Lysine Residues 1020/1024 within the Cell Cycle Regulatory Domain 1. *Journal of Biological Chemistry*, *280*(11), 10264–10276. https://doi.org/10.1074/jbc.M408748200

Bouzinab, K., Summers, H., Zhang, J., Stevens, M. F. G., Moody, C. J., Turyanska, L., Thomas, N. R., Gershkovich, P., Ashford, M. B., Vitterso, E., Storer, L. C. D., Grundy, R., & Bradshaw, T. D. (2019). In search of effective therapies to overcome resistance to Temozolomide in brain tumours. *Cancer Drug Resistance*, *2*, 1018-1031. https://doi.org/10.20517/cdr.2019.64

Bronner, D. N., O'Riordan, M. X. D., & He, Y. (2013). Caspase-2 mediates a Brucella abortus RB51-induced hybrid cell death having features of apoptosis and pyroptosis. *Frontiers in Cellular and Infection Microbiology*, *3*(83), 1-11. https://doi.org/10.3389/fcimb.2013.00083

Brosh, R., Shalgi, R., Liran, A., Landan, G., Korotayev, K., Nguyen, G. H., Enerly, E., Johnsen, H., Buganim, Y., Solomon, H., Goldstein, I., Madar, S., Goldfinger, N., Børresen-Dale, A., Ginsberg, D., Harris, C. C., Pilpel, Y., Oren, M., & Rotter, V. (2008). P53-repressed miRNAs are involved with E2F in a feed-forward loop promoting proliferation. *Molecular Systems Biology*, *4*(1), 229. https://doi.org/10.1038/msb.2008.65

Brown-Suedel, A. N., & Bouchier-Hayes, L. (2020). Caspase-2 Substrates: To Apoptosis, Cell Cycle Control, and Beyond. *Frontiers in Cell and Developmental Biology*, *8*, 610022. https://doi.org/10.3389/fcell.2020.610022

Brüsehafer, K., Manshian, B. B., Doherty, A. T., Zaïr, Z. M., Johnson, G. E., Doak, S. H., & Jenkins, G. J. S. (2016). The clastogenicity of 4NQO is cell-type dependent and linked to cytotoxicity, length of exposure and p53 proficiency. *Mutagenesis*, *31*(2), 171–180. https://doi.org/10.1093/mutage/gev069

Bukeirat, M., Sarkar, S. N., Hu, H., Quintana, D. D., Simpkins, J. W., & Ren, X. (2016). MiR-34a regulates blood–brain barrier permeability and mitochondrial function by targeting cytochrome c. *Journal of Cerebral Blood Flow & Metabolism*, *36*(2), 387–392. https://doi.org/10.1177/0271678X15606147

Burgering, B. M. T., & Medema, R. H. (2003). Decisions on life and death: FOXO Forkhead transcription factors are in command when PKB/Akt is off duty. *Journal of Leukocyte Biology*, *73*(6), 689–701. https://doi.org/10.1189/jlb.1202629

Cai, Y., & Li, Y. (2019). Upregulation of miR-29b-3p protects cardiomyocytes from hypoxia-induced apoptosis by targeting TRAF5. *Cellular & Molecular Biology Letters*, *24*(1), 27. https://doi.org/10.1186/s11658-019-0151-3

Caldecott, K. W. (2003). DNA Single-Strand Break Repair and Spinocerebellar Ataxia. *Cell*, *112*(1), 7–10. https://doi.org/10.1016/S0092-8674(02)01247-3

Canman, C. E., Lim, D.-S., Cimprich, K. A., Taya, Y., Tamai, K., Sakaguchi, K., Appella, E., Kastan, M. B., & Siliciano, J. D. (1998). Activation of the ATM Kinase by Ionizing Radiation and Phosphorylation of p53. *Science*, *281*(5383), 1677–1679. https://doi.org/10.1126/science.281.5383.1677

Cao, X., Cai, Z., Liu, J., Zhao, Y., Wang, X., Li, X., & Xia, H. (2017). MiRNA-504 inhibits p53-dependent vascular smooth muscle cell apoptosis and may prevent aneurysm formation. *Molecular Medicine Reports*, *16*(3), 2570–2578. https://doi.org/10.3892/mmr.2017.6873

Caporali, S., Falcinelli, S., Starace, G., Russo, M. T., Bonmassar, E., Jiricny, J., & D'Atri, S. (2004). DNA Damage Induced by Temozolomide Signals to both ATM and ATR: Role of the Mismatch Repair System. *Molecular Pharmacology*, *66*(3), 478-491.

Carracedo, A., & Pandolfi, P. P. (2008). The PTEN–PI3K pathway: Of feedbacks and cross-talks. *Oncogene*, *27*(41), 5527–5541. https://doi.org/10.1038/onc.2008.247

Chai, C., Wu, H., Wang, B., Eisenstat, D. D., & Leng, R. P. (2018). MicroRNA-498 promotes proliferation and migration by targeting the tumor suppressor PTEN in breast cancer cells. *Carcinogenesis*, *39*(9), 1185–1196. https://doi.org/10.1093/carcin/bgy092

Chang, L., Zhou, G., Soufan, O., & Xia, J. (2020). miRNet 2.0: Network-based visual analytics for miRNA functional analysis and systems biology. *Nucleic Acids Research*, *48*(W1), W244–W251. https://doi.org/10.1093/nar/gkaa467

Chang, T.-C., Wentzel, E. A., Kent, O. A., Ramachandran, K., Mullendore, M., Lee, K. H., Feldmann, G., Yamakuchi, M., Ferlito, M., Lowenstein, C. J., Arking, D. E., Beer, M. A., Maitra, A., & Mendell, J. T. (2007). Transactivation of miR-34a by p53 Broadly Influences Gene Expression and Promotes Apoptosis. *Molecular Cell*, *26*(5), 745–752. https://doi.org/10.1016/j.molcel.2007.05.010

Chang, Y.-C., Jan, K.-Y., Cheng, C.-A., Liao, C.-B., & Liu, Y.-C. (2008). Direct involvement of the tumor suppressor p53 in nucleotide excision repair. *DNA Repair*, *7*(5), 751–761. https://doi.org/10.1016/j.dnarep.2008.01.019

Chapman, K. E., Doak, S. H., & Jenkins, G. J. S. (2015). Acute Dosing and p53-Deficiency Promote Cellular Sensitivity to DNA Methylating Agents. *Toxicological Sciences*, *144*(2), 357–365. https://doi.org/10.1093/toxsci/kfv004

Chatterjee, N., & Walker, G. C. (2017). Mechanisms of DNA damage, repair, and mutagenesis: DNA Damage and Repair. *Environmental and Molecular Mutagenesis*, *58*(5), 235–263. https://doi.org/10.1002/em.22087

Chaudhry, M. A. (2007). Base excision repair of ionizing radiation-induced DNA damage in G1 and G2 cell cycle phases. *Cancer Cell International*, *7*(1), 15. https://doi.org/10.1186/1475-2867-7-15

Chen, Y., Lun, A. T. L., Smyth, G. K. (2016). From reads to genes to pathways: differential expression analysis of RNA-Seq experiments using Rsubread and the edgeR quasi-likelihood pipeline. *F1000Research*, *5*(1438), 1-48. https://doi.org/10.12688/f1000research.8987.2

Chen, A.-H., Qin, Y.-E., Tang, W.-F., Tao, J., Song, H., & Zuo, M. (2017). MiR-34a and miR-206 act as novel prognostic and therapy biomarkers in cervical cancer. *Cancer Cell International*, *17*(1), 63. https://doi.org/10.1186/s12935-017-0431-9

Chen, B., Duan, L., Yin, G., Tan, J., & Jiang, X. (2013b). Simultaneously expressed miR-424 and miR-381 synergistically suppress the proliferation and survival of renal cancer cells—Cdc2 activity is up-regulated by targeting WEE1. *Clinics*, *68*(6), 825–833. https://doi.org/10.6061/clinics/2013(06)17

Chen, G., Sun, W., Hua, X., Zeng, W., & Yang, L. (2018). Long non-coding RNA FOXD2-AS1 aggravates nasopharyngeal carcinoma carcinogenesis by modulating miR-363-5p/S100A1 pathway. *Gene*, *645*, 76–84. https://doi.org/10.1016/j.gene.2017.12.026

Chen, H.-C., Kanai, M., Inoue-Yamauchi, A., Tu, H.-C., Huang, Y., Ren, D., Kim, H., Takeda, S., Reyna, D. E., Chan, P. M., Ganesan, Y. T., Liao, C.-P., Gavathiotis, E., Hsieh, J. J., & Cheng, E. H. (2015). An interconnected hierarchical model of cell death regulation by the BCL-2 family. *Nature Cell Biology*, *17*(10), 1270–1281. https://doi.org/10.1038/ncb3236

Chen, S., Liu, R., Wang, Q., Qi, Z., Hu, Y., Zhou, P., & Wang, Z. (2019). MiR-34s negatively regulate homologous recombination through targeting RAD51. *Archives of Biochemistry and Biophysics*, *666*, 73–82. https://doi.org/10.1016/j.abb.2019.03.017

Chen, T. C., Cho, H. Y., Wang, W., Barath, M., Sharma, N., Hofman, F. M., & Schönthal, A. H. (2014). A Novel Temozolomide–Perillyl Alcohol Conjugate Exhibits Superior Activity against Breast Cancer Cells In Vitro and Intracranial Triple-Negative Tumor Growth In Vivo. *Molecular Cancer Therapeutics*, *13*(5), 1181-1193. https://doi.org/10.1158/1535-7163.MCT-13-0882

Chen, X., Chen, J., Gan, S., Guan, H., Zhou, Y., Ouyang, Q., & Shi, J. (2013a). DNA damage strength modulates a bimodal switch of p53 dynamics for cell-fate control. *BMC Biology*, *11*(1), 73. https://doi.org/10.1186/1741-7007-11-73

Cheng, M., Rizwan, A., Jiang, L., Bhujwalla, Z. M., & Glunde, K. (2017). Molecular Effects of Doxorubicin on Choline Metabolism in Breast Cancer. *Neoplasia*, *19*(8), 617–627. https://doi.org/10.1016/j.neo.2017.05.004

Cheng, Q., Chen, L., Li, Z., Lane, W. S., & Chen, J. (2009). ATM activates p53 by regulating MDM2 oligomerization and E3 processivity. *The EMBO Journal*, *28*(24), 3857–3867. https://doi.org/10.1038/emboj.2009.294

Cheng, Y., Xiang, G., Meng, Y., & Dong, R. (2016). MiRNA-183-5p promotes cell proliferation and inhibits apoptosis in human breast cancer by targeting the PDCD4. *Reproductive Biology*, *16*(3), 225–233. https://doi.org/10.1016/j.repbio.2016.07.002

Cheng, Y., Zhao, W., Zhang, X., Sun, L., Yang, H., Wang, Y., Cao, Y., Chu, Y., & Liu, G. (2018). Downregulation of microRNA-1 attenuates glucose-induced apoptosis by regulating the liver X receptor α in cardiomyocytes. *Experimental and Therapeutic Medicine*, *16*, 1814-1824. https://doi.org/10.3892/etm.2018.6388

Cimmino, A., Calin, G. A., Fabbri, M., Iorio, M. V., Ferracin, M., Shimizu, M., Wojcik, S. E., Aqeilan, R. I., Zupo, S., Dono, M., Rassenti, L., Alder, H., Volinia, S., Liu, C., Kipps, T. J., Negrini, M., & Croce, C. M. (2005). *MiR-15* and *miR-16* induce apoptosis by targeting BCL2. *Proceedings of the National Academy of Sciences*, *102*(39), 13944–13949. https://doi.org/10.1073/pnas.0506654102

Cimprich, K. A., & Cortez, D. (2008). ATR: An essential regulator of genome integrity. *Nature Reviews Molecular Cell Biology*, *9*(8), 616–627. https://doi.org/10.1038/nrm2450

Conrad, E., Polonio-Vallon, T., Meister, M., Matt, S., Bitomsky, N., Herbel, C., Liebl, M., Greiner, V., Kriznik, B., Schumacher, S., Krieghoff-Henning, E., & Hofmann, T. G. (2016). HIPK2 restricts SIRT1 activity upon severe DNA damage by a phosphorylation-controlled mechanism. *Cell Death & Differentiation*, *23*(1), 110–122. https://doi.org/10.1038/cdd.2015.75

Curtin, J. F., & Cotter, T. G. (2004). JNK Regulates HIPK3 Expression and Promotes Resistance to Fas-mediated Apoptosis in DU 145 Prostate Carcinoma Cells. *Journal of Biological Chemistry*, *279*(17), 17090–17100. https://doi.org/10.1074/jbc.M307629200

Dai, Y., & Grant, S. (2010). New Insights into Checkpoint Kinase 1 in the DNA Damage Response Signaling Network. *Clinical Cancer Research*, *16*(2), 376–383. https://doi.org/10.1158/1078-0432.CCR-09-1029

Darzynkiewicz, Z., Juan, G., Li, X., Gorczyca, W., Murakami, T., & Traganos, F. (1997). Cytometry in Cell Necrobiology: Analysis of Apoptosis and Accidental Cell Death (Necrosis). *Cytometry*, *27*, 1-20.

De Almodóvar, C. R., Ruiz-Ruiz, C., Rodríguez, A., Ortiz-Ferrón, G., Redondo, J. M., & López-Rivas, A. (2004). Tumor Necrosis Factor-related Apoptosis-inducing Ligand (TRAIL) Decoy Receptor TRAIL-R3 Is Up-regulated by p53 in Breast Tumor Cells through a Mechanism Involving an Intronic p53-binding Site. *Journal of Biological Chemistry*, *279*(6), 4093–4101. https://doi.org/10.1074/jbc.M311243200

De Zio, D., Cianfanelli, V., & Cecconi, F. (2013). New Insights into the Link Between DNA Damage and Apoptosis. *Antioxidants & Redox Signaling*, *19*(6), 559–571. https://doi.org/10.1089/ars.2012.4938

Deng, X., Gao, F., Flagg, T., Anderson, J., & May, W. S. (2006). Bcl2's Flexible Loop Domain Regulates p53 Binding and Survival. *Molecular and Cellular Biology*, *26*(12), 4421–4434. https://doi.org/10.1128/MCB.01647-05

Denli, A. M., Tops, B. B. J., Plasterk, R. H. A., Ketting, R. F., & Hannon, G. J. (2004). Processing of primary microRNAs by the Microprocessor complex. *Nature*, *432*(7014), 231–235. https://doi.org/10.1038/nature03049

Dhanasekaran, D. N., & Reddy, E. P. (2017). JNK-signaling: A multiplexing hub in programmed cell death. *Genes & Cancer*, *8*(9–10), 682–694. https://doi.org/10.18632/genesandcancer.155

Dobin, A., Davis, C. A., Schlesinger, F., Drenkow, J., Zaleski, C., Jha, S., Batut, P., Chaisson, M., & Gingeras, T. R. (2013). STAR: Ultrafast universal RNA-seq aligner. *Bioinformatics*, *29*(1), 15–21. https://doi.org/10.1093/bioinformatics/bts635

Dolezalova, D., Mraz, M., Barta, T., Plevova, K., Vinarsky, V., Holubcova, Z., Jaros, J., Dvorak, P., Pospisilova, S., & Hampl, A. (2012). MicroRNAs Regulate p21Waf1/Cip1 Protein Expression and the DNA Damage Response in Human Embryonic Stem Cells. *Stem Cells*, *30*(7), 1362–1372. https://doi.org/10.1002/stem.1108

Duan, Y., Dong, X., Nie, J., Li, P., Lu, F., Ma, D., & Ji, C. (2018). Wee1 kinase inhibitor MK-1775 induces apoptosis of acute lymphoblastic leukemia cells and enhances the efficacy of doxorubicin involving downregulation of Notch pathway. *Oncology Letters*. https://doi.org/10.3892/ol.2018.9291

Edlich, F. (2018). BCL-2 proteins and apoptosis: Recent insights and unknowns. *Biochemical and Biophysical Research Communications*, *500*(1), 26–34. https://doi.org/10.1016/j.bbrc.2017.06.190

Eich, M., Roos, W. P., Nikolova, T., & Kaina, B. (2013). Contribution of ATM and ATR to the Resistance of Glioblastoma and Malignant Melanoma Cells to the Methylating Anticancer Drug Temozolomide. *Molecular Cancer Therapeutics*, *12*(11), 2529–2540. https://doi.org/10.1158/1535-7163.MCT-13-0136

Einsele-Scholz, S., Malmsheimer, S., Bertram, K., Stehle, D., Johänning, J., Manz, M., Daniel, P. T., Gillissen, B. F., Schulze-Osthoff, K., & Essmann, F. (2016). Bok is a genuine multi-BH-domain protein that triggers apoptosis in the absence of Bax and Bak. *Journal of Cell Science*, *129*(15), 3054–3054. https://doi.org/10.1242/jcs.193946

El-deiry, W. S., Tokino, T., Velculescu, V. E., Levy, B. D., Parsons, R., Trent, J. M., Lin, D., Mercer, W. E., Kinzler, K. W., Vogelstein, B. (1993). WAF1, a Potential Mediator of p53

Tumor Suppression. *Cell*, *75*(4), 817-825. https://doi.org/10.1016/0092-8674(93)90500-P

Elmore, S. (2007). Apoptosis: A Review of Programmed Cell Death. *Toxicologic Pathology*, *35*(4), 495–516. https://doi.org/10.1080/01926230701320337

Ensminger, M., Iloff, L., Ebel, C., Nikolova, T., Kaina, B., & Löbrich, M. (2014). DNA breaks and chromosomal aberrations arise when replication meets base excision repair. *Journal of Cell Biology*, *206*(1), 29–43. https://doi.org/10.1083/jcb.201312078

Espinosa-Diez, C., Wilson, R., Chatterjee, N., Hudson, C., Ruhl, R., Hipfinger, C., Helms, E., Khan, O. F., Anderson, D. G., & Anand, S. (2018). MicroRNA regulation of the MRN complex impacts DNA damage, cellular senescence, and angiogenic signaling. *Cell Death & Disease*, *9*(6), 632. https://doi.org/10.1038/s41419-018-0690-y

Eto, K., Goto, S., Nakashima, W., Ura, Y., & Abe, S.-I. (2012). Loss of programmed cell death 4 induces apoptosis by promoting the translation of procaspase-3 mRNA. *Cell Death & Differentiation*, *19*(4), 573–581. https://doi.org/10.1038/cdd.2011.126

Fan, C.-H., Liu, W.-L., Cao, H., Wen, C., Chen, L., & Jiang, G. (2013). O6-methylguanine DNA methyltransferase as a promising target for the treatment of temozolomide-resistant gliomas. *Cell Death & Disease*, *4*(10), e876–e876. https://doi.org/10.1038/cddis.2013.388

Fava, L. L., Bock, F. J., Geley, S., & Villunger, A. (2012). Caspase-2 at a glance. *Journal of Cell Science*, *125*(24), 5911–5915. https://doi.org/10.1242/jcs.115105

Feitsma, H., Akay, A., & Cuppen, E. (2008). Alkylation damage causes MMR-dependent chromosomal instability in vertebrate embryos. *Nucleic Acids Research*, *36*(12), 4047–4056. https://doi.org/10.1093/nar/gkn341

Feng, L., Hollstein, M., & Xu, Y. (2006). Ser46 Phosphorylation Regulates p53-Dependent Apoptosis and Replicative Senescence. *Cell Cycle*, *5*(23), 2812–2819. https://doi.org/10.4161/cc.5.23.3526

Feng, Z., Zhang, C., Wu, R., & Hu, W. (2011). Tumor suppressor p53 meets microRNAs. *Journal of Molecular Cell Biology*, *3*(1), 44–50. https://doi.org/10.1093/jmcb/mjq040

Flamant, L., Notte, A., Ninane, N., Raes, M., & Michiels, C. (2010). Anti-apoptotic role of HIF-1 and AP-1 in paclitaxel exposed breast cancer cells under hypoxia. *Molecular Cancer*, *9*(1), 191. https://doi.org/10.1186/1476-4598-9-191

Floyd, D. H., Zhang, Y., Dey, B. K., Kefas, B., Breit, H., Marks, K., Dutta, A., Herold-Mende, C., Synowitz, M., Glass, R., Abounader, R., & Purow, B. W. (2014). Novel Anti-Apoptotic MicroRNAs 582-5p and 363 Promote Human Glioblastoma Stem Cell Survival via Direct Inhibition of Caspase 3, Caspase 9, and Bim. *PLoS ONE*, *9*(5), e96239. https://doi.org/10.1371/journal.pone.0096239

Freeburg, E. M., Goyeneche, A. A., Telleria, C. M. (2009). Mifepristone abrogates repopulation of ovarian cancer cells in between courses of cisplatin treatment. *International Journal of Oncology*, *34*(3), 743-755. https://doi.org/10.3892/ijo_00000200

Freeman, A. K., & Monteiro, A. N. (2010). Phosphatases in the cellular response to DNA damage. *Cell Communication and Signaling*, *8*(1), 27. https://doi.org/10.1186/1478-811X-8-27

Fuchs, R. P., Isogawa, A., Paulo, J. A., Onizuka, K., Takahashi, T., Amunugama, R., Duxin, J. P., & Fujii, S. (2021). Crosstalk between repair pathways elicits double-strand breaks in alkylated DNA and implications for the action of temozolomide. *ELife*, *10*, e69544. https://doi.org/10.7554/eLife.69544

Fuentealba, R. A., Liu, Q., Kanekiyo, T., Zhang, J., & Bu, G. (2009). Low Density Lipoprotein Receptor-related Protein 1 Promotes Anti-apoptotic Signaling in Neurons by Activating Akt Survival Pathway. *Journal of Biological Chemistry*, *284*(49), 34045–34053. https://doi.org/10.1074/jbc.M109.021030

Fugger, K., & West, S. C. (2016). Keeping homologous recombination in check. *Cell Research*, *26*(4), 397–398. https://doi.org/10.1038/cr.2016.25

Galluzzi, L., Vitale, I., Aaronson, S. A., Abrams, J. M., Adam, D., Agostinis, P., Alnemri, E. S., Altucci, L., Amelio, I., Andrews, D. W., Annicchiarico-Petruzzelli, M., Antonov, A. V., Arama, E., Baehrecke, E. H., Barlev, N. A., Bazan, N. G., Bernassola, F., Bertrand, M. J. M., Bianchi, K., … Kroemer, G. (2018). Molecular mechanisms of cell death: Recommendations of the Nomenclature Committee on Cell Death 2018. *Cell Death & Differentiation*, *25*(3), 486–541. https://doi.org/10.1038/s41418-017-0012-4

Gao, X., Qiao, Y., Han, D., Zhang, Y., & Ma, N. (2012). Enemy or partner: Relationship between intronic micrornas and their host genes. *IUBMB Life*, *64*(10), 835–840. https://doi.org/10.1002/iub.1079

Garcia-Moreno, A., López-Domínguez, R., Villatoro-García, J. A., Ramirez-Mena, A., Aparicio-Puerta, E., Hackenberg, M., Pascual-Montano, A., & Carmona-Saez, P. (2022). Functional Enrichment Analysis of Regulatory Elements. *Biomedicines*, *10*(3), 590. https://doi.org/10.3390/biomedicines10030590

Gatei, M., Scott, S. P., Filippovitch, I., Soronika, N., Lavin, M. F., Weber, B., & Khanna, K. K. (2000). Role for ATM in DNA Damage-induced Phosphorylation of BRCA1. *Cancer Research*, *60*, 3299-3304.

Gatei, M., Sloper, K., Sörensen, C., Syljuäsen, R., Falck, J., Hobson, K., Savage, K., Lukas, J., Zhou, B.-B., Bartek, J., & Khanna, K. K. (2003). Ataxia-telangiectasia-mutated (ATM)

and NBS1-dependent Phosphorylation of Chk1 on Ser-317 in Response to Ionizing Radiation. *Journal of Biological Chemistry*, *278*(17), 14806–14811. https://doi.org/10.1074/jbc.M210862200

Gillies, J. K., & Lorimer, I. A. J. (2007). Regulation of $p27^{Kip1}$ by miRNA 221/222 in Glioblastoma. *Cell Cycle*, *6*(16), 2005–2009. https://doi.org/10.4161/cc.6.16.4526

Gim, J., Won, S., & Park, T. (2016). LPEseq: Local-Pooled-Error Test for RNA Sequencing Experiments with a Small Number of Replicates. *PLoS ONE*, *11*(8), e0159182. https://doi.org/10.1371/journal.pone.0159182

Göhler, T., Sabbioneda, S., Green, C. M., & Lehmann, A. R. (2011). ATR-mediated phosphorylation of DNA polymerase η is needed for efficient recovery from UV damage. *Journal of Cell Biology*, *192*(2), 219–227. https://doi.org/10.1083/jcb.201008076

Goldmacher, V. S., Cuzick, R. A., & Thilly, W. G. (1986). Isolation and partial characterization of human cell mutants differing in sensitivity to killing and mutation by methylnitrosourea and N-methyl-N'-nitro-N-nitrosoguanidine. *Journal of Biological Chemistry*, *261*(27), 12462–12471. https://doi.org/10.1016/S0021-9258(18)67110-8

Gouws, C., & Pretorius, P. J. (2011). O6-methylguanine-DNA methyltransferase (MGMT): Can function explain a suicidal mechanism? *Medical Hypotheses*, *77*(5), 857–860. https://doi.org/10.1016/j.mehy.2011.07.055

Grieco, F. A., Sebastiani, G., Juan-Mateu, J., Villate, O., Marroqui, L., Ladrière, L., Tugay, K., Regazzi, R., Bugliani, M., Marchetti, P., Dotta, F., & Eizirik, D. L. (2017). MicroRNAs miR-23a-3p, miR-23b-3p, and miR-149-5p Regulate the Expression of Proapoptotic BH3-Only Proteins DP5 and PUMA in Human Pancreatic β-Cells. *Diabetes*, *66*(1), 100–112. https://doi.org/10.2337/db16-0592

Guo, X., Liu, Q., Wang, G., Zhu, S., Gao, L., Hong, W., Chen, Y., Wu, M., Liu, H., Jiang, C., & Kang, J. (2013). MicroRNA-29b is a novel mediator of Sox2 function in the regulation of somatic cell reprogramming. *Cell Research*, *23*(1), 142–156. https://doi.org/10.1038/cr.2012.180

Gupta, D., Lin, B., Cowan, A., & Heinen, C. D. (2018). ATR-Chk1 activation mitigates replication stress caused by mismatch repair-dependent processing of DNA damage. *Proceedings of the National Academy of Sciences*, *115*(7), 1523–1528. https://doi.org/10.1073/pnas.1720355115

Gupta, S., Sathishkumar, S., & Ahmed, M. M. (2010). Influence of Cell Cycle Checkpoints and p53 Function on the Toxicity of Temozolomide in Human Pancreatic Cancer Cells. *Pancreatology*, *10*(5), 565–579. https://doi.org/10.1159/000317254

Gutierrez, R., Thompson, Y., R. O'Connor, T. (2018). DNA direct repair pathways in cancer. *AIMS Medical Science*, *5*(3), 284–302. https://doi.org/10.3934/medsci.2018.3.284

Hakem, R. (2008). DNA-damage repair; the good, the bad, and the ugly. *The EMBO Journal*, *27*(4), 589–605. https://doi.org/10.1038/emboj.2008.15

Han, J., Flemington, C., Houghton, A. B., Gu, Z., Zambetti, G. P., Lutz, R. J., Zhu, L., & Chittenden, T. (2001). Expression of *bbc3* , a pro-apoptotic BH3-only gene, is regulated by diverse cell death and survival signals. *Proceedings of the National Academy of Sciences*, *98*(20), 11318–11323. https://doi.org/10.1073/pnas.201208798

Han, N., Yuan, F., Xian, P., Liu, N., Liu, J., Zhang, H., Zhang, H., Yao, K., & Yuan, G. (2019). GADD45a Mediated Cell Cycle Inhibition Is Regulated By P53 In Bladder Cancer. *OncoTargets and Therapy*, *12*, 7591–7599. https://doi.org/10.2147/OTT.S222223

Hanakahi, L. A., West, S. C. (2002). Specific interaction of IP_6 with human Ku70/80, the DNA-binding subunit of DNA-PK. *The EMBO Journal*, *21*(8), 2038-2044.

Hanna, J., Hossain, G. S., & Kocerha, J. (2019). The Potential for microRNA Therapeutics and Clinical Research. *Frontiers in Genetics*, *10*, 478. https://doi.org/10.3389/fgene.2019.00478

Hashimoto, K., & Todo, T. (2013). Mitotic slippage underlies the relationship between p53 dysfunction and the induction of large micronuclei by colcemid. *Mutagenesis*, *28*(4), 457–464. https://doi.org/10.1093/mutage/get021

He, Y., & Kaina, B. (2019). Are There Thresholds in Glioblastoma Cell Death Responses Triggered by Temozolomide? *International Journal of Molecular Sciences*, *20*(7), 1562. https://doi.org/10.3390/ijms20071562

He, Y., Roos, W. P., Wu, Q., Hofmann, T. G., & Kaina, B. (2019). The SIAH1–HIPK2–p53ser46 Damage Response Pathway is Involved in Temozolomide-Induced Glioblastoma Cell Death. *Molecular Cancer Research*, *17*(5), 1129–1141. https://doi.org/10.1158/1541-7786.MCR-18-1306

Helton, E. S., & Chen, X. (2007). P53 modulation of the DNA damage response. *Journal of Cellular Biochemistry*, *100*(4), 883–896. https://doi.org/10.1002/jcb.21091

Hermeking, H. (2012). MicroRNAs in the p53 network: micromanagement of tumour suppression. *Nature Reviews Cancer*, *12*, 613-626. https://doi.org/10.1038/nrc3318

Hernandez-Valencia, J., Garcia-Villa, E., Arenas-Hernandez, A., Garcia-Mena, J., Diaz-Chavez, J., & Gariglio, P. (2018). Induction of p53 Phosphorylation at Serine 20 by Resveratrol Is Required to Activate p53 Target Genes, Restoring Apoptosis in MCF-7 Cells Resistant to Cisplatin. *Nutrients*, *10*(9), 1148. https://doi.org/10.3390/nu10091148

Hirao, A., Kong, Y.-Y., Matsuoka, S., Wakeham, A., Ruland, J., Yoshida, H., Liu, D., Elledge, S. J., & Mak, T. W. (2000). DNA Damage-Induced Activation of p53 by the Checkpoint Kinase Chk2. *Science*, *287*(5459), 1824–1827. https://doi.org/10.1126/science.287.5459.1824

Hirose, Y., Berger, M. S., & Pieper, R. O. (2001). p53 Effects Both the Duration of G_2/M Arrest and the Fate of Temozolomide-treated Human Glioblastoma Cells. *Cancer Research*, *61*, 1957-1963

Höck, J., & Meister, G. (2008). The Argonaute protein family. *Genome Biology*, *9*(2), 210. https://doi.org/10.1186/gb-2008-9-2-210

Hoeijmakers, J. H. J. (2001). Genome maintenance mechanisms for preventing cancer. *Nature*, *411*(6835), 366–374. https://doi.org/10.1038/35077232

Hong, D. S., Kang, Y.-K., Borad, M., Sachdev, J., Ejadi, S., Lim, H. Y., Brenner, A. J., Park, K., Lee, J.-L., Kim, T.-Y., Shin, S., Becerra, C. R., Falchook, G., Stoudemire, J., Martin, D., Kelnar, K., Peltier, H., Bonato, V., Bader, A. G., … Beg, M. S. (2020). Phase 1 study of MRX34, a liposomal miR-34a mimic, in patients with advanced solid tumours. *British Journal of Cancer*, *122*(11), 1630–1637. https://doi.org/10.1038/s41416-020-0802-1

Hou, C., Wang, X., & Du, B. (2020). LncRNA MCM3AP-AS1 promotes the development of oral squamous cell carcinoma by inhibiting miR-363-5p. *Experimental and Therapeutic Medicine*, *20*(2), 978–984. https://doi.org/10.3892/etm.2020.8738

Hu, H., Du, L., Nagabayashi, G., Seeger, R. C., & Gatti, R. A. (2010). ATM is down-regulated by N-Myc–regulated microRNA-421. *Proceedings of the National Academy of Sciences*, *107*(4), 1506–1511. https://doi.org/10.1073/pnas.0907763107

Hu, H., & Gatti, R. A. (2011). MicroRNAs: New players in the DNA damage response. *Journal of Molecular Cell Biology*, *3*(3), 151–158. https://doi.org/10.1093/jmcb/mjq042

Hu, Y., Guo, F., Zhu, H., Tan, X., Zhu, X., Liu, X., Zhang, W., Yang, Q., & Jiang, Y. (2020). Circular RNA-0001283 Suppresses Breast Cancer Proliferation and Invasion via MiR-187/HIPK3 Axis. *Medical Science Monitor*, *26*, e921502 https://doi.org/10.12659/MSM.921502

Hu, Y., Petit, S. A., Ficarro, S. B., Toomire, K. J., Xie, A., Lim, E., Cao, S. A., Park, E., Eck, M. J., Scully, R., Brown, M., Marto, J. A., & Livingston, D. M. (2014). PARP1-Driven Poly-ADP-Ribosylation Regulates BRCA1 Function in Homologous Recombination–Mediated DNA Repair. *Cancer Discovery*, *4*(12), 1430–1447. https://doi.org/10.1158/2159-8290.CD-13-0891

Huang, C.-Y., Pai, P.-Y., Kuo, C.-H., Ho, T.-J., Lin, J.-Y., Lin, D.-Y., Tsai, F.-J., Padma, V. V., Kuo, W.-W., & Huang, C.-Y. (2017). P53-mediated miR-18 repression activates HSF2 for IGF-IIR-dependent myocyte hypertrophy in hypertension-induced heart failure. *Cell Death & Disease*, *8*(8), e2990. https://doi.org/10.1038/cddis.2017.320

Huang, J.-W., Wang, Y., Dhillon, K. K., Calses, P., Villegas, E., Mitchell, P. S., Tewari, M., Kemp, C. J., & Taniguchi, T. (2013). Systematic Screen Identifies miRNAs That Target RAD51 and RAD51D to Enhance Chemosensitivity. *Molecular Cancer Research*, *11*(12), 1564–1573. https://doi.org/10.1158/1541-7786.MCR-13-0292

Huang, Y., Tong, J., He, F., Yu, X., Fan, L., Hu, J., Tan, J., & Chen, Z. (2015b). MiR-141 regulates TGF-β1-induced epithelial-mesenchymal transition through repression of HIPK2 expression in renal tubular epithelial cells. *International Journal of Molecular Medicine*, *35*(2), 311–318. https://doi.org/10.3892/ijmm.2014.2008

Huang, Y.-Z., Zhang, J., Shao, H.-Y., Chen, J.-P., & Zhao, H.-Y. (2015a). MicroRNA-191 promotes osteosarcoma cells proliferation by targeting checkpoint kinase 2. *Tumor Biology*, *36*(8), 6095–6101. https://doi.org/10.1007/s13277-015-3290-9

Ifeadi, V., & Garnett-Benson, C. (2012). Sub-Lethal Irradiation of Human Colorectal Tumor Cells Imparts Enhanced and Sustained Susceptibility to Multiple Death Receptor Signaling Pathways. *PLoS ONE*, *7*(2), e31762. https://doi.org/10.1371/journal.pone.0031762

Imani, S., Zhang, X., Hosseinifard, H., Fu, S., & Fu, J. (2017). The diagnostic role of microRNA-34a in breast cancer: A systematic review and meta-analysis. *Oncotarget*, *8*(14), 23177–23187. https://doi.org/10.18632/oncotarget.15520

Inomata, Y., Abe, T., Tsuda, M., Takeda, S., & Hirota, K. (2021). Division of labor of Y-family polymerases in translesion-DNA synthesis for distinct types of DNA damage. *PLoS ONE*, *16*(6), e0252587. https://doi.org/10.1371/journal.pone.0252587

Inoue, Y., Kitagawa, M., & Taya, Y. (2007). Phosphorylation of pRB at Ser612 by Chk1/2 leads to a complex between pRB and E2F-1 after DNA damage. *The EMBO Journal*, *26*(8), 2083–2093. https://doi.org/10.1038/sj.emboj.7601652

Ito, M., Ohba, S., Gaensler, K., Ronen, S. M., Mukherjee, J., & Pieper, R. O. (2013). Early Chk1 Phosphorylation Is Driven by Temozolomide-Induced, DNA Double Strand Break- and Mismatch Repair-Independent DNA Damage. *PLoS ONE*, *8*(5), e62351. https://doi.org/10.1371/journal.pone.0062351

Ivanovska, I., Ball, A. S., Diaz, R. L., Magnus, J. F., Kibukawa, M., Schelter, J. M., Kobayashi, S. V., Lim, L., Burchard, J., Jackson, A. L., Linsley, P. S., & Cleary, M. A. (2008). MicroRNAs in the miR-106b Family Regulate p21/CDKN1A and Promote Cell

Cycle Progression. *Molecular and Cellular Biology*, *28*(7), 2167–2174. https://doi.org/10.1128/MCB.01977-07

Jabbur, J. R., Huang, P., & Zhang, W. (2000). DNA damage-induced phosphorylation of p53 at serine 20 correlates with p21 and Mdm-2 induction in vivo. *Oncogene*, *19*(54), 6203–6208. https://doi.org/10.1038/sj.onc.1204017

Jayarama, S., Li, L.-C., Ganesh, L., Mardi, D., Kanteti, P., Hay, N., Li, P., & Prabhakar, B. S. (2014). MADD Is a Downstream Target of PTEN in Triggering Apoptosis: MADD Is a Downstream Target of PTEN. *Journal of Cellular Biochemistry*, *115*(2), 261–270. https://doi.org/10.1002/jcb.24657

Jenkins, G. J. S., Zaïr, Z., Johnson, G. E., & Doak, S. H. (2010). Genotoxic thresholds, DNA repair, and susceptibility in human populations. *Toxicology*, *278*(3), 305–310. https://doi.org/10.1016/j.tox.2009.11.016

Jia, B., Liu, W., Gu, J., Wang, J., Lv, W., Zhang, W., Hao, Q., Pang, Z., Mu, N., Zhang, W., & Guo, Q. (2019a). MiR-7-5p suppresses stemness and enhances temozolomide sensitivity of drug-resistant glioblastoma cells by targeting Yin Yang 1. *Experimental Cell Research*, *375*(1), 73–81. https://doi.org/10.1016/j.yexcr.2018.12.016

Jia, R., & Wang, C. (2020). MiR-29b-3p Reverses Cisplatin Resistance by Targeting COL1A1 in Non-Small-Cell Lung Cancer A549/DDP Cells. *Cancer Management and Research*, *12*, 2559–2566. https://doi.org/10.2147/CMAR.S246625

Jia, Y., Lin, R., Jin, H., Si, L., Jian, W., Yu, Q., & Yang, S. (2019b). MicroRNA-34 suppresses proliferation of human ovarian cancer cells by triggering autophagy and apoptosis and inhibits cell invasion by targeting Notch 1. *Biochimie*, *160*, 193–199. https://doi.org/10.1016/j.biochi.2019.03.011

Jin, X., Cai, L., Wang, C., Deng, X., Yi, S., Lei, Z., Xiao, Q., Xu, H., Luo, H., & Sun, J. (2018). CASC2/miR-24/miR-221 modulates the TRAIL resistance of hepatocellular carcinoma cell through caspase-8/caspase-3. *Cell Death & Disease*, *9*(3), 318. https://doi.org/10.1038/s41419-018-0350-2

Joshi, V., Upadhyay, A., Kumar, A., & Mishra, A. (2017). Gp78 E3 Ubiquitin Ligase: Essential Functions and Contributions in Proteostasis. *Frontiers in Cellular Neuroscience*, *11*, 259. https://doi.org/10.3389/fncel.2017.00259

Kaina, B., & Christmann, M. (2019). DNA repair in personalized brain cancer therapy with temozolomide and nitrosoureas. *DNA Repair*, *78*, 128–141. https://doi.org/10.1016/j.dnarep.2019.04.007

Kaina, B., Christmann, M., Naumann, S., & Roos, W. P. (2007). MGMT: Key node in the battle against genotoxicity, carcinogenicity and apoptosis induced by alkylating agents. *DNA Repair*, *6*(8), 1079–1099. https://doi.org/10.1016/j.dnarep.2007.03.008

Kaina, B., Margison, G. P., & Christmann, M. (2010). Targeting O 6-methylguanine-DNA methyltransferase with specific inhibitors as a strategy in cancer therapy. *Cellular and Molecular Life Sciences*, *67*(21), 3663–3681. https://doi.org/10.1007/s00018-010-0491-7

Kaina, B., Thomas, A.D., Visser, H., Hengstler, J.G., Frötschl, R. (2021). Do Carcinogens Have a Threshold Dose? The Pros and Cons. In: Reichl, FX., Schwenk, M. (eds) *Regulatory Toxicology*. https://doi.org/10.1007/978-3-030-57499-4_55

Kannappan, R., Mattapally, S., Wagle, P. A., & Zhang, J. (2018). Transactivation domain of p53 regulates DNA repair and integrity in human iPS cells. *American Journal of Physiology-Heart and Circulatory Physiology*, *315*(3), H512–H521. https://doi.org/10.1152/ajpheart.00160.2018

Karimian, A., Ahmadi, Y., & Yousefi, B. (2016). Multiple functions of p21 in cell cycle, apoptosis and transcriptional regulation after DNA damage. *DNA Repair*, *42*, 63–71. https://doi.org/10.1016/j.dnarep.2016.04.008

Kass, E. M., Ahn, J., Tanaka, T., Freed-Pastor, W. A., Keezer, S., & Prives, C. (2007). Stability of Checkpoint Kinase 2 Is Regulated via Phosphorylation at Serine 456. *Journal of Biological Chemistry*, *282*(41), 30311–30321. https://doi.org/10.1074/jbc.M704642200

Kato, M., Paranjape, T., Ullrich, R., Nallur, S., Gillespie, E., Keane, K., Esquela-Kerscher, A., Weidhaas, J. B., & Slack, F. J. (2009). The mir-34 microRNA is required for the DNA damage response in vivo in C. elegans and in vitro in human breast cancer cells. *Oncogene*, *28*(25), 2419–2424. https://doi.org/10.1038/onc.2009.106

Kaufmann, W. K., & Paules, R. S. (1996). DNA damage and cell cycle checkpoints. *The FASEB Journal*, *10*(2), 238–247. https://doi.org/10.1096/fasebj.10.2.8641557

Kawai, S., & Amano, A. (2012). BRCA1 regulates microRNA biogenesis via the DROSHA microprocessor complex. *Journal of Cell Biology*, *197*(2), 201–208. https://doi.org/10.1083/jcb.201110008

Khan, A. A., Betel, D., Miller, M. L., Sander, C., Leslie, C. S., & Marks, D. S. (2009). Transfection of small RNAs globally perturbs gene regulation by endogenous microRNAs. *Nature Biotechnology*, *27*(6), 549–555. https://doi.org/10.1038/nbt.1543

Khuu, C., Jevnaker, A.-M., Bryne, M., & Osmundsen, H. (2014). An investigation into anti-proliferative effects of microRNAs encoded by the miR-106a-363 cluster on human carcinoma cells and keratinocytes using microarray profiling of miRNA transcriptomes. *Frontiers in Genetics*, *5*(246), 1-14. https://doi.org/10.3389/fgene.2014.00246

Kim, H., Tu, H.-C., Ren, D., Takeuchi, O., Jeffers, J. R., Zambetti, G. P., Hsieh, J. J.-D., & Cheng, E. H.-Y. (2009). Stepwise Activation of BAX and BAK by tBID, BIM, and PUMA Initiates Mitochondrial Apoptosis. *Molecular Cell*, *36*(3), 487–499. https://doi.org/10.1016/j.molcel.2009.09.030

Klapacz, J., Pottenger, L. H., Engelward, B. P., Heinen, C. D., Johnson, G. E., Clewell, R. A., Carmichael, P. L., Adeleye, Y., & Andersen, M. E. (2016). Contributions of DNA repair and damage response pathways to the non-linear genotoxic responses of alkylating agents. *Mutation Research/Reviews in Mutation Research*, *767*, 77–91. https://doi.org/10.1016/j.mrrev.2015.11.001

Knizhnik, A. V., Roos, W. P., Nikolova, T., Quiros, S., Tomaszowski, K. H., Christmann, M., & Kaina, B. (2013). Survival and death strategies in glioma cells: autophagy, senescence and apoptosis triggered by a single type of temozolomide-induced DNA damage. *PloS ONE*, *8*(1), e55665. https://doi.org/10.1371/journal.pone.0055665

Kodama, M., Otsubo, C., Hirota, T., Yokota, J., Enari, M., & Taya, Y. (2010). Requirement of ATM for Rapid p53 Phosphorylation at Ser46 without Ser/Thr-Gln Sequences. *Molecular and Cellular Biology*, *30*(7), 1620–1633. https://doi.org/10.1128/MCB.00810-09

Kos, A., Olde Loohuis, N. F. M., Wieczorek, M. L., Glennon, J. C., Martens, G. J. M., Kolk, S. M., & Aschrafi, A. (2012). A Potential Regulatory Role for Intronic microRNA-338-3p for Its Host Gene Encoding Apoptosis-Associated Tyrosine Kinase. *PLoS ONE*, *7*(2), e31022. https://doi.org/10.1371/journal.pone.0031022

Krejci, L., Altmannova, V., Spirek, M., & Zhao, X. (2012). Homologous recombination and its regulation. *Nucleic Acids Research*, *40*(13), 5795–5818. https://doi.org/10.1093/nar/gks270

Krishnan, K., Steptoe, A. L., Martin, H. C., Wani, S., Nones, K., Waddell, N., Mariasegaram, M., Simpson, P. T., Lakhani, S. R., Gabrielli, B., Vlassov, A., Cloonan, N., & Grimmond, S. M. (2013). MicroRNA-182-5p targets a network of genes involved in DNA repair. *RNA*, *19*(2), 230–242. https://doi.org/10.1261/rna.034926.112

Krokan, H. E., & Bjoras, M. (2013). Base Excision Repair. *Cold Spring Harbor Perspectives in Biology*, *5*(4), a012583. https://doi.org/10.1101/cshperspect.a012583

Kumar, A., Ghosh, S., & Chandna, S. (2015). Evidence for microRNA-31 dependent Bim-Bax interaction preceding mitochondrial Bax translocation during radiation-induced apoptosis. *Scientific Reports*, *5*(1), 15923. https://doi.org/10.1038/srep15923

Kumar, N., Moreno, N. C., Feltes, B. C., Menck, C. F., & Houten, B. V. (2020). Cooperation and interplay between base and nucleotide excision repair pathways: From DNA lesions to proteins. *Genetics and Molecular Biology*, *43*(1), e20190104. https://doi.org/10.1590/1678-4685-gmb-2019-0104

Kumar, N., Raja, S., & Van Houten, B. (2020). The involvement of nucleotide excision repair proteins in the removal of oxidative DNA damage. *Nucleic Acids Research*, *48*(20), 11227–11243. https://doi.org/10.1093/nar/gkaa777

Kumar, S. (2009). Caspase 2 in apoptosis, the DNA damage response and tumour suppression: Enigma no more? *Nature Reviews Cancer*, *9*, 897-903. https://doi.org/10.1038/nrc2745.

Kuribayashi, K., Krigsfeld, G., Wang, W., Xu, Ji., Mayes, P. A., Dicker, D. T., Wu, G. S., & El-Deiry, W. S. (2008). TNFSF10 (TRAIL), a p53 target gene that mediates p53-dependent cell death. *Cancer Biology & Therapy*, *7*(12), 2034–2038. https://doi.org/10.4161/cbt.7.12.7460

Lai, J., Xin, J., Fu, C., & Zhang, W. (2020). CircHIPK3 promotes proliferation and metastasis and inhibits apoptosis of renal cancer cells by inhibiting MiR-485-3p. *Cancer Cell International*, *20*(1), 248. https://doi.org/10.1186/s12935-020-01319-3

Lai, J., Yang, H., Zhu, Y., Ruan, M., Huang, Y., & Zhang, Q. (2019). MiR-7-5p-mediated downregulation of PARP1 impacts DNA homologous recombination repair and resistance to doxorubicin in small cell lung cancer. *BMC Cancer*, *19*(1), 602. https://doi.org/10.1186/s12885-019-5798-7

Lai, X., Gupta, S. K., Schmitz, U., Marquardt, S., Knoll, S., Spitschak, A., Wolkenhauer, O., Pützer, B. M., & Vera, J. (2018). MiR-205-5p and miR-342-3p cooperate in the repression of the E2F1 transcription factor in the context of anticancer chemotherapy resistance. *Theranostics*, *8*(4), 1106–1120. https://doi.org/10.7150/thno.19904

Lang, C., Xu, M., Zhao, Z., Chen, J., & Zhang, L. (2018). MicroRNA-96 expression induced by low-dose cisplatin or doxorubicin regulates chemosensitivity, cell death and proliferation in gastric cancer SGC7901 cells by targeting FOXO1. *Oncology Letters*, *16*, 4020-4026. https://doi.org/10.3892/ol.2018.9122

Lee, J., Kumagai, A., & Dunphy, W. G. (2001). Positive Regulation of Wee1 by Chk1 and 14-3-3 Proteins. *Molecular Biology of the Cell*, *12*(3), 551–563. https://doi.org/10.1091/mbc.12.3.551

Lee, J.-H., Goodarzi, A. A., Jeggo, P. A., & Paull, T. T. (2010). 53BP1 promotes ATM activity through direct interactions with the MRN complex. *The EMBO Journal*, *29*(3), 574–585. https://doi.org/10.1038/emboj.2009.372

Lee, R. C., Feinbaum, R. L., & Ambros, V. (1993). The C. elegans heterochronic gene lin-4 encodes small RNAs with antisense complementarity to lin-14. *Cell*, *75*(5), 843–854. https://doi.org/10.1016/0092-8674(93)90529-Y

Lee, S.-H., Meng, X. W., Flatten, K. S., Loegering, D. A., & Kaufmann, S. H. (2013). Phosphatidylserine exposure during apoptosis reflects bidirectional trafficking between plasma membrane and cytoplasm. *Cell Death & Differentiation*, *20*(1), 64–76. https://doi.org/10.1038/cdd.2012.93

Lee, Y., Kim, M., Han, J., Yeom, K.-H., Lee, S., Baek, S. H., & Kim, V. N. (2004). MicroRNA genes are transcribed by RNA polymerase II. *The EMBO Journal*, *23*(20), 4051–4060. https://doi.org/10.1038/sj.emboj.7600385

Leslie, P. L., Franklin, D. A., Liu, Y., & Zhang, Y. (2018). P53 Regulates the Expression of LRP1 and Apoptosis through a Stress Intensity-Dependent MicroRNA Feedback Loop. *Cell Reports*, *24*(6), 1484–1495. https://doi.org/10.1016/j.celrep.2018.07.010

Lezina, L., Purmessur, N., Antonov, A. V., Ivanova, T., Karpova, E., Krishan, K., Ivan, M., Aksenova, V., Tentler, D., Garabadgiu, A. V., Melino, G., & Barlev, N. A. (2013). MiR-16 and miR-26a target checkpoint kinases Wee1 and Chk1 in response to p53 activation by genotoxic stress. *Cell Death & Disease*, *4*(12), e953. https://doi.org/10.1038/cddis.2013.483

Li, G.-M. (2008). Mechanisms and functions of DNA mismatch repair. *Cell Research*, *18*(1), 85-98. https://doi.org/10.1038/cr.2007.115

Li, H., Handsaker, B., Wysoker, A., Fennell, T., Ruan, J., Homer, N., Marth, G., Abecasis, G., Durbin, R., & 1000 Genome Project Data Processing Subgroup. (2009). The Sequence Alignment/Map format and SAMtools. *Bioinformatics*, *25*(16), 2078–2079. https://doi.org/10.1093/bioinformatics/btp352

Li, J.-H., Xiao, X., Zhang, Y.-N., Wang, Y.-M., Feng, L.-M., Wu, Y.-M., & Zhang, Y.-X. (2011b). MicroRNA miR-886-5p inhibits apoptosis by down-regulating Bax expression

in human cervical carcinoma cells. *Gynecologic Oncology*, *120*(1), 145–151. https://doi.org/10.1016/j.ygyno.2010.09.009

Li, L., Guan, Y., Chen, X., Yang, J., & Cheng, Y. (2021). DNA Repair Pathways in Cancer Therapy and Resistance. *Frontiers in Pharmacology*, *11*, 629266. https://doi.org/10.3389/fphar.2020.629266

Li, Q., Liu, J., Jia, Y., Li, T., & Zhang, M. (2020). MiR-623 suppresses cell proliferation, migration and invasion through direct inhibition of XRCC5 in breast cancer. *Aging*, *12*(11), 10246–10258. https://doi.org/10.18632/aging.103182

Li, R., Zhang, H., & Zheng, X. (2018). MiR-34c induces apoptosis and inhibits the viability of M4e cells by targeting BCL2. *Oncology Letters*, *15*, 3357-3361. https://doi.org/10.3892/ol.2017.7640

Li, W., Wu, H., Li, Y., Pan, H., Meng, T., & Wang, X. (2016). MicroRNA-143 promotes apoptosis of osteosarcoma cells by caspase-3 activation via targeting Bcl-2. *Biomedicine & Pharmacotherapy*, *80*, 8–15. https://doi.org/10.1016/j.biopha.2016.03.001

Li, X., & Heyer, W.-D. (2008). Homologous recombination in DNA repair and DNA damage tolerance. *Cell Research*, *18*(1), 99–113. https://doi.org/10.1038/cr.2008.1

Li, Y., Jiang, J., Liu, W., Wang, H., Zhao, L., Liu, S., Li, P., Zhang, S., Sun, C., Wu, Y., Yu, S., Li, X., Zhang, H., Qian, H., Zhang, D., Guo, F., Zhai, Q., Ding, Q., Wang, L., & Ying, H. (2018). MicroRNA-378 promotes autophagy and inhibits apoptosis in skeletal muscle. *Proceedings of the National Academy of Sciences*, *115*(46), E10849-E10858. https://doi.org/10.1073/pnas.1803377115

Li, Z., Ni, M., Li, J., Zhang, Y., Ouyang, Q., & Tang, C. (2011a). Decision making of the p53 network: Death by integration. *Journal of Theoretical Biology*, *271*(1), 205–211. https://doi.org/10.1016/j.jtbi.2010.11.041

Li, Z., Pearlman, A. H., & Hsieh, P. (2016). DNA mismatch repair and the DNA damage response. *DNA Repair*, *38*, 94–101. https://doi.org/10.1016/j.dnarep.2015.11.019

Liang, M., Yao, G., Yin, M., Lü, M., Tian, H., Liu, L., Lian, J., Huang, X., & Sun, F. (2013). Transcriptional cooperation between p53 and NF-κB p65 regulates microRNA-224 transcription in mouse ovarian granulosa cells. *Molecular and Cellular Endocrinology*, *370*(1–2), 119–129. https://doi.org/10.1016/j.mce.2013.02.014

Liao, X.-H., Zheng, L., He, H.-P., Zheng, D.-L., Wei, Z.-Q., Wang, N., Dong, J., Ma, W.-J., & Zhang, T.-C. (2015). STAT3 regulated ATR via microRNA-383 to control DNA damage to affect apoptosis in A431 cells. *Cellular Signalling*, *27*(11), 2285–2295. https://doi.org/10.1016/j.cellsig.2015.08.005

Liebl, M. C., & Hofmann, T. G. (2019). Cell Fate Regulation upon DNA Damage: P53 Serine 46 Kinases Pave the Cell Death Road. *BioEssays*, *41*(12), 1900127. https://doi.org/10.1002/bies.201900127

Ling, H., Fabbri, M., & Calin, G. A. (2013). MicroRNAs and other non-coding RNAs as targets for anticancer drug development. *Nature Reviews Drug Discovery*, *12*(11), 847–865. https://doi.org/10.1038/nrd4140

Linke, S. P., Sengupta, S., Khabie, N., Jeffries, B. A., Buchhop, S., Miska, S., Henning, W., Pedeux, R., Wang, X. W., Hofseth, L. J., Yang, Q., Garfield, S. H., & Harris, C. C. (2003). p53 Interacts with hRAD51 and hRAD54, and Directly Modulates Homologous Recombination. *Cancer Research*, *63*, 2596-2605.

Liu, B., Qu, J., Xu, F., Guo, Y., Wang, Y., Yu, H., & Qian, B. (2015). MiR-195 suppresses non-small cell lung cancer by targeting CHEK1. *Oncotarget*, *6*(11), 9445–9456. https://doi.org/10.18632/oncotarget.3255

Liu, G., & Chen, X. (2006). DNA Polymerase η, the Product of the Xeroderma Pigmentosum Variant Gene and a Target of p53, Modulates the DNA Damage Checkpoint and p53 Activation. *Molecular & Cellular Biology*, *26*(4), 1398-1413. https://doi.org/10.1128/MCB.26.4.1398-1413.2006

Liu, H. L., Huang, C. Y., Chen, J. Y., Wang, H. Y. J., Chen, P. Y., & Wei, K. C. (2014). Pharmacodynamic and therapeutic investigation of focused ultrasound-induced blood-brain barrier opening for enhanced temozolomide delivery in glioma treatment. *PloS ONE*, *9*(12), e114311. https://doi.org/10.1371/journal.pone.0114311

Liu, J. C., Lerou, P. H., & Lahav, G. (2014). Stem cells: Balancing resistance and sensitivity to DNA damage. *Trends in Cell Biology*, *24*(5), 268–274. https://doi.org/10.1016/j.tcb.2014.03.002

Liu, J., Zhang, C., Zhao, Y., & Feng, Z. (2017). MicroRNA Control of p53: MicroRNAs and p53. *Journal of Cellular Biochemistry*, *118*(1), 7–14. https://doi.org/10.1002/jcb.25609

Liu, Q., Fu, H., Sun, F., Zhang, H., Tie, Y., Zhu, J., Xing, R., Sun, Z., & Zheng, X. (2008). MiR-16 family induces cell cycle arrest by regulating multiple cell cycle genes. *Nucleic Acids Research*, *36*(16), 5391–5404. https://doi.org/10.1093/nar/gkn522

Liu, X., Yue, P., Khuri, F. R., & Sun, S.-Y. (2004). P53 Upregulates Death Receptor 4 Expression through an Intronic p53 Binding Site. *Cancer Research*, *64*(15), 5078–5083. https://doi.org/10.1158/0008-5472.CAN-04-1195

Lizé, M., Pilarski, S., & Dobbelstein, M. (2010). E2F1-inducible microRNA 449a/b suppresses cell proliferation and promotes apoptosis. *Cell Death & Differentiation*, *17*(3), 452–458. https://doi.org/10.1038/cdd.2009.188

Llambi, F., Wang, Y.-M., Victor, B., Yang, M., Schneider, D. M., Gingras, S., Parsons, M. J., Zheng, J. H., Brown, S. A., Pelletier, S., Moldoveanu, T., Chen, T., & Green, D. R. (2016). BOK Is a Non-canonical BCL-2 Family Effector of Apoptosis Regulated by ER-Associated Degradation. *Cell*, *165*(2), 421–433. https://doi.org/10.1016/j.cell.2016.02.026

Loewer, A., Batchelor, E., Gaglia, G., & Lahav, G. (2010). Basal Dynamics of p53 Reveal Transcriptionally Attenuated Pulses in Cycling Cells. *Cell*, *142*(1), 89–100. https://doi.org/10.1016/j.cell.2010.05.031

Loewer, A., Karanam, K., Mock, C., & Lahav, G. (2013). The p53 response in single cells is linearly correlated to the number of DNA breaks without a distinct threshold. *BMC Biology*, *11*(114). https://doi.org/10.1186/1741-7007-11-114

Lorge, E., Moore, M. M., Clements, J., O'Donovan, M., Fellows, M. D., Honma, M., Kohara, A., Galloway, S., Armstrong, M. J., Thybaud, V., Gollapudi, B., Aardema, M. J., & Tanir, J. Y. (2016). Standardized cell sources and recommendations for good cell culture practices in genotoxicity testing. *Mutation Research/Genetic Toxicology and Environmental Mutagenesis*, *809*, 1–15. https://doi.org/10.1016/j.mrgentox.2016.08.001

Loughery, J., Cox, M., Smith, L. M., & Meek, D. W. (2014). Critical role for p53-serine 15 phosphorylation in stimulating transactivation at p53-responsive promoters. *Nucleic Acids Research*, *42*(12), 7666–7680. https://doi.org/10.1093/nar/gku501

Loughery, J., & Meek, D. (2013). Switching on p53: An essential role for protein phosphorylation? *Biodiscovery*, *8*(1), e8946. https://doi.org/10.7750/BioDiscovery.2013.8.1

Lu, K., Wang, J., Song, Y., Zhao, S., Liu, H., Tang, D., Pan, B., Zhao, H., & Zhang, Q. (2015). MiRNA-24-3p promotes cell proliferation and inhibits apoptosis in human breast cancer by targeting p27Kip1. *Oncology Reports*, *34*(2), 995–1002. https://doi.org/10.3892/or.2015.4025

Lu, X., Nguyen, T.-A., Zhang, X., & Donehower, L. A. (2008). The Wip1 phosphatase and Mdm2: Cracking the 'Wip' on p53 stability. *Cell Cycle*, *7*(2), 164–168. https://doi.org/10.4161/cc.7.2.5299

Luo, H., Liang, H., Chen, Y., Chen, S., Xu, Y., Xu, L., Liu, J., Zhou, K., Peng, J., Guo, G., Lai, B., Song, L., Yang, H., Liu, L., Peng, J., Liu, Z., Tang, L., Chen, W., & Tang, H. (2018). MiR-7-5p over-expression suppresses cell proliferation and promotes apoptosis through inhibiting the ability of DNA damage repair of PARP-1 and BRCA1 in TK6 cells exposed to hydroquinone. *Chemico-Biological Interactions*, *283*, 84–90. https://doi.org/10.1016/j.cbi.2018.01.019

Luo, W., Li, G., Yi, Z., Nie, Q., & Zhang, X. (2016). E2F1-miR-20a-5p/20b-5p auto-regulatory feedback loop involved in myoblast proliferation and differentiation. *Scientific Reports*, *6*(1), 27904. https://doi.org/10.1038/srep27904

Macurek, L., Benada, J., Müllers, E., Halim, V. A., Krejčíková, K., Burdová, K., Pecháčková, S., Hodný, Z., Lindqvist, A., Medema, R. H., & Bartek, J. (2013). Downregulation of Wip1 phosphatase modulates the cellular threshold of DNA damage signaling in mitosis. *Cell Cycle*, *12*(2), 251–262. https://doi.org/10.4161/cc.23057

Marechal, A., & Zou, L. (2013). DNA Damage Sensing by the ATM and ATR Kinases. *Cold Spring Harbor Perspectives in Biology*, *5*(9), a012716. https://doi.org/10.1101/cshperspect.a012716

Marqués-Torrejón, M. Á., Porlan, E., Banito, A., Gómez-Ibarlucea, E., Lopez-Contreras, A. J., Fernández-Capetillo, Ó., Vidal, A., Gil, J., Torres, J., & Fariñas, I. (2013). Cyclin-Dependent Kinase Inhibitor p21 Controls Adult Neural Stem Cell Expansion by Regulating Sox2 Gene Expression. *Cell Stem Cell*, *12*(1), 88–100. https://doi.org/10.1016/j.stem.2012.12.001

Matsuoka, S., Rotman, G., Ogawa, A., Shiloh, Y., Tamai, K., & Elledge, S. J. (2000). Ataxia telangiectasia-mutated phosphorylates Chk2 *in vivo* and *in vitro*. *Proceedings of the National Academy of Sciences*, *97*(19), 10389–10394. https://doi.org/10.1073/pnas.190030497

Matt, S., & Hofmann, T. G. (2016). The DNA damage-induced cell death response: A roadmap to kill cancer cells. *Cellular and Molecular Life Sciences*, *73*(15), 2829–2850. https://doi.org/10.1007/s00018-016-2130-4

Mayo, L. D., Seo, Y. R., Jackson, M. W., Smith, M. L., Guzman, J. R., Korgaonkar, C. K., & Donner, D. B. (2005). Phosphorylation of Human p53 at Serine 46 Determines Promoter Selection and whether Apoptosis Is Attenuated or Amplified. *Journal of Biological Chemistry*, *280*(28), 25953–25959. https://doi.org/10.1074/jbc.M503026200

McGeary, S. E., Lin, K. S., Shi, C. Y., Pham, T. M., Bisaria, N., Kelley, G. M., & Bartel, D. P. (2019). The biochemical basis of microRNA targeting efficacy. *Science*, *366*(6472), eaav1741. https://doi.org/10.1126/science.aav1741

Menolfi, D., & Zha, S. (2020). ATM, ATR and DNA-PKcs kinases—the lessons from the mouse models: Inhibition ≠ deletion. *Cell & Bioscience*, *10*(1), 8. https://doi.org/10.1186/s13578-020-0376-x

Min, H., Turck, C. W., Nikolic, J. M., & Black, D. L. (1997). A new regulatory protein, KSRP, mediates exon inclusion through an intronic splicing enhancer. *Genes & Development*, *11*(8), 1023–1036. https://doi.org/10.1101/gad.11.8.1023

Miyamoto, S., Guzman, R. C., Osborn, R. C., & Nandi, S. (1988). Neoplastic transformation of mouse mammary epithelial cells by in vitro exposure to N-methyl-N-nitrosourea. *Proceedings of the National Academy of Sciences*, *85*(2), 477-481.

Miyazaki, T., Kim, Y.-S., Yoon, J., Wang, H., Suzuki, T., & Morse, H. C. (2014). The 3′–5′ DNA Exonuclease TREX1 Directly Interacts with Poly(ADP-ribose) Polymerase-1 (PARP1) during the DNA Damage Response. *Journal of Biological Chemistry*, *289*(47), 32548–32558. https://doi.org/10.1074/jbc.M114.547331

Mobarra, N., Shafiee, A., Rad, S. M. A. H., Tasharrofi, N., Soufi-zomorod, M., Hafizi, M., Movahed, M., kouhkan, F., & Soleimani, M. (2015). Overexpression of microRNA-16 declines cellular growth, proliferation and induces apoptosis in human breast cancer cells. *In Vitro Cellular & Developmental Biology - Animal*, *51*(6), 604–611. https://doi.org/10.1007/s11626-015-9872-4

Mogilyansky, E., & Rigoutsos, I. (2013). The miR-17/92 cluster: A comprehensive update on its genomics, genetics, functions and increasingly important and numerous roles in health and disease. *Cell Death & Differentiation*, *20*(12), 1603–1614. https://doi.org/10.1038/cdd.2013.125

Mojas, N., Lopes, M., & Jiricny, J. (2007). Mismatch repair-dependent processing of methylation damage gives rise to persistent single-stranded gaps in newly replicated DNA. *Genes & Development*, *21*(24), 3342–3355. https://doi.org/10.1101/gad.455407

Moll, U. M., and Petrenko, O. (2003). The MDM2-p53 Interaction. *Molecular Cancer Research*, *1*(14), 1001-1008.

Moore, R., Ooi, H. K., Kang, T., Bleris, L., & Ma, L. (2015). MiR-192-Mediated Positive Feedback Loop Controls the Robustness of Stress-Induced p53 Oscillations in Breast Cancer Cells. *PLoS Computational Biology*, *11*(12), e1004653. https://doi.org/10.1371/journal.pcbi.1004653

Müller, M., Wilder, S., Bannasch, D., Israeli, D., Lehlbach, K., Li-Weber, M., Friedman, S. L., Galle, P. R., Stremmel, W., Oren, M., & Krammer, P. H. (1998). P53 Activates the CD95 (APO-1/Fas) Gene in Response to DNA Damage by Anticancer Drugs. *Journal of Experimental Medicine*, *188*(11), 2033–2045. https://doi.org/10.1084/jem.188.11.2033

Nagata, S., Nagase, H., Kawane, K., Mukae, N., & Fukuyama, H. (2003). Degradation of chromosomal DNA during apoptosis. *Cell Death & Differentiation*, *10*(1), 108–116. https://doi.org/10.1038/sj.cdd.4401161

Nair, R. R., Bagheri, M., & Saini, D. K. (2015). Temporally distinct roles of ATM and ROS in genotoxic-stress-dependent induction and maintenance of cellular senescence. *Journal of Cell Science*, *128*(2), 342–353. https://doi.org/10.1242/jcs.159517

Nakagawa, K., Taya, Y., Tamai, K., & Yamaizumi, M. (1999). Requirement of ATM in Phosphorylation of the Human p53 Protein at Serine 15 following DNA Double-Strand Breaks. *Molecular and Cellular Biology*, *19*(4), 2828–2834. https://doi.org/10.1128/MCB.19.4.2828

Nakano, K., & Vousden, K. H. (2001). PUMA, a Novel Proapoptotic Gene, Is Induced by p53. *Molecular Cell*, *7*(3), 683–694. https://doi.org/10.1016/S1097-2765(01)00214-3

Nakazawa, K., Dashzeveg, N., & Yoshida, K. (2014). Tumor suppressor p53 induces miR-1915 processing to inhibit Bcl-2 in the apoptotic response to DNA damage. *FEBS Journal*, *281*(13), 2937–2944. https://doi.org/10.1111/febs.12831

Newlands, E. S., Stevens, M. F. G., Wedge, S. R., Wheelhouse, R. T., & Brock, C. (1997). Temozolomide: A review of its discovery, chemical properties, pre-clinical development and clinical trials. *Cancer Treatment Reviews*, *23*(1), 35–61. https://doi.org/10.1016/S0305-7372(97)90019-0

Niida, H., Katsuno, Y., Banerjee, B., Hande, M. P., & Nakanishi, M. (2007). Specific Role of Chk1 Phosphorylations in Cell Survival and Checkpoint Activation. *Molecular and Cellular Biology*, *27*(7), 2572–2581. https://doi.org/10.1128/MCB.01611-06

Niu, M., Gao, D., Wen, Q., Wei, P., Pan, S., Shuai, C., Ma, H., Xiang, J., Li, Z., Fan, S., Li, G., & Peng, S. (2016). MiR-29c regulates the expression of miR-34c and miR-449a by targeting DNA methyltransferase 3a and 3b in nasopharyngeal carcinoma. *BMC Cancer*, *16*(1), 218. https://doi.org/10.1186/s12885-016-2253-x

Noonan, E. M., Shah, D., Yaffe, M. B., Lauffenburger, D. A., & Samson, L. D. (2012). *O* 6-Methylguanine DNA lesions induce an intra-S-phase arrest from which cells exit into apoptosis governed by early and late multi-pathway signaling network activation. *Integrative Biology*, *4*(10), 1237–1255. https://doi.org/10.1039/c2ib20091k

Nowsheen, S., & Yang, E. S. (2013). The intersection between DNA damage response and cell death pathways. *Experimental Oncology*, *34*(3), 243-254.

Oda, K., Arakawa, H., Tanaka, T., Matsuda, K., Tanikawa, C., Mori, T., Nishimori, H., Tamai, K., Tokino, T., Nakamura, Y., & Taya, Y. (2000). P53AIP1, a Potential Mediator of p53-Dependent Apoptosis, and Its Regulation by Ser-46-Phosphorylated p53. *Cell*, *102*(6), 849–862. https://doi.org/10.1016/S0092-8674(00)00073-8

Özören, N., & El-Deiry, W. S. (2002). Defining Characteristics of Types I and II Apoptotic Cells in Response to TRAIL. *Neoplasia*, *4*(6), 551–557. https://doi.org/10.1038/sj.neo.7900270

Pećina-Šlaus, N., Kafka, A., Salamon, I., & Bukovac, A. (2020). Mismatch Repair Pathway, Genome Stability and Cancer. *Frontiers in Molecular Biosciences*, *7*, 122. https://doi.org/10.3389/fmolb.2020.00122

Peddu, C., Zhang, S., Zhao, H., Wong, A., Lee, E. Y. C., Lee, M. Y. W. T., & Zhang, Z. (2018). Phosphorylation Alters the Properties of Pol η: Implications for Translesion Synthesis. *iScience*, *6*, 52–67. https://doi.org/10.1016/j.isci.2018.07.009

Peng, C., Chen, Z., Wang, S., Wang, H.-W., Qiu, W., Zhao, L., Xu, R., Luo, H., Chen, Y., Chen, D., You, Y., Liu, N., & Wang, H. (2016). The Error-Prone DNA Polymerase κ Promotes Temozolomide Resistance in Glioblastoma through Rad17-Dependent Activation of ATR-Chk1 Signaling. *Cancer Research*, *76*(8), 2340–2353. https://doi.org/10.1158/0008-5472.CAN-15-1884

Perfettini, J.-L., Castedo, M., Nardacci, R., Ciccosanti, F., Boya, P., Roumier, T., Larochette, N., Piacentini, M., & Kroemer, G. (2005). Essential role of p53 phosphorylation by p38 MAPK in apoptosis induction by the HIV-1 envelope. *Journal of Experimental Medicine*, *201*(2), 279–289. https://doi.org/10.1084/jem.20041502

Pernaute, B., Spruce, T., Smith, K. M., Sánchez-Nieto, J. M., Manzanares, M., Cobb, B., & Rodríguez, T. A. (2014). MicroRNAs control the apoptotic threshold in primed

pluripotent stem cells through regulation of BIM. *Genes & Development*, *28*(17), 1873–1878. https://doi.org/10.1101/gad.245621.114

Perona, R., Moncho-Amor, V., Machado-Pinilla, R., Belda-Iniesta, C., & Sánchez Pérez, I. (2008). Role of CHK2 in cancer development. *Clinical and Translational Oncology*, *10*(9), 538–542. https://doi.org/10.1007/s12094-008-0248-5

Pichiorri, F., Suh, S.-S., Rocci, A., De Luca, L., Taccioli, C., Santhanam, R., Zhou, W., Benson, D. M., Hofmainster, C., Alder, H., Garofalo, M., Di Leva, G., Volinia, S., Lin, H.-J., Perrotti, D., Kuehl, M., Aqeilan, R. I., Palumbo, A., & Croce, C. M. (2010). Downregulation of p53-inducible microRNAs 192, 194, and 215 Impairs the p53/MDM2 Autoregulatory Loop in Multiple Myeloma Development. *Cancer Cell*, *18*(4), 367–381. https://doi.org/10.1016/j.ccr.2010.09.005

Piotto, C., Biscontin, A., Millino, C., & Mognato, M. (2018). Functional validation of miRNAs targeting genes of DNA double-strand break repair to radiosensitize non-small lung cancer cells. *Biochimica et Biophysica Acta (BBA) - Gene Regulatory Mechanisms*, *1861*(12), 1102–1118. https://doi.org/10.1016/j.bbagrm.2018.10.010

Podhorecka, M., Skladanowski, A., & Bozko, P. (2010). H2AX Phosphorylation: Its Role in DNA Damage Response and Cancer Therapy. *Journal of Nucleic Acids*, *2010*, 1–9. https://doi.org/10.4061/2010/920161

Porter, J. R., Fisher, B. E., & Batchelor, E. (2016). P53 Pulses Diversify Target Gene Expression Dynamics in an mRNA Half-Life-Dependent Manner and Delineate Co-regulated Target Gene Subnetworks. *Cell Systems*, *2*(4), 272–282. https://doi.org/10.1016/j.cels.2016.03.006

Pothof, J., Verkaik, N. S., van IJcken, W., Wiemer, E. A. C., Ta, V. T. B., van der Horst, G. T. J., Jaspers, N. G. J., van Gent, D. C., Hoeijmakers, J. H. J., & Persengiev, S. P.

(2009). MicroRNA-mediated gene silencing modulates the UV-induced DNA-damage response. *The EMBO Journal*, *28*(14), 2090–2099. https://doi.org/10.1038/emboj.2009.156

Pratt, A. J., & MacRae, I. J. (2009). The RNA-induced Silencing Complex: A Versatile Gene-silencing Machine. *Journal of Biological Chemistry*, *284*(27), 17897–17901. https://doi.org/10.1074/jbc.R900012200

Puccini, J., Dorstyn, L., & Kumar, S. (2013). Caspase-2 as a tumour suppressor. *Cell Death & Differentiation*, *20*(9), 1133–1139. https://doi.org/10.1038/cdd.2013.87

Quiros, S., Roos, W. P., & Kaina, B. (2010). Processing of O^6-methylguanine into DNA double-strand breaks requires two rounds of replication whereas apoptosis is also induced in subsequent cell cycles. *Cell Cycle*, *9*(1), 168–178. https://doi.org/10.4161/cc.9.1.10363

Rahman, M., Lovat, F., Romano, G., Calore, F., Acunzo, M., Bell, E. H., & Nana-Sinkam, P. (2014). MiR-15b/16-2 Regulates Factors That Promote p53 Phosphorylation and Augments the DNA Damage Response following Radiation in the Lung. *Journal of Biological Chemistry*, *289*(38), 26406–26416. https://doi.org/10.1074/jbc.M114.573592

Rapti, S.-M., Kontos, C. K., Christodoulou, S., Papadopoulos, I. N., & Scorilas, A. (2017). MiR-34a overexpression predicts poor prognostic outcome in colorectal adenocarcinoma, independently of clinicopathological factors with established prognostic value. *Clinical Biochemistry*, *50*(16–17), 918–924. https://doi.org/10.1016/j.clinbiochem.2017.06.004

Raut, S. K., Singh, G. B., Rastogi, B., Saikia, U. N., Mittal, A., Dogra, N., Singh, S., Prasad, R., & Khullar, M. (2016). MiR-30c and miR-181a synergistically modulate p53–p21

pathway in diabetes induced cardiac hypertrophy. *Molecular and Cellular Biochemistry*, *417*(1–2), 191–203. https://doi.org/10.1007/s11010-016-2729-7

Razumilava, N., Bronk, S. F., Smoot, R. L., Fingas, C. D., Werneburg, N. W., Roberts, L. R., & Mott, J. L. (2012). MiR-25 targets TNF-related apoptosis inducing ligand (TRAIL) death receptor-4 and promotes apoptosis resistance in cholangiocarcinoma. *Hepatology*, *55*(2), 465–475. https://doi.org/10.1002/hep.24698

Reed, S., & Quelle, D. (2014). p53 Acetylation: Regulation and Consequences. *Cancers*, *7*(1), 30–69. https://doi.org/10.3390/cancers7010030

Ren, L., Li, F., Di, M., Fu, Y., Hui, Y., Xiao, G., Sun, Q., Liu, Y., Ren, D., & Du, X. (2017). MicroRNA-187 regulates gastric cancer progression by targeting the tumor suppressor CRMP1. *Biochemical and Biophysical Research Communications*, *482*(4), 597–603. https://doi.org/10.1016/j.bbrc.2016.11.079

Ren, Z., He, H., Zuo, Z., Xu, Z., Wei, Z., & Deng, J. (2019). The role of different SIRT1-mediated signaling pathways in toxic injury. *Cellular & Molecular Biology Letters*, *24*(1), 36. https://doi.org/10.1186/s11658-019-0158-9

Reynolds, P., Cooper, S., Lomax, M., & O'Neill, P. (2015). Disruption of PARP1 function inhibits base excision repair of a sub-set of DNA lesions. *Nucleic Acids Research*, *43*(8), 4028–4038. https://doi.org/10.1093/nar/gkv250

Ritchie, M. E., Phipson, B., Wu, D., Hu, Y., Law, C. W., Shi, W., & Smyth, G. K. (2015). Limma powers differential expression analyses for RNA-sequencing and microarray studies. *Nucleic Acids Research*, *43*(7), e47. https://doi.org/10.1093/nar/gkv007

Robeson, A. C., Lindblom, K. R., Wojton, J., Kornbluth, S., & Matsuura, K. (2018). Dimer-specific immunoprecipitation of active caspase-2 identifies TRAF proteins as novel

activators. *The EMBO Journal*, *37*(14), e97072. https://doi.org/10.15252/embj.201797072

Robinson, M. D., McCarthy, D. J., & Smyth, G. K. (2010). edgeR: A Bioconductor package for differential expression analysis of digital gene expression data. *Bioinformatics*, *26*(1), 139–140. https://doi.org/10.1093/bioinformatics/btp616

Robu, M., Shah, R. G., Petitclerc, N., Brind'Amour, J., Kandan-Kulangara, F., & Shah, G. M. (2013). Role of poly(ADP-ribose) polymerase-1 in the removal of UV-induced DNA lesions by nucleotide excision repair. *Proceedings of the National Academy of Sciences*, *110*(5), 1658–1663. https://doi.org/10.1073/pnas.1209507110

Rocha, C. R. R., Silva, M. M., Quinet, A., Cabral-Neto, J. B., & Menck, C. F. M. (2018). DNA repair pathways and cisplatin resistance: An intimate relationship. *Clinics*, *73*, e478s. https://doi.org/10.6061/clinics/2018/e478s

Rokhlin, O. W., Scheinker, V. S., Taghiyev, A. F., Bumcrot, D., Glover, R. A., & Cohen, M. B. (2008). MicroRNA-34 mediates AR-dependent p53-induced apoptosis in prostate cancer. *Cancer Biology & Therapy*, *7*(8), 1288–1296. https://doi.org/10.4161/cbt.7.8.6284

Roos, W. P., & Kaina, B. (2013). DNA damage-induced cell death: From specific DNA lesions to the DNA damage response and apoptosis. *Cancer Letters*, *332*(2), 237–248. https://doi.org/10.1016/j.canlet.2012.01.007

Roos, W. P., Thomas, A. D., & Kaina, B. (2016). DNA damage and the balance between survival and death in cancer biology. *Nature Reviews Cancer*, *16*(1), 20–33. https://doi.org/10.1038/nrc.2015.2

Rundle, S., Bradbury, A., Drew, Y., & Curtin, N. (2017). Targeting the ATR-CHK1 Axis in Cancer Therapy. *Cancers*, *9*(12), 41. https://doi.org/10.3390/cancers9050041

Safa, A. R. (2013). Roles of c-FLIP in Apoptosis, Necroptosis, and Autophagy. *Journal of Carcinogenesis & Mutagenesis*, *suppl. 6* (003). https://doi.org/10.4172/2157-2518.S6-003

Saito, S., Goodarzi, A. A., Higashimoto, Y., Noda, Y., Lees-Miller, S. P., Appella, E., & Anderson, C. W. (2002). ATM Mediates Phosphorylation at Multiple p53 Sites, Including Ser46, in Response to Ionizing Radiation. *Journal of Biological Chemistry*, *277*(15), 12491–12494. https://doi.org/10.1074/jbc.C200093200

Saleh, A. D., Savage, J. E., Cao, L., Soule, B. P., Ly, D., DeGraff, W., Harris, C. C., Mitchell, J. B., & Simone, N. L. (2011). Cellular Stress Induced Alterations in MicroRNA let-7a and let-7b Expression Are Dependent on p53. *PLoS ONE*, *6*(10), e24429. https://doi.org/10.1371/journal.pone.0024429

Sanphui, P., & Biswas, S. C. (2013). FoxO3a is activated and executes neuron death via Bim in response to β-amyloid. *Cell Death & Disease*, *4*(5), e625. https://doi.org/10.1038/cddis.2013.148

Santo, E. E., Stroeken, P., Sluis, P. V., Koster, J., Versteeg, R., & Westerhout, E. M. (2013). FOXO3a Is a Major Target of Inactivation by PI3K/AKT Signaling in Aggressive Neuroblastoma. *Cancer Research*, *73*(7), 2189–2198. https://doi.org/10.1158/0008-5472.CAN-12-3767

Saraste, A. (2000). Morphologic and biochemical hallmarks of apoptosis. *Cardiovascular Research*, *45*(3), 528–537. https://doi.org/10.1016/S0008-6363(99)00384-3

Scaffidi, C. (1998). Two CD95 (APO-1/Fas) signaling pathways. *The EMBO Journal*, *17*(6), 1675–1687. https://doi.org/10.1093/emboj/17.6.1675

Scharer, O. D. (2013). Nucleotide Excision Repair in Eukaryotes. *Cold Spring Harbor Perspectives in Biology*, *5*(10), a012609. https://doi.org/10.1101/cshperspect.a012609

Schilling, T., Schleithoff, E. S., Kairat, A., Melino, G., Stremmel, W., Oren, M., Krammer, P. H., & Müller, M. (2009). Active transcription of the human FAS/CD95/TNFRSF6 gene involves the p53 family. *Biochemical and Biophysical Research Communications*, *387*(2), 399–404. https://doi.org/10.1016/j.bbrc.2009.07.063

Schulze-Osthoff, K., Ferrari, D., Los, M., Wesselborg, S., & Peter, M. E. (1998). Apoptosis signaling by death receptors. *European Journal of Biochemistry*, *254*(3), 439–459. https://doi.org/10.1046/j.1432-1327.1998.2540439.x

Seo, Y. R., Fishel, M. L., Amundson, S., Kelley, M. R., & Smith, M. L. (2002). Implication of p53 in base excision DNA repair: In vivo evidence. *Oncogene*, *21*(5), 731–737. https://doi.org/10.1038/sj.onc.1205129

Shen, T., & Huang, S. (2012). The Role of Cdc25A in the Regulation of Cell Proliferation and Apoptosis. *Anti-Cancer Agents in Medicinal Chemistry*, *12*(6), 631–639. https://doi.org/10.2174/187152012800617678

Shi, X., Kachirskaia, I., Yamaguchi, H., West, L. E., Wen, H., Wang, E. W., Dutta, S., Appella, E., & Gozani, O. (2007). Modulation of p53 Function by SET8-Mediated Methylation at Lysine 382. *Molecular Cell*, *27*(4), 636–646. https://doi.org/10.1016/j.molcel.2007.07.012

Shieh, S.-Y., Ahn, J., Tamai, K., Taya, Y., & Prives, C. (2000). The human homologs of checkpoint kinases Chk1 and Cds1 (Chk2) phosphorylate p53 at multiple DNA damage-

inducible sites. *Genes & Development*, *14*(3), 289–300. https://doi.org/10.1101/gad.14.3.289

Shiotani, B., Nguyen, H. D., Håkansson, P., Maréchal, A., Tse, A., Tahara, H., & Zou, L. (2013). Two Distinct Modes of ATR Activation Orchestrated by Rad17 and Nbs1. *Cell Reports*, *3*(5), 1651–1662. https://doi.org/10.1016/j.celrep.2013.04.018

Shiotani, B., & Zou, L. (2009). Single-Stranded DNA Orchestrates an ATM-to-ATR Switch at DNA Breaks. *Molecular Cell*, *33*(5), 547–558. https://doi.org/10.1016/j.molcel.2009.01.024

Smeenk, L., van Heeringen, S. J., Koeppel, M., Gilbert, B., Janssen-Megens, E., Stunnenberg, H. G., & Lohrum, M. (2011). Role of p53 Serine 46 in p53 Target Gene Regulation. *PLoS ONE*, *6*(3), e17574. https://doi.org/10.1371/journal.pone.0017574

Soussi, T. (2010). The history of p53: A perfect example of the drawbacks of scientific paradigms. *EMBO Reports*, *11*(11), 822–826. https://doi.org/10.1038/embor.2010.159

Speidel, D., Helmbold, H., & Deppert, W. (2006). Dissection of transcriptional and non-transcriptional p53 activities in the response to genotoxic stress. *Oncogene*, *25*(6), 940–953. https://doi.org/10.1038/sj.onc.1209126

Spizzo, R., Nicoloso, M. S., Lupini, L., Lu, Y., Fogarty, J., Rossi, S., Zagatti, B., Fabbri, M., Veronese, A., Liu, X., Davuluri, R., Croce, C. M., Mills, G., Negrini, M., & Calin, G. A. (2010). MiR-145 participates with TP53 in a death-promoting regulatory loop and targets estrogen receptor-α in human breast cancer cells. *Cell Death & Differentiation*, *17*(2), 246–254. https://doi.org/10.1038/cdd.2009.117

Stiewe, T., & Pützer, B. M. (2000). Role of the p53-homologue p73 in E2F1-induced apoptosis. *Nature Genetics*, *26*(4), 464–469. https://doi.org/10.1038/82617

Stiff, T., O'Driscoll, M., Rief, N., Iwabuchi, K., Löbrich, M., & Jeggo, P. A. (2004). ATM and DNA-PK Function Redundantly to Phosphorylate H2AX after Exposure to Ionizing Radiation. *Cancer Research*, *64*(7), 2390–2396. https://doi.org/10.1158/0008-5472.CAN-03-3207

Strobel, H., Baisch, T., Fitzel, R., Schilberg, K., Siegelin, M. D., Karpel-Massler, G., Debatin, K.-M., & Westhoff, M.-A. (2019). Temozolomide and Other Alkylating Agents in Glioblastoma Therapy. *Biomedicines*, *7*(3), 69. https://doi.org/10.3390/biomedicines7030069

Su, C., Huang, D., Liu, J., Liu, W., & Cao, Y. (2019). MiR-27a-3p regulates proliferation and apoptosis of colon cancer cells by potentially targeting BTG1. *Oncology Letters*, *18*, 2825-2834. https://doi.org/10.3892/ol.2019.10629

Sullivan, K. D., Galbraith, M. D., Andrysik, Z., & Espinosa, J. M. (2018). Mechanisms of transcriptional regulation by p53. *Cell Death & Differentiation*, *25*(1), 133–143. https://doi.org/10.1038/cdd.2017.174

Surova, O., & Zhivotovsky, B. (2013). Various modes of cell death induced by DNA damage. *Oncogene*, *32*(33), 3789–3797. https://doi.org/10.1038/onc.2012.556

Suzuki, H. I., Yamagata, K., Sugimoto, K., Iwamoto, T., Kato, S., & Miyazono, K. (2009). Modulation of microRNA processing by p53. *Nature*, *460*(7254), 529–533. https://doi.org/10.1038/nature08199

Syed, A., & Tainer, J. A. (2018). The MRE11–RAD50–NBS1 Complex Conducts the Orchestration of Damage Signaling and Outcomes to Stress in DNA Replication and Repair. *Annual Review of Biochemistry*, *87*(1), 263–294. https://doi.org/10.1146/annurev-biochem-062917-012415

Taira, N., Nihira, K., Yamaguchi, T., Miki, Y., & Yoshida, K. (2007). DYRK2 Is Targeted to the Nucleus and Controls p53 via Ser46 Phosphorylation in the Apoptotic Response to DNA Damage. *Molecular Cell*, *25*(5), 725–738. https://doi.org/10.1016/j.molcel.2007.02.007

Tan, X., Tang, H., Bi, J., Li, N., & Jia, Y. (2018). MicroRNA-222-3p associated with *Helicobacter pylori* targets HIPK2 to promote cell proliferation, invasion, and inhibits apoptosis in gastric cancer. *Journal of Cellular Biochemistry*, *119*(7), 5153–5162. https://doi.org/10.1002/jcb.26542

Tang, Y., Zhao, W., Chen, Y., Zhao, Y., & Gu, W. (2008). Acetylation Is Indispensable for p53 Activation. *Cell*, *133*(4), 612–626. https://doi.org/10.1016/j.cell.2008.03.025

Tang, Y.-J., Wu, W., Chen, Q.-Q., Liu, S.-H., Zheng, Z.-Y., Cui, Z.-L., Xu, J.-P., Xue, Y., & Lin, D.-H. (2022). MiR-29b-3p suppresses the malignant biological behaviors of AML cells via inhibiting NF-κB and JAK/STAT signaling pathways by targeting HuR. *BMC Cancer*, *22*(1), 909. https://doi.org/10.1186/s12885-022-09996-1

Tarasov, V., Jung, P., Verdoodt, B., Lodygin, D., Epanchintsev, A., Menssen, A., Meister, G., & Hermeking, H. (2007). Differential Regulation of microRNAs by p53 Revealed by Massively Parallel Sequencing: MiR-34a is a p53 Target That Induces Apoptosis and G1-arrest. *Cell Cycle*, *6*(13), 1586–1593. https://doi.org/10.4161/cc.6.13.4436

Thornborrow, E. C., Patel, S., Mastropietro, A. E., Schwartzfarb, E. M., & Manfredi, J. J. (2002). A conserved intronic response element mediates direct p53-dependent transcriptional activation of both the human and murine bax genes. *Oncogene*, *21*(7), 990–999. https://doi.org/10.1038/sj.onc.1205069

Tibbetts, R. S., Brumbaugh, K. M., Williams, J. M., Sarkaria, J. N., Cliby, W. A., Shieh, S.-Y., Taya, Y., Prives, C., & Abraham, R. T. (1999). A role for ATR in the DNA damage-

induced phosphorylation of p53. *Genes & Development*, *13*(2), 152–157. https://doi.org/10.1101/gad.13.2.152

Tong, Z., Cui, Q., Wang, J., & Zhou, Y. (2019). TransmiR v2.0: An updated transcription factor-microRNA regulation database. *Nucleic Acids Research*, *47*(D1), D253–D258. https://doi.org/10.1093/nar/gky1023

Toyooka, T., Ishihama, M., & Ibuki, Y. (2011). Phosphorylation of Histone H2AX Is a Powerful Tool for Detecting Chemical Photogenotoxicity. *Journal of Investigative Dermatology*, *131*(6), 1313–1321. https://doi.org/10.1038/jid.2011.28

Trabucchi, M., Briata, P., Garcia-Mayoral, M., Haase, A. D., Filipowicz, W., Ramos, A., Gherzi, R., & Rosenfeld, M. G. (2009). The RNA-binding protein KSRP promotes the biogenesis of a subset of microRNAs. *Nature*, *459*(7249), 1010–1014. https://doi.org/10.1038/nature08025

Trenner, A., & Sartori, A. A. (2019). Harnessing DNA Double-Strand Break Repair for Cancer Treatment. *Frontiers in Oncology*, *9*, 1388. https://doi.org/10.3389/fonc.2019.01388

Tsuchiya, N., Izumiya, M., Ogata-Kawata, H., Okamoto, K., Fujiwara, Y., Nakai, M., Okabe, A., Schetter, A. J., Bowman, E. D., Midorikawa, Y., Sugiyama, Y., Aburatani, H., Harris, C. C., & Nakagama, H. (2011). Tumor Suppressor *miR-22* Determines p53-Dependent Cellular Fate through Post-transcriptional Regulation of p21. *Cancer Research*, *71*(13), 4628–4639. https://doi.org/10.1158/0008-5472.CAN-10-2475

Tsuda, M., Ogawa, S., Ooka, M., Kobayashi, K., Hirota, K., Wakasugi, M., Matsunaga, T., Sakuma, T., Yamamoto, T., Chikuma, S., Sasanuma, H., Debatisse, M., Doherty, A. J., Fuchs, R. P., & Takeda, S. (2019). PDIP38/PolDIP2 controls the DNA damage tolerance pathways by increasing the relative usage of translesion DNA synthesis over template switching. *PLoS ONE*, *14*(3), e0213383. https://doi.org/10.1371/journal.pone.0213383

Tsui, K.-H., Chiang, K.-C., Lin, Y.-H., Chang, K.-S., Feng, T.-H., & Juang, H.-H. (2018). BTG2 is a tumor suppressor gene upregulated by p53 and PTEN in human bladder carcinoma cells. *Cancer Medicine*, *7*(1), 184–195. https://doi.org/10.1002/cam4.1263

Tu, R., Kang, W., Yang, X., Zhang, Q., Xie, X., Liu, W., Zhang, J., Zhang, X.-D., Wang, H., & Du, R.-L. (2018). USP49 participates in the DNA damage response by forming a positive feedback loop with p53. *Cell Death & Disease*, *9*(5), 553. https://doi.org/10.1038/s41419-018-0475-3

Tubbs, A., & Nussenzweig, A. (2017). Endogenous DNA Damage as a Source of Genomic Instability in Cancer. *Cell*, *168*(4), 644–656. https://doi.org/10.1016/j.cell.2017.01.002

Valledor, A. F., Hsu, L.-C., Ogawa, S., Sawka-Verhelle, D., Karin, M., & Glass, C. K. (2004). Activation of liver X receptors and retinoid X receptors prevents bacterial-induced macrophage apoptosis. *Proceedings of the National Academy of Sciences*, *101*(51), 17813–17818. https://doi.org/10.1073/pnas.0407749101

Van Jaarsveld, M. T. M., Deng, D., Ordoñez-Rueda, D., Paulsen, M., Wiemer, E. A. C., & Zi, Z. (2020). Cell-type-specific role of CHK2 in mediating DNA damage-induced G2 cell cycle arrest. *Oncogenesis*, *9*(3), 35. https://doi.org/10.1038/s41389-020-0219-y

Vasudevan, S. (2012). Posttranscriptional Upregulation by MicroRNAs: Posttranscriptional Upregulation by MicroRNAs. *Wiley Interdisciplinary Reviews: RNA*, *3*(3), 311–330. https://doi.org/10.1002/wrna.121

Vermeulen, K., Van Bockstaele, D. R., & Berneman, Z. N. (2003). The cell cycle: A review of regulation, deregulation and therapeutic targets in cancer: *Cell cycle regulation and deregulation*. *Cell Proliferation*, *36*(3), 131–149. https://doi.org/10.1046/j.1365-2184.2003.00266.x

Vigneswara, V., & Ahmed, Z. (2020). The Role of Caspase-2 in Regulating Cell Fate. *Cells*, *9*(5), 1259. https://doi.org/10.3390/cells9051259

Vindigni, A., & Gonzalo, S. (2013). The Two Faces of DNA Repair: Disease and Therapy. *Science of Medicine*, *110*(4), 314-319.

Visconti, R., Della Monica, R., & Grieco, D. (2016). Cell cycle checkpoint in cancer: A therapeutically targetable double-edged sword. *Journal of Experimental & Clinical Cancer Research*, *35*(1), 153. https://doi.org/10.1186/s13046-016-0433-9

Visser, H., & Thomas, A. D. (2021). MicroRNAs and the DNA damage response: How is cell fate determined? *DNA Repair*, *108*, 103245. https://doi.org/10.1016/j.dnarep.2021.103245

Wajant, H., Pfizenmaier, K., & Scheurich, P. (2003). Tumor necrosis factor signaling. *Cell Death & Differentiation*, *10*(1), 45–65. https://doi.org/10.1038/sj.cdd.4401189

Walker, J. C., & Harland, R. M. (2009). MicroRNA-24a is required to repress apoptosis in the developing neural retina. *Genes & Development*, *23*(9), 1046–1051. https://doi.org/10.1101/gad.1777709

Wang, D., Hou, Q., Zhao, L., Gao, J., Xiao, Y., & Wang, A. (2019). Programmed cell death factor 4 enhances the chemosensitivity of colorectal cancer cells to Taxol. *Oncology Letters*, *18*, 1402-1408. https://doi.org/10.3892/ol.2019.10398

Wang, H.-Q., Yu, X.-D., Liu, Z.-H., Cheng, X., Samartzis, D., Jia, L.-T., Wu, S.-X., Huang, J., Chen, J., & Luo, Z.-J. (2011). Deregulated miR-155 promotes Fas-mediated apoptosis in human intervertebral disc degeneration by targeting FADD and caspase-3. *The Journal of Pathology*, *225*(2), 232–242. https://doi.org/10.1002/path.2931

Wang, J., He, J., Su, F., Ding, N., Hu, W., Yao, B., Wang, W., & Zhou, G. (2013). Repression of ATR pathway by miR-185 enhances radiation-induced apoptosis and proliferation inhibition. *Cell Death & Disease*, *4*(6), e699. https://doi.org/10.1038/cddis.2013.227

Wang, J., Jia, Z., Zhang, C., Sun, M., Wang, W., Chen, P., Ma, K., Zhang, Y., Li, X., & Zhou, C. (2014b). MiR-499 protects cardiomyocytes from H_2O_2-induced apoptosis via its effects on *Pdcd4* and *Pacs2*. *RNA Biology*, *11*(4), 339–350. https://doi.org/10.4161/rna.28300

Wang, J., Lu, M., Qiu, C., & Cui, Q. (2010). TransmiR: A transcription factor–microRNA regulation database. *Nucleic Acids Research*, *38*(suppl. 1), D119–D122. https://doi.org/10.1093/nar/gkp803

Wang, Q., Goldstein, M., Alexander, P., Wakeman, T. P., Sun, T., Feng, J., Lou, Z., Kastan, M. B., & Wang, X.-F. (2014a). Rad17 recruits the MRE11-RAD50-NBS1 complex to regulate the cellular response to DNA double-strand breaks. *The EMBO Journal*, *33*(8), 862–877. https://doi.org/10.1002/embj.201386064

Wang, Q., Yang, X., Zhou, X., Wu, B., Zhu, D., Jia, W., Chu, J., Wang, J., Wu, J., & Kong, L. (2020). MiR-3174 promotes proliferation and inhibits apoptosis by targeting FOXO1 in hepatocellular carcinoma. *Biochemical and Biophysical Research Communications*, *526*(4), 889–897. https://doi.org/10.1016/j.bbrc.2020.03.152

Wang, S., & El-Deiry, W. S. (2003). TRAIL and apoptosis induction by TNF-family death receptors. *Oncogene*, *22*(53), 8628–8633. https://doi.org/10.1038/sj.onc.1207232

Wang, X. Q., Redpath, J. L., Fan, S. T., & Stanbridge, E. J. (2006). ATR dependent activation of Chk2. *Journal of Cellular Physiology*, *208*(3), 613–619. https://doi.org/10.1002/jcp.20700

Wang, X., Zhenchuk, A., Wiman, K. G., & Albertioni, F. (2009). Regulation of p53R2 and its role as potential target for cancer therapy. *Cancer Letters*, *276*(1), 1–7. https://doi.org/10.1016/j.canlet.2008.07.019

Wang, Y., Sun, J., Wei, X., Luan, L., Zeng, X., Wang, C., & Zhao, W. (2017). Decrease of miR-622 expression suppresses migration and invasion by targeting regulation of DYRK2 in colorectal cancer cells. *OncoTargets and Therapy*, *10*, 1091–1100. https://doi.org/10.2147/OTT.S125724

Wang, Y., & Taniguchi, T. (2013). MicroRNAs and DNA damage response: Implications for cancer therapy. *Cell Cycle*, *12*(1), 32–42. https://doi.org/10.4161/cc.23051

Ward, I. M., Minn, K., van Deursen, J., & Chen, J. (2003). P53 Binding Protein 53BP1 Is Required for DNA Damage Responses and Tumor Suppression in Mice. *Molecular and Cellular Biology*, *23*(7), 2556–2563. https://doi.org/10.1128/MCB.23.7.2556-2563.2003

Wee, P., & Wang, Z. (2017). Epidermal Growth Factor Receptor Cell Proliferation Signaling Pathways. *Cancers*, *9*(5), 52. https://doi.org/10.3390/cancers9050052

Wei, D., Yu, G., & Zhao, Y. (2019). MicroRNA-30a-3p inhibits the progression of lung cancer via the PI3K/AKT by targeting DNA methyltransferase 3a. *OncoTargets and Therapy*, *12*, 7015–7024. https://doi.org/10.2147/OTT.S213583

Wesolowski, J. R., Rajdev, P., & Mukherji, S. K. (2010). Temozolomide (Temodar). *American Journal of Neuroradiology*, *31*(8), 1383–1384. https://doi.org/10.3174/ajnr.A2170

Williams, A. B., & Schumacher, B. (2016). P53 in the DNA-Damage-Repair Process. *Cold Spring Harbor Perspectives in Medicine*, *6*(5), a026070. https://doi.org/10.1101/cshperspect.a026070

Wilsker, D., Petermann, E., Helleday, T., & Bunz, F. (2008). Essential function of Chk1 can be uncoupled from DNA damage checkpoint and replication control. *Proceedings of the National Academy of Sciences*, *105*(52), 20752–20757. https://doi.org/10.1073/pnas.0806917106

Wilson, R., Espinosa-Diez, C., Kanner, N., Chatterjee, N., Ruhl, R., Hipfinger, C., Advani, S. J., Li, J., Khan, O. F., Franovic, A., Weis, S. M., Kumar, S., Coussens, L. M., Anderson, D. G., Chen, C. C., Cheresh, D. A., & Anand, S. (2016). MicroRNA regulation of endothelial TREX1 reprograms the tumour microenvironment. *Nature Communications*, *7*(1), 13597. https://doi.org/10.1038/ncomms13597

Winter, M., Sombroek, D., Dauth, I., Moehlenbrink, J., Scheuermann, K., Crone, J., & Hofmann, T. G. (2008). Control of HIPK2 stability by ubiquitin ligase Siah-1 and checkpoint kinases ATM and ATR. *Nature Cell Biology*, *10*(7), 812–824. https://doi.org/10.1038/ncb1743

Wyatt, M. D., & Pittman, D. L. (2006). Methylating Agents and DNA Repair Responses: Methylated Bases and Sources of Strand Breaks. *Chemical Research in Toxicology*, *19*(12), 1580–1594. https://doi.org/10.1021/tx060164e

Xia, X. Y., Yu, Y. J., Ye, F., Peng, G. Y., Li, Y. J., & Zhou, X. M. (2020). MicroRNA-506-3p inhibits proliferation and promotes apoptosis in ovarian cancer cell via targeting SIRT1/AKT/FOXO3a signaling pathway. *Neoplasma*, *67*(02), 344–353. https://doi.org/10.4149/neo_2020_190517N441

Xiao, J., Lin, H., Luo, X., Luo, X., & Wang, Z. (2011). miR-605 joins p53 network to form a p53: MiR-605 :Mdm2 positive feedback loop in response to stress: miR-605 in the p53 gene network. *The EMBO Journal*, *30*(3), 524–532. https://doi.org/10.1038/emboj.2010.347

Xiao, M., Li, J., Li, W., Wang, Y., Wu, F., Xi, Y., Zhang, L., Ding, C., Luo, H., Li, Y., Peng, L., Zhao, L., Peng, S., Xiao, Y., Dong, S., Cao, J., & Yu, W. (2017). MicroRNAs activate gene transcription epigenetically as an enhancer trigger. *RNA Biology*, *14*(10), 1326–1334. https://doi.org/10.1080/15476286.2015.1112487

Xie, Q.-H., He, X.-X., Chang, Y., Sun, S., Jiang, X., Li, P.-Y., & Lin, J.-S. (2011). MiR-192 inhibits nucleotide excision repair by targeting ERCC3 and ERCC4 in HepG2.2.15 cells. *Biochemical and Biophysical Research Communications*, *410*(3), 440–445. https://doi.org/10.1016/j.bbrc.2011.05.153

Xie, Y., Wei, R.-R., Huang, G.-L., Zhang, M.-Y., Yuan, Y.-F., & Wang, H.-Y. (2014). Checkpoint kinase 1 is negatively regulated by miR-497 in hepatocellular carcinoma. *Medical Oncology*, *31*(3), 844. https://doi.org/10.1007/s12032-014-0844-4

Xin, Y., Zhang, H.-B., Tang, T.-Y., Liu, G.-H., Wang, J.-S., Jiang, G., & Zhang, L.-Z. (2014). Low-dose radiation-induced apoptosis in human leukemia K562 cells through mitochondrial pathways. *Molecular Medicine Reports*, *10*(3), 1569–1575. https://doi.org/10.3892/mmr.2014.2381

Xu, P., Li, X., Liang, Y., Bao, Z., Zhang, F., Gu, L., Kosari, S., & Liu, W. (2022). PmiRtarbase: A positive miRNA-target regulations database. *Computational Biology and Chemistry*, *98*, 107690. https://doi.org/10.1016/j.compbiolchem.2022.107690

Xu, R., Garcia-Barros, M., Wen, S., Li, F., Lin, C.-L., Hannun, Y. A., Obeid, L. M., & Mao, C. (2017). Tumor suppressor p53 links ceramide metabolism to DNA damage response through alkaline ceramidase 2. *Cell Death & Differentiation*. https://doi.org/10.1038/s41418-017-0018-y

Xu, S., Huang, H., Chen, Y., Deng, Y., Zhang, B., Xiong, X., Yuan, Y., Zhu, Y., Huang, H., Xie, L., & Liu, X. (2016). DNA damage responsive miR-33b-3p promoted lung cancer

cells survival and cisplatin resistance by targeting p21$^{WAF1/CIP1}$. *Cell Cycle*, *15*(21), 2920–2930. https://doi.org/10.1080/15384101.2016.1224043

Yan, F., Liu, H., Hao, J., & Liu, Z. (2012). Dynamical Behaviors of Rb-E2F Pathway Including Negative Feedback Loops Involving miR449. *PLoS ONE*, *7*(9), e43908. https://doi.org/10.1371/journal.pone.0043908

Yan, H., Xue, G., Mei, Q., Wang, Y., Ding, F., Liu, M.-F., Lu, M.-H., Tang, Y., Yu, H., & Sun, S. (2009). Repression of the miR-17-92 cluster by p53 has an important function in hypoxia-induced apoptosis. *The EMBO Journal*, *28*(18), 2719–2732. https://doi.org/10.1038/emboj.2009.214

Yang, F., Kemp, C. J., & Henikoff, S. (2015). Anthracyclines induce double-strand DNA breaks at active gene promoters. *Mutation Research*, *773*, 9–15. https://doi.org/10.1016/j.mrfmmm.2015.01.007

Yang, H., Yan, B., Liao, D., Huang, S., & Qiu, Y. (2015). Acetylation of HDAC1 and degradation of SIRT1 form a positive feedback loop to regulate p53 acetylation during heat-shock stress. *Cell Death & Disease*, *6*(5), e1747. https://doi.org/10.1038/cddis.2015.106

Yang, L., Zhao, W., Wei, P., Zuo, W., & Zhu, S. (2017). Tumor suppressor p53 induces miR-15a processing to inhibit neuronal apoptosis inhibitory protein (NAIP) in the apoptotic response DNA damage in breast cancer cell. *American Journal of Translational Research*, *9*(2), 683-691.

Yang, Y., Yang, Z., Zhang, R., Jia, C., Mao, R., Mahati, S., Zhang, Y., Wu, G., Sun, Y. na, Jia, X. yan, Aimudula, A., Zhang, H., & Bao, Y. (2021). MiR-27a-3p enhances the cisplatin sensitivity in hepatocellular carcinoma cells through inhibiting PI3K/Akt

pathway. *Bioscience Reports*, *41*(12), BSR20192007. https://doi.org/10.1042/BSR20192007

Yao, L., Zhu, Z., Wu, J., Zhang, Y., Zhang, H., Sun, X., Qian, C., Wang, B., Xie, L., Zhang, S., & Lu, A. G. (2019). MicroRNA-124 regulates the expression of p62/p38 and promotes autophagy in the inflammatory pathogenesis of Parkinson's disease. *The FASEB Journal*, *33*(7), 8648–8665. https://doi.org/10.1096/fj.201900363R

Ye, W., Xue, J., Zhang, Q., Li, F., Zhang, W., Chen, H., Huang, Y., & Zheng, F. (2014). MiR-449a functions as a tumor suppressor in endometrial cancer by targeting CDC25A. *Oncology Reports*, *32*(3), 1193–1199. https://doi.org/10.3892/or.2014.3303

Yin, X., Ge, J., Ge, X., Gao, J., Su, X., Wang, X., Zhang, Q., & Wang, Z. (2021). MiR-363-5p modulates regulatory T cells through STAT4-HSPB1-Notch1 axis and is associated with the immunological abnormality in Graves' disease. *Journal of Cellular and Molecular Medicine*, *25*(19), 9364–9377. https://doi.org/10.1111/jcmm.16876

York, S. J., & Modrich, P. (2006). Mismatch Repair-dependent Iterative Excision at Irreparable O6-Methylguanine Lesions in Human Nuclear Extracts. *Journal of Biological Chemistry*, *281*(32), 22674–22683. https://doi.org/10.1074/jbc.M603667200

Yoshioka, K., Yoshioka, Y., & Hsieh, P. (2006). ATR Kinase Activation Mediated by MutSα and MutLα in Response to Cytotoxic O6-Methylguanine Adducts. *Molecular Cell*, *22*(4), 501–510. https://doi.org/10.1016/j.molcel.2006.04.023

Yu, N., Huangyang, P., Yang, X., Han, X., Yan, R., Jia, H., Shang, Y., & Sun, L. (2013). MicroRNA-7 Suppresses the Invasive Potential of Breast Cancer Cells and Sensitizes Cells to DNA Damages by Targeting Histone Methyltransferase SET8. *Journal of Biological Chemistry*, *288*(27), 19633–19642. https://doi.org/10.1074/jbc.M113.475657

Yu, S., Zeng, Y., & Sun, X. (2018). Neuroprotective effects of p53/microRNA-22 regulate inflammation and apoptosis in subarachnoid hemorrhage. *International Journal of Molecular Medicine*, *41*, 2406-2412. https://doi.org/10.3892/ijmm.2018.3392

Yuan, L.-Q., Zhang, T., Xu, L., Han, H., & Liu, S.-H. (2021). MiR-30c-5p inhibits glioma proliferation and invasion via targeting Bcl2. *Translational Cancer Research*, *10*(1), 337–348. https://doi.org/10.21037/tcr-19-2957

Yun, T., Yu, K., Yang, S., Cui, Y., Wang, Z., Ren, H., Chen, S., Li, L., Liu, X., Fang, M., & Jiang, X. (2016). Acetylation of p53 Protein at Lysine 120 Up-regulates Apaf-1 Protein and Sensitizes the Mitochondrial Apoptotic Pathway. *Journal of Biological Chemistry*, *291*(14), 7386–7395. https://doi.org/10.1074/jbc.M115.706341

Zaman, M. S., Chen, Y., Deng, G., Shahryari, V., Suh, S. O., Saini, S., Majid, S., Liu, J., Khatri, G., Tanaka, Y., & Dahiya, R. (2010). The functional significance of microRNA-145 in prostate cancer. *British Journal of Cancer*, *103*(2), 256–264. https://doi.org/10.1038/sj.bjc.6605742

Zang, Y.-S., Zhong, Y.-F., Fang, Z., Li, B., & An, J. (2012). MiR-155 inhibits the sensitivity of lung cancer cells to cisplatin via negative regulation of Apaf-1 expression. *Cancer Gene Therapy*, *19*(11), 773–778. https://doi.org/10.1038/cgt.2012.60

Zannini, L., Delia, D., & Buscemi, G. (2014). CHK2 kinase in the DNA damage response and beyond. *Journal of Molecular Cell Biology*, *6*(6), 442–457. https://doi.org/10.1093/jmcb/mju045

Zeman, M. K., & Cimprich, K. A. (2014). Causes and consequences of replication stress. *Nature Cell Biology*, *16*(1), 2–9. https://doi.org/10.1038/ncb2897

Zhan, X.-H., Xu, Q.-Y., Tian, R., Yan, H., Zhang, M., Wu, J., Wang, W., & He, J. (2017). MicroRNA16 regulates glioma cell proliferation, apoptosis and invasion by targeting Wip1-ATM-p53 feedback loop. *Oncotarget*, *8*(33), 54788–54798. https://doi.org/10.18632/oncotarget.18510

Zhang, Z. Y., Fu, S. L., Xu, S. Q., Zhou, X., Liu, X. S., Xu, Y. J., Zhao, J. P., & Wei, S. (2014a). By downregulating Ku80, hsa-miR-526b suppresses non-small cell lung cancer. *Oncotarget*, *6*(3), 1462-1477. https://doi.org/10.18632/oncotarget.2808

Zhang, B., Shetti, D., Fan, C., & Wei, K. (2019). MiR-29b-3p promotes progression of MDA-MB-231 triple-negative breast cancer cells through downregulating TRAF3. *Biological Research*, *52*(1), 38. https://doi.org/10.1186/s40659-019-0245-4

Zhang, J., Ma, Y., Zhang, Y., Niu, S., Chu, M., & Zhang, Z. (2021). Angiogenesis is Inhibited by Arsenic Trioxide Through Downregulation of the CircHIPK3/miR-149-5p/FOXO1/VEGF Functional Module in Rheumatoid Arthritis. *Frontiers in Pharmacology*, *12*, 751667. https://doi.org/10.3389/fphar.2021.751667

Zhang, J., Stevens, M. F. G., & Bradshaw, T. D. (2012). Temozolomide: Mechanisms of Action, Repair and Resistance. *Current Molecular Pharmacology*, *5*, 102-114.

Zhang, J., Willers, H., Feng, Z., Ghosh, J. C., Kim, S., Weaver, D. T., Chung, J. H., Powell, S. N., & Xia, F. (2004). Chk2 Phosphorylation of BRCA1 Regulates DNA Double-Strand Break Repair. *Molecular and Cellular Biology*, *24*(2), 708–718. https://doi.org/10.1128/MCB.24.2.708-718.2004

Zhang, M., Liu, J., Li, M., Zhang, S., Lu, Y., Liang, Y., Zhao, K., & Li, Y. (2018). Insulin-like growth factor 1/insulin-like growth factor 1 receptor signaling protects against cell apoptosis through the PI3K/AKT pathway in glioblastoma cells. *Experimental and Therapeutic Medicine*, *16*, 1477-1482. https://doi.org/10.3892/etm.2018.6336

Zhang, Q., Wu, X., & Yang, J. (2021). MiR-194-5p protects against myocardial ischemia/reperfusion injury via MAPK1/PTEN/AKT pathway. *Annals of Translational Medicine*, *9*(8), 654–654. https://doi.org/10.21037/atm-21-807

Zhang, X., Wan, G., Berger, F. G., He, X., & Lu, X. (2011). The ATM Kinase Induces MicroRNA Biogenesis in the DNA Damage Response. *Molecular Cell*, *41*(4), 371–383. https://doi.org/10.1016/j.molcel.2011.01.020

Zhang, X.-P., Liu, F., & Wang, W. (2011). Two-phase dynamics of p53 in the DNA damage response. *Proceedings of the National Academy of Sciences*, *108*(22), 8990–8995. https://doi.org/10.1073/pnas.1100600108

Zhang, Y., & Hunter, T. (2014). Roles of Chk1 in cell biology and cancer therapy. *International Journal of Cancer*, *134*(5), 1013–1023. https://doi.org/10.1002/ijc.28226

Zhang, Z., Lei, B., Wu, H., Zhang, X., & Zheng, N. (2017). Tumor suppressive role of miR-194-5p in glioblastoma multiforme. *Molecular Medicine Reports*, *16*(6), 9317–9322. https://doi.org/10.3892/mmr.2017.7826

Zhang, Z.-C., Li, Y.-Y., Wang, H.-Y., Fu, S., Wang, X.-P., Zeng, M.-S., Zeng, Y.-X., & Shao, J.-Y. (2014b). Knockdown of miR-214 Promotes Apoptosis and Inhibits Cell Proliferation in Nasopharyngeal Carcinoma. *PLoS ONE*, *9*(1), e86149. https://doi.org/10.1371/journal.pone.0086149

Zheng, J. H., Grace, C. R., Guibao, C. D., McNamara, D. E., Llambi, F., Wang, Y.-M., Chen, T., & Moldoveanu, T. (2018). Intrinsic Instability of BOK Enables Membrane Permeabilization in Apoptosis. *Cell Reports*, *23*(7), 2083-2094. https://doi.org/10.1016/j.celrep.2018.04.060

Zhou, Q., & Gallo, J. M. (2009). Differential effect of sunitinib on the distribution of temozolomide in an orthotopic glioma model. *Neuro-Oncology*, *11*(3), 301–310. https://doi.org/10.1215/15228517-2008-088

Zhou, Y., Zhao, Z., Yan, L., & Yang, J. (2021). MiR-485-3p promotes proliferation of osteoarthritis chondrocytes and inhibits apoptosis via Notch2 and the NF-κB pathway. *Immunopharmacology and Immunotoxicology*, *43*(3), 370–379. https://doi.org/10.1080/08923973.2021.1918150

Zhu, J., Dou, Z., Sammons, M. A., Levine, A. J., & Berger, S. L. (2016). Lysine methylation represses p53 activity in teratocarcinoma cancer cells. *Proceedings of the National Academy of Sciences*, *113*(35), 9822–9827. https://doi.org/10.1073/pnas.1610387113

Zou, L., & Elledge, S. J. (2003). Sensing DNA Damage Through ATRIP Recognition of RPA-ssDNA Complexes. *Science*, *300*(5625), 1542–1548. https://doi.org/10.1126/science.1083430

Zou, Y.-F., Liao, W.-T., Fu, Z.-J., Zhao, Q., Chen, Y.-X., & Zhang, W. (2017). MicroRNA-30c-5p ameliorates hypoxia-reoxygenation-induced tubular epithelial cell injury via HIF1α stabilization by targeting SOCS3. *Oncotarget*, *8*(54), 92801–92814. https://doi.org/10.18632/oncotarget.21582

Appendix A

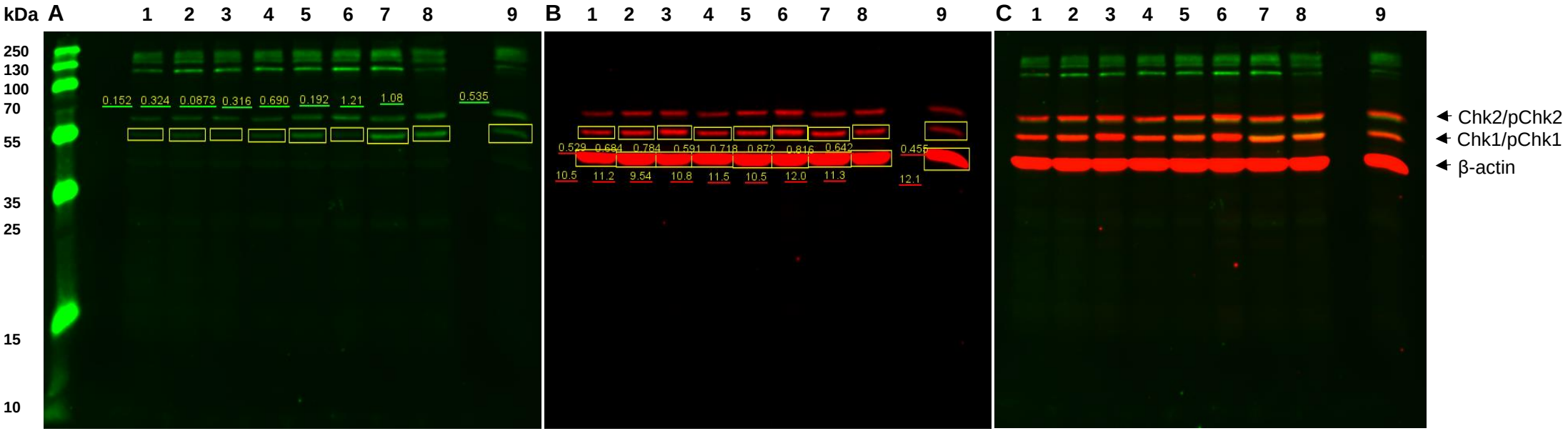

Figure 35. Illustration of protein normalisation and quantification.

All images are from the same immunoblot at different wavelengths to identify overlapping total and phospho-proteins, bound to respective fluorescently labelled secondary antibodies. For demonstration purposes, only Chk1/pChk1, and β-actin (loading control) is highlighted (boxed bands) to illustrate how protein expression was quantified. **A**: pChk1 (ser345). **B**: Chk1 and β-actin. **C**: Merged image of pChk1 (ser345), Chk1, and β-actin. Lanes 1 - 3 represent DMSO-treated samples 4 h, 18 h, and 36 h post-exposure; 4 - 6 represents 30TMZ-treated samples 4 h, 18 h, and 36 h post-exposure; 7 - 9 represents 900TMZ-treated samples 4 h, 18 h, and 36 h post-exposure. Using Image Studio™ Lite software, protein bands were selected and fluorescent signal intensity measured (automatically correcting for background signal based on a pre-determined margin above and below each band). Protein expression was normalised against β-actin by dividing the band from each sample by a lane normalisation factor, calculated by dividing the β-actin signal for each sample by the highest β-actin signal. For example, all β-actin signals will be divided by the β-actin signal of lane 9 (**B**) (12.1), as this is the highest. This produces proportions which is then used

to normalise Chk1/pChk1 levels for respective samples. For example, the normalised Chk1 (**B**) and pChk1 (**A**) signals for lane 1 is; 0.61 (0.529/(10.5/12.1)) and 0.18 (0.152/(10.5/12.1)) respectively. Subsequently, the level of pChk1 was normalised against Chk1 by dividing the pChk1 signal by that of Chk1 (i.e., 0.18/0.61), indicating that the normalised pChk1 signal is 0.3.

Appendix B

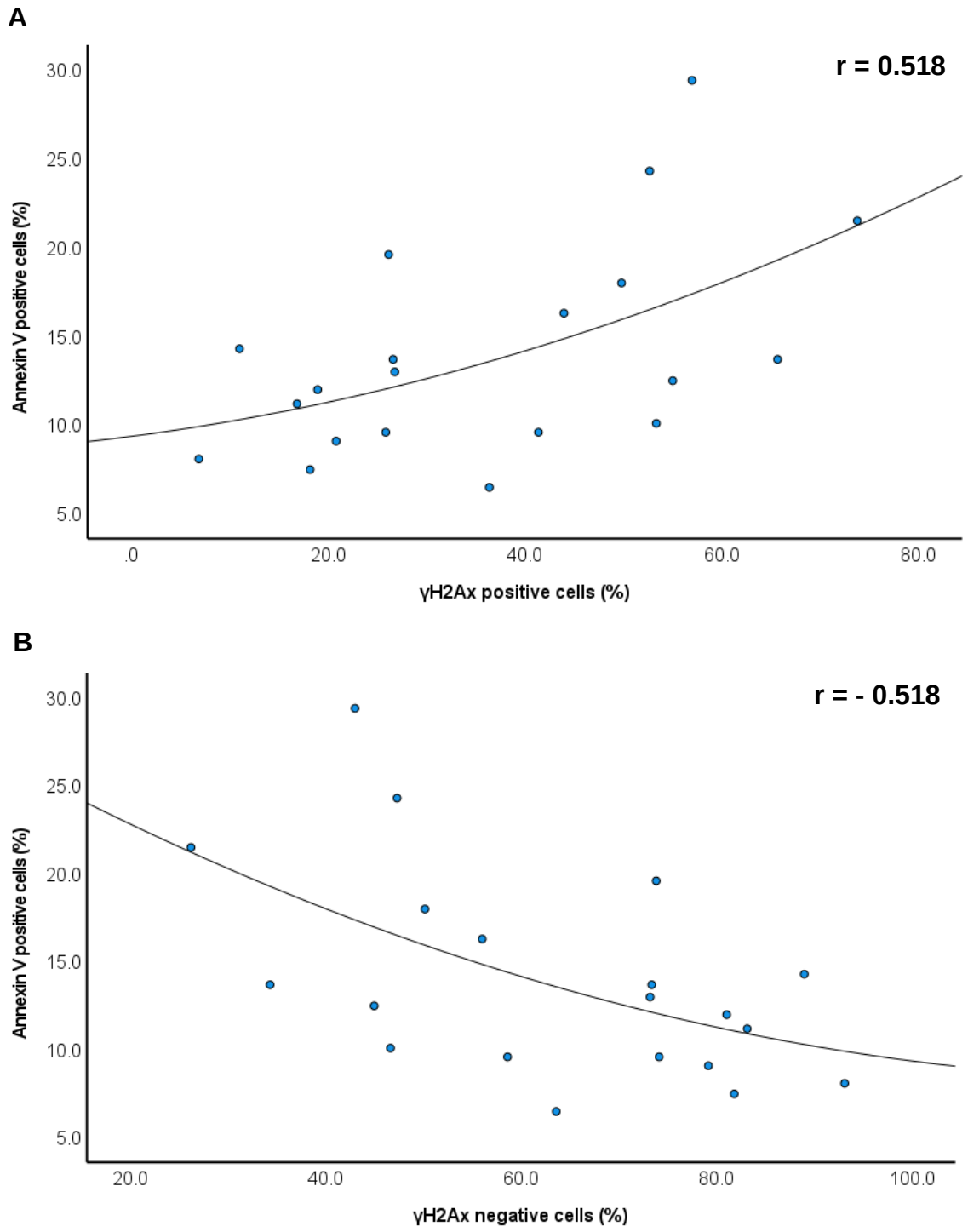

Figure 36. Correlation between γH2Ax and apoptosis.

TK6 cells were treated with DMSO and a range of TMZ doses for 1 h. Samples were collected 24 h post-exposure, probed with Annexin V-FITC and analysed with flow cytometry. Spearman correlation demonstrates a significant non-linear positive association between γH2Ax positive cells and percentage annexin V positive cells (**A**), whereas the reverse is true for γH2Ax negative cells (**B**). Data represents individual

samples of three (**n = 3**) biological repeats, except for 30TMZ (γH2Ax foci) where only two biological repeats were available.

Appendix C

Table 10. Quality assessment of small RNAseq RNA samples

Sample ID	GENEWIZ ID	Sample Type	Sample Vol.(ul)	Nanodrop 2000				DNA Qubit		RNA Qubit		TapeStation			QC Note
				Actual Nucleic Acid Conc. (ng/ul)	Total Amount (ng)	A260/A280	A260/A230	Actual Nucleic Acid Conc. (ng/ul)	Total Amount (ng)	Actual Nucleic Acid Conc. (ng/ul)	Total Amount (ng)	Average Size for DNA	RIN for RNA	DV 200 (for RNA)	
PRE	SCG9385	Total RNA	47	NA	NA	NA	NA	NA	NA	548.00	25756.00	NA	10.0	89.77	
DMSO-4H	SCG9386	Total RNA	47	NA	NA	NA	NA	NA	NA	520.00	24440.00	NA	10.0	86.67	
DMSO-18H	SCG9387	Total RNA	47	NA	NA	NA	NA	NA	NA	708.00	33276.00	NA	10.0	91.91	
DMSO-36H	SCG9388	Total RNA	47	NA	NA	NA	NA	NA	NA	642.00	30174.00	NA	9.5	81.26	
30TMZ-4H	SCG9389	Total RNA	47	NA	NA	NA	NA	NA	NA	568.00	26696.00	NA	10.0	89.27	
30TMZ-18H	SCG9390	Total RNA	47	NA	NA	NA	NA	NA	NA	844.00	39668.00	NA	10.0	92.43	
30TMZ-36H	SCG9391	Total RNA	47	NA	NA	NA	NA	NA	NA	1020.00	47940.00	NA	9.8	90.48	
900TMZ-4H	SCG9392	Total RNA	47	NA	NA	NA	NA	NA	NA	484.00	22748.00	NA	9.8	87.72	
900TMZ-18H	SCG9393	Total RNA	47	NA	NA	NA	NA	NA	NA	808.00	37976.00	NA	10.0	90.85	
900TMZ-36H	SCG9394	Total RNA	47	NA	NA	NA	NA	NA	NA	1060.00	49820.00	NA	9.7	90.10	

QC Note Legend for RNA

1	2	3	4
Not enough starting material	RIN<6	DV200<70	DNA Spot Check >10%

Appendix D

A

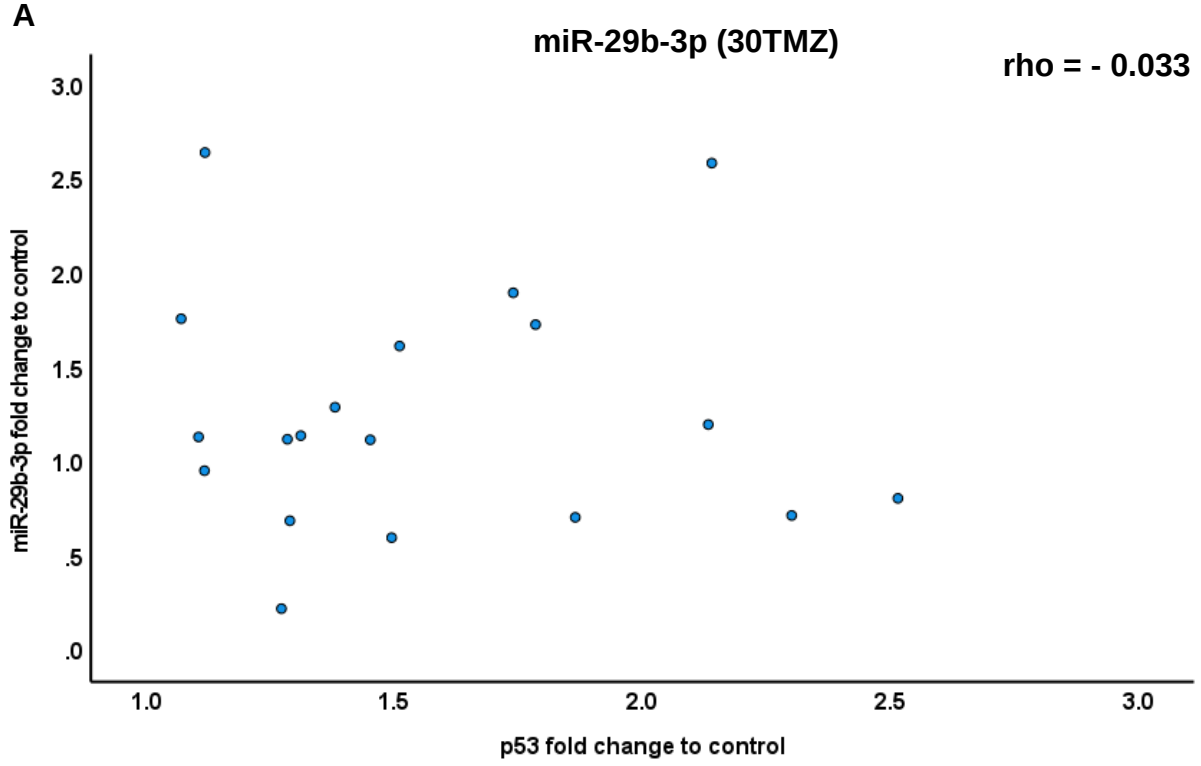

B

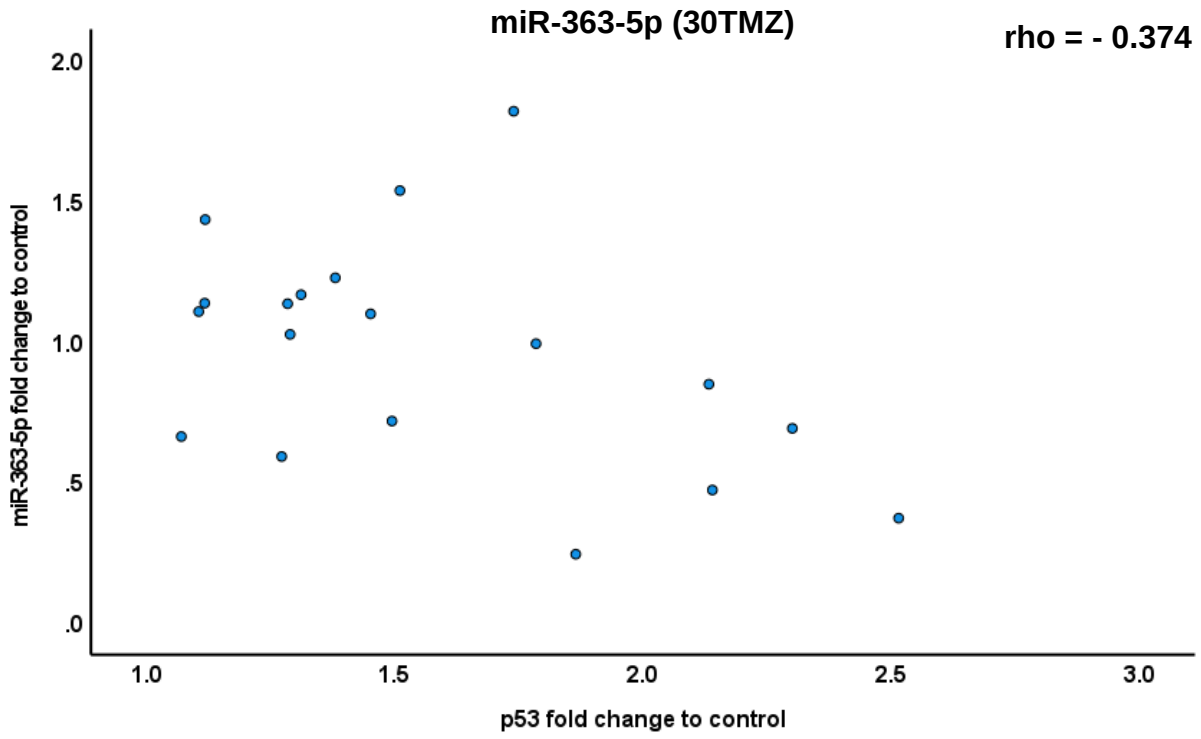

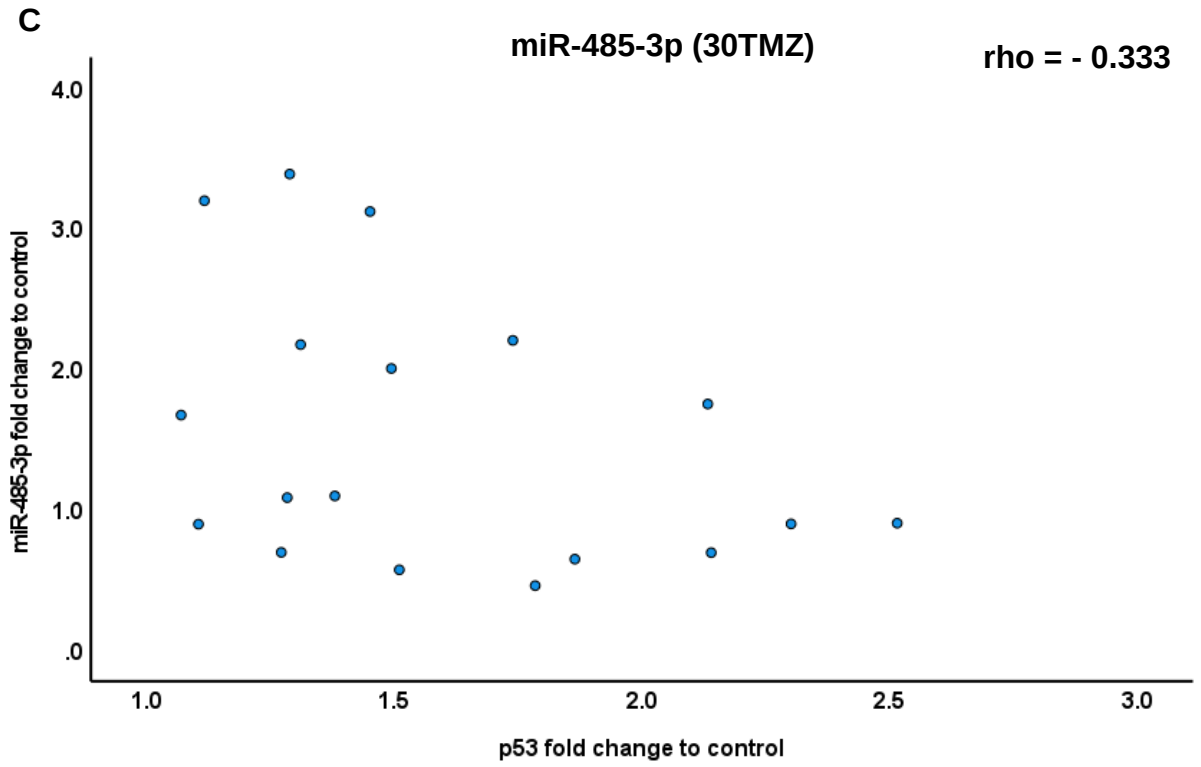

Figure 37. Correlation between p53 and miRNA expression among 30TMZ-treated cells.

Fold changes of p53 measured 4 h, 18 h, 36 h post-exposure to 30TMZ were correlated with fold changes in miR-29b-3p (**A**), miR-363-5p (**B**), and miR-485-3p (**C**) expression following the same treatment and corresponding time-frames. Figures are representative of one of multiple correlation combinations. Scatter plots represent individual data points of at least six (**n = 6**) biological replicates. No significant ($p < 0.05$) correlation is seen for any comparisons as determined by Spearman correlation.

A

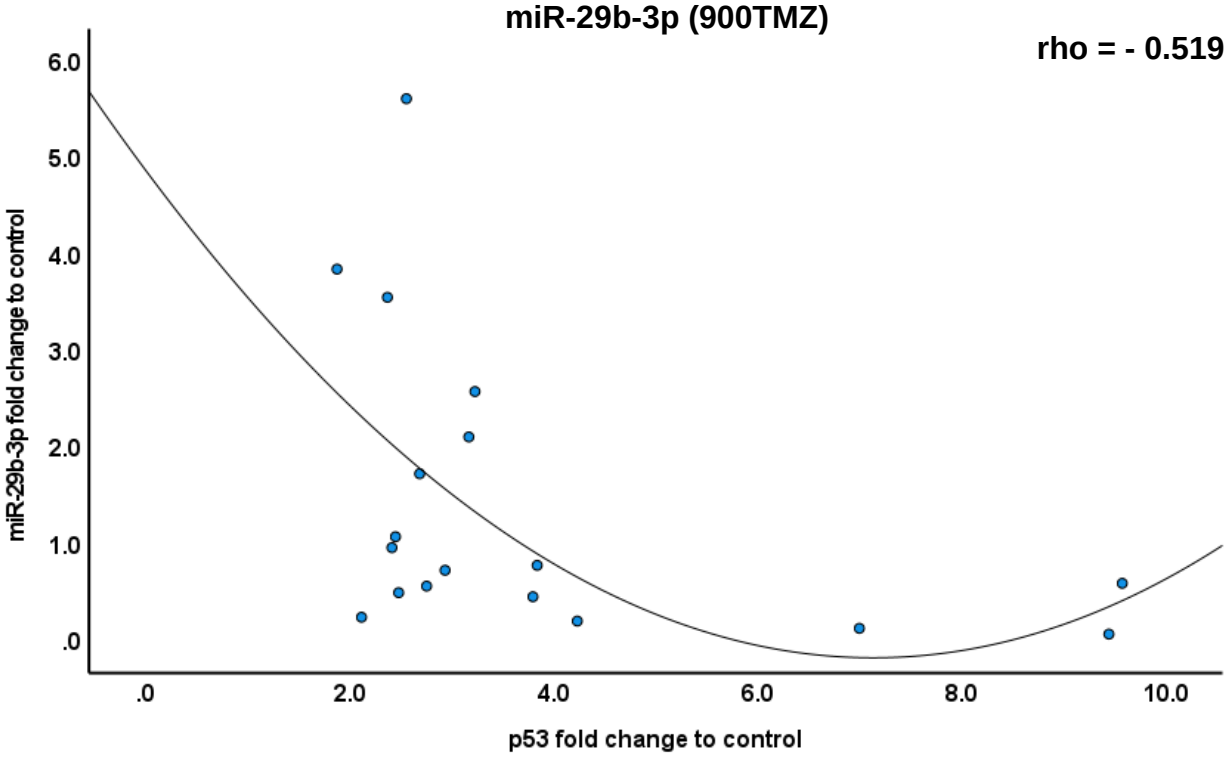
miR-29b-3p (900TMZ)
rho = - 0.519
miR-29b-3p fold change to control
6.0
5.0
4.0
3.0
2.0
1.0
.0
.0
2.0
4.0
6.0
8.0
10.0
p53 fold change to control

B

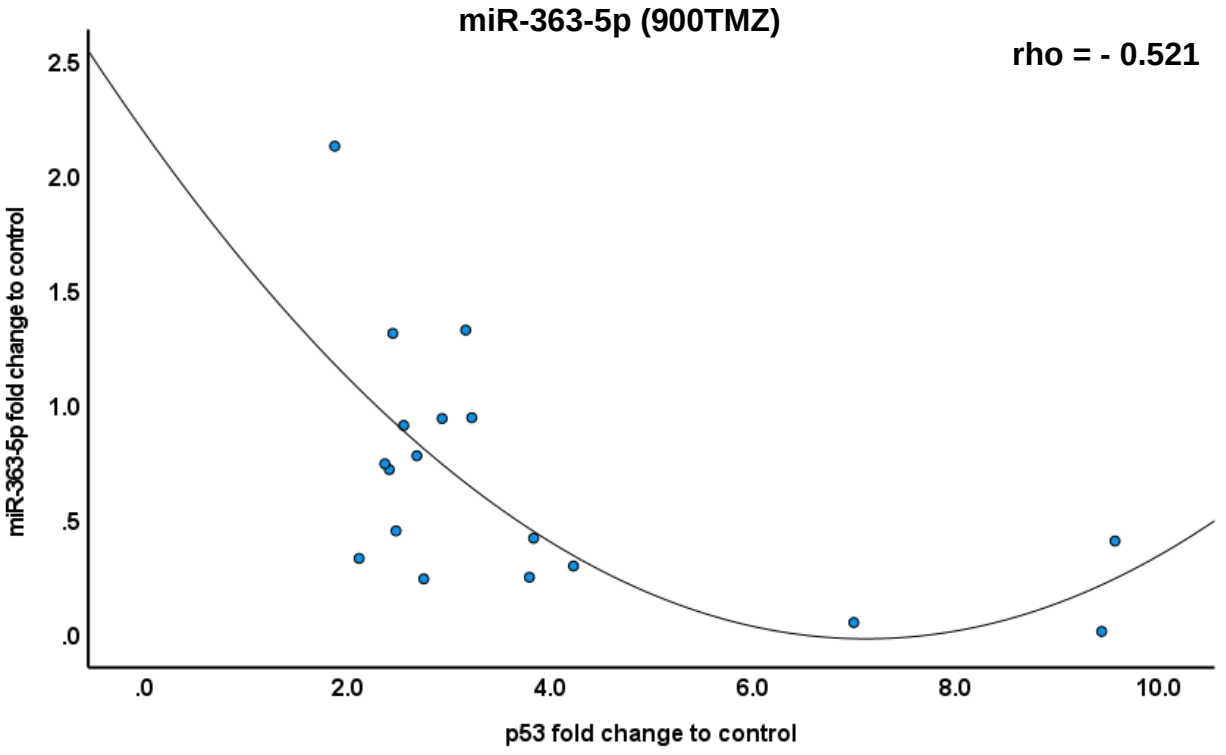
miR-363-5p (900TMZ)
rho = - 0.521
miR-363-5p fold change to control
2.5
2.0
1.5
1.0
.5
.0
.0
2.0
4.0
6.0
8.0
10.0
p53 fold change to control

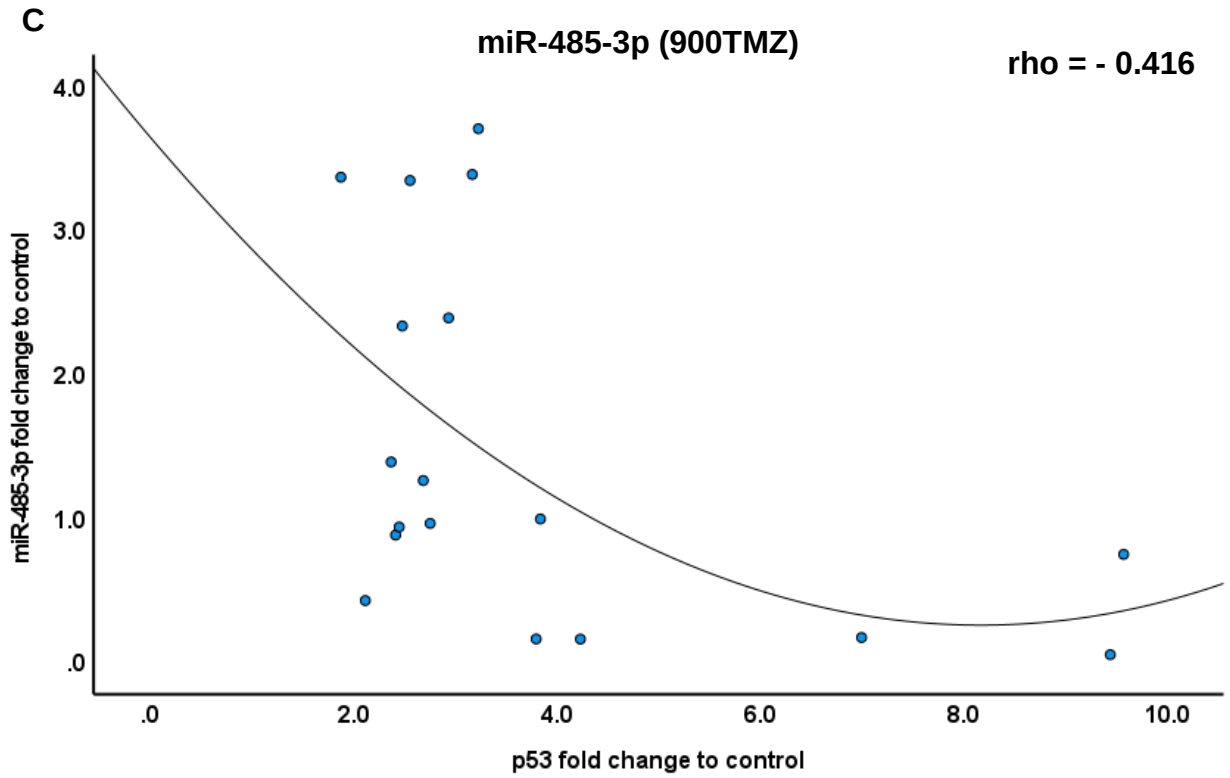

Figure 38. Correlation between p53 and miRNA expression among 900TMZ-treated cells.

Fold changes of p53 measured 4 h, 18 h, 36 h post-exposure to 900TMZ were correlated with fold changes in miR-29b-3p (**A**), miR-363-5p (**B**), and miR-485-3p (**C**) expression following the same treatment and corresponding time-frames. Figures are representative of one of multiple correlation combinations. Scatter plots represent individual data points of at least six (**n = 6**) biological replicates. A significant ($p < 0.05$) negative correlation is seen between p53 and miR-363-5p as determined by Spearman correlation.

Table 11. Spearman correlation p-values of all sampling iteration combinations

30TMZ			
Combination	**miR-29b-3p**	**miR-363-5p**	**miR-485-3p**
1	0.892	0.115	0.176
2	0.814	0.464	0.176
3	0.562	0.464	0.295
4			0.072
5			0.072
6			0.163
7			**0.036***
8			**0.036***
9			0.076
900TMZ			
1	**0.027***	**0.027***	0.086
2	**0.033***	**0.019***	**0.029***
3	0.055	**0.021***	**0.029***
4	**0.042***		
5	**0.041***		
6	**0.020***		
7	**0.030***		
8	**0.042***		
9	0.056		

Note - * indicates statistical significance as determined by Spearman's correlation.

Appendix E

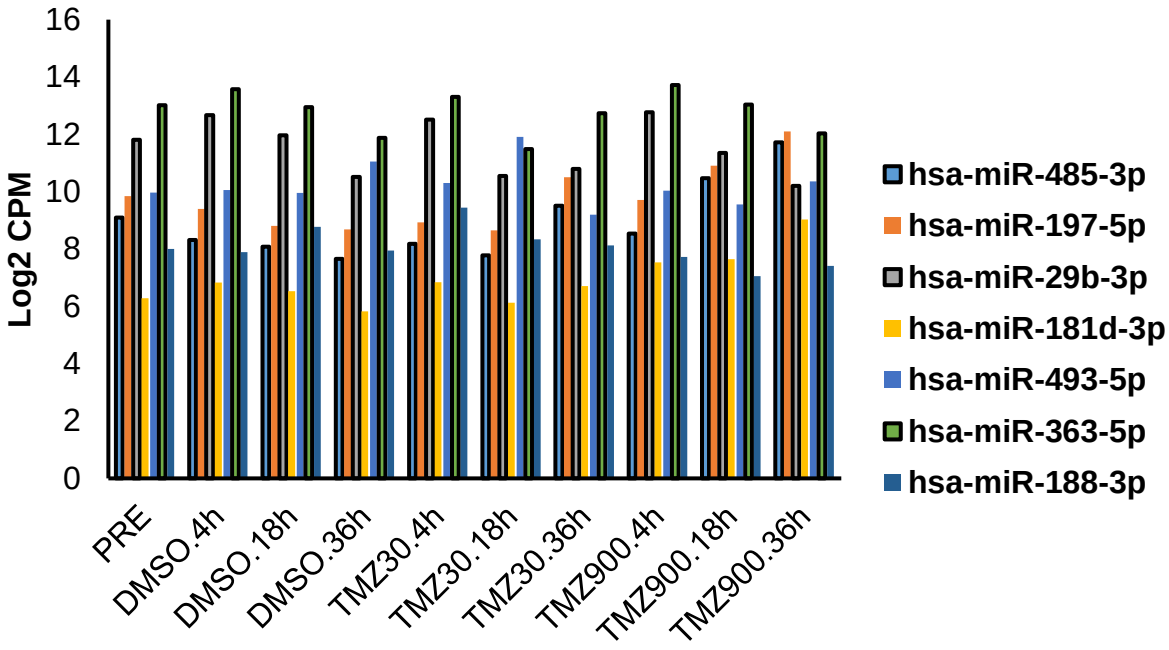

Figure 39. Log2 normalised CPM of selected miRNAs.

Among the seven originally selected miRNAs for investigation, miR-29b-3p, miR-363-5p, and miR-485-3p consistently had the highest expression among most groups. Therefore, these were selected for further investigation.